F ◆ Y ◆ 8 ◆ 7

UCRL--53689-87

DE88 010415

Institutional Research and Development

Lawrence Livermore National Laboratory

UCRL-53689-87
Distribution Categories
UC-2, 13

Acknowledgments

The Institutional Research and Development (IR&D) Program for FY87 was directed by Michael M. May, Associate Director at Large. John F. Holtzrichter, Claire E. Max, and Gordon L. Struble served as technical staff with Jeannie Maniz as Resource Manager.

The following people served on the publication staff for the FY87 IR&D annual report:

Scientific Editor	Gordon L. Struble
Publication Editor	Gloria M. Lawler
Editors	Richard B. Crawford Robert D. Kirvel Timothy M. Peck Judyth K. Prono Barbara S. Strack
Designer and Art Coordinator	John M. Zych
Layout Support	Julia Z. Deal
Art Support	George A. Kitrinos Raymond A. Marazzi
Composition Support	J. Louisa Cardoza
Production Support	The Design Group

We wish to thank George F. Bing and Jane T. Staehle for careful reading of the entire manuscript.

Contents

Exploratory Research in the Disciplines

Exploratory Research in the Disciplines (continued)

Physics

Director's Initiatives

Biotechnology

The Compact Torus

Supercomputer Research and Development

University of California Institutes

Institute of Geophysics and Planetary Physics

University of California Institutes (continued)

Individual Awards

Individual Awards (continued)

Introduction

Michael M. May

Lawrence Livermore Laboratory's (LLNL's) Institutional Research and Development (IR&D) Program, established in 1984, is funded by a 2% assessment on the Laboratory's operating budget. The program fosters exploratory work to advance science and technology, disciplinary research to develop innovative solutions to problems in various scientific fields, and long-term interdisciplinary research in support of LLNL's defense and energy missions. In managing the program, our policy is to use IR&D funds for research on innovative ideas in LLNL's areas of expertise and for developing new areas of expertise that we perceive to be in the national interest.

We support four categories of research. The first—Exploratory Research in the Disciplines—is managed by departments and divisions (Biomedical and Environmental Research, Chemistry and Materials Science, Computation, Earth Sciences, Engineering, Nuclear Chemistry, and Physics). We channel funds toward pioneering work in these disciplines. The second—Director's Initiatives—is devoted to a few larger projects selected by the LLNL Director. The third—Individual Awards—funds promising research outside the usual programmatic channels. We award funds on the basis of scientific excellence, potential impact, and leverage for future funding. In FY87, 125 applications for individual awards were submitted, and 38 were funded.

The fourth category—University of California (UC) Institutes—arises from the fact that LLNL is part of the nation's academic and research establishment. It collaborates with many UC campuses and also with other universities. The IR&D Program partially supports joint Laboratory-University research groups that LLNL and UC have created to focus effort on an important set of problems.

For FY87, the total IR&D budget was $16.8 million: $7.6 million for Exploratory Research in the Disciplines; $3.4 million for Director's Initiatives; $3.7 million for Individual Awards; and $1.8 million for the support of UC Institutes.

The technical accomplishments of each project and of each institute funded in FY87 are presented in this report, along with goals for FY88. The projects were chosen because we expect them to advance research in important areas that would otherwise not be funded or to support somewhat risky projects that promise a high payoff.

We are continually reappraising the IR&D Program. In particular, we seek new candidates for the Director's Initiatives, and we are constantly reassessing the work in progress. We make adjustments to further LLNL's policy of using the IR&D Program to fund innovative ideas with a high potential for enhancing programmatic activities of national importance.

Exploratory Research in the Disciplines

Lawrence Livermore National Laboratory

Chemistry and Materials Science

Overview

Thomas T. Sugihara

The Chemistry and Materials Science Department supports research in a broad range of disciplines—areas as diverse as x-ray optics and spectroscopy, the magnetic properties of cryogenic hydrogen isotopes, superconducting metal oxides, polymer development, photoactivated catalysis, and nuclear magnetic resonance imaging. In FY87, IR&D funding made possible an innovative project in each of these areas. The outcome of this work is expected to have a long-term impact on defense, laser, and energy programs at LLNL.

Our research in x-ray optics led to the design and synthesis of multilayer optic structures, each consisting of thin alternating layers of two elements. We found them to be well suited for use in intense x-ray light sources. A multilayer structure made of rhodium and carbon served successfully as a monochromator for extreme ultraviolet radiation. In addition, multilayer x-ray Cassegrain telescopes were used for solar observation at 17.2 nm, giving 1.2-arc second resolution.

We used extended x-ray absorption fine structure (EXAFS) and x-ray absorption near-edge structure (XANES) analyses to investigate properties of semiconductors important in thermoelectric devices. These analyses employ synchrotron radiation to yield local structure data, such as bond distances and coordination number, and chemical state information, such as oxidation state and electron energy levels. This work was conducted on the LLNL beamline at the Stanford Synchrotron Radiation Laboratory and at the Brookhaven National Synchrotron Light Source.

Several other projects focused on the synthesis and processing of unusual new materials. In midyear, we began the development of useful forms of high-temperature, superconducting metal oxides. This work, which challenges our expertise in ceramics and in vapor deposition of thin films, is expected to expand in FY88. Another materials project—the study of polymers that can be synthesized as rigid helical rods—was completed, but we will continue to investigate the application of these polymers as low-density foams and as optically active films. In a third materials project, we prepared a photoactivated catalyst for hydrogenation and other fuel-related reactions. The new catalyst is made from silica aerogel doped with photoactive ions as the chromophore. We plan to continue the study of its properties in FY88.

We also made progress toward achieving spin polarization in deuterium-tritium (D-T)—a condition that can greatly reduce the amount of laser energy needed to ignite D-T fuel for inertial confinement fusion. We synthesized a D-T system that had a higher percentage of molecular DT than conventional mixtures. The triton relaxation time—a factor critical in achieving spin polarization—was increased to the order of several seconds. The thermal conductivity of solid tritium was also measured and found to be significantly larger than expected.

Also completed is the development of a nuclear magnetic resonance spectrometer, capable of imaging mobile protons in solid samples. We obtained a spatial resolution of about 20×20 μm.

Overall, the Chemistry and Materials Science Department received $1,076,000 in IR&D funds for FY87.

FY87: $259,000
FY88: $160,000

X-Ray Thin Film Studies

Principal Investigator:
Troy W. Barbee, Jr.

We designed and synthesized multilayer optics for the soft x-ray (100- to 3000-eV) and extreme ultraviolet (30- to 100-eV) regions of the spectrum. Experiments conducted at the Stanford Synchrotron Radiation Laboratory (SSRL) showed that these optics can be used as dispersive elements in monochromators. A new multilayer optic exhibited unique dispersive properties, making possible soft x-ray and extreme ultraviolet instrumentation that is conceptually new.

Optical elements encompass a wide range of devices, all directed to the efficient manipulation of light to achieve specific physical ends. In the past decade, a new generation of optics for x rays has emerged. Foremost among these advances has been the use of vapor condensation in a controllable manner to deposit thin films, forming multilayer structures.

These structures are perfect enough to be considered synthetic crystals with large periods. They are perfect in the sense that their layers are sufficiently periodic for them to be used as wavelength-dispersive, analyzing crystals in the x-ray, soft x-ray, and extreme ultraviolet (EUV) spectral domains.

These unique materials are typically synthesized by atom-by-atom processes. In the work described here, we used magnetron sputter deposition to build structures with up to 500 layers, each about 0.6 to 20 nm thick.

Our work has three specific objectives:

- To characterize multilayer optic structures.
- To apply these optics to synchrotron radiation instrumentation.
- To use the unique capabilities of these optics and the instrumentation to determine the optical constants of condensed matter.

We synthesized and characterized simple mutilayer structures of rhodium-carbon (Rh-C), molybdenum-silicon (Mo-Si), and 304 stainless steel-silicon (304 SS-Si). We made several structures from all three materials, each structure with a different, but constant, period d_0. The Table shows the spectral range of application and the range of d_0 values for each material.

The reflectivities R, measured for these multilayers at wavelengths λ, were greater than 50% of those calculated for ideal multilayer structures, and some reflectivities were the best ever achieved: For Rh-C with $d_0 = 3.92$ nm, R was 35% for $\lambda = 4.47$ nm at a Bragg angle θ of 35°; for Mo-Si with $d_0 = 8.0$ nm, R was 59% for $\lambda = 15.2$ nm at $\theta = 90°$.

From two Rh-C multilayers made of 250 layer pairs with $d_0 = 1.908$ nm, we made a two-crystal, multilayer, vacuum monochromator and used it to measure the photoelectric absorption coefficient of silicon in the vicinity of its K edge at 1839 eV, of aluminum in the vicinity of its K edge at 1559 eV, of magnesium in the vicinity of its K edge at 1303 eV, of copper in the vicinity of its L edges at 932 eV, and of nickel in the vicinity of its L edges at 853 eV. Figure 1 shows that the measurements at the K edge of aluminum agree closely with calculated results for the SSRL monochromator beamline. The structure observed in the experimental data (from about 1.6 to 1.9 keV) is due to near-edge electronic effects of extended x-ray absorption fine structure (EXAFS). The EXAFS is caused by the atomic arrangement of the aluminum atoms in the sample. This measurement of EXAFS using a multilayer two-crystal monochromator is the first of its kind. It demonstrates the potential capability of multilayers to provide high resolution.

Table **Characteristics of multilayer structures synthesized for use as optics.**

Material	Spectral range (eV)	Range of periods (nm)
Rh-C	100–283 600–3000	1.91–8.0
Mo-Si	40–100 800–1830	3.0–35
304 SS-SI	250–700	2.4–5.5

Cassegrain telescopes containing optics coated with Mo-Si multilayer structures were used to obtain high-resolution, wide-field x-ray images—the first such images ever taken with multilayer optics. The 1.0- to 1.5-arc second resolution image in Figure 2, one of 13 taken with a single Cassegrain telescope, shows light from the excited emission lines of Fe(IX) and Fe(X) at a temperature of 1.0 to 1.3 × 10^6 K in the solar corona. The Mo-Si multilayer optic coatings had a period of 19.2 nm, a normal-incidence reflectivity of 38 to 42% at λ = 17.2 nm, and a two-reflection resolution of ~15. The telescope was launched on a Nike/Black Brandt rocket from White Sands Missile Range, N.M. This work was done in collaboration with the Center for

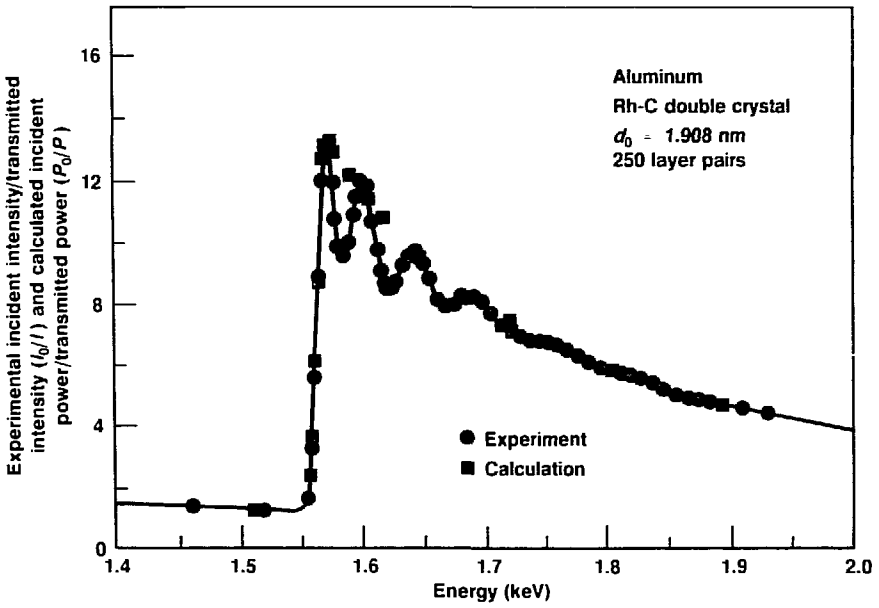

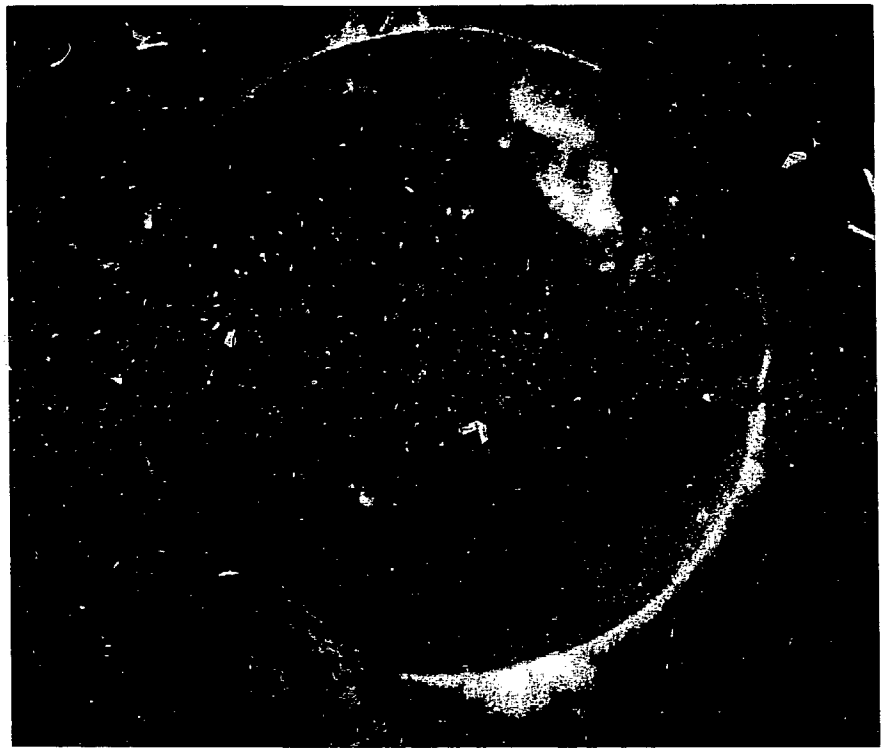

Fig. 1 (*Above*). The absorption edge profile, measured on 2.05-μm aluminum foil by a two-crystal, multilayer monochromator, compared with calculations.

Fig. 2. First high-resolution, wide-field x-ray image of the sun to be obtained with multilayer-coated optics. A Cassegrain telescope, having its concave (1.2-m radius) primary element and convex (0.5-m radius) secondary element coated with Mo-Si multilayers, was used to obtain this image. The coating consisted of twenty 19.2-nm periods that had ~40% reflectivity at normal incidence in a 6.5% band pass centered on 17.2-nm light.

Space Science and Astrophysics at Stanford University and the Space Sciences Laboratory of the Marshall Space Flight Center.

In FY88, we will investigate the scanning capabilities of the monochromator and develop ultra-high-resolution optics. These optics will be used to measure the scattering and absorption cross sections in the soft x-ray and EUV spectra. To allow absorption-edge contrast imaging with submicron resolution, we also plan to develop a tunable x-ray microscope in the soft x-ray and EUV range.

References

Barbee, T. W., Jr. (June 1987), "Multilayer Structures: Atomic Engineering in Its Infancy," *Proceedings NATO Advanced Study Institute—Physics, Fabrication, and Application of Multilayered Structures*, Ile de Bendor, France.

Barbee, T. W., Jr., P. Pianetta, R. Redaelli, R. Tatchyn, and T. W. Barbee, III (1987), "Molybdenum-Silicon Multilayer Monochromator for the Extreme Ultraviolet," *Appl. Phys. Lett.* **25**, 1841.

Cole, A. J., M. H. Key, A. Ridgeley, D. A. Brown, P. A. Norreys, E. R. Wooding, and T. W. Barbee, Jr. (1987), "A Pinhole Camera for Monochromatic X-Ray Imaging," *Opt. Commun.* **62**, 1.

Gardner, D. S., K. C. Saraswat, and T. W. Barbee, Jr. (June 16, 1987), (to Board of Trustees of the Leland Stanford Junior University), *Layered Aluminum and Aluminum/Silicon with Titanium and Tungsten for Multilevel Interconnects*, U.S. Patent 4,673,623.

Green, M., M. Richter, J. Kortright, T. W. Barbee, Jr., R. Carr, and I. Lindau (September 1987), "Scanning Tunneling Microscopy of X-Ray Optics," *Proceedings of the Conference on Scanning Tunneling Microscopy*, Oxnard, Calif. (to be published in *J. Vac. Sci. Technol.*).

Pan, L., P. L. King, P. Pianetta, D. Seligson, and T. W. Barbee, Jr. (June 1987), "Synchrotron-Based X-Ray Lithography at Stanford University," *Proceedings of the Conference on Synchrotron Radiation Instrumentation*, University of Wisconsin, Madison, Wis. (to be published in *Nucl. Instrum. Methods*).

Pianetta, P. and T. W. Barbee, Jr. (June 1987), "Applications of Multilayers to Synchrotron Radiation," *Proceedings of the Conference on Synchrotron Radiation Instrumentation*, University of Wisconsin, Madison, Wis. (to be published in *Nucl. Instrum. Methods*).

Thompson, A. C., Y. Wu, J. H. Underwood, and T. W. Barbee, Jr. (1987), "Focussing of Synchrotron Radiation X-Ray Beams Using Synthetic Multilayer Mirrors," *Nucl. Instrum. Methods* **A255**, 603.

Walker, A. B. C., Jr., T. W. Barbee, Jr., R. B. Hoover, and J. F. Lindblom, "XUV Images of the Solar Corona with a Normal-Incidence Cassegrain Multilayer Telescope," submitted to *Science*.

Walker, A. B. C., Jr., J. Lindblom, R. B. Hoover, and T. W. Barbee, Jr. (September 1987), "Monochromatic X-Ray and XUV Imaging with Multilayer Optics," *SPIE Proceedings on X-Ray and EUV Astronomy*, Nice, France.

FY87: $232,000
FY88: $180,000

Metal-Doped Beta-Boron Thermoelectric Materials

Principal Investigator: Joe Wong
Co-Investigator: Glen A. Slack[a]

[a]General Electric Research Laboratory, Schenectady, N.Y.

We used two types of x-ray absorption spectrum analyses—extended x-ray absorption fine structure (EXAFS) and x-ray absorption near-edge structure (XANES)—to investigate the bonding and local atomic structure of 3d, 4d, and 5d transition metals doped in beta-rhomboidal boron. The work was performed with synchrotron radiation.

Beta-boron is a semiconductor with a band gap of 1.5 eV. Hard and refractory with a melting point of 2300 K, it meets the criteria for potentially high thermoelectric efficiency: It consists of small atoms and has a large number of them (105) per unit cell.

It is made up of compact, polyhedral units of 10 and 12 boron (B) atoms, and isolated B atoms, all linked by strong, directional, covalent bonds (Hoard et al., 1970). These structural and bonding features create a very open structure. If we assume that the B atom radius R_B is 0.88 Å, the filled space amounts to only 36%. Thus, the beta-boron structure contains holes that can accommodate atoms of many metals in the periodic table.

Our work takes advantage of the atom-specificity of x-ray absorption spectroscopy to elucidate the bonding and local structure of metal dopants in beta-boron. We hope to gain an understanding of physico-chemical behavior that might be exploited for thermoelectric applications.

We conducted two runs at the Brookhaven National Synchrotron Light Source with the x-ray ring generating 2.5 GeV of electron energy and 75 to 100 mA of injection current. We completed a series of K-edge measurements on all 3d metals (Sc, Ti, ..., Ni, Cu) in beta-boron. We also studied concentration dependence in Ti, V, Cr, Fe, Co, Ni, and Cu systems and the spectral variation caused by double-doping with V and Cu. In addition, we used two 4d dopants, Zr and Nb, and two 5d dopants, Hf and Ta, to study the effects of atom size. We chose the d metals to study because their electron-rich structure complements the electron-deficient boron structure. The diborides of Sc, Ti, V, Cr, Zr, Hf, and Ta were also studied as reference compounds to aid in modeling the local environment of the metal dopant in beta-boron. The doped materials were prepared at General Electric Research Laboratory, Schenectady, N.Y., by means of a melt-grown technique carried out above 2300°C in ambient argon at 50 atm pressure.

Figure 1 shows normalized XANES spectra for a series of 3d metal dopants at 1 at.% concentration in beta-boron. The zero-energy points correspond with the first inflection point in the derivative spectrum of the respective pure metal. For metals earlier in the periodic table—Ti, V, and Cr in particular—several well-resolved transitions up to 24 eV are evident. The pre-edge feature at 1 to 2 eV is a $1s \rightarrow 3d$ transition that is normally dipole-forbidden. The rather strong presence of this transition indicates appreciable overlap of the d states with the p states of the metal dopants (Wong et al., 1984). Two well-defined bound states at 7 and 11 eV are also evident. As the d states are progressively filled in the series from Ti to Cu, the pre-edge feature at 1 to 2 eV becomes less well defined. It disappears in the spectra of Co, Ni, and Cu. Similarly, the doublet feature below 10 eV becomes less resolved, finally merging into the curve as a shoulder. This progression is evident in the series from Mn through Cu. The features at 17 eV and above are due to lattice scattering (Lytle et al., 1987).

We determined by EXAFS analysis and by varying the concentration that V and Cr, in concentrations up to 1 at.%, occupy the A_1 site in beta-boron (Hoard et al., 1970). In this site, the dopants have 12 neighboring B atoms at a bond distance of 2.15 Å. Ti, Fe, and Mn, at the same concentration, occupy the A_1 site and also the less symmetrical D site, which has 14 neighboring B atoms. Ni, in concentrations above 0.5 at.%, goes into both the A_1 and D sites, whereas Cu at 1 at.% goes into three different sites: A_1, D, and E.

We obtained XANES spectra for V and Cu in two doubly-doped beta-

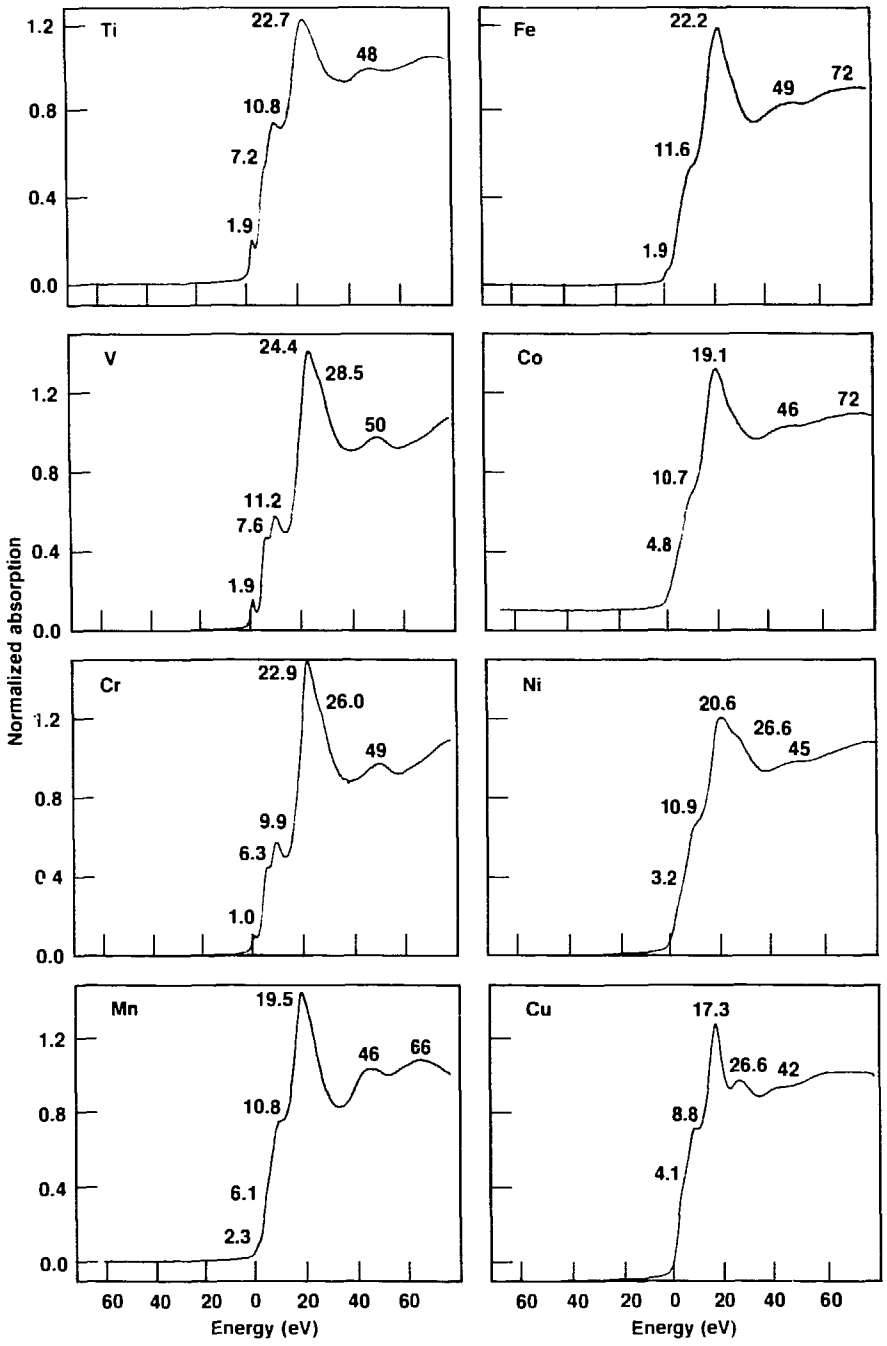

Fig. 1. K-edge XANES spectra of 3d metal dopants in beta-boron.

boron systems—one containing 1 at.% V and 1 at.% Cu, and the other containing 1 at.% V and 3 at.% Cu. The spectra are identical to those produced by the two metals when used as single dopants. The similarity of these spectra indicates that the local structure and electronic configuration around the V atom are not significantly affected by the presence of Cu in the boron lattice and vice versa. It demonstrates conclusively that there is no interaction between two dissimilar dopants.

L_3-edge XANES spectra of pure Ta metal, TaB_2, and Ta dopant in beta-boron (Figure 2) were a good source of information about the crystallographic environment of the metal dopants. Because the L_3 edge results from exciting the core 2p state to some final d states (which are quite empty in Ta), high intensity is observed in the principal absorption maximum—the so-called white line. Such L_3 spectra may be deconvoluted into a Lorentzian and an arctangent step function (Horsley, 1981). TaB_2 consists of alternate layers of metal and boron stacked along the c axis. Each Ta atom has six equidistant closest Ta neighbors in its plane and 12 equidistant B neighbors—six in the plane above and six in the plane below. In a corresponding manner, each B atom has three B neighbors in its plane and forms six bonds with Ta. Accordingly, the deconvoluted spectra, shown by dotted lines in Figures 2(a) and 2(b), yield a single Lorentzian, indicating a single crystallographic site for Ta. In contrast, the deconvoluted spectrum of Ta in beta-boron is best fitted with

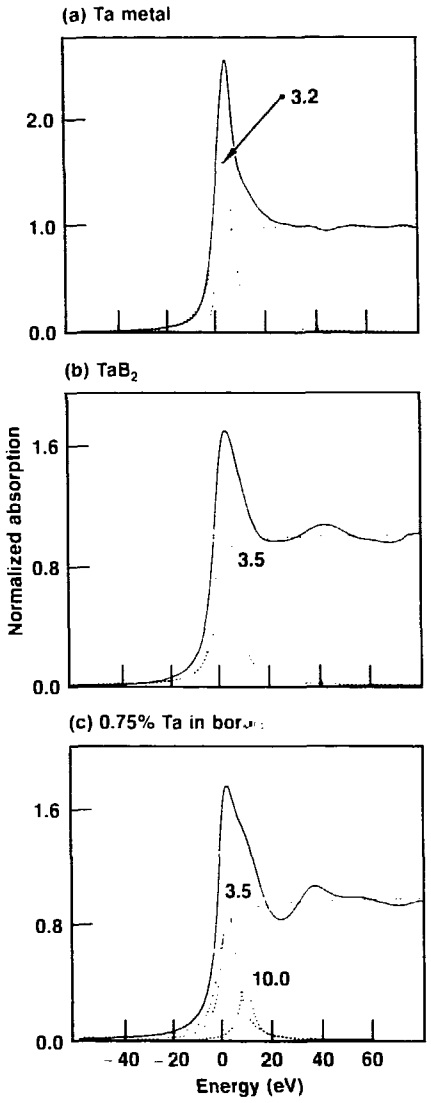

Fig. 2. L_3-edge XANES spectra of Ta (solid lines) and deconvoluted Lorentzian and arctangent functions (dotted lines).

two Lorentzians, as shown in Figure 2(c). This spectral analysis suggests that Ta occupies multiple sites in beta-boron.

In FY88, we plan to complete EXAFS analyses of these series of metal-doped boron materials and to correlate our results with recent crystallographic findings (Slack et al., 1987). We will also design and construct an experimental end station on a powerful, hard x-ray, wiggler beamline at the Stanford Synchrotron Radiation Laboratory. This will allow further studies with synchrotron radiation on high-temperature superconductors, interfacial structure at the junctions of dissimilar materials, and optical materials for lasers. We also plan to use the station for microtomography studies and x-ray scattering experiments at high temperature and pressure.

References

Hoard, J. L., D. B. Sullenger, C. H. L. Kennard, and R. E. Hughes (1970), "The Structure Analysis of Beta-Rhombohedral Boron," *J. Solid State Chem.* **1**, 268.

Horsley, J. A. (1981), "Relationship Between the $L_{2,3}$ X-Ray Absorption Edge Resonances and the d-Orbital Occupancy in Compounds of Platinum and Iridium," *J. Chem. Phys.* **76**, 1451.

Lytle, F. W., R. B. Greegor, and A. J. Panson (1987), "Discussion of X-Ray Absorption Near-Edge Structure: Application to Cu in High-T_c Superconductors," *Phys. Rev. B* **37** (in press).

Slack, G. A., C. Hejna, M. Garbauskas, and J. S. Kasper (1987), "X-Ray Study of Transition Metal Dopants in Beta-Boron," *J. Solid State Chem.* (in press).

Wong, J., F. W. Lytle, R. P. Messmer, and D. H. Maylotte (1984), "K-Edge Absorption Spectra of Selected Vanadium Compounds," *Phys. Rev. B* **30**, 5596.

Synthesis and Characterization of High-Temperature Superconducting Ceramics

Principal Investigator:
Richard L. Landingham

We took advantage of the interdisciplinary strength of LLNL and its available equipment to prepare substantial quantities of high-quality $YBa_2Cu_3O_{(7-\delta)}$ superconducting materials. These superconductors have a perovskite-like crystalline structure. We produced them in a variety of forms differing in oxygen content and are now evaluating their properties.

Materials fabrication is the key to research on the new high-temperature superconductors that have so widely captured public attention (Cava et al., 1987; Wu et al., 1987). Our major goal is to rapidly establish our ability to produce these materials by sophisticated fabrication techniques developed at LLNL. We set out to prepare Y-Ba-Cu-O, the material system currently known to have superconducting capability at the highest temperature, and to investigate its crystalline structure, purity, and physical properties. Our plans called for forming quantities of powder of a reproducible quality into appropriate components and making them available for evaluation by researchers in other disciplines. These samples are being tested under a variety of conditions such as ultra-high static pressures and dynamic pressures (Hor et al., 1987), high-radiation flux, magnetic fields, and microwave-cavity environments.

Another of our goals is to correlate improvements in the quality and characteristics of the material with these test conditions. This correlation, based on interdisciplinary cooperation, will help us to establish optimal synthesis and fabrication techniques. We will then use our expertise in the fabrication of layered materials to produce microchemically controlled films with known stoichiometry for advanced solid-state experiments.

At the start of this project in June 1987, we concentrated on learning what was already known about the selected material. We gathered information rapidly by visiting outside facilities such as IBM, Lawrence Berkeley Laboratory, and AT&T, and by inviting guest experts to speak at LLNL.

Because most progress had been achieved with cold-pressed and sintered components of $YBa_2Cu_3O_{6.8}$, our fabrication effort first focused on cold-pressing and sintering. The two main problems with this approach had been the lack of compositional uniformity on a submicron scale and low density (≤90% of theoretical). By cold-pressing and sintering $YBa_2Cu_3O_{(7-\delta)}$ (nicknamed "123 compound"), we achieved densities to 94% of theoretical. Although improved over previous results, this value is insufficient to give optimal mechanical properties and may limit current density in bulk conductors. To achieve higher densities with this method, we are evaluating parameters such as particle size,

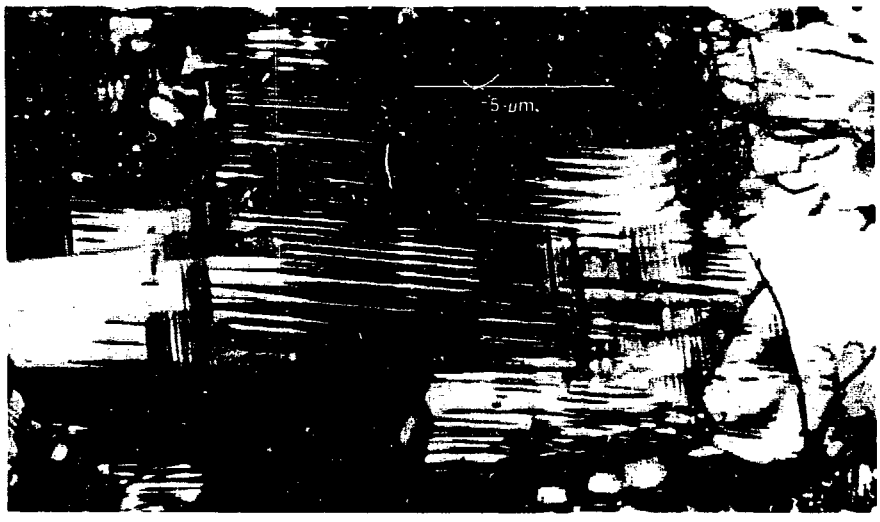

Microstructure of a $YBa_2Cu_3O_{(7-\delta)}$ compound fabricated to full density by the belt-piston technique (650°C at 300,000 psi for 1/2 h).

sintering temperature, and sintering environment.

By another method—the belt-piston (BP) method—we were able to achieve higher densities—up to 99%. We were the first to produce bulk 123 compound of nearly full density that levitates at liquid nitrogen temperatures. The BP process was carried out at the LLNL ultra-high-pressure facility. To $YBa_2Cu_3O_{6.8}$ powder, we applied pressures greater than 300,000 psi at temperatures up to 650°C in an air or oxygen environment. We pressed the compound into the form of small bars 1/2 in. in diameter and 1 in. long, achieving maximum density (<1% porosity) by applying heat at 630°C for 1/2 h with a pressure of 300,000 psi (see the Figure). We are now evaluating the properties of these bars.

We used a third method—hot isostatic pressure (HIP)—to fabricate components from 123 powder. Attempts to make larger bars (5/8 in. in diameter by 5 in. long) at lower pressures (around 30,000 psi) produced samples of about 90% density, if the temperature was not higher than 700°C. Fully dense bars were achieved at 750°C, but lower oxygen content caused a decrease in their superconducting properties. Above 650°C, the superconductors were transformed from the orthorhombic to the tetragonal phase even in 5 atm of oxygen. We were able to convert the surfaces of these fully dense, tetragonal materials back to the orthorhombic phase by heat treatments between 450 and 600°C in an oxygen atmosphere. The properties of these surfaces are now under study.

As we improved the density of the superconducting components, we began to have problems in achieving good electrical contacts with them. To study the interface between the superconductors and various metals that might serve as contacts, we embedded such metals in and around the 123 powder before the HIP and BP runs. Stainless steel cans placed around 123 powder in BP runs formed bonds with no observed interface layers. Nickel cans also formed bonds during HIP runs at 750°C, but a 50-μm intermediate layer was created. Copper cans formed a green intermediate layer, which allowed easy removal of the can from the 123 compound.

We also embedded four platinum electrodes in the 123 powder before the HIP and BP runs and observed a thin film at the interfaces at temperatures between 600 and 750°C. Silver rings were likewise embedded, and, according to microprobe analysis, they showed good bonding with no sign of interface reactions. More specimens containing silver rings are being prepared to measure the current density of the bulk 123 compound. The silver sections will serve as connection bus bars.

In FY88, we plan the intensive study of samples that have already been prepared. They will be subjected to several types of analyses: scanning tunneling microscopy, transmission electron microscopy, Auger analysis, and neutron diffraction. Dynamic compaction studies will be conducted on some samples, and others will serve as sputter targets for thin-film deposition. In addition, we plan to substitute new elements for selected elements in the present superconductor system to improve the properties of 123 compound.

References

Cava, R. J., R. B. van Dover, B. Batlogg, and E. A. Rietman (1987), "Bulk Superconductivity at 36 K in $La_{1.8}Sr_{0.2}CuO_4$," *Phys. Rev. Lett.* **58**, 408.

Hor, P. H., L. Gao, R. L. Meng, Z. J. Huang, Y. Q. Wang, K. Forster, J. Vassilious, C. W. Chu, M. K. Wu, J. R. Ashburn, and C. J. Torng (1987), "High-Pressure Study of the New Y-Ba-Cu-O Superconducting Compound System," *Phys. Rev. Lett.* **58**, 911.

Landingham, R. L. and D. C. Hagerty (1987), "Densification of Superconducting Ceramic Powders ($YBa_2Cu_3O_{6.8}$) by Belt-Piston (BP) Techniques," 20th Annual Convention of the International Metallographic Society, Monterey, Calif., July 27-30.

Landingham, R. L. and D. C. Hagerty (1987), "Densification of Superconducting Ceramic Powders ($YBa_2Cu_3O_{6.8}$) by Hot Isostatic Pressing (HIP) Techniques," 20th Annual Convention of the International Metallographic Society, Monterey, Calif., July 27-30.

Wu, M. K., J. R. Ashburn, C. J. Torng, P. H. Hor, R. L. Meng, L. Gao, Z. J. Huang, Y. Q. Wang, and C. W. Chu (1987), "Superconductivity at 93 K in a New Mixed-Phase Y-Ba-Cu-O Compound System," *Phys. Rev. Lett.* **58**, 908.

FY87, $135,000

Rigid-Rod Polymers

Principal Investigators:
Lucy M. Hair, Robert C. Cook, and Mark M. Green[a]

[a]Polytechnic University, Brooklyn, N.Y.

We used isocyanate (IC) and isonitrile (IN) comonomers to build cross-linked, rigid-rod, polymer gels that may ultimately have application in industrial, military, and consumer goods. Later we synthesized longer-chain, cross-linking IC and IN comonomers to act as bridges in the gel structure, believing they would produce stronger gels. In FY87, we developed ten cross-linked gel systems incorporating these bridges and found that localized regions of micro-gel formed, rather than a cohesive gel structure. This result perhaps indicates that the longer bridges reacted with the chain backbone. We also studied the contribution of torsional oscillations and helix reversals to the stiffness of polymer chains—an important concern in the design of strong, cross-linked structures.

The polymer families of isocyanates and isonitriles are unique in that they form as helical, wormlike rods due to a conflict between electronic and steric forces. They are well-suited for the creation of novel cross-linked systems and for theoretical studies because the pendant group R can vary widely without loss of helicity and, therefore, without loss of backbone rigidity. This single characteristic means that

- The polymers can be cross-linked through a reactive pendant group.
- Ideal (non-hydrogen-bonded), non-cross-linked, rigid-rod gels can be made.
- The polymers can be synthesized to have only one sense of the helix—either a left-hand or right-hand twist.

Our primary objectives were to make polymer gel and network systems and then to investigate their structures and properties. These steps lead to our secondary objectives: the development of gels and foams that can be used in the separation of stereoisomers, in the capture of trace chemicals, as low-density materials in the LLNL Laser Fusion Program, or as optically active coatings.

In FY85, we synthesized the first cross-linked gels composed of rigid-rod polymers by simultaneously co-polymerizing and cross-linking IC comonomers or IN comonomers. The chemical structures of the comonomers are shown as (a), (b), and (c) in the Table.

In FY86, we showed that it is possible to exert rough control over the molecular weights of non-cross-linked IC polymers. We did so by adjusting the molar ratio of the comonomers to butyl-lithium, the initiator used for the polymerization reaction. We also found optically active polymers to be more rigid than those that are not optically active—a discovery implying that materials made from optically active polymers would be inherently stronger. Despite the evidence for increased stiffness, we did not use optically active materials to make significant amounts of polymer. We made this decision to keep the syntheses simple and devote more resources to the study of the cross-linked, rigid-rod systems.

After careful screening of co-monomers for cross-linking capability, we synthesized 20 gel systems, but subsequent solvent-swelling studies showed a low degree of cross-linking. Space-filling models of the polymer and models of pendant-chain mobility indicated that this was due to the inaccessibility of the cross-linking comonomer: It was mostly buried in the rigid rod and thus not available for reaction. To overcome this problem, we synthesized the di-isocyanatodecane comonomer, shown in the Table as (d), and a new, unnamed IN comonomer, (e) and (f) in the Table. Both were expected to provide significantly longer cross-linking bridges in the polymer gels.

In FY87, we synthesized gels incorporating these new comonomers. In gels made with the IN comonomer, we observed local regions of micro-gel rather than a cohesive gel structure. We then performed Soxhlet extractions with chloroform on two types of

polyisonitrile gels: those made with the shorter IN cross-linking comonomers [(b) and (c) in the Table] and those made with the new, longer IN comonomer. The extracts and residues showed the amount of the shorter comonomers in the gel to be >85% and the amount of the longer comonomers to be >75%. The 10% difference is not large enough to account for the micro-gel formation. The chemical identity of the solubilized extracts will be determined by ^{13}C and ^{1}H nuclear magnetic resonance spectroscopy and by mass spectrometry.

Swelling studies to measure the thermodynamic interaction between solvent and gel are needed to determine the molecular weight between cross-links. In preliminary studies with five solvents, we found that the solubility parameter δ of poly (n-hexyl-isocyanate) cross-linked gel systems is equal to or less than that of cyclohexane: 8.2 Hildebrands [(calories/cm^3)^2]. Further swelling studies with a broader range of solvents will pinpoint the solubility parameter more accurately. We will then use these values in Gaussian and worm-like network equations as well as in an equation of our own to determine the molecular weight between cross-links.

Our theoretical work in FY87 turned toward answering specific questions about the structure, stiffness, and solution properties of individual polymer chains as necessary preparation to a study of the mechanical properties of the corresponding cross-linked materials. We first showed by an examination of local chain dynamics that the stiffness of poly (n-alkyl-isocyanates) can be completely explained by the existence of torsional oscillations in the chain backbone. Next, a careful examination of the data from local molecular spectroscopic probes revealed that polyisocyanates synthesized from a racemic mixture of optically active comonomers owe their apparent flexibility to helix reversals. These two studies solve a nagging problem described in the polyisocyanate literature and show us that helix-reversals drastically affect the mechanical properties of polyisocyanates in a cross-linked material.

Table Comonomer pairs.

Cross-linking bridge	Backbone only
a. $OCN(CH_2)_6NCO$ Di-isocyanatohexane	$CH_3(CH_2)_5NCO$ Hexyl isocyanate
b. $CN(CH_2)_6NC$ Di-isonitrile hexane	$CH_3(CH_2)_3NC$ Butyl isonitrile
c. $CN(CH_2)_6NC$ Di-isonitrile hexane	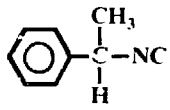 α-phenethyl isonitrile
d. $OCN(CH_2)_{10}NCO$ Di-isocyanatodecane	$CH_3(CH_2)_3NCO$ Butyl isocyanate
e. 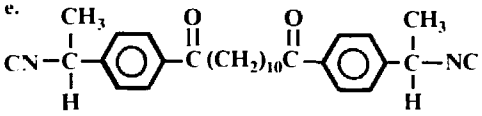	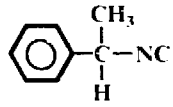
f. 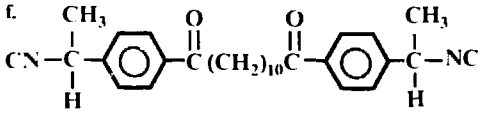	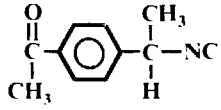

References

Cook, R. (1987). "Flexibility in Rigid Rod Poly (n-Alkyl-Isocyanates)." *Macromolecules* **20**, 1961.

Green, M. M., R. A. Gross, R. Cook, and F. C. Schilling (1987). "Broken Worm and Worm-Like Models for Polyisocyanates." *Macromolecules* **20**, 2636.

Lucht, L. M., P. K. Shell, and R. C. Cook (1986). "Rigid Rod Foams." *Laser Program Annual Report 85*, Lawrence Livermore National Laboratory, Livermore, Calif., UCRL-50021-85.

Luchi, L. M., P. K. Shell, R. Cook, A. R. Cook, M. M. Green, R. A. Gross, and M. Reidy (1986). "Gels from Rigid Rod Polymer Isocyanate Systems." *Proceedings of the ACS Division of Polymeric Materials: Science and Engineering* 55, 846.

FY87 $90,000
FY88 $100,000

Photoactivated Heterogeneous Catalysis on Aerogels

An SiO_2 aerogel, doped with a photoactive ion, was found to be an effective photocatalyst for the synthesis of C_1 to C_8 hydrocarbons from a hydrogen-carbon monoxide mixture. Simulated sunlight was the energy source.

Principal Investigator:
Carlos A. Colmenares
Co-Investigators:
S. Michael Angel,
Richard Gaver,[a] John F. Poco,
William E. Elsholz, and
Cheryl L. Evans

[a]San Jose State University, San Jose, Calif.

In FY87, we developed an SiO_2 aerogel doped with photochemically active ions to be used as a heterogeneous catalyst. By using this aerogel to catalyze the hydrogenation of CO (the Fischer-Tropsch process), we succeeded in producing a range of hydrocarbon products from methane to octane. This reaction was carried out at room temperature and 1 atm of pressure. The activation and reaction energy came from a solar-simulator lamp. The details of this experiment, including product quantities, will be reported in FY88.

We also carried out other reactions using the same catalyst: the hydrogenolysis of ethane ($H_2 + C_2H_6 = 2CH_4$) and the hydrogenation of ethylene ($H_2 + C_2H_4 = C_2H_6$). However, the method we used to determine the product quantities was not sufficiently sensitive. These reactions are being repeated, and their products will be determined by gas chromatography, as was done for the CO-hydrogenation products.

In FY88, we plan to design and carry out experiments to determine the wavelength dependence and energy-transfer mechanism of reactions catalyzed by doped aerogels. We also plan to produce ThO_2 aerogels (both plain and doped with photoactive ions), characterize them spectroscopically, and use them to catalyze the reactions described above. Finally, we plan to experiment with a variety of dopants in SiO_2 and ThO_2 aerogels.

FY87, $142,000

Increasing the Nuclear Polarization Memory Time

Principal Investigator:
P. Clark Souers

We are working toward the nuclear-spin polarization of frozen deuterium-tritium (D–T) to make possible its use as a "super" fuel for inertial confinement fusion (ICF). We can achieve this only if the material has a long polarization memory time. Toward this end, we increased the triton memory time (longitudinal nuclear relaxation time) from 0.3 s to 7 s.

Nuclear-spin polarization of deuterium-tritium (D-T)—a state in which the nuclear magnetic moments are aligned parallel to each other—greatly increases the efficiency of using this material as a fuel for ICF. The cross section for fusion between polarized deuterium and tritium nuclei is expected to be 50% higher than the corresponding cross section for unpolarized nuclei (Kulsrud et al., 1982). Polarization must be carried out in solid D-T. This material is solid at temperatures from 1.4 to 4.2 K.

The memory time for spin polarization—the length of time polarization can be maintained—must be relatively long. But in regular D-T, which has a composition of 25% T_2, 50% DT, and 25% D_2, free molecular rotation shortens the triton's memory time to an unacceptable 0.3 s. If the material were nonradioactive HD, one could wait for natural catalysis to cause this time to increase, but the radioactivity from tritium constantly produces rotationally excited T_2 molecules. The deuteron does not cause the same problem because its smaller magnetic moment gives it a longer memory time. Thus the memory time of the triton is the major obstacle to spin polarization.

We found that the memory time of solid D-T can be manipulated by changing its composition. We produced a material consisting of 85 to 94 mol % molecular DT from the reaction of lithium tritide and deuterated methyl alcohol. When frozen to 5 K, the DT exhibited a memory time of 1 s. By adding normal H_2, we increased the memory time to 6 to 10 s (see the Figure).

Super-pure molecular DT is clearly the best form of D-T fuel for nuclear polarization. In the future, we will try to isolate this compound. The task may prove difficult because DT decomposes under tritium radioactivity with a $1/e$ time constant of 100 h. We will also continue our efforts to lengthen the triton's memory time. In addition, we plan to obtain and study electron spin resonance data to determine the mechanism of nuclear spin polarization in DT, with the ultimate goal of building a polarization facility.

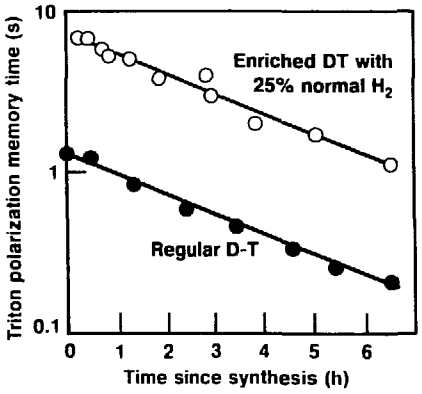

The triton polarization memory time increases twentyfold in enriched molecular DT with normal H_2 added. This result shows the feasibility of changing the memory time by proper synthesis of the sample. The decrease with time is due to radiation-induced catalysis of the rotationally excited H_2 in the sample.

References

Kulsrud, K. M., H. P. Furth, E. J. Valeo, and M. Goldhaber (1982), "Fusion Reactor Plasmas with Polarized Nuclei," *Phys. Rev. Lett.* **49**, 1248.

Souers, P. C., E. M. Fearon, E. R. Mapoles, J. R. Gaines, J. D. Sater, and P. A. Fedders (1986), "Nuclear Spin Polarization of Solid Deuterium-Tritium," *J. Vac. Sci. Technol. A* **4**, 1118.

Nuclear Magnetic Resonance Imaging

Principal Investigator:
Raymond L. Ward
Co-Investigators:
Alvin S. Maddux, Jr.,
Walter G. Boyle, Jr.,
Philip E. Harben, Wendy L. Swan,
James A. Happe, and Todd Felver[a]

[a]Sandia National Laboratories,
Livermore, Calif.

Nuclear magnetic resonance (NMR) imaging is a nondestructive technique used to characterize materials. By building magnetic field gradients into standard NMR pulse experiments, we have been able to obtain two-dimensional proton-spin-density maps with resolution approaching 100 μm. We have also made progress in obtaining slice images through materials. One of our major achievements in FY87 was to determine the homogeneity of a low-density, solid foam by imaging the distribution of mobile fluids loaded into the foam.

One objective of our research was to explore NMR imaging as a method for determining the homogeneity of polymers—in particular, low-density foams. To do this work, we began modification of an NMR spectrometer that was made available to us by Sandia National Laboratories, Livermore, Calif. Most of this modification is complete, but our slice-selection and data presentation capabilities need improvement.

Slice selection—the ability to choose a slice through a material to image—is critical in improving image resolution. Without it, the resolution of our x-y images would be limited by the sample size in the z direction. (That is, all spatial information along the z axis would be integrated into the image, regardless of the sample size. If the sample were too large, resolution would suffer.) We worked on two promising techniques for slice selection: rf modulation and multipulse excitation.

Using the first technique, we shaped rf pulses by modulating the rf with the sinc function

$$\frac{\sin x}{x} ,$$

where $x = t/T$ and $T = 2/G_z D_z$. G_z is the gradient field strength in the z direction, D_z is the slice thickness, and t is one-half the width of the sinc pulse, limited to the first zero crossing. This modulation scheme yields a uniform, rectangular, frequency-domain slice.

The multipulse excitation technique employs a Dante sequence—a series of short rf pulses. Using this technique, we produced selective excitation of resonances by alternating delays with rf pulse nutation.

To improve the presentation of our NMR images, we focused on the data accumulation time. Image contrast improves as the data accumulation time is increased and as signals are averaged over these longer periods. Yet because NMR imaging is a technique that might be used in a high-production environment, it is important to keep the time as short as possible. The best resolution reported in the literature was 10 to 13 μm for a slice thickness of 220 μm and four slices per experiment. On the same type of equipment, we obtained 20-μm resolution and reasonable contrast with 15 min of data accumulation. By increasing the data-accumulation time to 1 h, we obtained excellent contrast.

We determined the homogeneity of two polymeric foams—polystyrene and TPX (poly-4-methylpentene-1)—both of which have application in LLNL programs. Our method was to load the solid materials with a mobile fluid by a vacuum technique and then image the fluid distribution. It is important that the imaged nuclei be mobile so that narrow resonances are produced. With current imaging techniques, it is not possible to image solid material directly because of inherently very broad line widths (>1 kHz).

We used water mixed with a small amount of surfactant to enable the fluid to penetrate the hydrophobic polymers without modifying them. NMR imaging showed that the two foams take up different amounts of water and surfactant. Furthermore, it revealed local imperfections in supposedly high-quality preparations of both materials. The NMR images also revealed that a technique used for preparing large amounts of polystyrene—freeze-drying the polymer from a cyclohexane-dioxane mixture—produced nonhomogeneous material. Polystyrene prepared in this way took up the loading solution in a highly anisotropic manner. Electron microscope studies confirmed the separation of the foam into two morphological types. Later, it was determined that the cyclohexane-dioxane mixture separated into two phases during the freeze-drying process, thereby producing the nonhomogeneous foam.

Computation

Overview

Robert R. Borchers
James R. McGraw

Our IR&D program for FY87 focused on two critical areas of research: the effective use of multiprocessor computing systems and the development of expert systems technology. Our greatest challenge for using new supercomputer systems is to develop cost-effective ways for multiple processors to cooperate in executing the largest possible computer codes. Such cooperation is difficult for the four-processor machines we have now, and machines with many more processors will soon be available. Our emphasis on expert systems, or more properly "knowledge engineering," stems from our belief that this technology can dramatically affect the quality and robustness of future software systems.

Three of our IR&D projects studied multiprocessing. Our work on multitasking algorithms for the Cray-2 produced a variety of experimental codes that run in a highly parallel mode, including one that has achieved a speed of 1.1 gigaflops (one billion floating-point operations per second). This work also helped us evaluate how to utilize the Cray-2 and instruct users on ways to make the transition to this system. Over the last three years, work on this project has yielded 22 publications related to putting application codes on a multiprocessor. Our work on SISAL (Streams and Iteration in a Single Assignment Language), a programming language, is a long-range research effort to simplify the interface programmers would use to write parallel programs. With our collaborators, we have produced prototype compilers for a variety of parallel machines. Also, our SISAL software has been adopted by over 20 national and international research groups. Our work on Cerberus, a shared-memory multiprocessor simulation project, has resulted in a simulator system that can analyze the performance of shared-memory, vector multiprocessors down to the level of individual memory accesses. It has also helped us study potential tools for mapping existing programs onto multiprocessors.

Two of our IR&D projects were directed toward evaluating knowledge engineering techniques. In our work on partial differential equations (PDEs), we have investigated ways to automatically transform specific physics equations into programs that can solve these equations. Significant progress has been made in developing our approach to representing knowledge in a form that will allow the necessary equation manipulations to take place. In our second project, a joint venture with the University of Georgia, we have been studying the potential of expert systems to make decisions for classifying electrochemical mechanisms. This work will give us insight into an expert system's ability to adjust its decisions based on continually revised information.

Overall, the Computation Department received $1,084,000 in IR&D funds for FY87.

Multiprocessing Algorithms for the Cray-2

Principal Investigators:
David V. Anderson,
Alice E. Koniges, and
Arthur A. Mirin

The goal of this project is to develop efficient numerical techniques for solving large-scale computational physics problems on multiprocessor computers. This involves modifying existing algorithms and developing new multitasking ones. Because computationally challenging problems are common in the field of plasma modeling, plasma physics problems provide an ideal test bed for our research.

Mainframe computers designed during the next decade or so will be multiprocessors. Thus, efficient multitasking techniques will be indispensable for large-scale scientific computing. We are developing schemes to enlarge the scope and size of problems that can be solved on large multiprocessors while simultaneously improving computational efficiency. Our results are applicable to computer configurations that range from the two- and four-processor machines now available to future systems with perhaps hundreds of proce sors. Our studies concentrate on five areas of research:

- General multitasking techniques.
- Iterative and direct matrix solvers.
- Particle simulation codes.
- Plasma turbulence modeling.
- Plasma magnetohydrodynamics (MHD) codes.

Several of our physics codes serve as test beds for studying multitasking techniques. Part of our effort has been to determine whether existing codes can be multitasked without excessive rewriting. Another part addresses the costs and benefits of implementing multitasking: these depend on the tasks' granularity (how long they can work without interacting with other tasks), on the system scheduler, and on the charging algorithm.

Our work on matrix solvers has concentrated on developing routines that exploit the newest capabilities of the Cray computers: indirect vectorization and multitasking. We have written several iterative matrix-solver packages based on conjugate gradient methods. These codes are now available to our users. In related work, a physics problem required a direct, as opposed to iterative, solver. We decided to use cyclic reduction for this problem because this method lends itself to multitasking. The resulting code has proved remarkably successful, yielding speeds in excess of a gigaflop on the Cray-2. The code is being used by several institutions to compare the speeds of various supercomputers.

From our work on three-dimensional particle-simulation codes, we have developed a model that exploits new hardware and software features of the Cray-2, such as its four processors and vector-indirection capability. The memory-fetch and vector-arithmetic operation times of the Cray-2 show that it is well-matched to the requirements of such codes. This match results from the Cray's large memory, which obviates the need for disk storage, and from its hardware vectorizing of constructs such as A(I(J)), which use indirect indices.

For one application of our plasma turbulence modeling, we had to simulate the dynamics governing drift waves. To solve this problem effectively in a multitasking environment, we used the concept of ensemble averaging, which naturally consists of independent events. A spinoff of this study has been research into developing pseudorandom number generators for multiprocessors. We have introduced a technique that provides reproducible, independent strings of pseudorandom numbers.

Our final research area involves the parallelization of evolutionary MHD calculations. A three-dimensional, resistive MHD code has been restructured to make use of multitasking. Because this program is representative of many codes that solve coupled systems of partial differential equations (PDEs) on a fixed grid, results should be applicable to a wide variety of disciplines. The remainder of this article describes our FY87 research in more detail.

General Multitasking Techniques. Six of our major codes now implement multitasking. The most recently converted code is our three-dimensional, evolutionary MHD code, TEMCO. It has been used to study multitasking performance as a function of task size and code field length. We have found that the Cray time-sharing system scheduler allows good overlap, provided the code is large and the task string (i.e., the set

of tasks available to run consecutively on a processor) is of medium-to-large granularity. We also created a theoretical model of a scheduler designed to predict multitasking performance (i.e., the degree of overlap). This model shows, for example, that on the Cray-2, assuming it takes 6 ms to obtain a second processor, a multitasking job must have a field length of at least 10.6 million words if an overlap factor of 3.5 (out of a maximum of 4) is to be attained. Even then the typical task must be over 1 s long. A contour plot of overlap as a function of job size and task length is shown in the Figure. The results of TEMCO agree well with the predictions of this model.

Studies using the turbulence code SIMU indicate that the degree of overlap is not significantly enhanced by having a larger number of tasks ready to run. One might think that partitioning work into many smaller tasks would improve performance by load balancing. Instead, having too many outstanding tasks ready to run can lead to extremely high memory charges.

Iterative Matrix Solvers. In many plasma physics problems, the implicit solution techniques used to solve the governing equations give rise to systems of linear equations whose matrix operator is sparse, with a distinctive pattern. While there are several iterative matrix-solution packages available for sparse matrices, their generality makes them too slow to be used in production physics codes. Therefore we have written several matrix packages that encompass a variety of common sparsity patterns while retaining the speed available from vectorization and multitasking.

The solution technique used in these packages for asymmetric matrices is either the conjugate gradient method applied to the normal equations (obtained by multiplying the linear system by the transpose of the operator matrix) or the biconjugate gradient (BCG) method. In both cases, we precondition the matrix using an incomplete LU decomposition. The choice of techniques for solving the matrices arose partially from a study conducted with ITPACK software from the University of Texas. Using ITPACK as a tool, we determined that many of our applications problems are ill-conditioned and thus require a robust preconditioning method. The incomplete LU decomposition, although notoriously hard to vectorize, is one of the most effective preconditioners known.

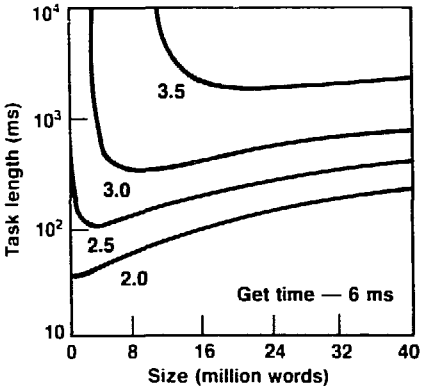

Contour plot of processor overlap for four equal tasks as a function of job size and task length, as predicted by our theoretical model (a 6-ms get time is assumed).

Vectorizing and multitasking the iterative solvers is accomplished at three different levels. At the lowest level, we use storage by diagonals to allow for direct vectorization of many of the operations. At the middle level, we use indirect vectorization (gather/scatter) when possible. This allows us to bring recursions to an outer loop while using indirect vectorization of the inner products in the innermost loop. The highest level consists of multitasking the recursive backsolve operations in the BCG method. We have created a library of these routines that includes solvers for single and coupled PDEs in two and three dimensions.

Direct Matrix Solvers. Our parallelized matrix solver (PAMS) code originated from a plasma physics equilibrium and stability calculation, but it is applicable to solving many parabolic and elliptic PDEs that arise in scientific and engineering disciplines. Typically, the equations are discretized by using spectral basis functions in two coordinates and finite elements or differences in the third. We have used three kinds of parallelization—functional unit overlap within a central processing unit (CPU), vectorization, and multitasking—to produce a very fast, executable code. Sustained speeds of 1.28 gigaflops (measured over intervals exceeding 10 CPUs) have been recorded. Improvements during the past year have allowed overall speeds of 1.1 gigaflops. PAMS is currently the fastest Cray-2 applications code running.

Plasma Turbulence Modeling. Our multitasked simulation code, SIMU, uses the concept of ensemble averaging to solve a prototypical, three-wave interaction problem. The use of ensemble averaging, as opposed to time averaging, turns the problem into an ideal candidate for multitasking. Because realizations of the dynamical equation can be grouped into arbitrarily sized packets, the multitasking nature of the code can be adapted for machines with an arbitrary number of processors—from four to four thousand.

To run SIMU and guarantee reproducible results independent of the multitasking, we need a means of

producing strings of pseudorandom numbers for each process. This problem is very important in all Monte Carlo calculations run on multiprocessor computers. We have devised a method for producing independent strings based on hopping through a pseudorandom number sequence at large intervals and picking a starting point for each process. This method is particularly useful for our application and shows promise for use in general Monte Carlo codes.

MHD Stability Calculations. The three-dimensional, resistive MHD code TEMCO has been restructured to use the multitasking capability of the Cray-2. Virtually all sections of the main time loop have been rewritten. In the process of rewriting, we compared CFT and CIVIC, two optimizing Fortran compilers, vis-a-vis vectorization. Most key areas of the time-integration module have been multitasked, including the coefficient computation, leapfrog advance, and implicit advance. As stated earlier, our analysis of multitasking efficiency and cost showed that from an algorithmic standpoint, good theoretical CPU overlap is attainable, but that actual multiprocessing efficiency is limited by the system scheduler. Because TEMCO is somewhat representative of many codes that solve coupled systems of PDEs on a fixed grid, results from this study should be applicable to a wide variety of physics models.

References

Anderson, D. V., A. R. Fry, R. Gruber, and A. Roy (1987), *Gigaflop Speed Algorithm for the Direct Solution of Large Block-Tridiagonal Systems in 3D Physics Applications*, Lawrence Livermore National Laboratory, Livermore, Calif., UCRL-96034; submitted to *J. Parallel Comput.*

Anderson, D. V., A. R. Fry, R. Gruber, and A. Roy (1987), "Plasma Physics at Gigaflops on the CRAY–2," 3rd Symposium on Science and Engineering on Cray Supercomputers, Minneapolis, Minn., September 9-11; Lawrence Livermore National Laboratory, Livermore, Calif., UCRL-96572.

Anderson, D. V., A. E. Koniges, and D. E. Shumaker (1987), *CPDES2: A Preconditioned Conjugate Gradient Solver for Linear Asymmetric Matrix Equations Arising from Coupled Partial Differential Equations in Two Dimensions*, Lawrence Livermore National Laboratory, Livermore, Calif., UCRL-96617; submitted to *Comput. Phys. Commun.*

Anderson, D. V., A. E. Koniges, and D. E. Shumaker (1987), *CPDES3: A Preconditioned Conjugate Gradient Solver for Linear Asymmetric Matrix Equations Arising from Coupled Partial Differential Equations in Three Dimensions*, Lawrence Livermore National Laboratory, Livermore, Calif., UCRL-96618; submitted to *Comput. Phys. Commun.*

Koniges, A. E. and D. V. Anderson (1987), "ILUBCG2: A Preconditioned Biconjugate Gradient Routine for the Solution of Linear Asymmetric Matrix Equations Arising from a 9-Point Discretization," *Comput. Phys. Commun.* **43**(2), 297.

Koniges, A. E. and D. V. Anderson (1987), "Vectorized and Multitasked Software Packages for Solving Asymmetric Matrix Equations," *Computer Methods for Partial Differential Equations VI*, R. Vichnevetsky and R. S. Stepleman, Eds. (Prentice-Hall, Englewood Cliffs, N.J.).

Koniges, A. E. and C. E. Leith (1987), *Parallel Processing of Random Number Generator for Monte Carlo Turbulence Simulation*, Lawrence Livermore National Laboratory, Livermore, Calif., UCRL-97474.

Mirin, A. A. (1987), *Predicting Multiprocessing Efficiency on the Cray Multiprocessors in a Time Sharing Environment/Application to a 3-D Magnetohydrodynamics Code*, Lawrence Livermore National Laboratory, Livermore, Calif., UCRL-97580.

FY87 $139,000

Cerberus: A Shared-Memory Multiprocessor Simulation Project

We have developed a simulation system to study architectural and software issues for shared-memory multiprocessors with up to 256 CPUs. Two of the issues investigated were hot spots and barrier synchronization.

Principal Investigators:
Eugene D. Brooks III,
Timothy S. Axelrod, and
Gregory A. Darmohray

The goal of the Cerberus project is to learn how to use hundreds of pipelined processors (each of supercomputer class) in a tightly coupled, shared-memory multiprocessor system. Both architectural and software issues are being examined. For this work, we have developed a multiprocessor simulation system, which is composed of a simulator for the scalable supercomputer architecture along with complete compiler and runtime support (Brooks et al., 1987). Development of the simulator was completed this year, and we have used the system to study hot spots in our multiprocessor architecture and parallel implementation of Gaussian linear-system solvers (Darmohray and Brooks, 1987).

In general terms, hot spots are bottlenecks that result when a number of multitasking algorithms all need to use the same page of memory at roughly the same time. We have found that hot spots will not be a severe problem for near-term multiprocessor systems. Although they have a time penalty that grows linearly with the number of processors, pipelining (or vectorizing) access to the hot spot will postpone serious impact on performance until hundreds of processors are involved.

In our study of parallel Gaussian solvers for linear systems, we examined both Gauss and Gauss-Jordan elimination without pivoting, comparing software and hardware support for barrier synchronization (Brooks, 1986). In the case of Gauss elimination, we found that for the smallest matrix (32 × 32), the hardware barrier has the greatest impact on performance, providing a speedup of 9.4 for 32 processors. This compares with a speedup of 4.9 for the software barrier, a speedup that changed little as we went from 16 to 32 processors. As the matrix size increases, however, the ratio of real work done to synchronization cost also increases, resulting in good speedups even for the software barrier.

For our largest matrix (128 × 128), the speedup of Gauss elimination with the hardware barrier is a little over 20 for 32 processors; with the software barrier, it is about 18. For 64 processors, the speedups are 30 and 20, respectively, with the speedup curve flattening out for the software barrier. Thus, if we want good parallel performance for a long-running job that iterates repetitively on small matrices, a hardware barrier will be needed. If the matrices are large, however, a software algorithm will be fast enough.

References

Brooks, E. D. (1986), "The Butterfly Barrier," *International J. Parallel Programming* **15**(4), 295.

Brooks, E. D., T. S. Axelrod, and G. A. Darmohray (October 1987), "The Cerberus Multiprocessor Simulator," Third SIAM Conference on Parallel Processing, Society for Industrial and Applied Mathematics, Los Angeles, Calif.

Darmohray, G. A. and E. D. Brooks (October 1987), "Gaussian Techniques on Shared Memory Multiprocessor Computers," Third SIAM Conference on Parallel Processing, Society for Industrial and Applied Mathematics, Los Angeles, Calif.

FY87 $239,000

Design and Development of SISAL

Principal Investigators:
Stephen K. Skedzielewski,
John T. Feo,
Rodney R. Oldehoeft, and
James R. McGraw

We are developing a general purpose language, SISAL, along with associated compiler techniques and runtime systems for executing programs on multiprocessor computers. Our efforts are focused on the large-scale numerical computations typically written at LLNL. In FY87, we extended SISAL's definition, revised and extended its intermediate form to include vectorization and preallocation of memory, and developed a runtime system that allows us to run SISAL on a variety of multiprocessor systems in native mode.

We are designing and implementing a high-level, functional language for a variety of parallel and vector processors. This language, SISAL (Streams and Iteration in a Single Assignment Language), is free of side effects and deadlock, and guarantees determinate results (McGraw et al., 1985). All parallelism is implicit in the semantics of the language. Users do not explicitly divide a task into subtasks and assign them to processors; this is done automatically by the compiler and the runtime system.

The SISAL project is a joint study in language and compiler design for multiprocessors. Much of the compiler analysis is done on an intermediate form called IF1 (Skedzielewski and Glauert, 1985) and on its extension IF2 (Welcome et al., 1986). These forms are machine-independent, lower-level, graphical representations of programs. They are well-suited for use by code optimizers (i.e., algorithms that restructure programs to make them run faster) within compilers. IF1 handles most common optimizations, such as common subexpression removal and loop invariance. IF2 addresses the memory management problems inherent in functional languages.

A goal of our project is to extend the research in functional languages into academia and industry. We work closely with groups at Colorado State University, the University of Manchester in England, and Digital Equipment Corporation. Each is developing a compiler for a different machine. Researchers at Carnegie-Mellon University have translated SISAL to W2, the programming language of the WARP systolic array computer, while researchers at the University of Southern California have translated IF1 to Occam, the machine language of the INMOS Transputer. Scientists at Stanford University use SISAL and IF1 to simulate multiprocessor performance for several theoretical models of multiprocessors (Sarkar, 1987). TRW and RCA Laboratories are considering using SISAL to program their new research machines.

During the past year we progressed in language research, compiler development, and interpreter improvements. We proposed three changes to the SISAL language: array definitions, higher order functions, and modules. The first two changes will allow SISAL programmers to write cleaner and more abstract codes. The third will allow us to use existing Fortran libraries.

IF1 language research is driven by the need for sophisticated code optimizers in SISAL. The intermediate form underwent its first major revision this year since its release in 1985. We included vectorizers and simplified the representation of iteration nodes from two forms to one. A student at the University of California, Davis (at Livermore), completed the design of an IF1 code optimizer that eliminates much unnecessary array copying by preallocating memory for composite data structures. A second student studied the ways that intermediate results can be saved and reused. This

work has applications in program development, debugging, and graphic systems.

We began research to map SISAL programs to models of parallel processors. How to assign the tasks of a parallel process to the resources of a parallel system is a fundamental problem facing the proponents of parallel processing. A graduate student at Stanford used our SISAL compiler and IF1 interpreter to simulate the execution of SISAL programs on a theoretical multiprocessor. His work is being used as the basis of a new project started this year to evaluate the architecture and performance of a variety of parallel processors.

We improved the interpreter for SISAL programs. It runs considerably faster and has new debugging features. We added vector operations and included a memory caching method.

Our most important accomplishment is the production of the first SISAL compilers for actual machines. With our collaborators at Colorado State University, we wrote a translator that accepts IF1 files and produces C programs; we also developed a runtime library that supports parallel processing on multiple machines. We successfully ported our system to a number of computers, including a Sequent Balance, multi-VAX, Cray-X/MP, SUN workstation, Encore, and Alliant. While the compiler and runtime systems are still immature, they do support the development and evaluation of parallel applications. We are finally able to run SISAL codes in native mode on truly parallel systems.

References

Feo, J. T. (1987). *The Livermore Loops in SISAL*, Lawrence Livermore National Laboratory, Livermore, Calif., UCID-22159.

McGraw, J. R., S. Skedzielewski, S. Allen, R. Oldehoeft, J. Glauert, C. Kirkham, W. Noyce, and R. Thomas (1985). *SISAL: Streams and Iteration in a Single Assignment Language, Language Reference Manual, Version 1.2*, Lawrence Livermore National Laboratory, Livermore, Calif., M-146, Rev. 1.

Oldehoeft, R. R. and D. C. Cann (1987). *Applicative Parallelism—Potential and Challenge*, Lawrence Livermore National Laboratory, Livermore, Calif., UCRL-96781; to be presented at the Hawaii International Conference on Systems Sciences, Kailua-Kone, Hawaii, January 1988.

Oldehoeft, R. R. and J. R. McGraw, *Mixed Applicative and Imperative Programs*, Lawrence Livermore National Laboratory, Livermore, Calif., UCRL-96244; submitted to *J. Parallel and Distributed Computing*.

Ranelletti, J. (1987). *Graph Transformation Algorithms for Array Memory Optimization in Applicative Languages*, Ph.D. dissertation, University of California, Davis.

Sarkar, V. (1987). *Partitioning and Scheduling Parallel Programs for Execution on Multiprocessors*, Stanford University, Computer Systems Laboratory, Stanford, Calif., CSL-TR-87-328.

Skedzielewski, S. K. and J. Glauert (1985). *IF1: An Intermediate Form for Applicative Languages*, Lawrence Livermore National Laboratory, Livermore, Calif., M-170.

Skedzielewski, S. K., R. K. Yates, and R. R. Oldehoeft, "DI, an Interactive Debugging Interpreter for Applicative Languages," *Proc. SIGPLAN'87 Symposium on Interpreters and Interpretive Techniques*, p. 102; also published in *SIGPLAN Notices* **22**(7), 102.

Welcome, M., S. K. Skedzielewski, R. K. Yates, and J. Ranelletti (1986). *IF2: An Applicative Language Intermediate Form with Explicit Memory Management*, Lawrence Livermore National Laboratory, Livermore, Calif., M-195.

FY87: $372,000
FY88: $285,000

Automatic Programming System for Solving Partial Differential Equations

We are creating an automatic programming system for physics problems that are based on partial differential equations derived from conservation laws. Our principal effort this past year went into developing a series of knowledge representation schemes that will provide the basis for implementing such a system.

Principal Investigators:
David Balaban, Joe Garbarini, and Kevin Olwell

The primary objective of this project is to develop an automatic programming system that will take as input a natural, two-dimensional, interactive mathematical specification of a partial-differential-equation (PDE) physics problem and produce an efficient program for computing an accurate numerical approximation of the solution. To achieve this objective, we have chosen to begin by developing a knowledge representation scheme (KRS). This KRS is an integrated, abstract model for all aspects of the automatic programming system. The rigor provided by this model will make it possible to isolate and solve critical research problems.

Because the project's scope is very large, we have narrowed our focus to physics problems based on PDEs derived from conservation laws. We then limited this work to a few specific problems from two classes of problems. The first class consists of traditional linear and nonlinear problems that do not have discontinuities (shocks). These problems are simple enough to allow us to systematically develop and test KRSs and yet complex enough to be useful in a number of engineering applications. We have selected three specific problems to work on: a one-dimensional diffusion equation, a one-dimensional wave equation, and a three-dimensional heat equation. The second class consists of compressible fluid-flow problems that involve discontinuities. These problems have both greater applicability and greater intrinsic difficulty. From this class, we have selected the one- and two-dimensional Euler equations.

The development of an automatic programming system to handle these problems is a highly interdisciplinary effort. It requires expertise in mathematical physics, PDEs, knowledge formalization, and advanced artificial-intelligence-based software implementation. It also requires extensive collaboration with researchers outside LLNL. We are working with researchers at Rutgers University; the University of Houston; Murray State University; Clarkson University; Vanderbilt University; the University of California, Berkeley; MathSoft, Inc.; and Tektronix, Inc.

Our automated programming system has declarative and procedural components. The declarative component is the system's overall KRS, which contains information about static data structures and how these structures relate. This KRS is partitioned into five parts, each of which is itself a KRS. The procedural component contains data transformations.

Figure 1 shows the processes and KRSs into which the automatic programming system is partitioned. The boxes represent knowledge bases, computer implementations of the KRSs. The circles represent processes, computer implementations of the procedural pieces into which the automatic programming system is partitioned. Lines with arrows at both ends represent the flow of information to and from knowledge bases. Lines with arrows at one end represent the flow of information from the user to the system, between processes in the system, and from the system to a computer that will run the generated code.

As stated, the system's declarative component is actually five separate KRSs. The first KRS is an unambiguous foundation upon which the other KRSs are built. These other four schemes contain the knowledge required to relate concepts at different levels. The initial levels are problem oriented; the final levels are code oriented.

The system's procedural component reflects the sequence of events that must take place when any numerical simulation is built up. As numbered in Figure 1, these events are:

0. Interact with the user: This process accepts user input of mathematical expressions in standard two-dimensional form as they would be written down on paper. The process removes any ambiguities from this input and passes it to other processes.

1. Get domain and partitioning

information: This process interactively accepts a graphical specification of the spatial and temporal problem domain and the way it is to be broken up for purposes of discretization. It produces a mathematical representation of this information.
2. Get continuous physics information: This process interactively accepts a specification of the problem in terms of differential equations and their constituent conservation laws. It produces a mathematical representation of this nondiscrete problem specification.
3. Determine discrete system of equations: This process transforms the problem's nondiscrete mathematical representation into a discrete approximation of the problem. Additional inputs may be required, depending on the class of problems being solved.
4. Determine solution scheme: This process transforms the problem's discrete approximation into a solution scheme that is amenable to computer implementation. It determines whether explicit or implicit solution schemes are to be used and computes matrix formulations of aspects of the solution (such as the Jacobian) if necessary.
5. Generate code: This process takes the solution scheme and generates the code. It is desirable to use specialized, high-level languages such as FIDIL (a finite-difference language extension to Fortran) in this process.

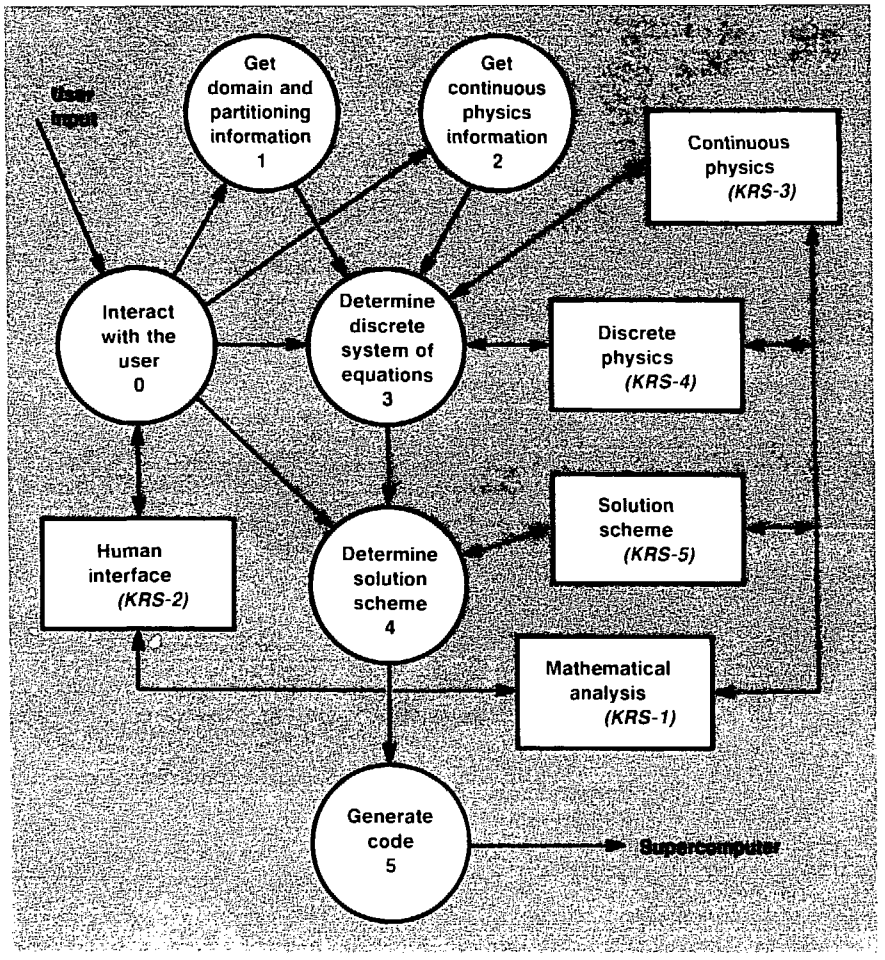

Fig. 1. Processes (circles) and KRSs (squares) of our automated programming system. The processes are numbered in sequence. The mathematical analysis KRS is the basis for the other four KRSs.

Some effort this year went into developing the human interface (process 0). After a study of existing human interface systems, we decided to use the commercially available MathStation (by MathSoft, Inc.) rather than develop our own system.

Our major effort went into developing KRSs that are powerful enough to handle the one-dimensional diffusion problem. Significant progress was made on the continuous physics, discrete physics, and mathematical analysis KRSs. Although the first two KRSs have not yet been implemented as knowledge bases, the progress made on them should make their implementation easy once the mathematical analysis KRS is completed.

The mathematical analysis KRS must be powerful enough to represent the mathematics required by the other KRSs in the automatic programming system. This knowledge base has an applicative structure: Its internal system has no variables or expressions, and it is based on a formalism derived from differential geometry, the language FP, and Bourbaki. This formalism contains none of the ambiguities inherent in conventional mathematical notation. The mathematical analysis KRS contains the underlying structures for an entire symbolic manipulation system that focuses on mathematical analysis as opposed to algebra. It properly handles functions and operators, which is not true of existing symbolic manipulation systems.

Table Examples of physics problems and their division into the four variables of our continuous physics KRS.

Physical problem	Observable	Density	Current	Source
Heat conduction	Temperature	Energy density	Heat flux	Heat sources
Elastic deformation	Displacement	Momentum density	Stress	External force
Fluid flow	Fluid density and velocity	Mass and momentum density	Flow rate and stress	Fluid sources and pressure gradient
Flow through porous media	Pressure	Mass density	Flow rate	Fluid sources
Electrodynamics	Potentials	Electric flux	Field tensor	Electric charge and current

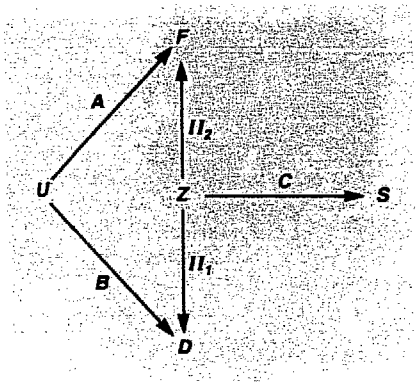

Fig. 2. The PDE relational diagram. Objects are function spaces representing observables *U*, densities *D*, sources *S*, space currents *F*, and space-time currents *Z*. Mappings are current relation *A*, density relation *B*, conservation law *C*, and standard projection operators Π_1 and Π_2.

The continuous physics KRS is a uniform framework for physics problems that have a continuous model based on conservation principles. The framework is based on three fundamental relations between observables, densities, currents, and sources. By viewing densities and currents as a space-time current, we can use the conservation law to relate densities, currents, and sources. A large number of physics problems may be viewed in this way; the Table lists a few of them.

The three fundamental relations in our continuous physics KRS are:
- Current relation *A*, which relates currents to observables.
- Density relation *B*, which relates densities to observables.
- Conservation law *C*, which relates densities, currents, and sources.

These three fundamental relations define a PDE via relation composition. The sequence of relation compositions is determined by the diagram in Figure 2.

The objects in the diagram are function spaces that represent observables *U*, densities *D*, sources *S*, space currents *F*, and space-time currents [$Z = (D, F)$]. The mappings in the diagram are the current relation *A*, the density relation *B*, the conservation law *C*, and the standard projection operators Π_1 and Π_2. In terms of the pieces, the PDE relation is $C \circ (A \times B)$, where $\circ$ represents relation composition and $\times$ represents the Cartesian product of two relations. To keep the notation simple, Figure 2 does not represent the problem's boundary or initial conditions. These can be added via a relation between the space-time flux and a product of function spaces representing the two sets of conditions.

The discrete physics KRS provides a framework for defining a discrete system of equations. Specifying the approximations of space-time current integrals on space-time partitions allows us to generate the discrete system of equations corresponding to the PDE. Evaluating space-time current integrals over cell faces becomes a mechanical process when the KRS selects the appropriate interpolation functions for cell faces and uses the appropriate pieces of the continuous physics KRS.

In continuing our work in FY88, we have defined six primary tasks to be pursued. In order of priority, they are:
1. Refine the mathematical analysis KRS.
2. Begin implementing the human interface: Install MathStation, create the human interface KRS, and create processes 0, 1, and 2.
3. Develop the continuous and discrete physics KRSs and process 3 to the point that we can create discrete systems of equations for the one-dimensional diffusion and Euler equations, and then for the other three equations.
4. Begin experimentation with FIDIL.
5. Develop the solution scheme KRS and process 3 to the point that we can create discrete systems of equations for our specific problems in the same order as in task 3.
6. Use FIDIL to generate Cray Fortran programs with these solution schemes.

Reference

Balaban, D., J. Garbarini, K. Olwell, W. Greiman, and S. Shlaer (1987), "On the Relational Modeling of Discrete PDE Problems," *Proc. IMACS Conference on AI, Expert Systems, and Languages in Modeling and Simulation*, Barcelona, Spain, June 2-4 (North-Holland, Amsterdam, Netherlands).

Development of an Expert System to Automate Routine Experiments

Principal Investigators: Hal R. Brand and James Anderson[a]

[a]University of Georgia, Athens.

The objective of this project is to develop software techniques that can close the experiment–analysis loop required to solve many routine analysis problems in chemistry. During FY87, work centered on constructing a knowledge-based expert system capable of classifying electrochemical mechanisms using cyclic voltammetry.

The solution to many problems in chemistry and related fields requires that certain exploratory experiments be conducted. Analysis of these experiments then directs further experimentation and analysis. This repetitive experiment–analysis process continues until a satisfactory solution is obtained. Defining this kind of iterative process requires significant expertise in the problem itself. Accordingly, automation has focused on merely automating some of the steps involved (e.g., data acquisition, instrument control, and portions of the data processing). Our work focuses on automating the whole routine-analysis process with intelligent software.

Our approach has been to start with a somewhat easy, single case and then try to generalize from it. To this end, we have been working on closing the experiment–analysis loop in cyclic voltammetry (CV) using a knowledge representation scheme (KRS). We chose the classification of electrochemical mechanisms with CV as the routine-analysis problem because it can easily be simplified to permit reasonable progress while exhibiting many of the complications inherent in routine analyses. Later, we can increase the problem's complexity.

During FY87, we designed a prototype expert system for classifying electrochemical mechanisms and began work on a knowledge base that could design CV experiments. The expert system is built from two separate but interacting knowledge bases: the experiment assistant (EA) and the CV. The EA knowledge base acquires and stores information by querying the user about the proposed experiment and conditions (e.g., electrodes, cell geometry, and solution composition). It then establishes constraints on the experiment and measurements to ensure that only physically reasonable values of experimental parameters are selected.

The CV knowledge base contains the knowledge to analyze experimental results and to determine when new experiments are required and how to design them in cooperation with the EA knowledge base. It also stores the results and analysis of the experiments conducted. We hope that eventually the expert system will have a deep enough understanding of CV mechanisms that, based on this understanding and on the accumulated data, it can then postulate probable mechanisms about which it has no specific knowledge.

To support the expert system, numerical CV feature-extraction routines were designed and constructed. Before features can be extracted from the data, the data must first be smoothed and corrected for nonideal behavior. To this end, we have developed both Fourier and Savitzky-Golay quadratic smoothing routines to increase the signal-to-noise ratio. We have also developed routines capable of correcting experimental data for both background charging current and reverse peak diffusion.

Finally, we constructed a CV simulator to test the expert system. The simulator presently simulates both ideal and noisy cyclic voltammograms for three common mechanistic cases: simple electron transfer (E), a chemical step preceding the electron transfer (CE), and a chemical step following the electron transfer (EC). The simulator treats both oxidation and reduction reactions for each possible mechanistic case. It can also simulate many nonideal cell behaviors. To aid in using the simulator, a user-friendly, menu-oriented interface has been included.

References

Anderson, J. L., M. Volk, R. Gonsher, and H. R. Brand (1987), "An Expert System for Cyclic Voltammetric Experimentation," Pittsburgh Conference on Analytical Chemistry, New Orleans, La., February 1988.

Brand, H. R., J. L. Anderson, M. Volk, and R. Gonsher (1987), "Frames and Rules: Artificial Intelligence Concepts in the Analytical Laboratory Using a Knowledge-Based Expert System," Pittsburgh Conference on Analytical Chemistry, New Orleans, La., February 1988.

Earth Sciences

Overview

Larry Schwartz

The Earth Sciences Department uses IR&D funds to develop capabilities needed for LLNL or Department of Energy (DOE) programs, to test hypotheses and prove feasibilities before seeking major program funding, and to contribute to earth sciences disciplines in order to attract new staff members and promote collaboration with outstanding scientists at other institutions.

The Department provides support in the areas of geochemistry, geophysics, seismology, geological engineering, and hydrology to programs such as Nuclear Test Containment, Treaty Verification, Nuclear Waste Management, Fossil Energy, and Weapons Materials. We also have a research effort supported through the Office of Basic Energy Sciences.

In FY87, we completed the staffing for our fluid-flow project to calculate complex hydrologic and geochemical phenomena in fractured geologic formations. We increased by 25 times the computational efficiency of a hydrothermal flow code introduced last year and developed the capability to model the miscible transport of up to four chemical species. We determined aluminum hydrolysis constants at temperatures to 250°C from solubility measurements of the mineral boehmite. From these data, we will be able to calculate better values for aqueous aluminum speciation and solubility in natural systems. In our project to build in situ sensors for high-temperature, high-pressure environments, we made long-distance (>500 ft) fiber-optic measurements of the temperature optrode. By pushing the capability of our diamond anvil cell to a new pressure record for a condensed gas—over 2 Mbar—we determined that xenon does not metallize, as predicted theoretically. We developed new procedures for fabricating dense, long rods of starting material in crystal-growth experiments on materials that constitute the deep interior of the earth's mantle. We developed a new algorithm for inverting seismic travel time data in complicated media with strong ray bending to increase our seismic imaging capability. We identified softening and agglomeration of coal as the major impediment to developing a good process for producing gasoline by pyrolysis of bituminous coal and initiated a series of laboratory experiments to learn why coal softens. Finally, our discovery of thermophilic microorganisms in geothermal wells could lead to new biotechnology applications.

In FY88, we will complete our work on hydrologic flow code capabilities, optrodes, crystal growth, and biotechnology. We will study crustal evolution in Northern California, begin a novel geochemical technique to infer pH in situ, and develop a facility for large-volume, high-pressure experimentation.

Overall, the Earth Sciences Department received $1,196,000 in IR&D funds for FY87.

FY87: $308,000
FY88: $200,000

Fluid Flow and Transport Modeling

Principal Investigators:
Thomas A. Buscheck,
Richard B. Knapp, John J. Nitao,
and Andrew F. B. Tompson

Applications in the areas of nuclear waste isolation, enhanced hydrocarbon recovery, geothermal energy, and groundwater contamination require significant advancements in modeling flow and transport in fractured heterogeneous porous media. We implemented simple reactive chemical transport in an existing hydrothermal flow code and addressed nonequilibrium fluid-rock geochemical interaction. We began code development on a general flow and transport simulator and a particle-tracking solute-transport model. With the addition of two more investigators in FY87, we broadened the scope of the project to include numerical-code design, theoretical development, and related experimental investigations.

Many LLNL and DOE programs apply porous-media flow and transport models in nuclear waste isolation, enhanced hydrocarbon recovery, geothermal energy, and groundwater contamination. The success of these models requires significant advancements in our conceptual understanding of the relevant physical processes as well as the continued development of numerical techniques and modeling philosophies to solve the corresponding mathematical statements. Many anticipated model applications involve complex, interacting physicochemical phenomena that occur in a variety of subsurface environments, including uniform, heterogeneous, and fractured porous media. Flow of multiphase liquids and gases, transport of various reactive chemical species in these phases, and transport of energy are among the phenomena of interest.

The ability to simulate simple flow and transport processes in uniform porous media has existed for years. However, the nature and complexity of many problems recently encountered strain our understanding of the physical behavior of these systems as well as the data and numerical techniques required in simulating them. Consequently, improved conceptual and mathematical models must be developed. Numerical-solution methods must be refined and improved not only to treat the new and diverse equation structures but also to develop more efficient and practical tools capable of addressing large, complex problems. In addition, improved mathematical models and simulators will ultimately require carefully designed and conducted experiments in order to calibrate their constitutive equations and to provide a basis for model validation. With two additional investigators in FY87, we broadened the scope of our project to include a balance of efforts in numerical-code design, in improved theoretical developments, and in experimental investigations for the calibration and validation of models.

Among our accomplishments in FY87 was the enhancement of LLNL's version of the TOUGH hydrothermal flow code (Preuss, 1985). Figures 1 and 2 apply to a study in which TOUGH simulated hydrothermal flow around a nuclear waste canister in an underground repository. We also incorporated the miscible transport of four chemical species in the aqueous phase. We verified the implementation of the chemical transport equation in a one-dimensional, nonreactive chemical transport problem and found mass conservation to be excellent. We added simple reactive transport to the code, using silica transport as a prototype example. Reactive silica transport was based on silica-water equilibria data (Rimstidt, 1979). The model allows for accompanying changes in the permeability, based upon an empirical permeability-versus-porosity relation.

We began modeling the reactive transport of multiple chemical species, including irreversible as well as reversible reactions. The chemical components in both the aqueous and solid phases may interact in a nonlinear fashion. Accomplishments for FY87 include initiating development of governing equations by volume-averaging techniques; importing an existing code, MTRANS, which treats the

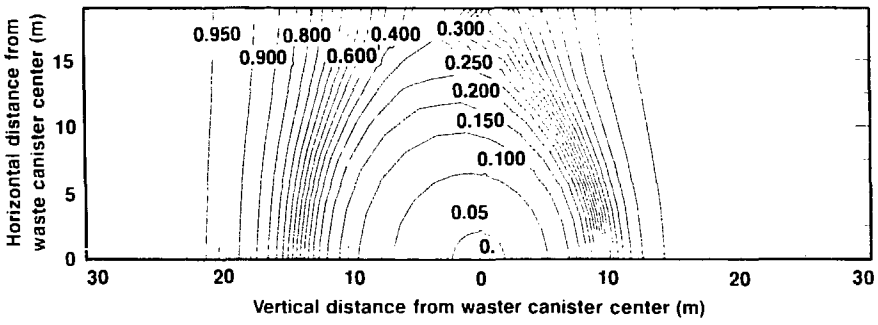

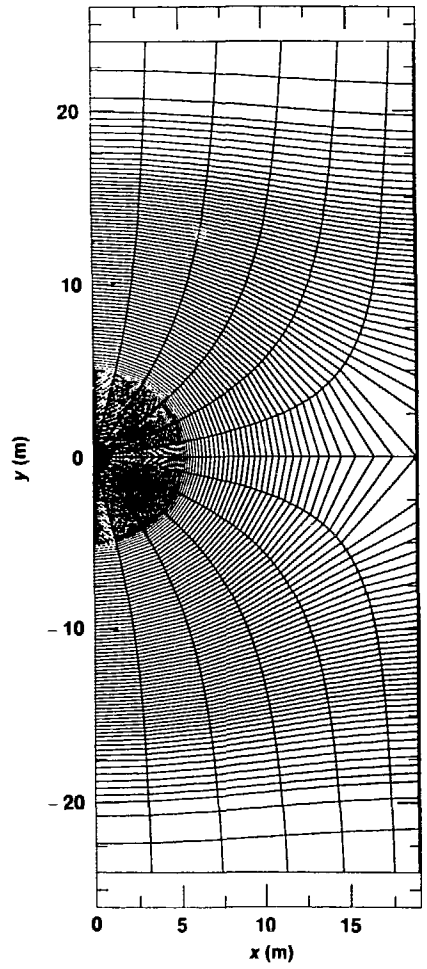

Fig. 1 (*Top*). A TOUGH simulation of the hydrological environment around a nuclear waste canister in an underground repository. It shows the liquid saturation contours in the rock as heat in the canister vaporizes water.

Fig. 2. The grid system used to perform the calculations for Figure 1.

homogeneous isothermal case for up to 12 species; and applying this code to an alkaline flood experiment taken from the literature in order to test the code's capabilities.

We are developing a general porous-media flow and transport code capable of addressing a wide range of applications. The flexible structure of this new code will allow it to be dimensioned and configured to address a specific problem. Many existing codes are limited because they are hardwired to address flow phenomena that may not be relevant to the problem of interest; the result is wasted computational effort. Moreover, modifying hardwired codes to address additional flow phenomena is typically time-consuming. We designed the new flow and transport code to allow the user (rather than the code developer) to make decisions about which flow phenomena are to be accounted for in the model. Its structure will facilitate additional code development and performance enhancements. Accomplishments in FY87 include the basic design of the code structure as well as significant progress in code development.

We also made progress in developing a preconditioned conjugate gradient-method linear-equation solver for our porous-media flow and transport codes. This solver will facilitate addressing very large problems.

We improved an alternative solute transport model based on a particle-tracking approach. This approach offers several advantages over conventional discrete methods, including the ability to track sharp fronts effectively, conserve mass exactly, and, in some cases, reduce computational costs sharply. Figure 3 shows the particle-tracking approach applied to solute transport. We also improved a three-dimensional "turning bands" random-field generator. Such simulators are widely used in the areas of geostatistics and hydrology for the generation of synthetic sets of highly variable physical quantities used in stochastic models of naturally heterogeneous systems. This particular code is one of the most efficient of its type available today.

Among our completed theoretical work is the refinement of a higher-order model for solute dispersion in porous media. More specifically, we developed a new functional representation of the dispersive flux that appears to be much more consistent with experimental observations than the conventional Fickian constitutive model. In addition, we reformulated the theory and developed constitutive relationships for the electrochemical and thermoelectric coupling coefficients used in the interpretation of self-potential surveys.

Work on several experimental investigations progressed during FY87. The particle-tracking transport model was used to simulate detailed solute motions through heterogeneous porous media (see Figure 3). Computer experiments were used to examine large-scale dispersive behavior in spatially variable flow fields. The results compared well with theoretical predictions based upon stochastic models of these systems.

We also coordinated experimental work conducted at the University of

California, Berkeley (Udell et al., 1987). Our objectives were to provide data regarding nonisothermal transport in porous media, to identify governing parameters responsible for observed phenomena, and to explore the major interactions expected within the unsaturated zone during steam restoration of an aquifer contaminated with a second-phase liquid. A series of experiments involving iso-enthalpic injection of dry steam into dry, partially saturated, and fully saturated porous media was completed. Theory was developed to describe the steam displacement of a second-phase liquid and the effect of gravity on the propagation velocity of the steam condensation front. The theory and the experimental data agreed.

In FY88, development of our general porous-media flow and transport code will continue. A prototype version of this code will be applied to isothermal problems in nuclear waste isolation and in contaminant transport, possibly including the evaluation of aquifer-restoration strategies for LLNL. After the general porous-media flow and transport code is complete, we will incorporate and test the preconditioned conjugate gradient-method linear-equation solver. We will eventually incorporate this solver into versions of our other flow codes. Work will also begin on incorporating an adaptive moving mesh to the general flow code. Additional development of this code will address nonisothermal applications and the transport of a second-phase liquid.

We will continue to develop the particle-tracking model in FY88, with emphasis on incorporating TOUGH and other flow codes and developing improved methods of estimating particle densities, or concentrations, from the results. In addition, we will include the ability to treat variably saturated transport problems. We will create additional computer simulations of solute transport through heterogeneous porous media with the particle-tracking model.

Our effort to model reactive chemical transport in FY88 will include validating the MTRANS code and applying it to the analysis of laboratory core tests being conducted for the Nuclear Waste Management Program. To develop a stationary-state reactive chemical-transport simulator, we will modify LLNL's EQ3/6 code. The refinement of the volume-averaging approach will also continue. We will complete and publish work related to the improved interpretation of self-potential surveys.

We will continue our cooperative research effort with the University of California to investigate the mechanisms of steam displacement of nonaqueous liquid-phase contaminants from aquifers. Work in

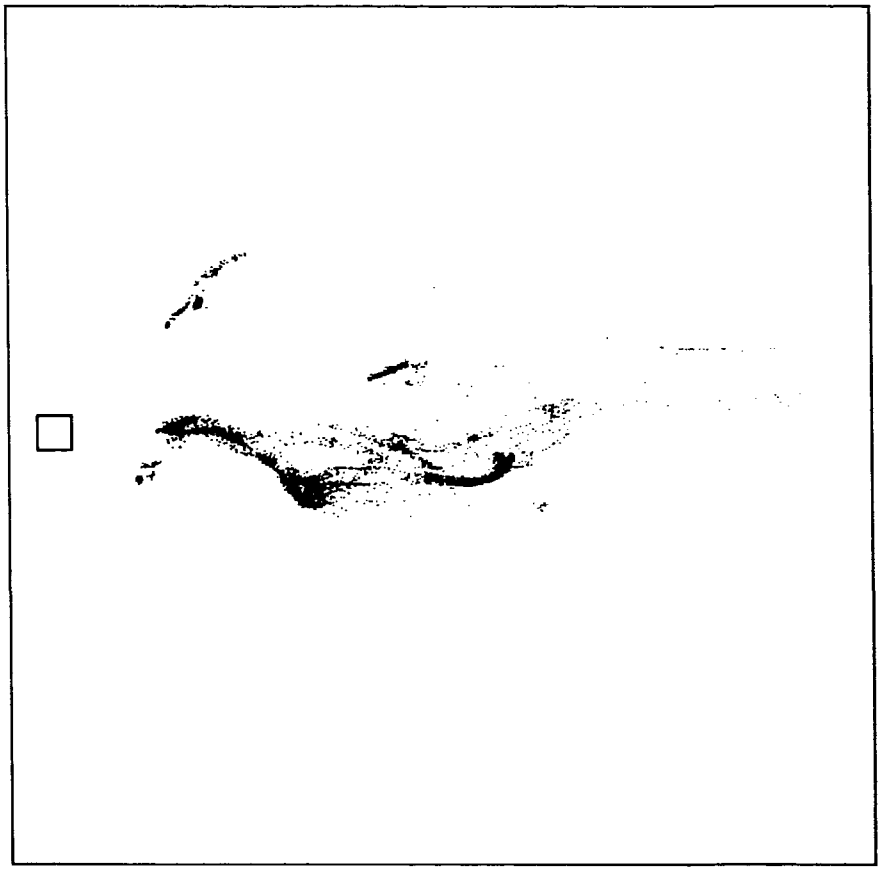

Fig. 3. Vertical projection of the distribution of solute mass (represented here as a collection of 8000 hypothetical particles) after release in the flow field from a small cubic region (located midway along the left vertical). The solute mass is moved by the groundwater flow as well as diffusion and dispersion processes. This kind of disordered mass distribution is typical of real conditions observed in the field and can be quantitatively studied and used to improve our ability to model actual groundwater contamination sites.

this area will be partly funded through a grant awarded by the University of California Toxic Substances Research and Teaching Program. Our contribution (as an associate researcher) will be to model the multidimensional scaled laboratory experiments of a multiple-well steamflood pattern designed to displace hydrocarbon contaminants to a central recovery well. This study will investigate the mechanisms of displacement in uniform and heterogeneous porous media under conditions of full and partial saturation. Work will also include studying displacement mechanisms governing the efficiency of conventional isothermal "pump and treat" recovery methods. The ultimate goal of this project is to conduct a pilot study in the field to demonstrate the effectiveness of steam displacement in aquifer restoration. From a modeling standpoint, these experiments represent outstanding opportunities to obtain carefully instrumented data for the purpose of model validation.

References

Preuss, K. (1985). *TOUGH User's Guide*. Lawrence Berkeley Laboratory, Berkeley, Calif., LBL-20700.

Rimstidt, J. D. (1979). *The Kinetics of Silica-Water Reactions*. Ph.D. dissertation, Pennsylvania State University, University Park, Pa.

Tompson, A. F. B. (1987). "On a New Functional Form for the Dispersive Flux in Porous Media," submitted to *Water Resources Research*; also published as Lawrence Livermore National Laboratory, Livermore, Calif., UCRL-97274.

Tompson, A. F. B. and D. Dougherty (1987). *On the Use of Particle Tracking Methods for Modeling Solute Transport in Porous Media*, abstract, Lawrence Livermore National Laboratory, Livermore, Calif., UCRL-97361.

Tompson, A. F. B., E. G. Vomvoris, and L. W. Gelhar (1987). *Numerical Simulation of Solute Transport in Randomly Heterogeneous Porous Media: Motivation, Model Development, and Application*, Lawrence Livermore National Laboratory, Livermore, Calif., UCID-21281.

Tompson, A. F. B. and R. Ababou (1986). "Use of the Three-Dimensional Turning Bands Simulator in Hydrology: Some Recent Developments and Applications," abstract, *Trans. Am. Geophys. Union*, **67**(44), 941.

Udell, K. S., J. Hunt, and N. Sitar (1987). *Removal of Nonaqueous Liquid Phase Contaminants from Aquifers by Steam Displacement*, proposal to the University of California Toxic Substances Research and Teaching Program, LEHR Facility, University of California, Davis, Calif., UCB Eng-6684.

New Applications of Fermat's Principle to Seismic Tomography

Principal Investigators:
James G. Berryman and
John J. Zucca

We developed a new algorithm for inverting travel-time data hat allows for strong ray bending. The method depends on Fermat's principle, which classifies rays into two groups. This grouping improves model convergence when integrated into the standard least-squares inversion.

Many areas in the earth sciences would benefit from an improved capability to deduce earth structure. On a regional scale, the understanding of volcanic plumbing systems is important for those who research or intend to produce geothermal power. On the local scale, seismic data for studies of enhanced oil recovery can indicate which formations are producing oil.

We are studying techniques to improve existing methods of seismic tomography. In particular, we are examining problems of large contrasts (>20%) in the seismic wave speed of the study area. To be successful in this effort, we need to develop new schemes for ray tracing and new methods of inversion to ensure convergence of the solution.

Our new method for two-dimensional tomography applies Fermat's principle to ray paths with strong bending. Fermat's principle classifies rays as feasible or nonfeasible. A nonfeasible ray has a shorter travel time than measured. This implies that travel time needs to be added to the ray path since Fermat's principle says that the minimum travel-time path is the true ray path. A feasible ray has a travel time greater than the measured value. In this case, Fermat's principle states that a shorter ray path might be found that could bring the calculated and measured travel times into closer agreement. This more systematic approach to modifying the starting model helps to ensure fast convergence and a smooth final model.

To help model areas with strong ray bending, we developed a new ray tracing method based on Monte Carlo methods and Fermat's principle. This approach ignores Snell's law at cell boundaries and searches for the minimum time path in an expanding ellipse around the initial straight-line path. The Figure shows the results of a ray tracing in a model that has a large low-velocity zone (LVZ) in the center of the model. Note that the ray paths bend significantly toward the LVZ. Our new method produces improved results over traditional techniques that rely on straight ray paths and simple least-squares inversion.

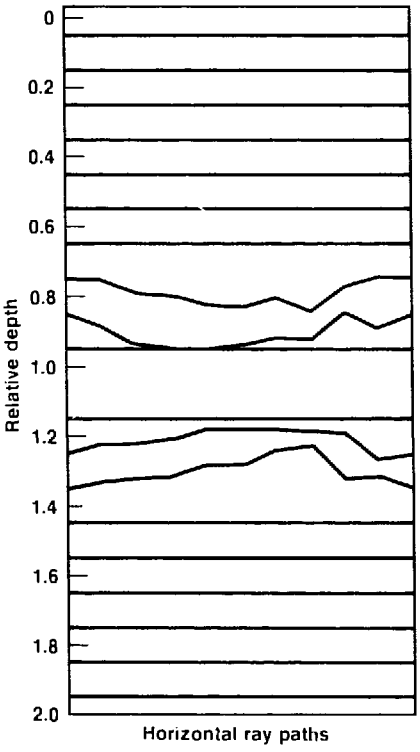

The Monte Carlo ray tracer finds the fastest ray paths when source and receiver are at the same depth. The theoretical model has a low-velocity zone in the middle at a relative depth of 1.0.

Reference

Beatty, J. A. and J. Berryman (1987), *Using the STOMP Program for Tomography with Strong Ray Bending*. Lawrence Livermore National Laboratory, Livermore, Calif., UCID-21157.

Geochemical Modeling of Natural Systems

Principal Investigators:
Kevin G. Knauss,
Kenneth J. Jackson,
William L. Bourcier, and
Thomas J. Wolery

Our measurements of the solubility and dissolution kinetics of various minerals in high-temperature aqueous solutions coupled with advanced algorithms to calculate activity coefficients of aqueous electrolyte species have improved our ability to accurately model geochemical interactions between mineral phases and aqueous solutions.

Our IR&D effort had two elements:

- Enhancement of our geochemical modeling code EQ3/6.
- Experimental measurements of the solubility and dissolution kinetics of various minerals to support code enhancement.

In the experimental segment, we measured the solubility of quartz and boehmite, and determined the dissolution kinetics of muscovite.

We measured the solubility of quartz as a function of NaCl concentration (from 2 to 5 molal) and temperature (from 150 to 350°C in 50° increments). The purpose of these measurements was to define the properties of aqueous silica in concentrated aqueous solutions. We made reversed solubility measurements by using Dickson-type, gold-bag rocking autoclaves. These experiments provided information formerly lacking in a database used by the EQ3/6 code and details concerning the role of water molecules in the formation of the activated complex controlling quartz dissolution.

We measured the solubility of boehmite as a function of pH and temperature in order to determine hydrolysis constants for aluminum. We made reversed measurements at 150, 200, and 250°C at pH 1, 2, 3.5, 5.5, 9, and 10. By using a ridge-regression technique to fit the measured solubility data to a stepwise set of assumed aqueous Al species, Al^{3+}, $AlOH^{2+}$, $Al(OH)_2^+$, $Al(OH)_3$, and $Al(OH)_4^-$, we determined the hydrolysis constants for Al to 250°C. We used the constants to calculate free energies for these species and incorporated the results into the EQ3/6 database. The code is now capable of modeling aqueous Al speciation and Al mineral solubility in high-temperature natural systems. The results of this solubility study and of the quartz study will permit more accurate prediction of the solubility behavior of alumino-silicate minerals in geothermal solutions.

Because no accurate data were previously available for the dissolution kinetics of muscovite, we carried out a set of experiments to determine the dissolution rate and to better understand the dissolution mechanism for this important rock-forming mineral. We determined the kinetics at 70°C as a function of pH. Our experiments were done far from equilibrium (as confirmed by calculation of chemical affinity) in single-pass, flow-through cells. After completing experiments at pH 1 through pH 13 at pH increments of 1 and determining the rates and mechanism controlling dissolution, we incorporated the values in the EQ3/6 database.

Over the past several years, we developed the EQ3/6 code to model the equilibrium chemistry of complex aqueous solutions. This code, which treats up to several hundred chemical species simultaneously, is used by DOE programs, major oil companies, the U.S. Geological Survey, and many of the world's major universities. It is probably the most comprehensive geochemical chemical-equilibrium code in the world today. Nevertheless, it has some limitations. Although it can adequately deal with solutions of low to moderately high ionic strength, it has difficulty calculating activity coefficients in concentrated solutions. Furthermore, although we recently added reaction kinetics to the code (dissolution and, to a lesser extent, precipitation), we have been limited by the lack of kinetics data. To reduce these limitations, we developed, tested, and incorporated into the code a new set of activity coefficient algorithms—hydration-theory equations.

After this enhancement, we developed an extensive database consisting of the variable parameters needed to evaluate the equations. We wrote a fitting program to regress the parameters and assembled a database of experimentally determined activity and osmotic-coefficient data for use in a fitting exercise. Fitting exercises using the experimental data for binary salt solutions showed that the hydration-theory equations can be used successfully to fit the activity and osmotic coefficient behavior of a wide variety of salts (see the Figure). Provisional values for the hydration number and ion-size parameters regressed from the fitting program seem physically realistic, but it remains to be shown that the equations and fitting code can simultaneously fit all the available data on binary solutions. Similarly, we must test the applicability of our calculations in multicomponent aqueous solutions.

Having removed many of the code's limitations, we now have a greatly improved capability to model a variety of important geological processes, including diagenetic processes, nuclear-waste disposal, the formation of many types of hydrothermal ore deposits, the formation of oil-field brines, and the utilization of hydrothermal energy.

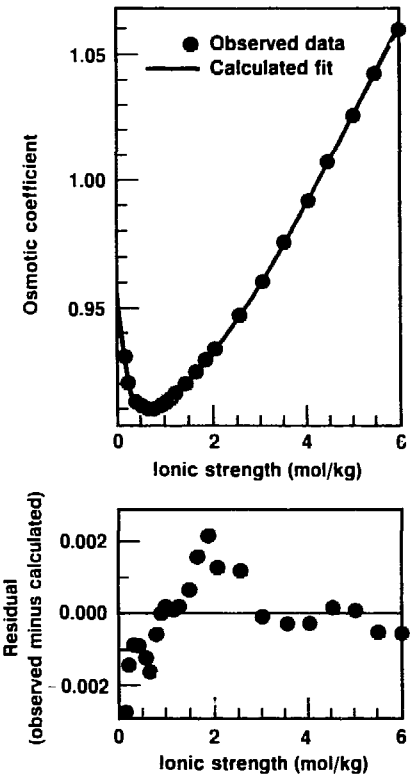

Comparison of osmotic coefficients calculated using the hydration theory equations and observed data versus ionic strength for $NaClO_4$.

References

Bourcier, W. L., K. G. Knauss, and K. J. Jackson (1987), "Aluminum Hydrolysis Constants to 250°C Determined from Boehmite Solubility Measurements," *Geol. Soc. Am. Abstr. Progrs.* **19**, 596.

Knauss, K. G. and T. J. Wolery (1987), "Muscovite Dissolution Kinetics as a Function of pH at 70°C," *Geol. Soc. Am. Abstr. Progrs.* **19**, 729.

Knauss, K. G. and T. J. Wolery (1987), "The Dissolution Kinetics of Quartz as a Function of pH and Time at 70°C," *Geochim. Cosmochim. Acta* (in press).

FY87 $215,000
FY88 $100,000

In Situ Measurements

Principal Investigators:
S. Michael Angel,
H. Michael Buettner, and
Paul W. Kasameyer

To understand the continuous changes in the earth's crust, we must be able to sample fluids from deep boreholes in situ without changing their chemical state. We are developing optical chemical sensors (optrodes) for a fiber-optic system to measure fluid properties and composition in hot, corrosive wells. Because these sensors use fluorescent inorganic ions and other inert indicators, they can work in very hot water for long periods. We can also use fluorescent inorganic ions doped into solid matrices as optrodes to measure pH.

The inability to sample or measure the chemical composition of brines in hot wells limits our understanding of in situ conditions in the crust of the earth. We are investigating the feasibility of making temperature and chemical measurements in wells at temperatures between 100 and 300°C by using optrodes.

Optrodes are optical transducers placed at the distal end of optical fibers. They produce a signal, usually fluorescence, in response to the parameter being measured. Optrodes have already proven useful at LLNL for remote in situ measurements of a variety of species, including pH in groundwater. By using a laser as the excitation light source and low-loss optical fibers, we can make measurements at distances up to 1 km, while certain measurements at 200 m are routine (see Figure 1). Our objective is to develop optrodes that expand this capability to temperatures at which in situ sampling methods usually fail.

Our research this year concentrated on using fluorescent inorganic ions in inert porous matrices to make measurements of two types: pH and temperature at temperatures over 100°C. Certain rare earths are particularly useful for such measurements because they are highly fluorescent and do not photodecompose upon intense laser irradiation.

Several candidates for a pH optrode were evaluated and found unsatisfactory. One pH indicator investigated is the uranyl ion. Uranyl, highly fluorescent and pH-dependent, could result in a useful pH optrode if it could be immobilized with the right oxidation state in a suitable matrix. Although we were successful in immobilizing the uranium in the lattice of calcium zirconolite, we could not maintain the correct oxidation state. We also tested beta-alumina, a natural solid ionic conductor of Na^+, H^+, and other ions, as the carrier matrix for this ion. Uranyl-doped beta-alumina samples were found to be sensitive to pH between 4 and 9 even at room temperature; this process was reversible. Several beta-alumina samples were tested at 100°C and above. These tests indicated that the samples lose mechanical strength in hot water quickly and are not suitable for high-temperature optrodes. We are currently investigating ways to improve the performance of this pH sensor.

Our other efforts focused on the development of a temperature optrode, necessary for corrections to the chemically sensitive optrodes. This effort provided the opportunity to develop and test design concepts for high-temperature optrodes through experiments with a relatively simple system.

We developed a temperature optrode using rare earth dopants in a porous ceramic matrix of calcium zirconolite. We selected calcium zirconolite as the carrier matrix because of its ability to immobilize rare earths and actinides in extremely corrosive environments without leaching. Because the dopant ions are incorporated into zirconium lattice sites in the crystal, they do not leach out of the crystal easily. Highly porous calcium zirconolite gels were made using sol-gel techniques. X-ray diffraction spectra of the sintered gels indicate that the samples, although highly porous, still have the zirconolite crystal structure.

We chose Eu(III) and Er (III) ions as the dopants for the temperature optrode since they can be doped into calcium zirconolite at high levels without affecting the structure of the matrix. Also, these ions fluoresce in a convenient region of the visible spectrum. Eu(III) has several emission bands that show large temperature effects when excited with the 488-nm line of an argon-ion laser. This convenient and powerful excitation source makes it possible to

use this optrode over long optical fibers.

We constructed temperature optrodes by attaching a small bead of the doped calcium zirconolite gel to the tip of a 320-μm-core, high-temperature optical fiber with a chemically resistant high-temperature ceramic glue. Er(III) was doped into the temperature optrode matrix as an internal intensity reference. With an absorption band near 488 nm, Er(III) can be excited simultaneously with Eu(III) and fluoresces in a convenient part of the spectrum. More importantly, the temperature coefficient of Er(III) complements that of Eu(III), decreasing as temperature increases and providing a more accurate temperature measurement. Figure 2 shows a calibration curve for this optrode up to 280°C. The optrode is sensitive to about 320°C.

Long-term testing of this sensor in water at 300°C and 10,000 psi indicates it is stable. Also, field tests in geothermal brine at 200 m indicate that the sensor can be used over a kilometer of optical fiber without further optimization.

The temperature optrode development demonstrated several important points:

- Highly porous calcium zirconolite materials will survive in high-temperature water for extended periods.
- Lanthanides do not leach out of this material in very hot water for long periods.
- Optrodes can be made of these materials.
- Optrodes can be used to make measurements in very hot water at high pressures.
- Optical fiber measurements can be made over very long distances in geothermal brine.

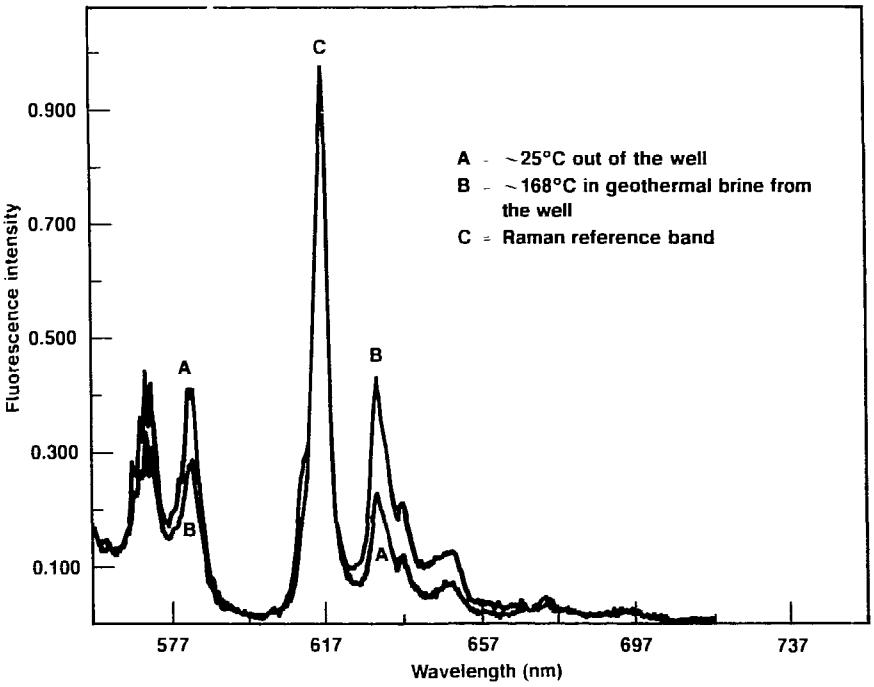

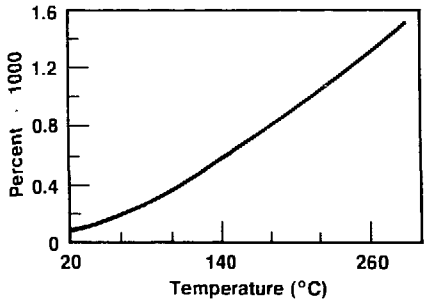

Fig. 1 (*Above*). Temperature measured in situ in geothermal brine over 200 m of optical fiber.

Fig. 2. Temperature optrode calibration curve. The percent change (versus 25°C) of the ratio of the fluorescence intensities of the Eu (III) and Er (III) peak intensities (plotted versus temperature).

We are deferring efforts on the pH optrode to test candidate eH (reducing potential) optrodes in FY88. Our initial studies will test lanthanide and transition metal ions incorporated into highly porous ceramics and inert polymer electrolytes.

References

Angel, S. M. (1987), "Development of Fiber-Optics Sensors for Temperature Measurement and Chemical Analysis in Geothermal Wells," *Transactions, Geothermal Resources Council* **11**, 155.

Angel, S. M. (1987), "Optrodes—Chemically Sensitive Fiber-Optic Sensors," *Spectroscopy* **2**, 4.

FY87: $10,000
FY88: $120,000

Design of a Large-Volume, High-Pressure Apparatus for Geophysical Research

Models of earth composition, structure, and evolution are constrained by the results of high-pressure and temperature experiments. We can extend the depth range of experimentation by increasing the upper-pressure limit. By modifying an existing design at LLNL, we can conduct experiments at pressures up to 0.25 Mbar.

Principal Investigators:
Fredrick J. Ryerson,
Leland L. Dibley,
Robert N. Schock,
and Hugh Heard[a]

[a]Deceased, 1987.

Generating higher pressures in larger volumes is a continuing requirement in geology, geophysics, materials science, and high-pressure physics. In the U.S., high-pressure research with large sample volumes (2 cm^3) developed rapidly in the 1950s during the race to produce a synthetic diamond. The piston-cylinder device developed during this extreme conditions and the recovery of sample material. This device is now widely used, but it can only handle pressures less than 0.06 Mbar, rendering depths greater than 200 km (the lower mantle) inaccessible to experimenters.

Diamond-cell and shock-wave experiments, important in extending the pressure range accessible to mantle and core. Unfortunately, since the volume of material used in the diamond cell is very small and the material used in shock-wave experiments is not recoverable, the application of these techniques is limited. In the last 25 years, however, a number of Japanese universities and research institutions have pioneered the use of a large-volume, high-pressure apparatus known as a multi-anvil sliding system (MAS). This system offers three advantages: a fourfold increase in pressure over the piston-cylinder, sample recoverability, and only small sacrifices in sample volume. The depth range of large-volume experimentation can be extended to 750 km, allowing investigation of 400- and 600-km seismic discontinuities from a mineralogic standpoint.

During FY87, we visited several existing MAS facilities in Japan to investigate which MAS is most compatible with our needs, which could fit the existing press frames at

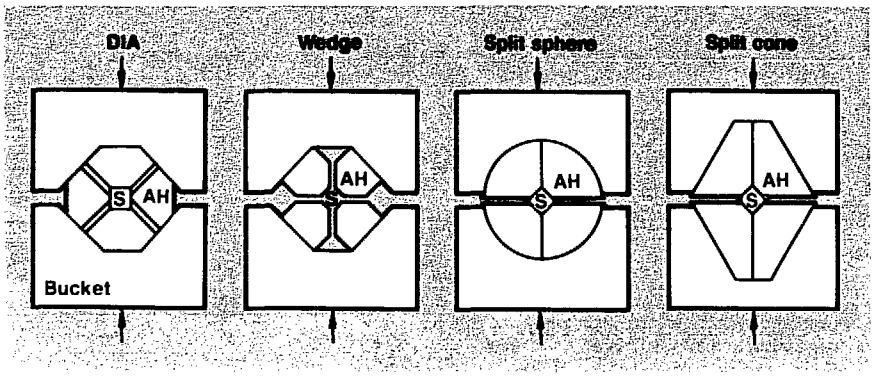

Schematic illustration of the various MAS designs. We compress the sample volume (S) by applying a uniaxial load to the buckets, which in turn drive the anvil heads (AH). We completed the split-cone design at LLNL during FY87.

LLNL, and which design of the currently operating systems could be improved.

Three types of MAS are currently in use in Japan: DIA, wedge, and split-sphere designs (see the Figure). In each case, tungsten carbide (WC) anvils are confined to a guide-block assembly in order to ensure alignment and synchronous application of force on the compressed volume. The DIA and wedge designs have the advantage of allowing in situ x-ray analysis but to date have only operated at 0.10 Mbar and at less than 1500°C. The split-sphere design does not allow x–ray access but operates at pressures up to 0.25 Mbar with temperatures as high as 2000°C. (Higher temperatures can be achieved with some sacrifice of pressure.) All of these devices can be operated in presses with capacities lower than 1000 metric tons. Therefore, we can adapt a 1200-ton press in the Earth Sciences Department at LLNL to this application.

We chose to modify the split-sphere design for use at LLNL because we can attain results at higher pressures and temperatures. With the preliminary design completed, final design drawings are now under review. The major modification incorporated in the LLNL design is the replacement of the split sphere by a split cone (see the Figure). The use of a split-cone design will allow easier alignment of the bucket and anvil assembly in the guide block.

Final drawings of the split-cone design were reviewed and put out for bid in December 1987. On the basis of discussions with possible suppliers, we expect that fabrication of the guide-block assembly and buckets could take as long as nine months. In the interim, we plan to visit the only U.S. laboratory operating a MAS (State University of New York at Stony Brook) to study furnace design for high-pressure applications and other routine operating procedures. Power supplies and other supporting equipment will be in place prior to the receipt of the guide-block assembly and buckets. After the guide blocks are installed in the 1200-ton press, initial testing and pressure calibration will begin. This facility may eventually function as a West Coast center for large-volume, high-pressure experimentation.

Advanced High-Pressure Diamond-Anvil Cell

Principal Investigators: Robin L. Reichlin and Raymond Jeanloz[a]

[a]University of California, Berkeley.

We extended the maximum pressure achieved for condensed gas samples in the diamond-anvil cell (DAC) from 1.4 to over 2 Mbar. We achieved higher pressures for materials with high shear strengths. We fabricated a modified DAC with superior alignment capability, successfully tested in the 1-Mbar region. With collaborators at the University of California, Berkeley, we measured the optical absorption and IR reflectivity of fayalite to 2.2 Mbar to understand the electronic character of this material under conditions relevant to the earth's interior.

The multi-year DAC program pushes the limits of maximum pressure capabilities for diamond-anvil cell experiments. In order to extend the pressure range of the DAC, we used calculational and experimental techniques to test modifications of diamond and sample geometries, new gasketing materials, and the cell and press. We explored the physical properties of geological materials in the multi-megabar pressure regime relevant to conditions in the earth's mantle and core.

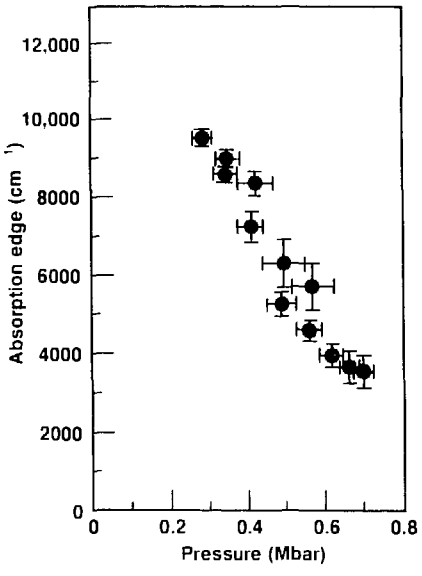

Optical absorption of fayalite at pressures below 0.9 Mbar. Extrapolation of absorption data corrected to 700 kbar indicates band-gap closure (i.e., metallization) at about 1 Mbar.

We increased the pressure capability of the DAC for soft samples. The highest pressures previously achieved for condensed gases were 1.2 to 1.4 Mbar (N_2, H_2, and Xe) and 1.7 for somewhat stiffer materials such as CsI (Reichlin et al., 1986). By experimenting with five different anvil designs in tests on Xe, we achieved a pressure above 2 Mbar. We have also achieved higher pressures in a significantly stiffer material (fayalite, 2.2 Mbar). We collected in situ optical absorption and reflectivity data on both of these materials.

With collaborators at the University of California, Berkeley, we collected optical absorption and electrical resistance data on fayalite below 0.9 Mbar that indicate fayalite should transform to a metallic state above 1 Mbar. (The Figure shows the optical-absorption data.) We also made IR reflectivity measurements to 2.2 Mbar and observed no free-electron behavior in this material.

We fabricated a new diamond cell, designed to have superior alignment capability and to be more accurately machinable than the standard Mao-Bell design. Preliminary tests prove the new design is far more easily aligned to the extreme precision required for DAC experiments. We achieved a pressure of 1 Mbar with this new design and will continue to test performance under extreme conditions.

References

Moss, W. and K. Goettel (1987), "Finite Element Design of Diamond Anvils," *Appl. Phys. Lett.* **50**, 1455.

Moss, W., J. Hallquist, R. Reichlin, K. Goettel, and S. Martin (1986), "Finite Element Analysis of the Diamond-Anvil Cell: Achieving 4.6 Mbar," *Appl. Phys. Lett.* **48**, 1258.

Reichlin, R., M. Ross, S. Martin, and K. Goettel (1986), "Metallization of CsI," *Phys. Rev. Lett.* **56**, 2858.

Reichlin, R., D. Schiferl, S. Martin, C. Vanderborg, and R. Mills (1985), "Optical Studies of Nitrogen to 130 GPa," *Phys. Rev. Lett.* **55**, 1464.

Williams, Q., R. Reichlin, S. Martin, E. Knittle, and R. Jeanloz (1987), "High-Pressure Electronic Properties of Fayalite," *Trans. Am. Geophys. Union* **68**, 1455.

Characterization of the Kinetics of Coal Pyrolysis

Principal Investigators: Alan K. Burnham and Myongsook S. Oh

As world petroleum supplies decrease, coal will become an important source of transportation fuels. In order to design efficient coal-processing plants and reduce costs, we must understand how coal rank (carbon content) influences the mechanism of coal pyrolysis. We used both tandem mass spectrometry and a simple total product detector to illustrate how coal pyrolysis characteristics relate to the formation of individual compounds.

Because of coal's complex structure, coal pyrolysis cannot be characterized by traditional chemical kinetics. Although alternate theories using activation-energy distributions are useful for process design, we need to understand the underlying chemical and physical processes involved. Our current objective is to better understand the relation between global chemical kinetic expressions used in process design and more detailed expressions involving individual compounds.

Coals vary widely in their pyrolysis characteristics. We chose eight Argonne premium coal samples for our work because of their diverse range of properties, high quality, and widespread use by other researchers. We measured total product formation rates at three heating rates from 5 to 50°C/min using a micropyrolysis apparatus. The flame-ionization detector of this apparatus is sensitive to all non-oxygenated (reduced) carbon atoms in the pyrolysis products. As coal rank increases, we found that the temperature at which the product formation rate is at a maximum increases, and the required activation-energy distribution width decreases. Both of these effects are due to the increasing carbon content of the samples. Coal becomes more carbonaceous as increased time and temperature related to deeper burial eliminate oxygen from its structure.

By using pyrolysis coupled with tandem mass spectrometry, we gained further insight into the effect of coal rank on kinetics. The increase in the total product formation temperature with coal rank results from two factors. First, the formation temperature of individual pyrolysis products increases from subbituminous to low volatile bituminous (see the Figure). Second, methane, which has a higher individual formation temperature than other pyrolysis products, accounts for an increasing proportion of the products as coal rank increases.

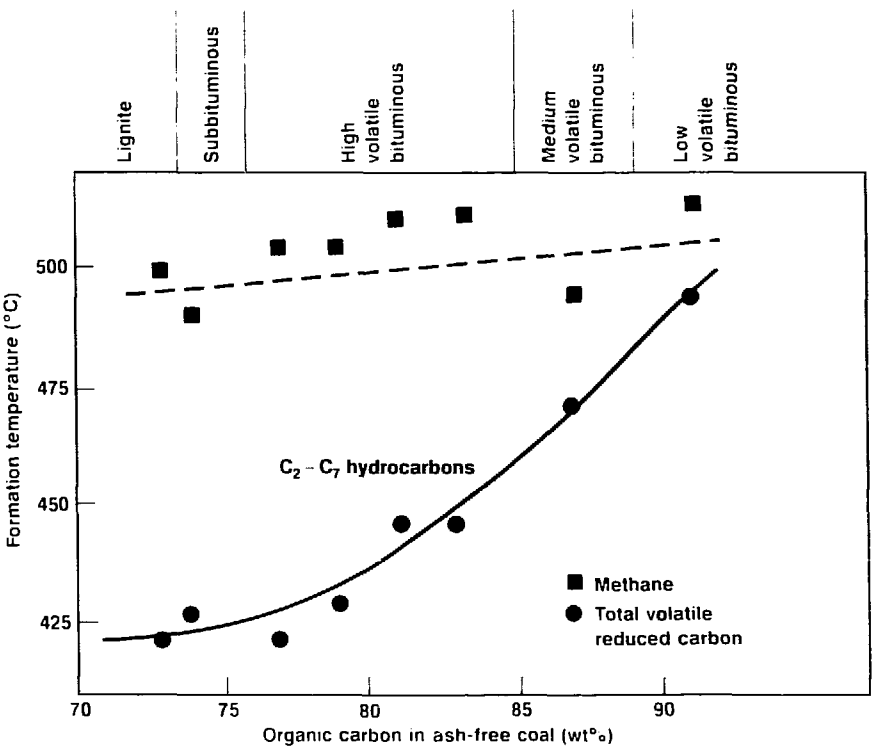

As coal rank increases, the the total product formation temperature and that of most individual pyrolysis products increases. The formation temperature here is the temperature at which the product formation rate was at a maximum when each of the eight coal samples was heated at 5 C/min.

FY87: $242,000
FY88: $225,000

Crystal Growth

Principal Investigators:
Morris Young and
Frederick J. Ryerson
Co-Investigator: Chol K. Syn

Laboratory-prepared, well-defined, single crystals—essential for geophysical and geochemical research—are largely unavailable. The Earth Sciences Department at LLNL initiated a crystal growth program to provide the U.S. earth sciences community with well-characterized, high-quality, single crystals.

To model the mechanisms controlling large-scale plate movements in the earth's upper mantle, geoscientists need to understand the physical and chemical properties of the materials that constitute the earth's outer shell. However, the availability of single crystals necessary for research to gain this understanding is low. One of our program goals is to establish LLNL as the lead laboratory for providing the U.S. earth sciences community with the crystals needed for research.

A second goal relates to the use of single crystals as tools for precision machining—important in the manufacture of highly complex devices for civilian and military applications. Single crystals of diamond have been used extensively in cutting nonferrous metals. However, ferrous metals and specialty metals (e.g., molybdenum, tungsten, and beryllium) cannot be machined with diamond because of their chemical affinity for carbon. Cubic boron nitride (cBN) is a leading candidate for machining such metals by virtue of its hardness, good thermal conductivity, and relative inertness with respect to ferrous metals. The major impediment in the implementation of cBN as a cutting tool component is the difficulty of fabricating large (3- to 5-mm, 1/2-carat) single crystals.

Our goal is to develop a process to synthesize single crystals of cBN and to assess the relation between synthesis conditions and tool performance. Synthesis will be carried out in the high-pressure facilities of the Earth Sciences Department. The cutting tools will be built and evaluated at other LLNL locations: the Large Optic Diamond Turning Machine (LODTM) facility and the Machine Fabrication Division (MFD).

In FY87, we built and equipped a crystal-growth laboratory at LLNL with funds from the Office of Basic Energy Sciences. One major piece of equipment we purchased is a thermal image furnace. Capable of reaching 2150°C, the furnace focuses the infrared radiation energy of two halogen lamps onto a melt zone area 1 cm in diameter and 0.5 cm long. A quartz tube encloses the crystal-growth chamber. We control the crystal-growth atmosphere by regulating the gas mixture flowing through the quartz tube. In this arrangement, high-melting-point silicate crystals can grow under controlled oxygen fugacity, which permits control of the crystal chemistry. We are now in the process of installing and calibrating the thermal image furnace. In addition to this furnace, the new laboratory will feature a material-synthesis furnace, powder-preparation equipment, a crystal cutting saw, and an optical microscope.

In order to gain hands-on experience with the thermal image furnace, we attempted to grow forsterite and fayalite crystals at the Westinghouse Research Center, Pittsburgh, Pa. We developed methods to mix, cold-press, and sinter starting material into feed rods of the proper shape and size at LLNL, and then conducted crystal-growth experiments at Westinghouse. A forsterite single crystal (grown in the [100] crystallographic direction) was perfectly clear, indicating high purity; however, it cracked during cool-down. The cracking problem persisted when crystals were grown at different rates and when they were

cooled at slower rates after growth. The crystal-cracking problem probably results from the thermal contraction strain induced by the large temperature gradient in the thermal image furnace. This problem can be alleviated by reducing the temperature gradient in the cool-down region of the furnace. We installed an after-heater in our new thermal image furnace to reduce the temperature gradient. Initial attempts to grow fayalite crystals resulted in crystal material with gross inhomogeneity caused by improper gas mixture in the crystal-growth chamber. Consequently, we installed a more precise gas delivery system in our new furnace.

For tool fabrication and testing, we obtained cBN single-crystal seeds grown by dynamic compaction from General Electric Company (GE), Columbus, Ohio. We also obtained crystals grown in a large-volume, high-pressure apparatus from the National Institute for Research in Inorganic Material (NIRIM) in Japan. In conjunction with personnel from LODTM and MFD, we attempted to fabricate the cBN into cutting tools at Edge Technologies, Indianapolis, Ind. Although successfully produced, tools made from the GE crystals performed poorly in tests on copper metal. The NIRIM crystal failed during tool fabrication.

In FY88, we will install all the equipment in our new crystal-growth laboratory. After becoming familiar with the characteristics and operation of the thermal image furnace, we plan to grow olivine [$(Mg, Fe)_2SiO_4$] with well-characterized stoichiometry and purity. Working closely with the earth sciences community, we will provide crystals needed for various research projects. We will also begin to grow diopside and melilite for ongoing diffusion experiments in the Earth Sciences Department. Having the unique capability of the thermal image furnace, we will cooperate with the laser material research community in growing laser-related crystals.

Because of difficulties in the fabrication and use of cBN tools, we will assign cBN synthesis a low priority in FY88. We will attempt to obtain additional single-crystal cBN from NIRIM and again try to fabricate tools for testing. Synthesis experiments will be postponed until the utility of cBN tools can be demonstrated.

Thermophilic Microorganisms in Geothermal Fluid

Principal Investigators:
Emilio Garcia, Robert T. Taylor, and Dana Isherwood

We analyzed geothermal fluids from three wells in Nevada and California for the presence of viable microorganisms. Using phase-contrast microscopy, we observed microorganisms with morphologies characteristic of extreme thermophiles. Preliminary studies indicate that some of the organisms can grow at temperatures as high as 105°C and can be successfully subcultured.

The purpose of this research is to characterize the viable thermophilic bacteria in certain geothermal fluids and to determine their potential uses in mineral recovery from geothermal wastes. Also of interest are other possible biotechnological applications that capitalize on the thermal stabilities of their indigenous protein catalysts (enzymes). After an initial survey to establish the presence of microorganisms in these geothermal fluids, we will determine conditions for their optimal culturing and isolation. This preliminary work is to be followed by studies to learn more about the physiological characteristics and potentially useful metabolic activities of these microorganisms. Such studies would include identifying specific enzymes or metal binders and regulating useful processes carried out by such bacteria. We expect that bacteria derived from such unusually high temperature, pressure, and salt environments will yield valuable information about cellular tolerance under extreme conditions. Subsequently, we may understand more accurately how microorganisms contribute to underground metal corrosion and subsurface geocycling of metals.

Using phase-contrast and electron microscopy, we have clearly established the presence of microorganisms in samples obtained from two 3000-ft geothermal wells at Steamboat Hills and Desert Park, Nevada, and from a 7000-ft well recently drilled by the U.S. Geological Survey at Cajon Pass, California. The waters from the first two sources had in situ temperatures of 200 to 204°C and pressures of about 2000 psi; the sample obtained from the deeper California well had an in situ temperature of 90°C and was under a hydrostatic pressure approaching 3000 psi.

In agreement with characteristics first noted by Brock (1986), many of the varied microorganisims we

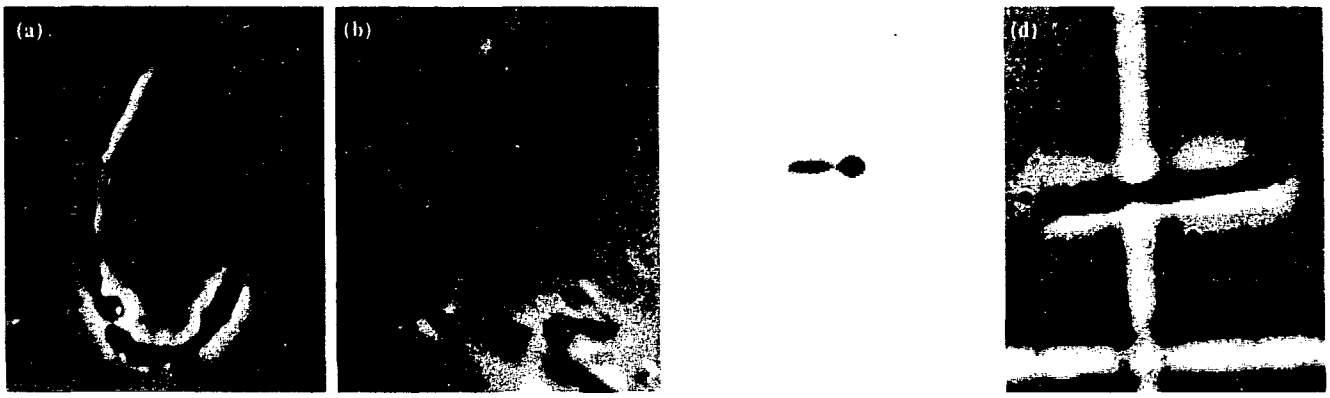

Phase-contrast photomicrographs of representative bacteria from several geothermal fluids: (a) Magnification of 2500× reveals a filamentous bacterium 5 to 10 μm in length, whose individual cells appear to be contained in a sheath; (b) some of the organisms have unique knob-like structures at each end of the cells; (c) others show bud-like structures, indicating a possible budding mode of cell division; (d) at least one organism closely resembles a recently isolated thermophile, *Pyrobaculum islandicum*.

observed microscopically have the unusual morphologies commonly associated with extreme thermophiles (see the Figure). Chemical composition data for all of the samples under study have guided the design of media and conditions for subculturing incubations. All water samples have a pH of 6 to 7.

We inoculated a variety of media formulated to support the growth of organisms present in low-nutrient, sulfate-containing, anaerobic environments with samples obtained from the two Nevada geothermal wells. We achieved limited growth and successful subculturing of a few of the microorganisms under anaerobic incubation as high as 105°C in sealed containers.

The immediate goal for FY88 is to increase the selection of organisms in the samples by optimizing growth conditions and media. This effort may address the possible high-pressure requirement of some of our isolates. Then we will design solid media to facilitate the isolation of pure cultures of these extreme thermophiles. The microorganisms will be characterized in terms of useful physiological capabilities (e.g., salt tolerance and metal binding). After characterization, we will initiate pertinent genetic and biochemical studies. This phase of the research should take approximately two years.

Reference

Brock, T. D. (1986), *The Thermophiles: General, Molecular, and Applied Microbiology* (John Wiley and Sons, New York).

Engineering

Overview

Dennis K. Fisher

Research in the Engineering Department is focused on identifying and developing emerging technologies needed to meet the future requirements of LLNL programs. Findings from the four projects funded by IR&D in FY87 will be applied in programs as diverse as Laser Isotope Separation, Nuclear Test, and Precision Engineering. In addition, the researchers often collaborate with investigators or sponsor research at universities, industrial technology centers, and other laboratories. These efforts enhance the quality of engineering tools and techniques available to LLNL.

All four studies funded in FY87 concern the need to understand the behavior of exotic materials. In the first project, a continuation of previous efforts, researchers are developing a basic understanding of how chips are formed from the interactions of components involved in single-point cutting. This machining process can produce highly reflective optics with extreme form accuracies and super-smooth finishes. In FY87, copper chips were produced with a nominal depth of 30 Å, a smoothness that challenges the resolution of scanning electron microscopes. Precision optics (e.g., grazing-incidence x-ray components for telescopes and diagnostic systems) with micrometer smoothnesses are particularly important for LLNL's Defense Systems Program and for the Strategic Defense Initiative.

The second project, a study of material properties, is directed toward obtaining data on the radiative and optical properties of pure liquid-metal surfaces. Such data are of particular importance to the Laser Isotope Separation Program, where the emissivity and reflectivity of liquid-metal films must be determined very precisely. In FY87, researchers used an apparatus they designed to simultaneously measure the radiative properties and determine the surface chemistry of samples of uranium and molten indium. From these efforts, the scientific community will have the first radiative property measurements of materials with known surface compositions.

A most powerful technique for unraveling the mysteries of materials is computer modeling. The third study focuses on the computer modeling of solid-state superlattices, among the most important materials to become available in the last decade. The models, which predict the effect of layer thickness and atomic composition on device properties, will help LLNL researchers design quantum-well lasers and heterojunction structures.

The final study forms the basis for the next generation of ultra-high-speed circuits and sensors used, for example, in downhole diagnostics, where ultra-fast digitizers are required. Such digitizers will almost invariably be made from gallium-arsenide integrated circuits, which can be much faster than integrated circuits made from silicon substrates. A gallium-arsenide digital recorder developed by Engineering displayed a 2.5-gigasample/second sampling rate, far better than the 0.5-gigasample/second rate possible with commercially available integrated circuits. In addition, redesigned logic cells for the recorder operate at 40% lower voltage, are 75% smaller, and use 70% less power than previous versions.

Overall, Engineering received $927,000 in IR&D funds in FY87.

FY87: $421,000

Chip Science: A Basic Study of the Single-Point Cutting Process

Principal Investigator:
Robert R. Donaldson
Co-Investigators:
Chol K. Syn, John S. Taylor, and Robert A. Riddle

We continued our study of cutting with ultra-sharp, single-point diamond tools. The single-point cutting process is a significant factor in the overall performance of precision machining of exotic components, such as radically aspheric optical surfaces for directed-energy research. This year we focused our experiments in two areas: determining the minimum attainable depth of cut for a diamond tool edge, a parameter which ultimately limits the figure accuracy and surface roughness, and addressing machinability issues for single-crystal silicon, a material of interest for cooled high-energy mirrors.

Our overall objective is to improve LLNL's capability in both accuracy and size of precision-machined components. Optical surfaces required for directed-energy research present unusually stringent demands. Our approach has been to combine LLNL expertise in three areas: Precision Engineering, for cutting experiments plus form and finish measurements; Materials Science, for additional characterization and insight into material behaviors; and Computation, for developing predictive models for cutting behavior.

Single-crystal diamond as a cutting tool material is uniquely able to sustain an extremely sharp edge, i.e., a small edge radius. As discussed in a previous report (Donaldson et al., 1987), the edge radius determines a minimum depth of cut, below which the tool disturbs the workpiece surface structure without removing material, degrading both the surface finish and the form accuracy. For conventional cutting tools, the edge radius is between 1 and 100 μm, depending on factors such as tool and workpiece materials, initial sharpening, and wear history. For high-quality diamond tools, the edge radius, although too small to measure with confidence, is theoretically predicted from surface-energy considerations to be a few nanometers.

This year we undertook to experimentally measure the minimum depth of cut. The cuts were performed on the Precision Engineering Research Lathe (PERL), which advances a cutting tool at an adequately low and uniform velocity for these tests. The tools were of a vee-point geometry, we used special diamond selection and sharpening techniques developed by Osaka University researchers who collaborated on this effort, and the workpiece was a fine-grained electroplated copper. By feeding laterally, to cut along one side of the vee, we were able to produce a continuous chip of rectangular cross section and extremely large aspect ratio. Tool-chip friction in the exit zone caused a folding behavior for thin chips that became progressively more convoluted as the depth of cut was reduced. Figure 1 shows the convoluted edge of a chip with a nominal cut depth of 3 nm; note that the chip material is thin enough to become translucent to the electron beam of a scanning electron microscope (SEM). The actual thickness is below the SEM resolution but is estimated to be no more than a few tens of nanometers, which is consistent with the depth of cut (uncut chip thickness) if the shear angle is small, as typically occurs for thin chips. Cuts with smaller depths—down to 1 nm—have also been made, with attendant increasing difficulty with SEM resolution. While the PERL has an exceptionally low level of vibration, amplitudes on the order of 1 nm in the chip-thickness direction are plausible, which would lead to large percentage variations in the actual depth of cut. Nonetheless, for all chip samples examined by the SEM, the degree of chip convolution increased with decreasing depth of cut, giving some qualitative assurance that progressively finer cuts were actually occurring. We conclude that while a quantitative lower limit to the depth

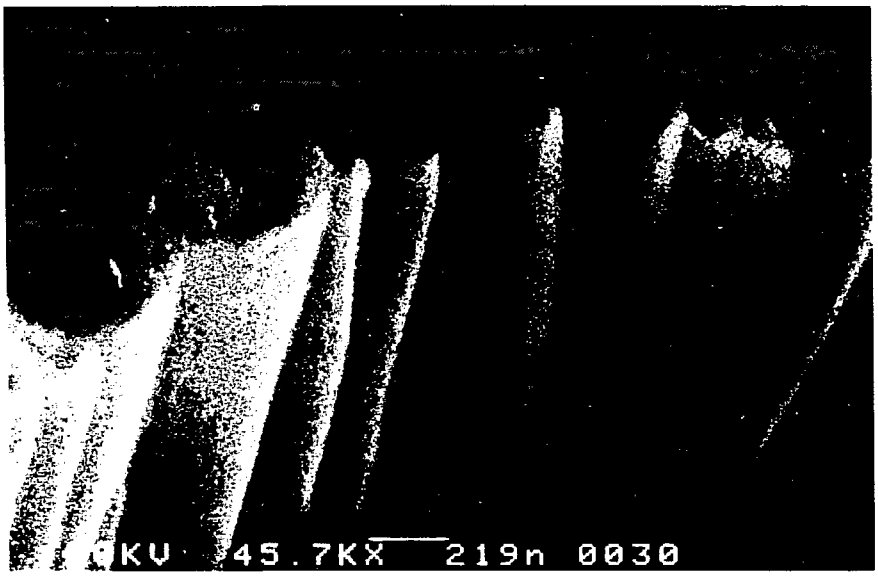

Fig. 1. High-magnification scanning electron micrograph of the edge of a copper chip machined with a 3-nm depth of cut, showing the convoluted folding of the thin chip that results from friction against the tool and regions that are translucent to the SEM.

of cut cannot be established by our currently available experimental equipment, it is no more than a few nanometers, and hence consistent with the theoretical estimate of the limiting diamond tool cutting edge radius.

The above results are more significant than may be obvious for more routine uses of diamond tools. A typical diamond tool has a circular nose profile extending over an arc exceeding 90°, so that workpiece contours containing both flat-facing and cylindrical turning can be addressed without reorienting the cutting tool. Also, the tool-nose radius is on the order of 1 mm, since high-quality single-crystal diamonds in larger sizes become prohibitively costly. The spiral progression of the tool nose across the workpiece leaves behind a circularly scalloped pattern of surface roughness, which can be limited to a specified amplitude by use of a sufficiently small tool advance per spindle revolution. A detailed analysis of the chip geometry shows that, regardless of the total thickness of the workpiece layer being removed, the chip thickness in the trailing edge or "scalloped" region is only a few nanometers. Since the trailing edge region defines the workpiece surface roughness, the fact that a diamond tool can cut rather than smear or otherwise disturb the surface at the nanometer level is important to its performance in producing mirror-finish components.

The second research area we studied during FY87 was the single-point diamond machining of silicon, a material of interest for liquid-cooled directed-energy optics because of its high thermal conductivity and low coefficient of thermal expansion. Although silicon is nominally brittle, evidence in the literature indicates a ductile-brittle transition, i.e., that a diamond tool can cut silicon in a ductile manner, without cracking, when the depth of cut is less than 100 nm. These earlier studies left open two important issues. First, they started with an optically polished, crack-free surface, and it was not obvious what would happen if the initial workpiece surface contained cracks, since these cracks might continue to propagate despite fine cuts. If so, rough-ground workpiece blanks would have to be polished crack-free before machining, a time-consuming and expensive step. Secondly, it was not clear how to interpret the 100-nm depth limit, e.g., if a workpiece blank arrived with an excess stock of 100 μm, would would it take 10^3 machining passes (an obviously impractical number) to avoid irrecoverable cracks? Finally, rapid wear of the diamond tool appeared to be a major issue, although no quantitative wear data were available.

To address tool wear, we did cutting tests dry (no cutting fluid) and with light lubricating oil, ethanol, and water. With dry or oil-lubricated cutting, the wear rate was rapid, about 2 μm per km of cutting distance (tool travel), and the surface roughness exceeded 10 nm rms after cutting only 0.5 km. In contrast, the wear rate with either ethanol or water was too small to measure accurately over the 0.5-km distance, but was at least two orders of magnitude lower and hence approached the level found in an earlier wear study on electroless nickel. The surface roughness was also lower, about 2.5 nm rms at the end of the test. The mechanism of wear reduction is unclear, and hence other still more effective cutting fluids may exist. The largest difficulty with both ethanol and water is thermal distortion from evaporative cooling, which might be addressed by

arranging for an essentially saturated local environment.

We gained insight into the ductile-brittle transition problem by examining the circular-arc "shoulder" left when a facing cut with a round-nosed tool stops before completion. Geometrical analysis of the sequence of laterally displaced tool-nose contact arcs shows that the uncut chip thickness decreases almost linearly from the original surface at the leading edge to nearly zero at the trailing edge. As shown in Figure 2, the degree of surface fracture also decreases from the leading to the trailing edge, leaving an essentially fracture-free final surface. This result is quite encouraging, since it indicates that the larger fractures higher up on the shoulder do not penetrate down to the level of the final surface, making it possible to produce undamaged final surfaces while removing a relatively thick layer from the workpiece. Further tests show that the behavior shown in Figure 2 is insensitive to the depth of cut (layer thickness), but varies with the feed rate. Below the 1.5 μm/rev of Figure 2, the damage-free zone moves up the shoulder toward the leading edge, while at larger feed rates, damage appears in the final surface, with the transition occurring at about 2 μm/rev.

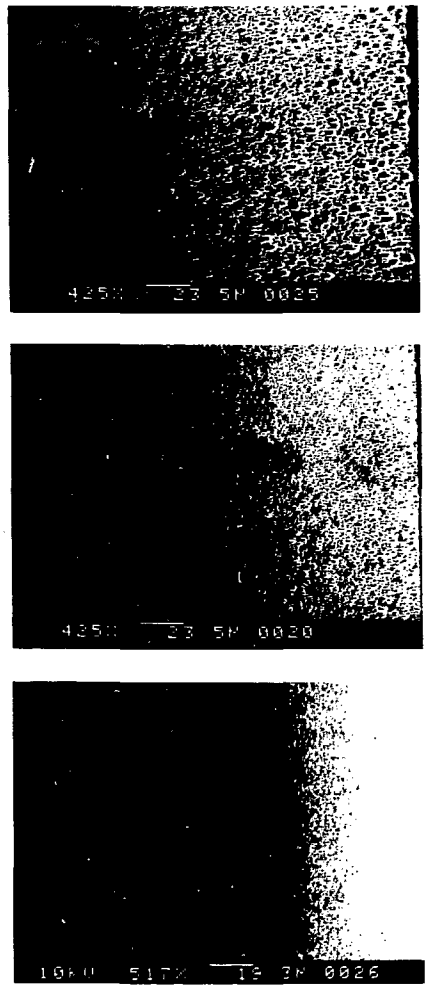

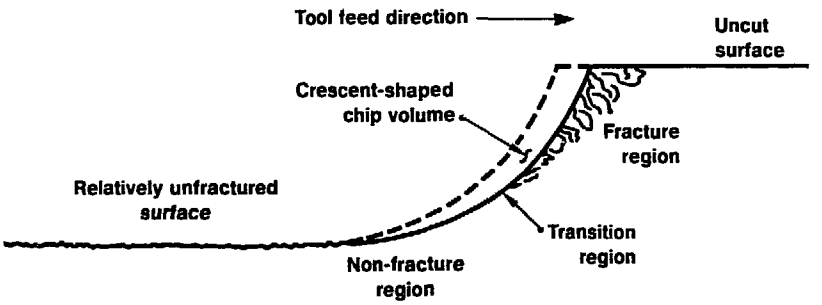

Fig. 2. (*Left*) **plan view of the shoulder region of the single-crystal silicon cut with a diamond tool at 1.5-μm feed/rev and 25-μm depth of cut, showing gradation of damage severity from leading to trailing edge, with damage-free final surface;** (*right*) **cross section of tool and shoulder geometry, showing decrease of uncut chip thickness from leading to trailing edge.**

References

Donaldson, R. R., C. K. Syn, J. S. Taylor, and R. A. Riddle (1987), "Chip Science: A Basic Study of the Single-Point Cutting Process," in Lawrence Livermore National Laboratory reports *Institutional Research and Development, FY86*, UCRL-53689-86, p. 72; *Engineering Research Annual Report, FY86*, UCID-19323-86, p. 35; ibid. UCID-19323-85-2, pp. 69-85; ibid., UCID-19323-85-1, p. 39.

Donaldson, R. R. and D. C. Thompson (1986), "Design and Performance of a Small Precision CNC Turning Machine," *CIRP Annals* **35**(1), 373.

Ikawa, N., M. Ohmori, S. Shimada, R. R. Donaldson, C. K. Syn, J. S. Taylor, and H. Yoshinaga (1987), "Minimum Thickness of Cutting in Micromachining (Report 2)—Chip Morphology at Nanometer Level" (in Japanese), Japan Society of Precision Engineering, Fall Meeting, Kofu, Yamanashi, Japan, October 12-14.

Riddle, R. A. (1986), *The Effect of Failure Criterion in the Numerical Modeling of Orthogonal Metal Cutting*," Lawrence Livermore National Laboratory, Livermore, Calif., UCRL-93745-ABS.

Syn, C. K., J. S. Taylor, and R. R. Donaldson (1986), "Diamond Tool Wear vs Cutting Distance on Electroless Nickel Mirrors," SPIE 30th Annual Symposium, San Diego, Calif., August 17-22, paper no. 676-26.

Taylor, J. S., C. K. Syn, T. T. Saito, and R. R. Donaldson (1986), "Surface Finish Measurements of Diamond-Turned Electroless-Nickel-Plated Mirrors," *Optical Engineering* **25**(9), 1013.

Taylor, J. S., C. K. Syn, R. R. Donaldson, and S. R. Patterson (1987), *Diamond Turning of Silicon for Optics Applications*, Lawrence Livermore National Laboratory, Livermore, Calif., UCID-21187.

FY87 $50,000

High-Temperature Radiant Properties of Metal Alloys

We have measured and reported the thermal radiative properties of surface-characterized high-purity metals and ceramics. The results of this study are now being used in the development of lightweight turbines for jet engines.

Principal Investigators:
Mark Havstad and
William McLean II

The optical properties of pure surfaces (emissivity, absorptivity, and reflectivity) and their underlying optical constants (index of refraction and extinction coefficient) are rarely known precisely enough for use in emerging technologies where these surfaces strongly influence performance. Liquid metals, for example, have such surface reactivity that both an ultra-high vacuum system (1×10^{-9} Torr or better) and a surface-characterizing apparatus are required to measure optical properties accurately. We developed an apparatus that measures emissivity and reflectivity of materials of known composition as functions of angle, temperature, wavelength, and polarization.

The Figure shows that, for sputter-cleaned uranium, normal spectral emissivity depends on wavelength. This dependence was long suspected, but unconfirmed until our experiments. The lower-wavelength (visible) emissivities are much higher than the longer (infrared) values.

We are also studying high-temperature ceramics that are used in the fabrication process of higher-performance rotors in advanced jet engines. We have data on one of three materials needed for finite-element calculations of heat flow and stress levels experienced as these turbine rotors cool after being cast.

In FY87, we integrated polarizing filters into our apparatus; we can now measure separately the reflectivity of light polarized parallel to and perpendicular to the plane of incidence, thereby making it possible to measure the optical constants of metals, even when their surfaces are molten and slightly curved. We can also analyze the polarization of the emission from hot samples to independently check our polarized reflection measurements. Computer programs that compute the complex index of refraction worked well for molten indium. We shall soon move on to molten uranium and stainless steel and begin to work with alloys.

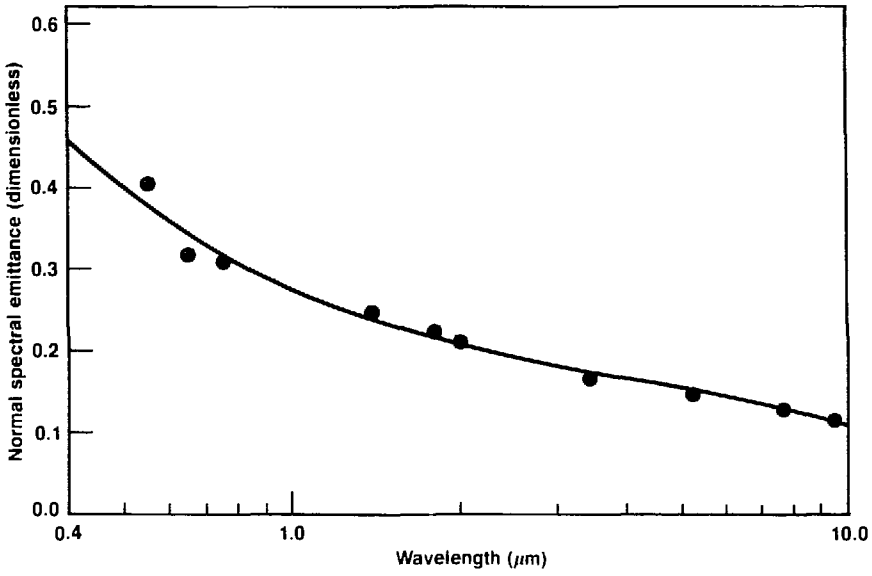

Normal spectral emittance of pure uranium measured in ultra-high vacuum. Auger electron spectroscopy performed in situ before and after the emissivity measurement verified surface composition.

FY87: $153,000

Calculations of Optical and Transport Properties of Solid-State Superlattices

Principal Investigators:
Jick H. Yee and William J. Orvis

Superlattice and quantum-well materials are produced by growing a stack of alternating layers of two different materials. Because they depend on the thickness and chemical composition of the layers, optical and transport properties of these materials can be tailored to a specific application. We are developing a general computer model based on pseudopotential techniques in energy-band theory to enable designers to calculate these properties for electron-device applications. Now that superlattice materials are available, a device designer is freed from the constraint of using the fixed material properties of a small number of semiconductor materials.

The objectives of this project are twofold:

- Construct a general computer model to investigate the physical properties of superlattice and quantum-well structure materials.
- Use this model to select suitable superlattice and quantum-well structure materials for electron-device applications.

A material's optical and transport properties, such as free carrier mobilities, optical absorption coefficient, and free carrier lifetimes, are determined by the material's crystal structure and chemical composition. These properties in turn determine whether a material is suitable for electronic devices. Hence, a material's properties can be selected by manipulating chemical composition and crystal structure. In the past, because few materials have optical and transport properties suitable for electronic applications, it was difficult to create devices for specific applications. A molecular beam epitaxy (MBE) machine now often makes it possible to tailor the optical and transport properties of a material to a prescribed electronic characteristic for an electron device.

A new class of materials, made by laying down alternating layers of two different materials in a stack, has optical and transport properties suitable for device applications. Since these materials are man-made, their properties are easily tailored by changing the thickness and the chemical composition of the layers. Materials in this new class are called superlattice or quantum-well structures.

Because superlattice and quantum-well structure materials have many potential applications, their optical and transport properties have been widely investigated. In spite of these efforts, more experimental and theoretical investigations of these materials' electronic properties are needed. To date, most theoretical studies on the electronic structure have been based on simple models for the potential energy of the electrons. Because some calculations neglected the spin-orbit coupling effect, their results do not apply to superlattice and quantum-well materials that are made from group 3, 4, or 5 compounds with small band gaps, such as indium antimonide. In addition, the investigations have concentrated primarily on the few superlattice and quantum-well materials that are made from compounds that have approximately the same size of unit cell.

The difference between our work and other investigations is that we use a realistic periodic potential in our models and include the effects of spin-orbit interactions in our calculations. Our computer model, which is based on a pseudopotential technique that can model realistic superlattice and quantum-well structures, is nearly completed. We have included the spin-orbital coupling effects in a superlattice, which were not included in the existing simpler models. Therefore, ours is the most complete model for computing the electron band structure of superlattice and quantum-well materials. Detailed data, such as the

pseudopotential form factors, the reciprocal lattice vectors, and the superlattice Brillouin zone, are being compiled, and we can soon begin coding.

In the meantime, we have also developed a simpler computer code to investigate the electron band structure of some superlattice and quantum-well materials for which the potential energy of the electrons can be approximated either by a square or triangular potential well (see the Figure). The results obtained from this investigation show that the wave functions of electrons in superlattice materials depend strongly on the shape of the wells. The energy-band structure diagrams for electrons in a number of simple superlattices were also calculated. From these energy-band diagrams, one can readily estimate the widths of the minibands by simply taking the difference between the energy of the highest and lowest energy state for each band within the first Brillouin zone.

In the near future, we will code our generalized models for Cray computers. We will then use this code to investigate the electron band structure and also the optical and transport properties of superlattice and quantum-well materials. From this investigation, we will select the most promising materials for electron device applications, such as laser diodes and heterojunction structures for LLNL programs.

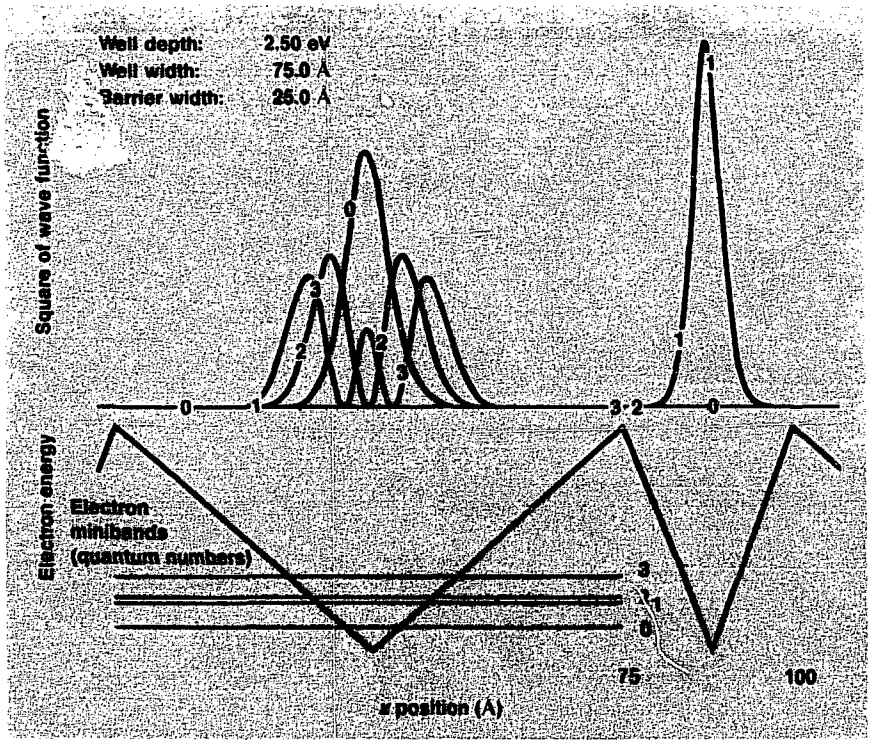

Energy bands, minibands, and square of the wave function for a superlattice structure that consists of alternating potential wells—typical of a doping superlattice. The square of the electron's wave function gives the probability of finding the electron at a particular location.

FY87 $303,000

GaAs High-Speed Circuits: Sample-and-Hold

Principal Investigators:
Steve P. Swierkowski and
Gregory A. Cooper

Our goals include developing a diagnostic integrated circuit (IC) that can sample transients at rates between 3 and 5 gigasamples/second. We are expanding wide-band electronics for diagnostics and sampling by introducing gallium arsenide (GaAs) systems with time resolutions in the range of 10 to 100 ps. (GaAs-based ICs are currently the fastest electronics technology.) We have demonstrated digital logic gates with 75-ps propagation times and analog sampling gates with 100-ps aperture times. Application in a prototype recording system has demonstrated a recording rate of 2.5 gigasamples/s.

Many high-energy physics experiments at LLNL require diagnostic recording systems for nonrepetitive, high-bandwidth transient waveforms. Additionally, wideband sensors for x rays, optical signals, and particles are almost always needed. Current instrumentation is frequently inadequate or impractical—especially for destructive experiments. Other programmatic needs in the wideband electronics arena include: x-ray sensors, optical sensors, wideband amplifiers, high-voltage noise supression/clipping circuits, photoconductive high-voltage switches, solid-state imaging, and high-bandwidth fiber-optic system components. To address LLNL's diverse experimental needs, we have expanded our IC capability from the existing silicon base into gallium arsenide (GaAs). We now use 1-μm gate transistors of the depletion-mode type, which are the baseline technology in industrial chips. Our integration level is lower than that of industry but suitable for most of the unorthodox, noncommercial circuit applications that we are pursuing.

We recently devoted much effort to advancing our GaAs devices to the state of the art. We are advancing toward heterostructure technology via molecular beam epitaxy (MBE) and electro-optic testing of ultra-high-speed circuits. Much of our work has been in conjunction with researchers at Stanford University (Rodwell et al., 1987), Amoco Corporation Research Center (Jain et al., 1987), and Howard University. Our processing technology is maturing with two test-vehicle transient-recording approaches: We have implemented low-risk hybrid and higher-risk integrated sample-and-hold schemes. The hybrid technology is now being used for diagnostics at the Nevada Test Site, and the integrated scheme has brought our skills to a practical and advanced level of maturity by pushing the limits of our IC performance parameters.

The hybrid sample-and-hold recording scheme was very successful on our first attempt, with a sampling rate of 2.5 gigasamples/s and a recording bandwidth of 1.7 GHz. One small-scale integration GaAs IC is used for each sample point. The points are obtained from a periodically tapped transmission line. We repackaged the instrument for field testing; the same GaAs ICs will be used, but the sampling rate will be doubled. An impr ved readout scheme will allow built-in self-calibration of gain and offset for this nearly completed effort. The theoretically estimated intrinsic aperture time of the GaAs sampling circuit is about 20 ps, but the external package parasitic inductance and the strobe pulse fall time will limit the effective aperture time to about 120 ps (Swierkowski and Cooper, 1987).

The integrated sample-and-hold chip that can record 20 samples is our highest-risk design. Our first effort was nearly fully functional and did sample, although not at full speed, and—more importantly—it performed well with nonuniform sampling intervals. Extensive circuit testing showed that the circuit speed was slowed by excessive interconnection capacitance caused by the metal support dielectric (polyimide). We have now developed an airbridge interconnect method that reduces the interconnection capacitance to the lowest possible value. The second-

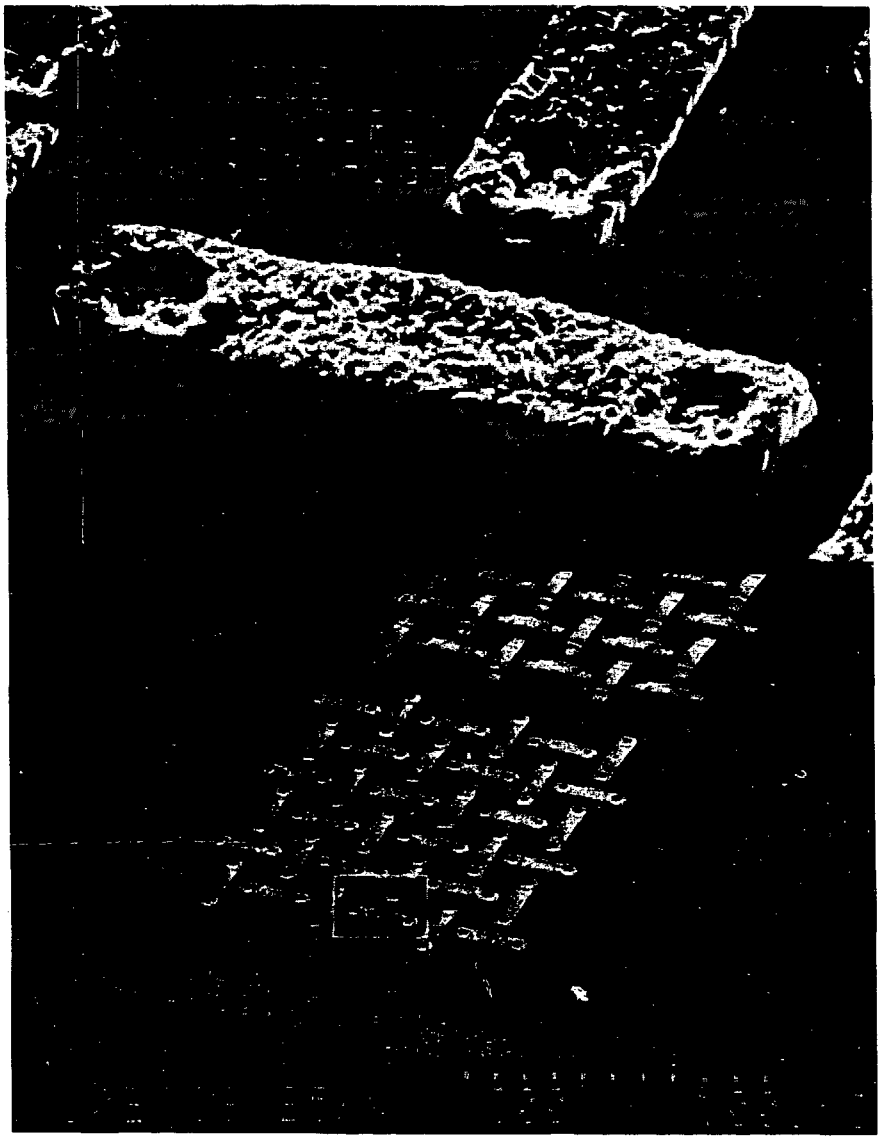

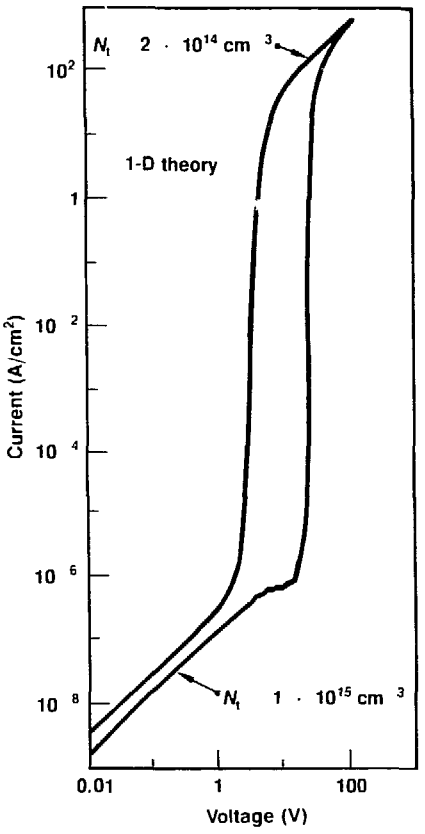

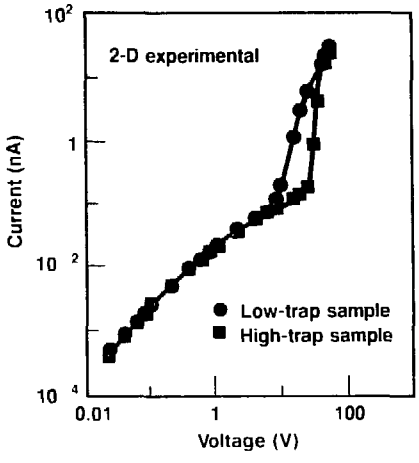

Fig. 1 *(Above).* **A split-field, dual-magnification image of an airbridge IC metal interconnect test structure with a cross-hatched, interwoven design. The second-level metal (bright features) is plated thick enough to be self-supporting, and air is the intermetal dielectric. This method for interconnecting ICs has the lowest possible parasitic capacitance.**

Fig. 2. Theoretical and experimental *I-V* leakage currents in GaAs ICs show qualitatively similar behavior over many orders of magnitude. This finding confirms our understanding of this phenomenon and allows us to implement preventive procedures. The complex effect depends on impurities (density N_t) and defects in the starting material, circuit processing, and circuit design and layout.

level metal is plated thickly enough to be self-supporting, and the intermetal dielectric is air. Figure 1 shows a cross-hatched, interwoven test pattern with alternating first- and second-level metals. The airbridge interconnect method should be the best by far for all of our very-high-speed IC projects. Testing also indicated that the variations in sampling intervals were caused by subcircuit parasitic leakage currents in the semi-insulating GaAs wafers, also known as backgating.

Our approach to this problem is two-sided. First, we will try to understand, quantify, and eliminate or greatly reduce the backgating phenomenon itself. Second, we are redesigning the circuit to be more tolerant or resistant to backgating. Significant progress has been made in both approaches, and successful circuit operation seems possible. We now understand the backgating phenomenon. Figure 2 shows that our experimental measurements confirm the features of a published model (Horio et al., 1986). We have identified several experimental approaches to alleviate this effect, which is endemic to the industry, and these processing experiments are currently in progress.

In summary, we have achieved short-duration (a few nanoseconds) transient digitization with record sampling rates and large bandwidths. Longer recording lengths now appear feasible with the recent progress in IC processing and circuit designs.

References

Horio, K., T. Ikoma, and H. Yanai (1986), "Computer-Aided Analysis of GaAs n-i-n Structures with a Heavily Compensated i-Layer," *IEEE Trans. Electron. Devices* **ED-33**(9), 1242.

Jain, R. K., X. C. Zhang, and S. P. Swierkowski (1987), "Electro-Optic Sampling Measurement of Picosecond Electrical Transients in GaAs FETs," *Technical Digest of the Conference on Lasers and Electro-Optics (CLEO)*.

Rodwell, M. J., C. J. Madden, B. T. Khuri-Yakub, D. M. Bloom, Y. C. Pao, N. S. Gabriel, and S. P. Swierkowski (1987), "Generation of 7.8-ps Electrical Transients on a Monolithic Nonlinear Transmission Line," submitted to *Electron. Lett.*

Swierkowski, S. P. and G. A. Cooper (1987), "GaAs High-Speed Circuits: Sample-and-Hold," *Electronics Engineering Thrust Area Report FY 86*, Lawrence Livermore National Laboratory, Livermore, Calif., UCRL-53700-87.

Nuclear Chemistry

Overview

Douglas A. Leich

The Nuclear Chemistry Division's primary mission is to provide diagnostic information on the performance of nuclear explosive devices by the use of radiochemical and isotopic techniques. We combine chemical and physical disciplines (e.g., inorganic and physical chemistry, geochemistry, radiochemistry, and nuclear physics) with expertise in radiation detection, isotope mass spectrometry, and data analysis. Applications of our work benefit such LLNL programs as Nuclear Test, Nuclear Waste Management, Treaty Verification, Safeguards Technology, Laser Isotope Separation, and Environmental Protection. Through IR&D-sponsored fundamental research in nuclear science and related disciplines, we can develop the scientific and technical leadership needed to most effectively contribute to LLNL programs.

In FY87, IR&D supported our experimental research in three fields: neutrino physics, isotope cosmochemistry, and condensed-matter physics. We also began development of several new techniques for chemical and isotopic measurements relevant to our future ability to support LLNL's mission.

We fabricated and began to assemble a major experiment to measure the mass of the electron antineutrino. Our experiment uses a gaseous atomic tritium source to eliminate all the known systematic problems associated with solid-state tritium sources.

Two major components of our cosmochemistry research program, our ^{187}Re half-life determination and our study of isotopic anomalies in meteorite chondrules, are nearing completion. In the former, we are now completing the measurement of nanogram quantities of osmium grown from rhenium sources. In the latter, we discovered titanium isotopic abundance variations that strongly support the view that the dust from which the chondrules formed dates from before the birth of the sun. We have also been applying our mass spectrometry techniques to problems in geochemistry.

Our research in condensed-matter physics, using annihilation radiation to measure the electronic structure of solids, was transferred early in FY87 from Nuclear Chemistry to the Chemistry and Materials Science Department.

We started three new IR&D projects in FY87 to develop high-sensitivity techniques for isotopic and chemical measurements. We assembled and are currently optimizing a photothermal deflection spectroscopy (PDS) system for measuring traces of lanthanides and actinides in solution. We also assembled a closely related photoacoustic spectroscopy (PAS) system to study the thermodynamic properties of actinides in solution. Finally, we developed a technique for precise isotopic analyses of nanogram quantities of osmium by inductively coupled plasma mass spectrometry (ICP-MS) and began the development of chemical techniques for future accelerator mass spectrometry (AMS) applications.

In FY88, we will calibrate and optimize the neutrino-mass experiment's high-resolution magnetic spectrometer with a ^{83m}Kr source and begin tritium measurements near the end of the fiscal year. We will begin to apply PAS and calorimetry techniques to study the solution thermodynamics of plutonium and uranium complexes. We will explore sensitivity-enhancement techniques for ICP-MS and develop ion-source techniques for AMS at the new LLNL tandem Van de Graaff accelerator. The cosmochemistry research project will conclude with the analysis and interpretation of data from our ^{187}Re half-life measurements and studies of titanium isotopic anomalies. We will complete our exploration of PDS and related photothermal techniques for submicromolar concentration measurements of actinide species.

Overall, the Nuclear Chemistry Division received $970,000 in IR&D funds in FY87.

FY87: $378,000
FY88: $350,000

Antineutrino Mass Measurement

Principal Investigators:
Wolfgang Stoeffl and
Daniel J. Decman
Co-Investigator:
Jon Engelage

We are building an apparatus to determine the electron antineutrino mass with a precision of a few electron volts (eV) by measuring the shape of tritium's beta-decay spectrum near its endpoint. Our spectrometer will have a toroidal magnetic field, a system to generate gaseous atomic tritium, and a new low-background counting system. We expect it to have a resolution at 23 keV of about 6 eV and to be in operation by spring 1988.

We are constructing a high-precision spectrometer to determine the shape of tritium's beta-decay spectrum very close to its endpoint as a means of measuring the rest mass of the electron antineutrino. The shape of any beta-decay spectrum depends on the distribution of energy and momentum among the three particles involved in beta decay: the recoiling atomic nucleus, the electron, and the neutrino. However, it is only at the extreme high end of the spectrum (where the electron has maximum energy and the momentum of the neutrino is almost zero) that the mass of the neutrino (if any) can have a measurable effect on this shape.

A precise measure of neutrino mass has been a goal of experimental physicists for decades. This measurement could impact issues ranging from how to account for the missing mass needed to close the universe to the validity of most modern Grand Unification Theories. In addition, a more precise value for the neutrino mass (even just setting an upper limit of 5 eV), together with the neutrino-burst data from the recent supernova, would greatly advance our understanding of this area of astrophysics.

All modern neutrino-mass experiments have been limited by systematic uncertainties and a background counting level that is high in comparison with the low beta-decay counting rate close to the endpoint. The systematic problems come mostly from having the tritium adsorbed in a solid. With a solid tritium source, calibration to determine the system resolution becomes impossible because there is no way to devise a corresponding solid calibration source. (It is not possible to substitute a calibration atom for tritium in a solid source or molecule without changing the chemical composition, and the effect of the chemical surroundings on the energy of the outgoing electron is too complex to be calculated precisely enough for our purposes.)

To avoid this difficulty, the tritium in our experiment will be in the form of a monatomic gas at low pressure (about 0.1 Pa) generated by an rf discharge. The source tube is kept at 100 K to prevent recombination of the atomic tritium. A series of high-speed pumps will collect escaping tritium before it can reach the spectrometer, send it to a cleaner, and recycle it back to the rf dissociator.

We will use the conversion-electron lines of ^{83m}Kr as a calibration standard: Because krypton is also a monatomic gas, the chemical environment (a good vacuum) will be the same as for the tritium. Hence we can directly determine our system's energy resolution.

Electrons from tritium atoms that decay in the source region will be guided into the large toroidal magnetic field of our spectrometer by a system of five solenoidal superconducting magnets. The field is produced by 72 current loops supported by the space frame shown in Figure 1. It will focus the electrons onto a cylindrical silicon detector that is segmented into 16 independent ring-shaped elements, each with its own amplifier system (Figure 2). The silicon detector has enough energy resolution to distinguish between "good" events (those that represent real beta decays) and background events (extraneous radioactive decays and secondary cosmic ray interactions).

In most spectrometers, the usual way to measure energy distribution is to vary the magnetic field systematically so as to "scan" the spectrum across the detector (observe one narrow slice of it at a time). This technique involves changing the current to the magnet, which implies that the heat dissipated will also change. For most purposes, this heating change is too small to affect the measurement.

Because of the extreme precision required in our experiment, we cannot tolerate thermal changes that could change the system geometry enough to introduce significant errors. To avoid this possibility, we will operate the spectrometer at a

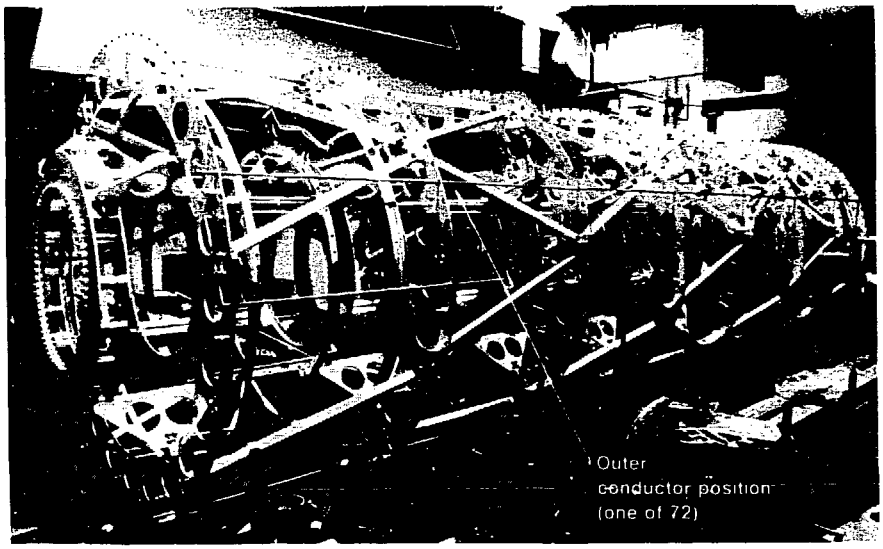

Fig. 1. The 8-m-long space frame for supporting the 72 current loops (not yet installed) that will produce our spectrometer's toroidal magnetic field. The large rings are 2 m in diameter.

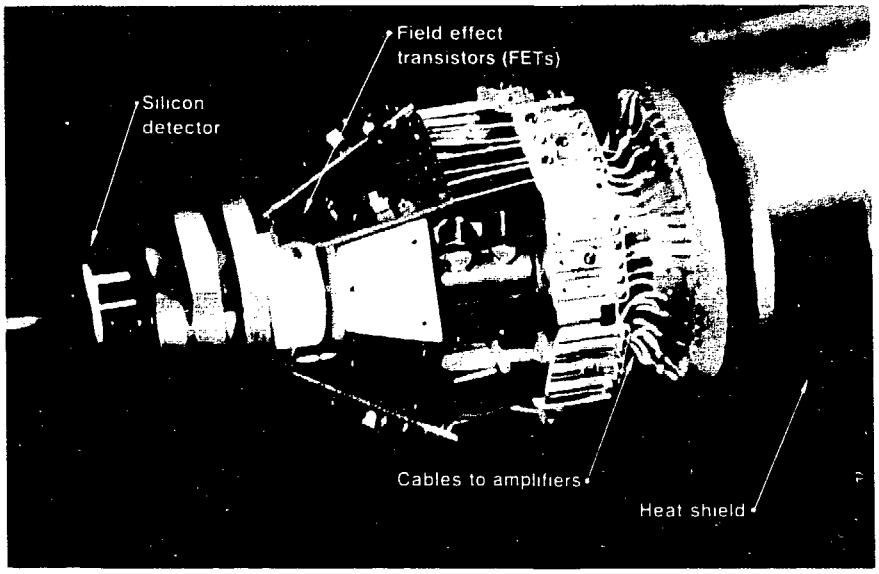

Fig. 2. The low-background silicon detector we plan to use in our neutrino-mass measurements. Preliminary tests indicate that its background counting rate is low enough to allow our spectrometer to detect the effects of any neutrino mass greater than 5 eV.

constant field (and constant current) and instead scan the spectrum by accelerating the emitted electrons with a variable electrostatic potential.

During FY87, we fabricated the hardware for the apparatus, completed a special nonmagnetic building to house it, and installed a large vacuum tank and source table. We leak-checked the vacuum tank and obtained pressures below about 2 μPa. We also obtained a good vacuum in the cryogenic source tube, both at room temperature and at liquid nitrogen temperature.

We expect to finish assembling the toroidal-field spectrometer early in 1988. We designed, constructed, and tested a source of ^{83m}Kr using commercially available ^{83}RbCl. We performed several tests of a 5-segment version of our 16-segment silicon detector and found that the background counting rate is low enough that our completed spectrometer should be able to detect the effects of any neutrino mass larger than 5 eV.

We will be devoting most of our time in FY88 to assembling and testing our apparatus. We expect to have an operating spectrometer system by spring of 1988. We plan to spend several months calibrating and optimizing the system, using an electron gun and the ^{83m}Kr source. After these tests are complete, we can introduce tritium into the system and start taking data.

FY87: $256,000
FY88: $50,000

Cosmochemistry Research

Principal Investigators: Sidney Niemeyer, G. Price Russ III, and George B. Hudson
Co-Investigators: Jeanne M. Bazan, Marc W. Caffee, Kenneth L. Cameron,[a] Julia C. Crowley,[b] Arthur R. Flegal,[a] Manfred Lindner, Gregory Nimz,[a] Henry F. Shaw, and Carol A. Velsko

[a]University of California, Santa Cruz.
[b]University of California, Davis.

Isotopic abundances and their variations from one sample to another yield clues to how the elements were synthesized in stars, how solid bodies formed in our solar system, and how chemical and tectonic processes have shaped our world. In FY87, we completed a second measurement of the ^{187}Re half-life, discovered titanium isotopic anomalies in meteorite chondrules, and completed our Rio Grande rift isotopic study. We also began a study of xenon in well gases to test whether ^{129}Xe anomalies are nonprimordial, i.e., generated in the earth's crust.

The overall objective of this research program is to advance our understanding of early solar-system processes and subsequent geochemical processes by measuring the variations in isotopic abundances that they produced. The isotope ^{187}Re has such a long half-life that measuring the ratio of ^{187}Re to its daughter ^{187}Os reveals clues to events that happened early in the life of the galaxy, long before our solar system began to form, and also promises to provide a valuable scheme for dating the formation of metallic and sulfide minerals in solar system bodies.

Isotopic anomalies in meteorites yield clues to the processes by which all the heavier elements were synthesized in the stars and also provide a means of tracing the early history of the solar system. Titanium isotopic anomalies are especially useful in deciding between alternative models of how dust formed and evolved in the early solar nebula.

In terrestrial geochemical studies, measurements of strontium, neodymium, lead, and noble-gas isotopic abundances help us to date geochemical events and to trace various geochemical fractionation processes. Increasingly, the isotopic compositions are augmented by analyses of specific trace-element abundances to further constrain our geochemical models.

In FY87, we established an experimental technique based on inductively coupled plasma (ICP) mass spectrometry to measure the ingrowth of nanogram quantities of ^{187}Os from ^{187}Re decay. We used this technique to analyze samples from a second rhenium source for a new ^{187}Re half-life determination. The results were in good agreement with those from our first source.

We also discovered anomalies in the abundance ratios of titanium isotopes in meteorite chondrules, the most prevalent constituent of the more primitive meteorites (see the Figure). In carbonaceous-chrondrite chondrules (e.g., those from the Allende meteorite), we generally find small excesses of ^{50}Ti. In the chondrules from ordinary chondrites (e.g., the Chainpur meteorite), we often find small deficits of ^{50}Ti.

The distribution of titanium isotopic anomalies in meteorites and their constituents supports the view that this isotopic diversity is a telltale clue to conditions in the clouds of primordial dust from which these chondrules and refractory-rich inclusions were formed. Work on silicon isotopes in the Allende meteorite also supports this view.

In terrestrial geochemistry, we developed a new hypothesis that ascribes observed variations in ^{129}Xe abundance to the decay of ^{129}I from spontaneous fission of ^{238}U rather than to the decay of primordial ^{129}I. This hypothesis has important implications for theories on how long outgassing and formation of the earth's crust could have taken.

In previous work, we analyzed gas from deep in the earth's mantle. In a new experiment to test this hypothesis, we found excess ^{129}Xe in a CO_2 well that is much more closely linked to crustal sources, which are unlikely to contain much primordial ^{129}I.

Our uranium-lead isotopic analyses of Rio Grande rift basalts

confirmed our earlier conclusion that they came from two chemically distinct reservoirs of magma in the mantle. The isotopic similarities of these basalts to other Western U.S. basalts and to ocean island basalts suggest that the same types of mantle reservoirs play important roles in generating many terrestrial basalts.

We established a technique for the precise analysis of lead isotopes in seawater, including for the first time the minor, nonradiogenic isotope. Early results clearly reveal a fine-scale isotopic structure in offshore water samples. This can be used to identify lead that comes from human activities and to study ocean currents and convective mixing processes.

Our objectives for FY88, the final year of this project, are to complete the analyses and data interpretation for our ^{187}Re half-life measurement and for our studies of titanium isotopic anomalies, and to publish the results. Other research directions that have been developed during the course of this project will be pursued separately, including a new IR&D project on Re-Os cosmochemistry.

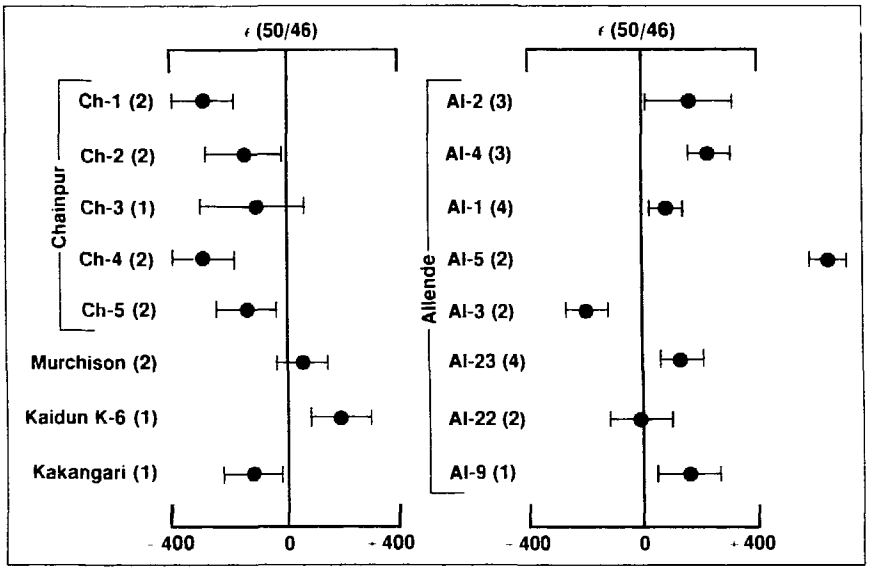

Titanium isotopic anomalies in chondrules. Each point represents the deviation of the ratios of ^{50}Ti to ^{46}Ti from that in natural titanium (in parts per million). Each result was obtained from the number of analyses shown in parentheses; errors are 2-sigma. Four of the eight chondrules from Allende, a carbonaceous chondrite, show well-resolved anomalies, usually excesses of ^{50}Ti. In contrast, the chondrules from Chainpur, an ordinary chondrite, typically show small deficits of ^{50}Ti, two of which are clearly resolved from the terrestrial composition.

References

Caffee, M. W. and G. B. Hudson (1987). "Excess ^{129}Xe in Terrestrial Samples, a Non-Primordial Origin," submitted to *Proc. 18th Lunar and Planetary Science Conference*.

Molini-Velsko, C., T. K. Mayeda, and R. N. Clayton (1986). "Isotopic Composition of Silicon in Meteorites," *Geochim. Cosmochim. Acta* **50**, 2719.

Niemeyer, S. (1986). "Ubiquitous Isotopic Anomalies in Ca, Ti, and Cr," *Proc. Sixth International Conference on Geochronology, Cosmochronology, and Isotope Geology*, Cambridge, England, June 30-July 4.

Niemeyer, S. (1987). "Titanium Isotopic Anomalies in Chondrules from Carbonaceous Chondrites," *Geochim. Cosmochim. Acta* (in press).

FY87: $35,000

Nuclear Solid State Research

Principal Investigators:
Michael J. Fluss,
Patrice E. A. Turchi, and
Charles E. Violet

We continued experiments using the annihilation radiation from positron-electron pairs to measure the electronic structure of solids. We also began high-pressure Mössbauer studies of plutonium alloys and effects studies in "hard-magnet" alloys. Nuclear Chemistry IR&D support ended with the transfer of the principal investigators to the Chemistry and Materials Science Department.

The focus of our efforts has been to characterize the electronic, magnetic, and atomic properties of condensed matter on a microscopic scale and to study the relation between the microscopic and macroscopic properties by using nuclear probe techniques. We combined theoretical and experimental methods, concentrating on a few technologically and fundamentally interesting materials systems. These include the electronic structure of transition metal alloys, heavy-fermion systems (including plutonium and its alloys), and radiation effects in permanent magnet materials, which are of potential interest to free-electron laser research.

We can now model the electronic structure of metal alloys and perform precise experiments on such systems. We completed the principal experimental apparatus needed (a two-dimensional angular correlation system) and tested it to meet the anticipated requirements for high electron-momentum resolution. The system consists of two large-area, position-sensitive gamma-ray detectors (Anger cameras) coupled to a multiparameter data-acquisition system.

We have been using this equipment and technique to study the new high-temperature superconductors lanthanum copper oxide (La_2CuO_4) and yttrium barium copper oxide ($YBa_2Cu_3O_7$). The deduced probability density for the positron wave function in the basal plane of La_2CuO_4 (Figure) shows that the positron is attracted most strongly to the oxygen atoms, less to the copper atoms, and is repelled by the lanthanum atoms. In $YBa_2Cu_3O_7$, the positrons tend to cluster near ordered vacancy strings. We hope this work will provide important new insights into the mechanism for high-temperature superconductivity.

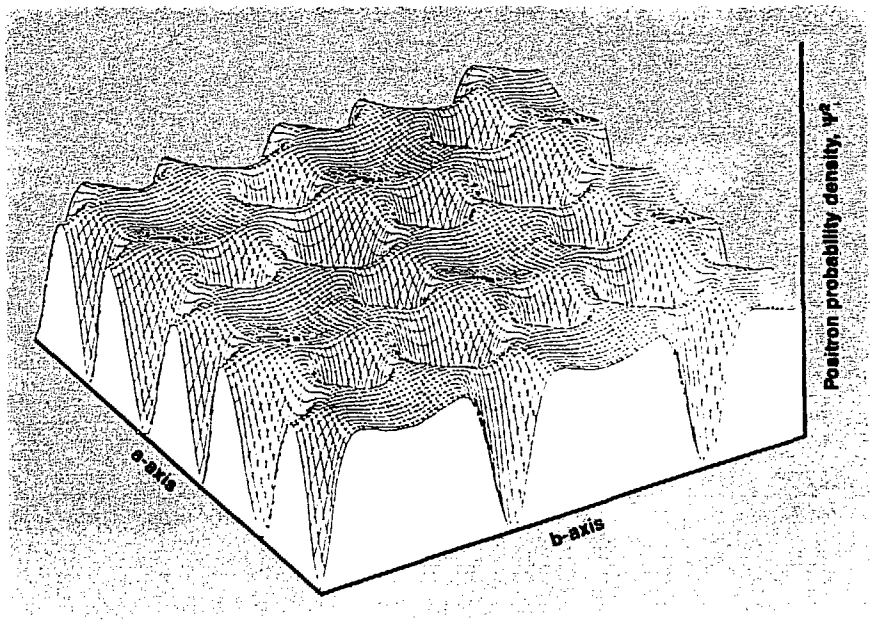

Positron probability density in the basal plane of the high-temperature superconducting material La_2CuO_4.

FY87: $53,000
FY88: $40,000

Ultrasensitive Laser Spectroscopy

Principal Investigator:
Robert J. Silva
Co-Investigator:
Richard E. Russo[a]

[a]Lawrence Berkeley Laboratory, Berkeley, Calif.

We are investigating the application of recently developed techniques of photothermal laser spectroscopy to the detection and study of actinide speciation at submicromolar solution concentrations. We have developed a photothermal deflection spectroscopy (PDS) system and determined, from measurements with Nd(III), that its sensitivity is about 200 times that of conventional absorption spectrometers.

The objective of this research is to investigate the application of recently developed photothermal laser spectroscopy techniques—photothermal deflection spectroscopy, thermal lensing spectroscopy, and photoacoustic spectroscopy—to the identification and quantification of actinide species in aqueous solutions at submicromolar concentrations. These techniques are potentially thousands of times more sensitive than conventional spectroscopic methods. The ability to identify and measure specific actinide species present at trace-level concentrations has become increasingly important to the measurement of thermodynamic properties, to high-level nuclear waste management research, and to environmental monitoring.

In our initial work, we assembled a photothermal deflection spectroscopy system using a Nd:YAG-pumped, pulsed dye laser for excitation and a helium-neon laser for probing (see the Figure). Using solutions of Nd(III), a good nonradioactive stand-in for trivalent actinides, we estimated a detection limit (signal/noise = 3) of 27 μmol/L from Beer's Law plots.

More recently, we used an argon-ion-pumped dye laser, modulated by a mechanical chopper, to develop a novel arrangement for background (solvent) subtraction in the PDS system. With this new arrangement, we estimated a detection limit of 5 μmol/L for Nd(III). This is about 1/200 the concentration detectable with conventional spectrometers. Although we used sample volumes of about 1 cm^3 in these measurements for convenience, it is possible to obtain good results with volumes only 1/10 as large.

In FY88, we propose to assemble a thermal lensing spectroscopy system using our existing equipment and to investigate the capability and sensitivity limitation of the system, again using solutions of Nd(III). At the end of the fiscal year, we expect to be able to assess the relative sensitivities and limitations of the three photothermal spectroscopy systems.

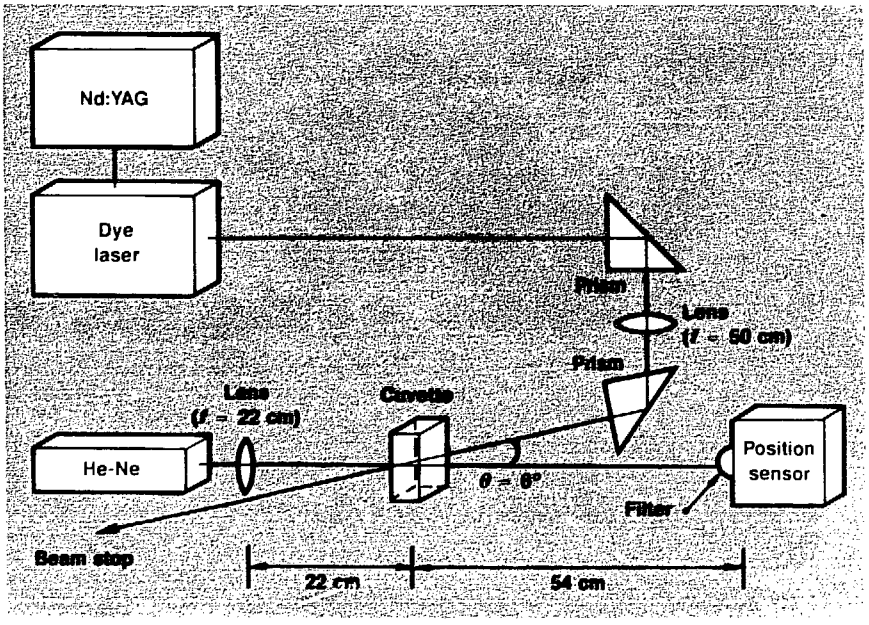

Experimental configuration for photothermal deflection spectroscopy.

References

Kliger, D. S. (1983), *Ultrasensitive Laser Spectroscopy* (Academic Press Inc., New York).

Russo, R. E. and R. J. Silva (1987), "Photothermal Spectroscopy Instrumentation for Sub-Micromolar Detection of Actinide Ions in Aqueous Solutions," The 11th Actinide Separation Conference, Lawrence Livermore National Laboratory, Livermore, Calif., June 1-4.

Thermodynamic Properties of the Actinide Elements

Principal Investigators:
Robert J. Silva and
Patricia A. Baisden
Co-Investigators:
Richard A. Torres and
Cynthia Palmer

Our measurements of the thermodynamic properties of actinide elements in aqueous solution will provide a concise and quantitative framework for understanding their chemical behavior under a wide variety of conditions. This knowledge will contribute to LLNL programs by helping us to develop novel actinide separation schemes and to predict the behavior of actinides in the environment.

We are investigating the chemical properties of actinide-element species in solution by measuring their free energies of formation and reaction enthalpies and entropies as a function of temperature, ionic strength, and redox conditions. These studies will generate a framework for understanding and predicting the chemical behavior of these elements under a wide variety of conditions. Because the actinide elements are the heaviest elements known, and because they and their daughters are among the more biologically hazardous nuclear-fuel-cycle radionuclides, studies of their chemical behavior offer both theoretical and practical benefits. Improved methods for isolating actinide elements from nuclear waste or test debris and for predicting their chemical behavior in the environment are important LLNL objectives.

To provide a much needed capability for measuring the free energies of formation of metal ions reacting with complexing agents and determining speciation at submicromolar concentrations, we have assembled and are testing a complete photoacoustic spectroscopy system (see the Figure). We also completed the design of a variable-temperature titration calorimeter to measure reaction enthalpies as a function of temperature.

In FY88, we will determine the sensitivity of our photoacoustic spectrometer and then begin studies of the hydrolysis and carbonate complexation of Pu(IV). We propose to investigate the feasibility of using laser-induced fluorescence to detect and study actinide ions in solution at subnanomolar concentrations. After we have constructed our variable-temperature calorimeter, established its sensitivity, and tested the complete system at elevated temperatures and pressures, we will begin studies of the heat of complexation of the uranyl ion UO_2^{++}

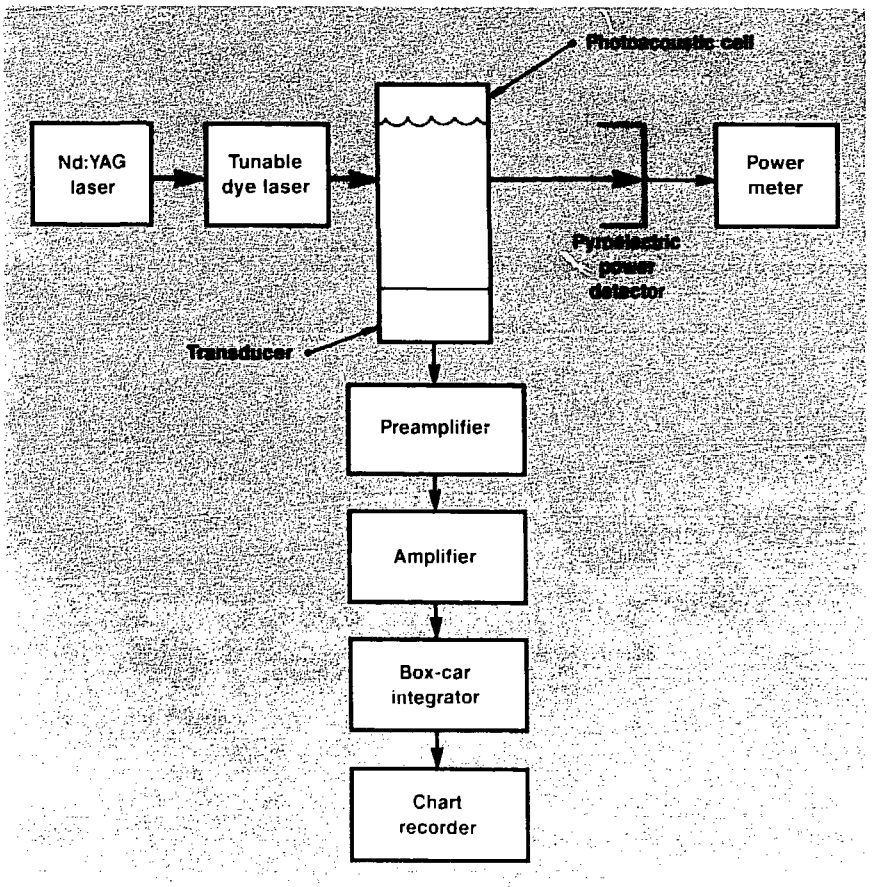

Experimental configuration for photoacoustic spectroscopy.

FY87: $133,000
FY88: $100,000

New Techniques for Measuring Isotopic Ratios

Principal Investigators:
G. Price Russ III and
Robert C. Finkel
Co-Investigators:
Douglas L. Phinney,
Kevin D. McKeegan, and
Jeanne M. Bazan

We are developing ways to measure isotope ratios in very small samples for elements and sample types not accessible by present techniques. This capability is needed in basic and applied research fields ranging from geochemistry to nuclear weapons diagnostics.

We are investigating three new isotope-measuring techniques: inductively coupled plasma mass spectrometry (ICP-MS), accelerator mass spectrometry (AMS), and secondary-ion mass spectrometry (SIMS).

ICP-MS can measure isotope ratios and elements in solution at concentrations less than parts per billion. To improve upon this performance, we are evaluating various data-collection schemes and sample-introduction systems. One of these, a special nebulizer, produced a tenfold improvement in sensitivity for multielement ICP-MS analyses from solution. In addition, we developed a sample introduction technique that gives our ICP-MS good sensitivity for nanogram-size samples of osmium. Isotopic compositions of the stable osmium tracers used in our rhenium half-life experiment measured in this way agree well with those of the supplier (Oak Ridge National Laboratory). We also developed methods to reduce the instrument's blank and sample-to-sample memory below the part-per-thousand level.

We are helping to develop AMS for use on the Physics Department's new tandem Van de Graaff accelerator. We are contributing our expertise in the development of ion-source chemical techniques for specific AMS applications and in high-mass-resolution ion optics to detect rare heavier isotopes (masses greater than 40).

We are also modifying the electronic controls of our SIMS instrument (ion microprobe) to enable it to operate in the high mass-resolution mode needed to avoid isobaric interferences (from other ions that have the same mass/charge ratio). Preliminary attempts to produce negative niobium ions for SIMS, while suppressing isobaric molybdenum and zirconium ions to improve resolution, gave promising results for possible AMS applications to nuclear test diagnostics. We also use the ion microprobe to simulate an AMS source in evaluating ways to ionize various elements to be analyzed with AMS.

In FY88, we will more fully explore how to apply the alternative sampling methods we have already used to enhance ICP-MS sensitivity for multielement and isotopic analyses. We will also install and test an AMS ion source and detection system on the new tandem Van de Graaff accelerator. We will continue to develop chemical techniques for AMS sample preparation—for example, those for measuring the long-lived radionuclides ^{36}Cl and ^{129}I.

With SIMS, we will be developing ways to measure the isotopic composition of oxygen in solids, which is useful for studying high-temperature superconductors and diffusion such as that in rock-fluid interactions. We will also develop the capability to measure osmium isotope ratios on the ion probe, so as to decide whether to use ICP-MS or SIMS in future rhenium-osmium studies.

References

Beer, J., G. Bonani, H. J. Hofman, M. Suter, A. Synal, W. Woelfli, H. Oeschger, U. Siegenthaler, and R. C. Finkel (1987). "^{10}Be Measurements on Polar Ice: Comparison of Arctic and Antarctic Records," *Nucl. Instrum. Methods* (in press).

McKeegan, K. D. (1987). "Oxygen Isotopic Abundances in Refractory Stratospheric Dust Particles: Proof of Extraterrestrial Origin," *Science* **237**, 1468.

Russ, G. P. III and J. M. Bazan (1987). "Isotopic Ratio Measurements with an Inductively Coupled Plasma Source Mass Spectrometer," *Spectrochim. Acta* **42B**, 49.

Russ, G. P. III, J. M. Bazan, and A. R. Date (1987). "Osmium Isotope Ratio Measurements by Inductively Coupled Plasma Source Mass Spectrometry," *Anal. Chem.* **59**, 984.

Physics

Overview

Bruce Tarter
John Nuckolls

The Physics Department's IR&D work has emphasized innovative and disciplinary research that could have a major long-term effect on LLNL's defense and energy programs. Our efforts are equally divided between projects that exploit advances in high-speed computers and those that are pushing the state of the art in experimental physics.

We made significant progress in projects related to magnetic and catalyzed fusion. Our effort to construct a comprehensive computer code to model magnetic fusion energy experiments was quite successful for mirror machines. The methodology developed has other applications and is now being used to build a general tokamak-modeling code. We are well along in fabricating a high-pressure cell for accelerator experiments to study the potential of muon-catalyzed fusion, and our project to search for quarks (possible fusion catalysts) should soon be gathering data.

Much of our computational work has focused on combining hydrodynamics with other processes. Our research on optimal methods for multiprocessor computers has led to the construction of a two-dimensional free-Lagrangian hydrodynamics code as a test vehicle; the anticipated addition of radiation transport will challenge these techniques. We used recent advances in chaos theory to model mixing at fluid interfaces, and the results will be incorporated in weapon-design codes. The expansion of our global-circulation model now allows us to include the effects of oceans on atmospheric circulation. We extended our atmospheric chemistry models to incorporate the presence of trace gases that, cumulatively, may affect the environment as much as do major constituents.

A different class of computational modeling has used large multidimensional Hartree-Fock codes to search for shape isomers as candidate nuclei for gamma-ray lasers. We hope to begin to study likely candidates in the next year.

We continued work on several experimental projects and initiated two new ones. In our laboratory x-ray-laser design project, we achieved substantially shorter wavelengths and are now close to the "water window" required for biological applications. We designed and began assembling the cryogenic apparatus needed to determine the electron neutrino mass at a level (less than 10 eV) that would yield important cosmological information. Test runs with implanted-ion tritium sources verified our procedures for acquiring and analyzing data and also gave a 27-eV statistical sensitivity in the neutron mass determination, which is consistent with other ongoing experiments. We also designed and began to assemble a compact, high-repetition, two-stage gas gun that will significantly enhance our high-pressure physics capability.

We began an intensive effort to metallize molecular hydrogen at high pressure in a diamond-anvil cell; this project will provide a benchmark for our theoretical models. Finally, we began a new project to use very-short-pulse (less than 100 fs) lasers to study the properties of dense plasmas at "preheat" conditions. The short pulse length allows us to heat solid materials to temperatures as high as several electron volts before the materials expand; we can then test and improve our theoretical models, which are quite uncertain in this regime of importance to weapons and inertial confinement physics.

Overall, the Physics Department received $2,300,000 in IR&D funds in FY87.

FY87 $229,000
FY88 $150,000

Computer Simulation of Magnetic Fusion Machines

We have developed an advanced general-purpose code development system called BASIS and applied it to programs that simulate the behavior of tandem-mirror and other magnetic fusion experiments.

Principal Investigators:
Paul F. Dubois and
Alex Friedman

The goals of this project, conducted jointly by the Physics Department and the Magnetic Fusion Energy (MFE) Division, are to design and implement an advanced general-purpose code development system and then use this system to build computational tools to further our understanding of controlled fusion experiments. Our intent was to introduce a computing environment that would enhance the productivity of code developers and code users alike. The first major application of this system was the MERTH tandem mirror code. It was expected that other BASIS codes would also be constructed as the system matured.

The BASIS code development system now supports about two dozen programs, including the MERTH tandem mirror simulation for which it was originally designed; MUMAK, a point-model tokamak plasma simulation; and TETRA, the national tokamak systems code. BASIS consists of

- A program (MAC) that processes a file containing descriptions of variables and functions.
- A program (MPPL) that preprocesses macros (including the output of MAC) and extended Fortran statements to make a standard Fortran source.
- A runtime resident package that provides database and memory management, and user interface functions.

Several utilities maintain programs and convert existing programs to BASIS. The user interface is now a complete programming language, including looping and conditional constructs, user function definition, and variable declarations. Through this language, the user of a BASIS program can set, display, and plot physics variables. All BASIS programs have this same user interface; a configuration procedure determines which physics modules are attached. We have written four manuals and have begun educational programs. The system is available on computers in the National Magnetic Fusion Energy Computer Center (NMFECC) and in the Livermore Computer Center (LCC).

MERTH is a useful tool for supporting tandem mirror experiments. We improved it by upgrading two of its components: the electron-cyclotron resonant-heating calculation and the TRQ plasma package. TRQ is a coupled-point model that employs both rate and constraint equations to advance the plasma forward in time. It was improved by the development of a consistent scheme for particle accounting and (most fundamentally) by a revised structure whereby rate and constraint equations are treated on a consistent footing and can be freely interchanged (as can the dependent variables that describe the

state of the plasma). The solution is carried out under the control of the differential-algebraic solver DASSL. For example, it is possible to solve for the particular value of a model parameter that yields a steady state at given temperatures and densities or to solve for densities or temperatures as functions of time. We have found very useful the capability to solve for a steady state directly without doing time-evolution of the equations. The knowledge gained while constructing this code has given us insight into how best to structure a rate code. Our greatest difficulty was in formulating accurate models to describe the physics of hot- and warm-electron distributions. Much work was devoted to this problem, but our understanding remains incomplete.

The BASIS system has become an important tool to be exploited in other projects, and work on it will continue. Further development of MERTH was suspended when the emphasis of the MFE program changed to concentrate on the tokamak approach to controlled fusion. A follow-on project, dedicated to the development of improved modeling capabilities for toroidal systems, is being initiated.

References

Benedetti, C. M., P. F. Dubois, P. C. Willmann, and Z. C. Motteler (1987), *BASIS User's Manual—A Supplement of Recent Improvements to BASIS*, Lawrence Livermore National Laboratory, Livermore, Calif., M-189 Supplement.

Dubois, P. F. (1987), "BASIS: Setting the Scientist Free," *NMFECC Buffer* (May 1987), p. 4, and *LLNL Tentacle* (August 1987).

Dubois, P. F. (1987), "MPPL: Making Fortran Bearable," *NMFECC Buffer* (June 1987), p. 19, and *LLNL Tentacle* (September 1987).

Dubois, P. F. (1986), *MPPL User's Manual*, Lawrence Livermore National Laboratory, Livermore, Calif., M-187.

Dubois, P. F. (1986), *Writing BASIS Packages*, Lawrence Livermore National Laboratory, Livermore, Calif., M-194.

Dubois, P. F. and Z. C. Motteler (1987), *BASIS User's Manual*, Lawrence Livermore National Laboratory, Livermore, Calif., M-189.

Friedman, A., M. E. Rensink, and W. M. Nevis (1987), "Consistency Issues and Improvements in the MERTH Code TRQ Package," *TMX-U Final Report*, G. D. Porter, Ed., Lawrence Livermore National Laboratory, Livermore, Calif., UCID-20981.

Hindmarsh, A. C. (1980), "LSODE and LSODI, Two New Initial Value Ordinary Differential Equation Solvers," *ACM-Signum Newsletter* **15**(4), 10.

Petzold, L. R. (1982), "A Description of DSSL: A Differential/Algebraic System Solver," *Proc. IMACS World Congress*, Montreal, Canada, August 1982, Sandia National Laboratories, Livermore, Calif., SAND82-8637.

FY87: $421,000
FY88: $310,000

Fusion Catalysis

Principal Investigators:
Berni J. Alder,
William B. Durham, and
Hugh Heard[a] (Muon Catalysis);
Charles Hendricks (Quark Search)

[a]Deceased, 1987.

We are exploring two approaches to catalyzed fusion. The major effort is focused on muon-catalyzed fusion, in which we are investigating optimum conditions to enhance the yield of the process. For a key series of experiments to be conducted at the Swiss Institute for Nuclear Research, we are constructing a high-temperature, moderate-pressure cell. Both theory and experiment predict that conditions obtained in our cell should produce the highest fusion rates ever achieved. In addition, we are using droplet generators and drop towers to search for long-lived quarks, which might be extraordinarily effective fusion catalysts. This scheme has a throughput many orders of magnitude higher than competing schemes and could test a variety of materials.

Muon-Catalyzed Fusion. We are building a vessel that holds DT mixtures at temperatures as high as 2000 K and pressures of 2000 atm. Our goal is to measure cycling rates and neutron generation at high temperature. In particular, we expect to be able to determine the peak in the cycling rate with temperature, even though recent experiments indicated the presence of nonequilibrium conditions with temperatures around 2000 K. Technical constraints on the apparatus are that the target be sufficiently large and the walls sufficiently thin so that enough muons enter the target to produce accurate results. Also, the modest pressures are needed to permit measurably nigh densities at these high temperatures. The DT mixture should also be free of any significant impurities. The apparatus will be built and tested at LLNL and then sent to the Swiss Institute for Nuclear Research in Villigen, Switzerland, for the muon experiments.

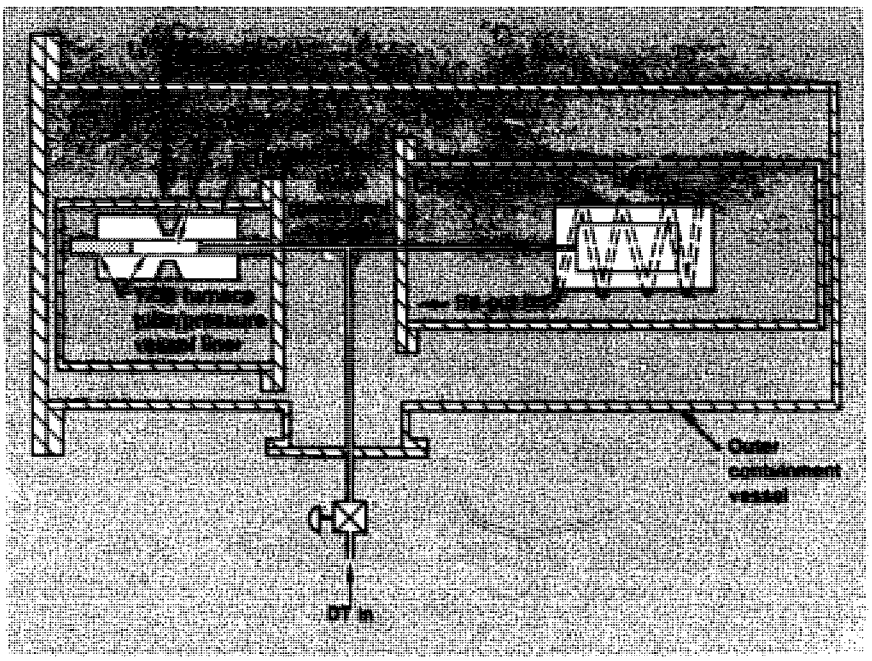

Apparatus for muon-catalyzed fusion.

The central part of the apparatus, shown in cross section in the Figure, is the target assembly (on the left-hand side of the drawing). The target assembly consists of a sealed metal liner surrounded by a ZrO_2 insulator, which in turn is surrounded by a pressure vessel made of high-strength beryllium-copper. The liner, which is made of TZM, a nearly pure molybdenum alloy, serves simultaneously as a leak-free container for the gas and a resistance heater. A test showed that an electrical current of approximately 800 A passed through the liner will

raise its central temperature to 2000 K. The target vessel is pressurized by a new, simpler design in which the DT is condensed in a cold trap by liquid helium at approximately 20 K. That trap is then connected to the target cell and the DT allowed to warm up to the desired temperature and pressure. The target cell has been tested with argon gas to 1700 K and 500 atm. Complete assembly and testing will occur early in FY88.

After we complete testing at LLNL, the major goal for FY88 is to ship the experimental assembly to the accelerator in Switzerland and perform measurements in the muon beam. Our secondary goal is to use the practical experience gained from the present vessel to design a second-generation vessel capable of achieving higher temperatures and pressures in larger-volume samples.

On the theoretical side, ca ations are now under way to improve the stripping probability value for the muon captured by the α particle in the fusion process. The error in this value is the most likely cause of the discrepancy between experiment and theory. In FY88, we also hope to improve the value for the Auger rate—that is, the electron emission rate—for the decay of the muon from the excited state to the ground state, so that we may investigate whether fusion can be made to take place in the excited state. The idea would be to use multiphoton excitation to remove the electrons, preventing decay. If this were possible, a much lower sticking probability in the excited state would result in a considerably larger neutron yield.

Quark Search. We concentrated on generating stable streams of droplets with diameters less than 20 μm. These droplets should be spaced at least 50 diameters apart. Their small size makes it possible to separate and detect 1/3, 2/3, and integer charges, and a small number of total integer charges, per droplet. We have also developed high-resolution, high-speed techniques for detecting the time and position of arrival of the particles at the endpoints of their trajectories.

During the next year, we will complete the detection system, perfect the particle-generation apparatus, and carry out the assay of a wide variety of materials—including samples of niobium offered for test by Professor William M. Fairbank of Stanford University and samples of materials that have been irradiated in high-energy accelerators at the Fermi and CERN laboratories.

Physics Codes for Parallel Processors

Principal Investigator:
Peter G. Eltgroth

We are exploring new approaches to the computer solution of problems of general interest to LLNL. Current investigation centers on developing a parallel code to treat hydrodynamics and radiation. The two-dimensional code FLIT2D uses novel data structures to allow maximum parallelism. The hydrodynamics has been successfully tested against other code results. Development continues with emphasis on parallel efficiency, realistic boundary treatment, and radiation physics.

The general goal of this investigation is to obtain solutions to a large class of physics problems with a high degree of computational parallelism. Specifically, it is desirable to break a problem up into work units equivalent to the update of a zone. Since many LLNL problems have at least tens of thousands of zones, this approach provides an abundance of work for multiprocessors now available. Vectorizing a code provides parallelism but at the expense of a computational style that is more rigid and less general than the high-level approach.

By returning to the original physics formulation of problems, we have developed new algorithms suitable for implementation on a wide variety of parallel computers. We devised computer codes to test the new ideas. These codes are written so that an arbitrary number of processors can be brought to bear on a problem without changing the source code in any way. The most fully developed code is FLIT2D, which is written in C with extensions to support multiprocessing. This physics code is based on a two-dimensional free-Lagrange treatment of multimaterial hydrodynamics. Other physical processes, such as radiation physics, will be added to the code as time permits. The code has been developed as if it were to be a production code, with general input-output capabilities and access to equation-of-state facilities. It runs on both uniprocessors and multiprocessors and is relatively portable from one multiprocessor to another. Its auxiliary packages will include graphics and a performance monitor that reports on its own efficiency. The hydrodynamics itself runs in a style equivalent to an implicit treatment, although technically it does not belong to either the implicit or explicit category.

Major effort in the past year went toward developing asynchronous physics solution details and a general code structure suitable for parallel computation. An arbitrary number of large work modules can be made available for parallel execution at a high level in the code. Physics subroutines can be coded without concern about implementing details of parallel execution.

References

Eltgroth, P. G. (1985), "Free Lagrangian Methods, Independent Time Steps, and Parallel Processing," *The Free Lagrange Method*, M. J. Fritts, W. P. Crowley, and H. Trease, Eds. (Springer-Verlag, New York), p. 114.

Eltgroth, P. G. (1986), "Physics Codes on Parallel Computers," *Proc. 1985 International Conference on Parallel Computing*, M. Feilmeier, G. Joubert, and U. Schendel, Eds. (Elsevier Science Publishing Company/B. V. North-Holland, New York), p. 213.

FY87: $54,000
FY88: $90,000

Enhanced Modeling Capabilities to Study Atmospheric Trace Gases

This project is designed to enhance LLNL's modeling capabilities to address key questions related to how trace gases affect climate and the ozone layer. We have begun to analyze and further develop the new zonally averaged model of the troposphere and stratosphere.

Principal Investigator:
Donald J. Wuebbles

The goal of this project is to extend LLNL's state-of-the art modeling capabilities to study trace gases and their influence on the global atmosphere. These models will also be applied to environmental problems.

We have improved both the numerical solution of atmospheric dynamical processes and the overall computational running time of the zonally averaged two-dimensional model of the troposphere and stratosphere. The overall numerical solution of the trace gas continuity equations has been changed to allow for the incorporation of an advanced technique for treating tracer transport. In addition, through more efficient treatment of the chemistry terms, we have improved the overall running time of the model by nearly a factor of 2 with no loss of accuracy. We began several studies (see the Figure) with the two-dimensional model to examine the combined effects of trace gases, solar cycle variations, and the nuclear test series on determining the trends in ozone since the late 1950s. This is the first time that a two-dimensional model has been used in an attempt to explain the observed ozone changes over this time period and the first time that a model of this complexity has been used to study the possible effects of the nuclear test series of the late 1950s and early 1960s.

In FY88, we plan to examine approaches for improving the theoretical capabilities of one-dimensional and two-dimensional models to represent global dynamical processes. In particular, we would like to improve the representation of chemistry-wave (chemical eddy) interactions and to study the potential importance for including the influence of semi-annual oscillation effects from Kelvin and gravity waves on the model-calculated distributions of trace species. We will begin model-validation studies to compare results with available satellite data.

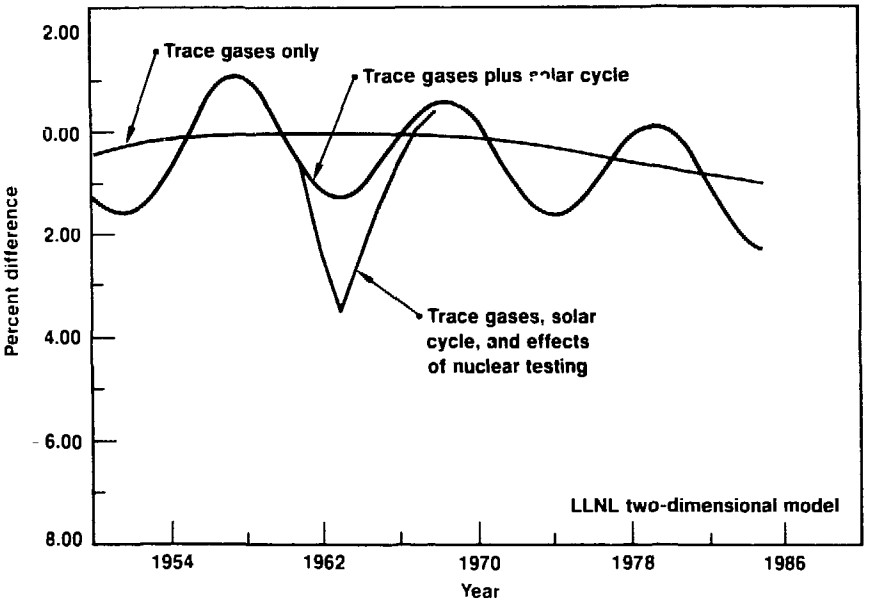

The change in the total ozone amount (averaged globally) relative to 1960 is shown for three different calculations made from our two-dimensional model of the troposphere and stratosphere. The flattest curve would be expected if the changes in the ozone over the past 35 years were due solely to trace gas emissions of chlorofluorocarbons (e.g., $CFCl_3$, CF_2Cl_2), methane (CH_4), and nitrous oxide (N_2O). The next curve adds in the calculated effects of changes in solar flux during the 11-year sunspot cycle. The third curve includes effects of atmospheric nuclear testing in the late 1950s and early 1960s. According to this model, trace gases accounted for only a small change in total ozone, but stratospheric nuclear tests resulted in a 2% global decrease in ozone in the early 1960s. Actual observations of the ozone amount agree well with the third curve predicted by our model.

Nonlinear Dynamics: Fluid Instabilities and Chaotic Systems

Principal Investigators:
James A. Viecelli
(Fluid Instabilities) and
Minh Duong-Van
(Chaotic Systems)

Our effort in nonlinear dynamics has two components. Extensive two-dimensional numerical simulations of the interfaces of Rayleigh-Taylor unstable materials have led to a statistical characterization of the mixed region. This is being translated to a set of prescriptions for more general hydrodynamics codes. Additionally, we have explored the fundamental properties of chaotic systems to extend our ability to predict the behavior of turbulent flow.

Fluid Instabilities. We are seeking a better understanding of fluid-mixing instabilities—in particular, the geometrical properties of the mixing region and the effect of compressibility on increasing the mixing rate.

In the case of Rayleigh-Taylor instability, Lyapunov exponents for the mix problem can be computed, and the fractal characteristics of the mixed region can be determined (Viecelli, 1987). More recent compressible hydrodynamic computations show that probability distributions for the chord lengths of ray paths through the mix can also be obtained. This quantity is of interest for radiation transport computations. Compressible flow runs are also providing data on turbulence amplification. We studied an implosion problem with a known similarity solution by numerical integration when the initial conditions are perturbed by a random eddy field. Eddy kinetic-energy density amplifications approaching 256× are obtained for this 16×-compression case of two-dimensional flow in the limit of viscosity with initial eddy kinetic energy going to zero.

Chaotic Systems. Nonlinear systems that manifest chaotic behavior constitute a major topic in theoretical physics. A key issue is the predictability of dynamical systems, which depends on whether the system is random or chaotic. If the system is random (infinite dimensions), the information required to make a prediction is infinite, and there is no hope for predictability. However, if a turbulent system is chaotic and has finite fractal dimensions, predictability may be possible. We have studied this question for several systems.

To focus on this topic, we studied the nature of turbulence on a lattice and also the information contained in time series of experimental data (Duong-Van, 1986; Duong-Van et al., 1986; Duong-Van and Feit, 1987). We next analyzed the continuation of Feigenbaum's work (1979 and 1980) on the bifurcation of the logistic map (or any quadratic map). At the onset of turbulence, Feigenbaum found that universal numbers α and δ fit all experimental data on the onset of turbulence. However, the theoretical ratio of the successive bifurcation power spectra differs from experimental data by a factor of 50. Furthermore, the power spectrum at the turbulent regime is flat and inconsistent with the data, which has a spectral index of –5/3. We found that to bring out the macroscopic limit, we should average by the technique described by Duong-Van (1986) and Duong-Van and Feit (1987). This result is described in Duong-Van (1987a).

The second topic we studied was the calculation of phase-transition phenomena with the strange-set mathematics developed by Feigenbaum et al. (1986). We were able to identify the free energy, entropy, internal energy, and temperature of thermodynamics with strange-set variables. Then the behavior of the specific heat as a function of lattice size could be determined (Duong-Van, 1987b and 1987c). We are looking into applying this work to develop a fast-switch design that may be rapid enough (picosecond switching) for use in power switches. This effort is a collaboration between F. Villa at Stanford University (SLAC) and J. H. Yee of LLNL's Electronic Engineering Department. Results from calculations at Stanford and from LLNL codes on gas breakdown show that it is feasible to develop a high-pressure switch in the picosecond regime (Villa, 1986; Khanaka et al., 1987).

References

Duong-Van, M. (1987a), "Macroscopic Chaos From Microscopic Fluctuations with Time Averaging," *Proceedings of the International Conference on the Physics of Chaos and Systems Far From Equilibrium*, M. Duong-Van, Ed. (Monterey, Calif., January 1987); submitted to *Phys. Rev. A*.

Duong-Van, M. (1987b), "Relation Between Maximization of Information and the Fokker-Planck Equation at the Phase Transition," submitted to *Nuclear Physics B (Field Theory and Statistical Mechanics)*.

Duong-Van, M. (1987c), "Phase Transition of Multifractal Maps," *Proceedings of the International Conference on the Physics of Chaos and Systems Far From Equilibrium*, M. Duong-Van, Ed. (Monterey, Calif., January 1987); also published in *Proceedings of the International Workshop on Nonlinear Phenomena*, G. Marx, Ed. (Lake Balaton, Hungary); submitted to *Phys. Rev. Lett.*

Duong-Van, M. (1986), "Instabilities on Turbulence and the Physics of Fixed Points," *Dimensions and Entropies in Chaotic Systems*, G. Meyer-Kress, Ed. (Springer-Verlag, New York), p. 171.

Duong-Van, M. and M. D. Feit (1987), "Comments on Power Spectra of Discrete Stochastic Time Series," *Phys. Lett. A* **119**, 388.

Duong-Van, M., M. D. Feit, M. Pound, and P. Keller (1986), "The Nature of Turbulence in a Triangular Lattice Gas Automaton," *Physica* **23D**, 448.

Feigenbaum, M. J. (1980), "The Transition to Aperiodic Behavior in Turbulent Systems," *Commun. Math. Phys.* **77**, 65.

Feigenbaum, M. J. (1979), "The Universal Matrix Properties of Nonlinear Transformations," *J. Stat. Phys.* **21**, 669.

Feigenbaum, M. J., M. H. Jensen, and I. Procaccia (1986), "Time Ordering and the Thermodynamics of Strange Sets: Theory and Experimental Tests," *Phys. Rev. Lett.* **57**, 1503.

Khanaka, M. D., M. Duong-Van, J. H. Yee, and D. J. Mayhall (1987), *Modeling Picosecond Switching Phenomenon in High-Pressure Gases and Its Possible Application for Pulsed Power*, Lawrence Livermore National Laboratory, Livermore, Calif., Director's IR&D proposal 88-03.

Viecelli, J. A. (1987), *Estimating Limits on Resolution and Predictability in Computations of Hydrodynamically Unstable Flows*, Lawrence Livermore National Laboratory, Livermore, Calif., UCRL-95592, Rev. 1; to be published in *J. Comput. Phys.* (February 1988).

Villa, F. (1986), *High Gradient LINAC Prototype*, Stanford Linear Accelerator Center, Stanford, Calif., SLAC-PUB-3875.

FY87: $104,000
FY88: $100,000

Global Circulation Models

Principal Investigators:
Curt Covey and Steven J. Ghan

Global circulation models (GCMs) simulate past and possible future climatic changes by numerically integrating the fluid dynamical equations of motion for the atmosphere with boundary conditions that incorporate various factors influencing the climate system. The GCM that we have modified and tested over the past few years is being used to study transport of heat in the atmosphere, atmospheric composition, and surface modifications.

Our overall goals are to maintain state-of-the-art GCM capability at LLNL and to use GCMs to examine a variety of questions about the atmosphere and climate of Earth and, possibly, other planets. Our near-term objectives are to apply our GCM to topics of current interest in climate dynamics, while enhancing the model's capabilities for treating atmospheric interactions with the land surface and the oceans.

We have obtained from the National Center for Atmospheric Research (NCAR) an improved version of their GCM that includes more realistic treatment of the planetary boundary layer, hence a more reliable computation of surface temperature. This year, the improved model was linked with simplified representations of sea ice and the upper mixed layer of the oceans, allowing the combined model to compute changes in these important components of the climate system. A Lagrangian trace-species transport model was joined to our GCM, permitting study of interactions between climate and atmospheric particles (e.g., from volcanoes or smoke from nuclear war) or chemical species. We have begun a series of experiments to assess the functional dependence of atmospheric heat transport on surface boundary conditions. Our first experiment involves the effects of topography on model-simulated atmospheric circulation (see the Figure). Finally, we have employed simpler one- and two-dimensional models to characterize interactions between the absorption of sunlight by a trace atmospheric constituent and the vertical transport of that constituent. Our results imply that parameterizations of unstable radiative-dynamical interactions need to be added to GCMs in order to fully simulate the lofting of particulate matter in situations as diverse as nuclear winter and Martian dust storms.

We plan to study interactions between atmospheric heat transport and climate as we continue with model development, particularly improvements in treatment of the ocean. The dependence of model-simulated atmospheric heat transport upon sea surface temperature gradient, land/sea distribution, and ocean heat transport will be assessed. (Preliminary investigations suggest that the climatic effect of a change in equator-to-pole transport of heat by the ocean—often cited as an important factor in both paleoclimatic and possible future climatic changes—may actually be offset by the atmosphere changing its heat transport in the opposite sense.) We will also use the coupled GCM-trace species transport model to continue assessing nuclear winter with particular emphasis on the effects of upper-atmospheric dust upon the lofting of lower-atmospheric smoke.

References

Covey, C. and E. Barron (1987), "The Role of Ocean Heat Transport in Climatic Change," *Earth Science Reviews* (in press).

Covey, C. and S. J. Ghan (1987), "Mesoscale Radiative-Dynamical Instability and Mars Dust Storms," *Bull. Am. Astron. Soc.* (in press).

Walton, J. J., M. C. MacCracken, and S. J. Ghan (1987), "A Global-Scale Lagrangian Trace Species Model of Transport, Transformation, and Removal Processes," submitted to *J. Geophys. Res.*

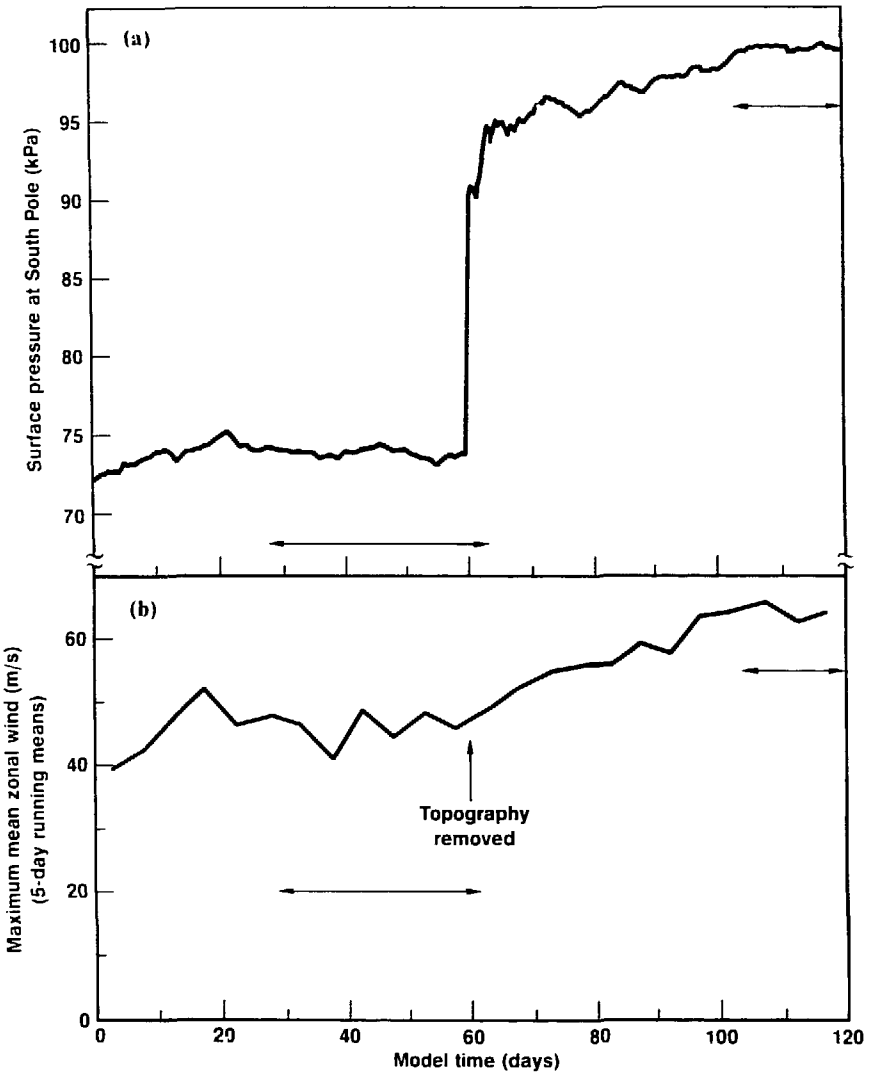

Response of the LLNL GCM to removal of topography, leaving a perfectly smooth Earth with all land at sea level. Surface pressure at the South Pole rises dramatically as the Antarctic Plateau abruptly drops from a 3-km altitude to sea level (*top*). A more subtle and interesting change due to the removal of mountains is the increase in intensity of the Northern Hemisphere winter jet stream (*bottom*), indicating significant changes in weather patterns and attendant transport of heat by the atmosphere. We are continuing to study these model-simulated changes, comparing the two time periods indicated by the double arrows.

Shape Isomers as Candidates for a Gamma-Ray Laser

Principal Investigator:
Morton S. Weiss

Building a gamma-ray laser will require energy-storage states that can transfer their energy to lasing states. Theoretical calculations are in progress to predict which nuclei will have the especially favored states, which are called electromagnetically decaying shape isomers.

We have undertaken a calculational program in nuclear theory to predict the existence of a new class of nuclear isomers with properties particularly promising as storage states for a gamma-ray laser. The rationale for this concept is the arguable inadequacy, for purposes of the gamma-ray laser, of ordinary isomers whose lifetimes are anomalous because they have atypical angular momenta relative to other nuclear levels of comparable energy. In particular, ordinary isomers have transition strengths of, at most, a fractionated single particle unit. In contrast, our hypothesized electromagnetically decaying shape isomers will have long lives because of their structure, will have the same angular momenta as their neighboring levels, and will be very highly collective in transition strength.

We have constructed static potential energy maps for appropriate nuclei by use of a constrained three-dimensional nuclear Hartree-Fock approximation. Figure 1, a one-dimensional projection of such a map, indicates a possible shape isomer. Figure 2 shows systematics for a particularly interesting regime, the mercury isotopes. While many of

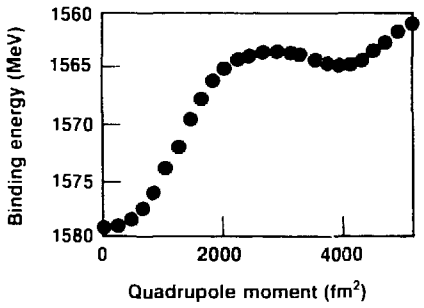

Fig. 1. Projection onto prolate symmetry axis of potential energy map for Os^{200}. The ground state has a quadrupole moment of zero. The valley at quadrupole moment 4000 indicates a possible shape isomer.

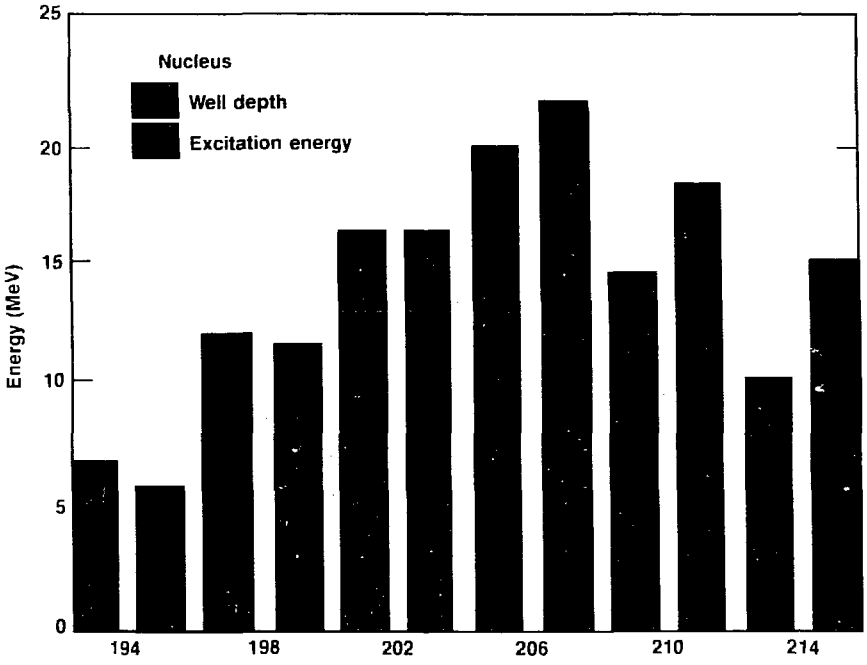

Fig. 2. Height and depth of the second minima for some representative mercury isotopes for two versions of the effective nuclear potential. In each pair, the left element represents the Skyrme III potential, and the right element represents the Skyrme M* potential. The numbers (194, 198, 202, etc.) represent the isotope masses.

these nuclei are likely to exhibit isomerism. Hg^{184} is a particularly promising candidate for experimental verification of these predictions. Static potential energy maps for many other nuclei have been completed, several with potential shape isomers.

We are now performing calculations to extend the nuclei for which static maps exist, and we are also calculating the actinide nuclei, a technically difficult enterprise. Several actinide nuclei exhibit experimentally observed fission shape isomerism and will serve as tests of our work. We have also begun to implement a theory for the nuclear dynamics. The latter task, although difficult, will enable us to calculate lifetimes and transition rates and will also represent a qualitative advance in our capacity to predict, ab initio, many elusive properties of atomic nuclei.

Laboratory X-Ray Lasers

Principal Investigator:
Mordecai D. Rosen

The goal of this project is to provide leadership in theory and design for a joint effort sponsored by LLNL's Physics Department, Laser Program, and Defense Sciences Program to develop the physics and technology of laboratory x-ray lasers, with special emphasis on biological applications. Analysis of Nova experimental results is under way, and design studies for further experiments, at the Nova laser facility and elsewhere, will be pursued in FY88.

In FY84, Novette experiments demonstrated, for the first time, x-ray lasing in the laboratory. Since then, our work has focused on attempts to understand the results and to design new schemes for more coherent lasing at shorter wavelengths, with a view toward applications.

We made progress in a wide variety of enterprises. Our effort in designing nickel-like (4d $\rightarrow$4p) laboratory x-ray lasers has paid off in our achieving a predicted gain as short as 50 Å (in ytterbium). This result puts us at the brink of the "water-window" needed for biological applications. (The water window is the frequency region between 22 and 44 Å in which the contrast is maximum between water and biological structures. At these frequencies, carbon and nitrogen molecules in biological specimens scatter x rays effectively, but oxygen in water does not. In other words, the x-ray beam will scatter off the biological specimen, not off the water surrounding it.)

A year ago, our $n = 3 \rightarrow 2$, hydrogen-like aluminum (39 Å) recombination design held the promise of only small gain. Now, new designs using the same material (with 10-ps irradiations) promise near double-digit gains. A new and different approach—using $n = 5 \rightarrow 3$, lithium-like calcium (39 Å)—was also designed this year. Preliminary experiments with lithium-like aluminum, helium-like aluminum, and lithium-like calcium have indeed shown promising data. Our preliminary attempts at holography of simple wires have been successful. (The Figure shows the apparatus for the holography experiments.) Contacts have been established with our eventual users—biologists within and outside LLNL. Double- and triple-pass mirror/cavity experiments were successful, and our post-shot analysis has been crucial in interpreting the results. Our understanding of the neon-like systems used in the original x-ray lasing experiments has deepened considerably. Absolute timing of the x-ray laser has confirmed our basic model and refuted competing models, and the $J = 0$ gain has been measured and is within a factor of 2 to 3 of theory. We have invented powerful new methods to predict refracting beam patterns. Comparison of our models and experimental data has led to detailed confirmation of the theoretical gain profile within the x-ray laser medium. In short, we have far exceeded our FY87 plans.

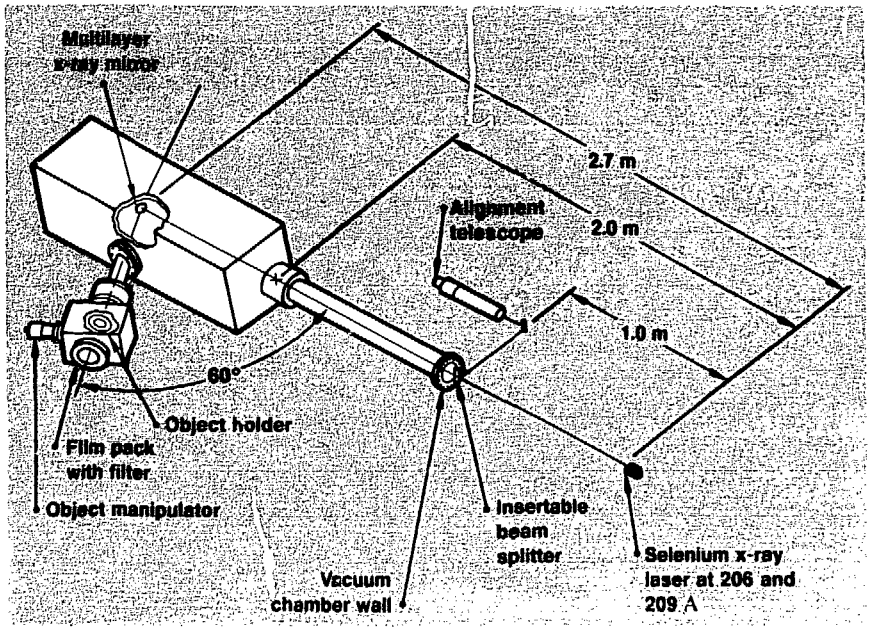

Experimental setup for x-ray holography with a neon-like selenium laser.

In FY88, we will analyze the huge body of data generated with Nova and in support experiments at KMS Fusion, Ann Arbor, Mich. Nickel-like europium and ytterbium will be analyzed in detail, and an optimal nickel-like tungsten laser (44 Å) will then be designed. Data from short-pulse (100-ps) attempts at recombination schemes (hydrogen- and lithium-like aluminum, lithium-like chromium and calcium) must be analyzed if we are to have confidence in proceeding to our ultimate goal of 10 ps. (Our calculations show that a 10-ps pulse is critical for a recombination/rapid-cooling scheme. The goal is to deliver high power quickly to heat the specimen and strip off electrons so that recombination occurs as the specimen cools rapidly.)

We will also analyze the holography and the results of a triple-pass experimental series. These experiments, along with our refraction codes, will allow us to design a full-coherence (master-oscillator/power-amplifier geometry) experiment. Work on other lasers at other labs will concentrate on $J = 0$ problems and absorption spectroscopy (ionization balance) and trapping issues. In the latter half of FY88, the Nova II beam will be restored to service with twice the power and with a short-pulse oscillator. These improvements will enable us to achieve shorter and shorter laser wavelengths as we work our way to the water window.

We will also work with other experiment designs, such as neodymium-like ($5f^3$–$5d$) uranium and photo-pumped recombination schemes. Both hold promise for reduced driver requirements.

References

Bailey, J., J. D. Kilkenny, Y. Lee, S. Maxon, J. H. Scofield, and D. Weber (1987), "Spot Spectroscopy of Highly Ionized Europium," *Phys. Rev. A* **35**, 2578.

Ceglio, N. M., J. E. Trebes, R. A. London, and D. P. Gaines (1987), *Time-Resolved Measurement of Double Pass Amplification of Spontaneous Emission at Soft X-Ray Wavelengths*, Lawrence Livermore National Laboratory, Livermore, Calif., UCRL-96785; submitted to *Phys. Rev. Lett.*

Charatis, G., G. E. Busch, C. L. Shepard, P. M. Campbell, and M. D. Rosen (1986), "Hydrodynamic Aspects of Se XRL Targets," *Proceedings, International Colloquium on XRLs*, P. Jaegle and A. Sureau, Eds. (Aussois, France, April 1986), *J. Phys. (Paris)* **47**, C6-89.

Eder, D. C., M. D. Rosen, R. W. Lee, J. E. Trebes, N. M. Ceglio, M. J. Eckart, B. J. MacGowan, R. L. Kauffman, and D. L. Matthews (1987), *Recombination X-Ray Lasers Using Hydrogen-like Magnesium and Aluminum*, Lawrence Livermore National Laboratory, Livermore, Calif., UCRL-96133; to be published in *J. Opt. Soc. Am. B.*

London, R. A. (1987), *Beam Optics of Exploding Foil Plasma X-Ray Lasers*, Lawrence Livermore National Laboratory, Livermore, Calif., UCRL-97091; to be published in *Phys. Fluids.*

MacGowan, B. J., S. Brown, E. M. Campbell, M. J. Eckart, P. L. Hagelstein, C. J. Keane, R. A. London, D. L. Matthews, D. G. Nilson, T. W. Phillips, M. D. Rosen, J. H. Scofield, G. Shimkaveg, A. Simon, R. Stewart, J. E. Trebes, D. A. Whelan, B. L. Whitten, and J. Woodworth (1986), "Lawrence Livermore National Laboratory X-Ray Laser Research: Recent Results," *Proc. SPIE 688, Multilayer Structures and Laboratory X-Ray Laser Research*, N. M. Ceglio and P. Dhez, Eds., p. 36.

MacGowan, B. J., S. Maxon, P. L. Hagelstein, C. J. Keane, R. A. London, D. L. Matthews, M. D. Rosen, J. H. Scofield, and D. A. Whelan (1987), *Demonstration of Soft X-ray Amplification in Ni-like Ions*, Lawrence Livermore National Laboratory, Livermore, Calif., UCRL-97235, to be published in *Phys. Rev. Lett.*

MacGowan, B. J., M. D. Rosen, M. J. Eckart, P. L. Hagelstein, D. L. Matthews, D. G. Nilson, T. W. Phillips, J. H. Scofield, G. Shimkaveg, J. E. Trebes, R. S. Walling, B. L. Whitten, and J. G. Woodworth (1987), "Observation of X-Ray Amplification in Neon-Like Molybdenum," *J. Appl. Phys.* **61**, 5243.

Matthews, D. L., M. D. Rosen, S. Brown, N. M. Ceglio, D. C. Eder, A. Hawryluk, C. J. Keane, R. A. London, B. J. MacGowan, S. Maxon, D. G. Nilson, J. H. Scofield, and J. E. Trebes (1987), "X-Ray Laser Research at the Lawrence Livermore National Laboratory Nova Laser Facility," *J. Opt. Soc. Am. B* **4**, 575.

Maxon, S., B. J. MacGowan, R. A. London, J. H. Scofield, M. D. Rosen, M. Chen, and P. L. Hagelstein (1987), *Calculation and Design of a Ni-Like Eu Soft X-Ray Laser*, Lawrence Livermore National Laboratory, Livermore, Calif., UCRL-97267; submitted to *Phys. Rev. Lett.*

Rosen, M. D., J. E. Trebes, B. J. MacGowan, P. L. Hagelstein, R. A. London, D. L. Matthews, D. G. Nilson, T. W. Phillips, D. A. Whelan, and V. L. Jacobs, *On the Dynamics of Collisional Excitation XRLs*, Lawrence Livermore National Laboratory, Livermore, Calif., UCRL-94859; to be published in *Phys. Rev. Lett.*

Determination of the Neutrino Rest Mass

Principal Investigators:
Orrin Fackler and
Marshall Mugge

Until 1980, when the results of a Russian experiment were published indicating a finite neutrino rest mass of about 30 eV, the neutrino had been assumed to have zero rest mass. The implications of a finite neutrino rest mass are profound. All other known elementary particles except the photon have finite rest mass. Since many more neutrinos were created in the "big bang" than other massive particles, even a very small neutrino mass would be sufficient for them to dominate the matter in the universe and hence could effect closure of the universe.

The overall objective of this experiment is to determine the neutrino mass to within a few electron volts by measuring the shape of the tritium beta-decay energy spectrum near its endpoint. To accomplish this, we are performing an integral experiment that uses an electrostatic spectrometer and a frozen tritium source. The use of an electrostatic spectrometer allows an accurately measurable resolution function that has sharply cut-off tails, very high acceptance, and higher neutrino-mass sensitivity to the integral spectrum shape with lower sensitivity to systematics than for an equivalent magnetic spectrometer. The use of frozen tritium as a source allows precise calculation of the molecular final states and solid-state effects to better than 0.2 eV.

We have completed fabrication and testing of the total electrostatic system, measured the resolution of the spectrometer, and acquired 100 days of data with a low-intensity,

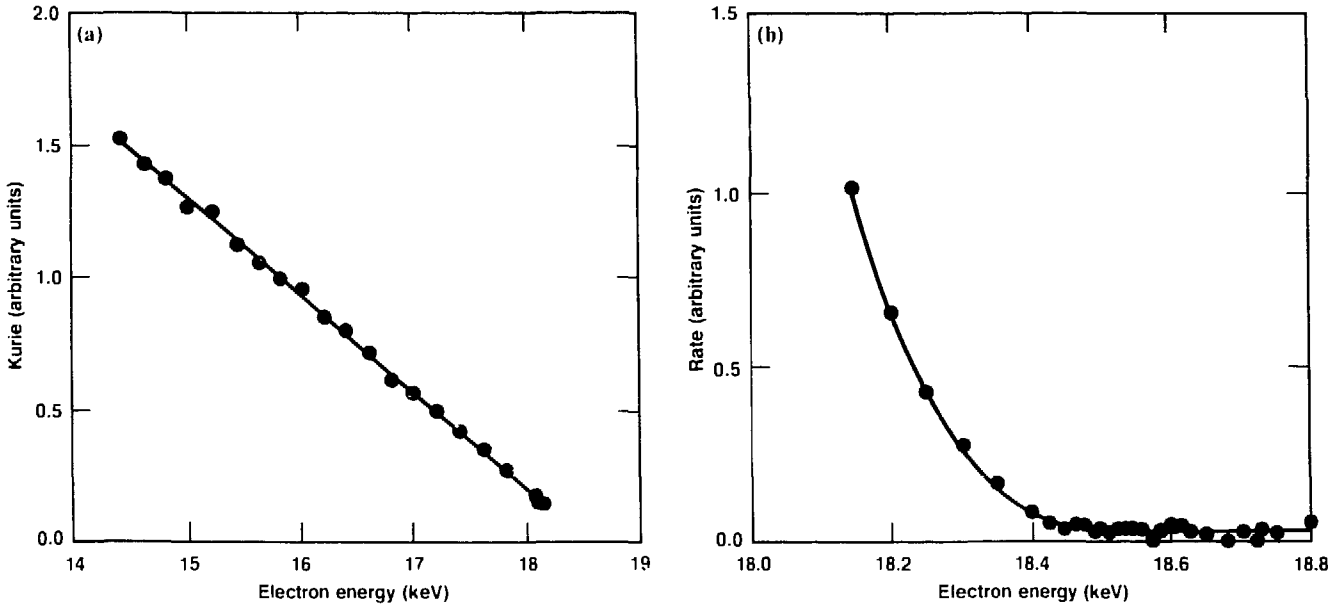

(a) Integral data from tritium beta-decay accumulated over 40 days are presented in the form of a Kurie plot. Plotted in this way, the data should fall on a straight line. A fit to this curve demonstrates a linearity in our data that easily satisfies the requirements of our experimental technique. (b) The actual integral spectrum of tritium beta-decay data near the endpoint. The curve is our best fit to that integral data and demonstrates that, even when using an ion-implanted source, we are able to achieve a 27-eV statistical sensitivity in the neutrino mass determination.

ion-implanted tritium source. These data have demonstrated that the present spectrometer has the designed 6-eV resolution and the required long-term stability. These data have also provided a base for development of analysis programs and allowed extensive studies of experimental backgrounds. From these studies, we identified both electrostatic and detector-associated backgrounds. The design of the cryogenic version of the experiment was modified to reduce these backgrounds. The Figure shows an analysis of 40 days of data. While these data are in no way indicative of the quality we expect to get from the frozen tritium source, they were sufficient to demonstate that our experiments work as designed. A preliminary fit to these data yielded a 27-eV statistical sensitivity in the neutrino mass determination. We have begun the final part of our experiment. The cryogenic design is complete, and fabrication is under way. Liquid-nitrogen shields for the frozen tritium source are now being installed. Highly accurate molecular corrections are complete, and energy-loss measurements have begun.

We will install the cryogenic spectrometer with a designed resolution of 3.2 eV in early 1988. We anticipate that design of a new computerized data acquisition and control system will be completed within months, in time to test components of the cryogenic system that will support the frozen tritium source. We expect fabrication and installation of the frozen tritium source to be completed in March 1988, with initial testing during the summer. Final data acquisition with this source is scheduled to begin in the fall of 1988.

Advanced Two-Stage Light-Gas Gun

Principal Investigator:
William J. Nellis

To meet increased demand for LLNL's two-stage light-gas gun, we designed an advanced version with a doubled shot rate that will be able to test materials at more extreme conditions and still handle twice the current rate of experiments. Eventually, we plan to house the existing gas gun and the advanced version in the same facility, where they can share common diagnostics and control systems.

Because of high demand for use of the LLNL two-stage light-gas gun by various Laboratory and University of California programs, we need a gas-gun facility with an increased shot rate. In addition, higher shock pressures and temperatures are needed both to probe matter at more extreme conditions for programmatic applications and also to study the physics of materials at more extreme conditions. We began in FY86 to design a facility that will include the present LLNL two-stage gun, modified to achieve projectile velocities between 10 and 11 km/s, and a second one-third-scale gun to achieve 8 km/s (the present limit) in more frequent experiments.

A two-stage gun one-third the size of our present gun and a target chamber were designed and ordered from commercial suppliers. This hardware was delivered in December 1987. Associated support and control systems have also been designed, ordered, and received. The new gun will be set up and tested in a temporary location in Building 341. A plan for an expanded gun facility to house both two-stage guns in Building 341, with a common control and diagnostic system, has been developed. The proposed plan places the gun facility in a red-badge area for easy access by University of California faculty and students. Such collaboration is conducted through the Institute of Geophysics and Planetary Physics.

The new gun system will be assembled and tested in FY88. With the gun, the current shot rate (roughly one per day) can be doubled or tripled. A new small-bore launch tube designed for the present gun would achieve velocities up to 11 km/s. Modified components for the present gun will be purchased, and high-velocity testing will begin.

Shock Synthesis of Novel Superconductors

Principal Investigator:
William J. Nellis

We are using shock waves produced by our two-stage light-gas gun to develop ways to make superconducting wire with recently discovered high-T_c oxide superconductors. We are also trying to synthesize new phases of these materials that may have even higher transition temperatures.

The purpose of this research is to produce novel superconductors by processing specimens at high dynamic pressures, densities, and temperatures with our two-stage light-gas gun and to characterize structure and properties. The latter experiments will be done at either LLNL or the University of California, San Diego, and at Stanford University. The goals are twofold: to process known high-T_c superconductors into useful applications, such as current-carrying wire, and to synthesize new metastable solid phases of potentially high-T_c superconductors with ultra-high critical electrical currents and magnetic fields. Both goals are feasible because dynamic pressures up to a megabar and temperatures up to a few thousand degrees kelvin are sufficient to compact or melt powders and to drive phase transitions in solids with quench rates up to 10^{12} bar/s and 10^{9} k/s.

We have shown that solids, powders, and films can be subjected to megabar pressures and then recovered intact for physical measurements. In pure niobium, a 0.6-Mbar shock pressure induces defects that increase the critical magnetic field by a factor of 2. We subjected a Nb$_3$Si alloy to 1 Mbar and induced a phase transition to a different crystal structure, with a complete resistive transition to the superconducting state at T_c = 18 K. The unshocked specimen did not superconduct above 1 K. Previous attempts to prepare this material have succeeded only when shock waves were used and produced specimens with only a weak inflection in electrical resistance. We are now trying to synthesize and stabilize new forms of the recently discovered high-T_c oxide superconductors, which may superconduct with T_c up to 240 K. We demonstrated the process of shock compaction of thin layers of powders in a copper matrix with a shock pressure of 150 kbar; we demonstrated complete melting and quenching with 600 kbar. In preliminary experiments, we used this method to embed powders of the ceramic superconductor $Pb_{1.2}Mo_6S_8$ into copper. We are now applying this method to the recently discovered high-T_c oxide superconductors in an attempt to learn how to use high dynamic pressure to make superconducting wire. We filed a patent application for the dynamic process to make superconducting wire, and we were recently informed that our application has been approved.

References

Nellis, W. J., W. H. Gourdin, and M. B. Maple (1987). *Shock-Induced Melting and Rapid Solidification*, Lawrence Livermore National Laboratory, Livermore, Calif., UCRL-96769; to be published in *Proc. 1987 APS Topical Conference on Shock Waves in Condensed Matter*.

Neumeier, J. J., W. J. Nellis, M. B. Maple, M. S. Torikachvili, and B. C. Sales (1987). *Superconductivity of a 15-Phase Nb Si Synthesized by Mbar Shock Pressure*, Lawrence Livermore National Laboratory, Livermore, Calif., UCRL-95814; to be published in *Proc. 1987 APS Topical Conference on Shock Waves in Condensed Matter*.

FY87 $64,000
FY88 $150,000

Femtosecond Laser Interaction Project

Principal Investigator:
Richard M. More

We are exploring the possibility of producing and studying matter at solid-state density at the high temperatures normally associated with plasma physics (1 to 100 eV). In the past year, we analyzed sub-picosecond laser reflectivity data taken by our collaborators at AT&T–Bell Laboratories, showed that the desired plasma conditions are indeed produced, and began acquisition of a femtosecond-range oscillator for the LLNL short-pulse laser facility.

Design calculations for nuclear weapons, as well as studies of weapons effects, rely heavily on theoretical data for equation of state and opacity of matter at conditions of extreme high-energy density. One especially important range is that produced by rapid energy deposition in solid matter—the so-called preheat condition in which matter reaches temperatures of 1 to 100 eV while still remaining at solid density. In this range, the available theories do not agree, and large uncertainties exist. Laboratory experimental techniques able to reach the temperatures of interest include shock compression, which unfortunately raises the density so that atomic repulsions dominate, and ablation, which produces large plasmas of varying density that are difficult to diagnose with precision. A new possibility arises with high-power lasers producing very short pulses in the sub-picosecond range. Such a laser can rapidly heat a thin layer of target material (2×10^{-5} cm, the optical skin depth), which subsequently expands in approximately 10^{-12} s. With sufficiently rapid diagnostics, the equation of state or opacity of this material can be measured to produce data of great scientific and program interest.

We have examined several key questions concerning this concept: Does the material reach thermal equilibrium in such a short timescale? What diagnostics will be sufficiently rapid? How large a laser facility is required? Because of the small total pulse energy (approximately 0.01 J), the required laser is relatively modest in size and cost. By means of newly developed short-pulse technology, lasers with the required short-pulse characteristics have been constructed at several locations, including the University of California, Berkeley, and AT&T–Bell Laboratories. Through collaboration with the Bell group, we have obtained preliminary reflectivity data for several target materials (Al, Si, and Cu). We analyzed these data with a new computer code (SPRINT) that calculates absorption and reflection of electromagnetic radiation, target heating, and thermal conduction using semiclassical statistical theories for high-temperature specific heat, equilibration time, and electrical and thermal conductivities. The results are in reasonably good agreement with the experiment. This agreement implies that target expansion is very small during the laser pulse. Thus the reflectivity appears to provide a workable first diagnostic. The SPRINT computer code has also been applied to predict damage thresholds for multilayer x-ray mirrors used in the Nova x-ray laser program.

To perform further exploratory studies, we have procured a specialized oscillator for an existing laser-amplifier system. Using pulse compression techniques, the extended system will produce high-intensity pulses in the sub-picosecond time domain. Future experiments with this laser will use delayed probe pulses to study target surface expansion (release-wave velocity). In addition, we plan to study the nonlinear optical response of metallic targets with the short-pulse laser, looking for a novel nonlinear Umklapp electron-phonon absorption process recently predicted by Laughlin, More, and Teller (1987).

Reference

Laughlin, R. B., R. M. More, and E. Teller (1987), "Nonlinear Resistivity Due to Spontaneous Emission of Phonons in Potassium," submitted to *Phys. Rev. A*.

More, R. M., K. H. Warren, and Z. Zinamon (1986), "Damage to Multilayer Mirrors in a Hostile Environment," *Proc. SPIE Int. Soc. Opt. Eng.* **688**, 134.

Insulator-to-Metal Transitions: Metallization of Molecular Hydrogen

Principal Investigators:
Marvin Ross, Robin L. Reichlin, and William C. Moss

High-pressure diamond-anvil studies have observed insulator-metal transitions in CsI and Br_2 near 1.1 Mbar. No transitions have been observed in xenon up to 1.7 Mbar. The objective of our project is to achieve the metallization of molecular hydrogen, which is expected to occur above 2 Mbar.

As a consequence of its simplicity, its possible applications, and the fundamental physics involved in its metallic phase, hydrogen has been the focus of considerable activity. Theoretical studies predict that at sufficiently high pressures (commonly thought to be between 2 and 4 Mbar), molecular hydrogen should undergo a phase transition into a metallic state. Quantum Monte Carlo calculations of the properties of hydrogen made by Ceperley and Alder (1987) predict a metallic transition near 3 Mbar. Whether molecular hydrogen undergoes a direct dissociation into an alkali-like metal or becomes a molecular metal before dissociating into a monatomic metal remains a major question. The latter possibility was not considered by Ceperley and Alder. Our objective is to determine accurately the pressure and density at which molecular hydrogen converts to metal and to examine the properties of the two phases.

Our program is organized to attain a succession of higher pressures by metallizing first CsI and Br_2 (near 1 Mbar) and then the inert gas xenon, which is believed to become metallic near 2 Mbar. Finally, we will attempt to metallize hydrogen at pressures near 3 Mbar.

We determined that CsI metallized in a diamond-anvil cell at a pressure of 1.1 Mbar by measuring its optical reflectivity (Reichlin et al., 1986). The pressure of the metallization transition is determined by a sharp rise in the reflectivity, which is synonymous with the appearance of a conducting phase. More recently, we made measurements on Br_2, the preliminary evaluation of which strongly indicates that we have observed metallization of this molecule also near 1.1 Mbar. Our diamond-anvil study on xenon has reached 1.7 Mbar, but no changes in the xenon sample are apparent. A sample of hydrogen has also been compressed to 1.3 Mbar, and no changes were observed. Work on these materials is continuing.

In our experiments with hydrogen, we have found that diamonds fracture at pressures as low as several hundred kbar. To achieve higher pressures without fracturing the diamond in the diamond-anvil cell, we are carrying out finite-element simulations to optimize the cell design. These calculations have shown that proper beveling of the diamond face can delay fracturing, and pressures up to 5 Mbar can be achieved in an empty cell (Moss and Goettel, 1987). Hydrogen samples have been loaded into cells made according to the new design, and compression studies are in progress.

References

Ceperley, D. M. and B. J. Alder (1987), "The Ground State of Solid Hydrogen at High Pressure," *Phys. Rev. B* **36**, 2092.

Moss, W. C. and K. A. Goettel (1987), "Finite Element Design of Diamond Anvils," *Appl. Phys. Lett.* **50**, 25.

Reichlin, R., M. Ross, S. Martin, and K. A. Goettel (1986), "Metallization of CsI," *Phys. Rev. Lett.* **56**, 2858.

Director's Initiatives

Lawrence Livermore National Laboratory

Biotechnology

Overview

Mortimer L. Mendelsohn

Funds for the Biomedical and Environmental Research Program were allocated to five areas of research from the IR&D Director's Initiatives and departmental sources. Here we describe the main purpose of each of these research activities.

Immunoassay Instrumentation. We are developing novel immunochemical sensors by pursuing two different instrumentation strategies. First, we are using the surface acoustic wave (SAW) method to detect oscillatory changes in thin films after the binding of antibody molecules. Second, we are using the evanescent wave to elicit antibody fluorescence immediately adjacent to the surface of an optical fiber. For our initial measurements in both detectors, we selected the monoclonal antibody Py-1, which can detect pesticide contamination in ground water.

Microbial Genetic Engineering. Two genes cloned from *Thiobacillus ferrooxidans* have been transferred into *Escherichia coli*. These genes are of interest because one fixes atmospheric nitrogen, and the other is involved in sulfur assimilation. Similarly, a gene cloned and transferred from *Clostridium pasteurianum* reduces toxic oxyanion selenate to the nontoxic element selenium.

Human Glycophorin Mutation. The glycophorin assay measures somatic mutation in human red blood cells. We found that blood samples from 92 cancer patients undergoing radiotherapy contained normal levels of mutant red blood cells. In contrast to results from survivors of the atomic bomb in Hiroshima and chemotherapy patients, localized cancer radiotherapy does not induce mutations, presumably because therapeutic doses sterilize rather than induce mutations in bone marrow.

Ecological Impacts of Nuclear Winter. By using experimental data and model simulations, we are studying the combined effects of low temperature and low levels of light at the plant, community, and regional levels. Tests on soybeans and loblolly pines subjected to a temperature of 15°C and light reduction of 99% reveal some delays but no significant effects on either growth or yield.

Nuclear Magnetic Resonance Imaging of Plants. We have used a large-bore, high-resolution nuclear magnetic resonance (NMR) imaging device to obtain images of living plant roots. This work was done in collaboration with scientists at the U.S. Department of Agriculture and General Electric. Our NMR images of undisturbed plants show the interactions of root and soil and mark the first time such fundamental processes have been directly observed under controlled conditions.

Overall, the Biomedical and Environmental Research Program received $947,000 in IR&D operating funds; an additional $35,000 in equipment funds was awarded for Microbial Genetic Engineering research.

Immunoassay Instrumentation

Principal Investigator:
Martin Vanderlaan

We are using two different instrumentation strategies to develop new sensors capable of detecting antibodies. Our goal is to incorporate antibodies into silicon nitride membranes or optical fibers that would then serve as novel instruments for making real-time immunochemical measurements.

In a collaborative effort with the University of California, Berkeley, we are developing new methods for attaching antigens to silicon nitride membranes. This work involves the microfabrication of surface acoustic wave (SAW) detectors for lambda waves. The basic strategy behind our effort takes advantage of the fact that the molecular weight of antibodies is large enough that their binding to the surface of silicon nitride membranes would be detectable as a change in the frequency of oscillation of a piezoelectric crystal.

For our initial measurements, we selected Py-1, which is a monoclonal antibody developed at LLNL. Among its other advantages, Py-1 recognizes a family of pesticides called synthetic pyrethroids. Instruments incorporating this antibody should be suitable for detecting pesticide contamination in ground water.

After a thin film of ZnO is sputtered onto a silicon nitride membrane for piezoelectric coupling, aluminum-interdigitated electrode transducers are evaporated onto the ZnO. A delay line serves as a feedback loop in a simple amplifier to produce oscillation. The frequency of vibration is low enough that there is little power loss into an overlying liquid. Thus, our measurements can be made on aqueous solutions.

We have evaluated several means for covalently coupling proteins to silicon nitride chips. To facilitate handling, we have evaluated relatively large (1-cm^2) chips via enzyme-linked immunoassay for their ability to bind antibody. We first attached an albumen antigen containing the meta-phenoxybenzoyl groups to the surface of the chip. Next, we incubated Py-1 with the chip because it is capable of recognizing the meta-phenoxybenzoyl groups. For evaluation purposes, we then incubated an enzyme-linked antibody to Py-1 with the chip.

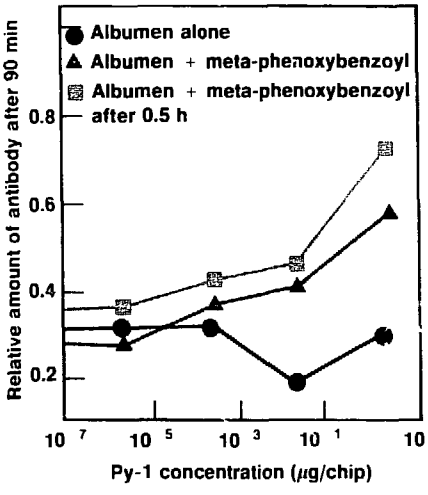

Fig. 1. Detection of antibody bound to silicon nitride chips. The monoclonal antibody Py-1 binds only on the chips containing the phenoxybenzoyl groups and not on those with albumen alone.

Figure 1 shows typical results from measurements of enzymatic activity. The results indicate that monoclonal antibody binding occurred only on the chips that contained the phenoxybenzoyl groups and not on those chips with albumen alone. After optimizing a method for applying the antigen to silicon nitride, we will be able to apply it to microfabricated membranes in an actual SAW detector.

Our second instrumentation study is a collaborative effort with researchers at the University of California, Davis. In this work, we are using antigens immobilized on optical fibers. The bound antibodies are coupled with fluorescein dye so that they can be easily detected by measuring fluorescence.

Optical fibers are first coated with phenoxybenzoyl-albumen and then incubated with the monoclonal antibody Py-1. Our measurements indicate that an increase in fluorescence depends on elapsed time and concentration of antibody, and that the increase is reversible. Figure 2 shows how the fluorescence changes with time as antibodies bind to a fiber and then are washed off.

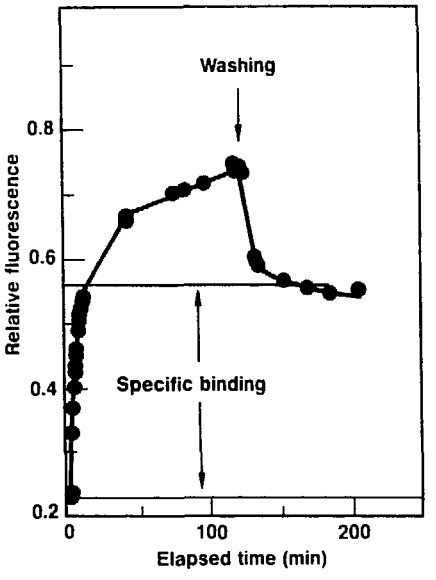

Fig. 2. Measurement of antibody fluorescence from optical fibers incubated with Py-1. The fluorescence increases with time as antibodies bind both specifically to the antigen and nonspecifically to the fiber. When the fiber is washed, nonspecifically adhered antibodies are removed.

We are currently studying the rates of these forward and reverse reactions.

In both of our immunoassay instrumentation studies, we selected the monoclonal antibody Py-1 as a starting point. However, once we have developed the basic principles of fabrication and our detectors have been optimized for Py-1, it should be possible to incorporate a variety of other antibodies that are sensitive to trace chemicals. The immunoassays developed at LLNL include, for example, antibodies to a variety of pesticides, cooked-food mutagens, and dioxin. Our goal for FY88 is to pursue both of our two instrumentation designs and to produce working prototypes of these detectors.

References

Vanderlaan, M., L. Stanker, and B. Watkins (1987). "Environmental Monitoring by Immunoassay," *Environ. Sci. Technol.* (in press).

Vanderlaan, M., L. Stanker, and B. Watkins (1987). "Immunoassays for Monitoring Toxic Chemicals," DOE Contractors Meeting, Monterey, Calif., June 23-26.

Microbial Genetic Engineering (Recombinant DNA) Biotechnology

Principal Investigator:
Emilio Garcia
Co-Investigators:
Robert T. Taylor and Ilona Fry

We are continuing to study two bacterial species with promising metal and metalloid detoxification-recovery potentials. We have cloned and characterized several genes from* Thiobacillus ferrooxidans, *including the genes that allow this iron-oxidizing bacterium to fix nitrogen directly from the atmosphere and a gene involved in sulfur assimilation. We have isolated a new plasmid from* T. ferrooxidans, *which appears potentially useful for the cloning and transferring of genes in this organism. We have also tested several* T. ferrooxidans *strains for heavy-metal resistance and identified one possessing resistance to nickel. The unique property of chromosome-associated metal resistance and the newly isolated plasmid will be used as tools in the development of techniques for the reversible introduction of genes into and out of the bacterial strains from which they were initially obtained. We have also cloned, from the gram-positive bacterium* Clostridium pasteurianum, *a gene that confers on* Escherichia coli *cells the ability to reduce the toxic oxyanion selenate to the nontoxic element selenium. Characterization of this gene and its product should yield information on the mechanisms of this important reductive process.

The bioconversion and bioleaching of metals and metalloids by microorganisms is probably one of the least publicized and most underrated areas of modern biotechnology. Although metals and metalloids are useful commodities, they present particularly difficult environmental problems because, unlike organic pollutants, they cannot be degraded. Instead, they are merely interconverted and recycled in the environment by geochemical action or by biological activities, such as oxidation, methylation, and reduction. Metals are usually found in nature as low-grade ores, and their economical recovery by microbial activity is another area of great potential interest.

We are studying two bacterial species that exhibit unique oxidative and reductive properties towards metals and metalloids. *Thiobacillus ferrooxidans* is an aerobe (an organism requiring oxygen) that can oxidize iron and sulfur compounds from mineral matter, with accompanying solubilization-separation of valuable metals or toxic metal pollutants. *Clostridium pasteurianum* is an anaerobic microorganism (one growing in the absence of oxygen) that can carry out the biological reduction of metallic oxyanions to their nontoxic, insoluble elemental forms. Our work has focused on the development of genetic techniques that will allow us to elucidate and manipulate the biochemical pathways involved in iron and sulfur oxidation in *Thiobacillus* and the uptake and reduction of selenate by *Clostridium*.

Our ultimate objective is to determine the steps and mechanisms used by these bacteria for bioconversions and bioleachings. In particular, we would like to apply the oxidative abilities of *T. ferrooxidans* to the recovery of strategic metals from fly ash, to the in situ leaching of minerals from underground deposits, and to the possible removal of pyritic sulfur from coal. We will apply the reductive capabilities of *C. pasteurianum* to the removal and recovery of elements, such as selenium, tellurium, and molybdenum, from agricultural, mining, and coal-cleaning wastewater. To fulfill our

aims, we have worked during the last two years on the development of genetic and recombinant DNA tools for these two microorganisms. The knowledge we are seeking would make possible the manipulation of one or more of the steps in the relevant biological processes and thereby render such bacteria useful alternatives for the removal, recovery, and detoxification of various industrial and energy-related inorganic waste by-products.

We used the genomic libraries of *T. ferrooxidans* and *C. pasteurianum* that were constructed last year to isolate the genetic material encoding key cellular processes in the two bacteria. From the obligate anaerobic bacterium *C. pasteurianum*, we cloned a gene that permits *E. coli* (an organism normally incapable of selenate reduction) to reductively convert the toxic, soluble compound selenate to the nontoxic, insoluble element selenium. Our work appears to be the first identification of the gene(s) involved in the reduction of selenate. It paves the way for the potential engineering of a Clostridial strain with an improved selenate detoxification capability. Our future research on this topic will be directed at the characterization of such genes and determinations of the rate-limiting steps in the reaction pathways catalyzed by the gene products. A high priority during FY88 will be the development of techniques for the reversible introduction of these genes into and out of the Clostridial strain from which they were initially obtained.

Using a homologous probe derived from an unrelated bacterium, we identified and then cloned in an *E. coli* host two genes from *T. ferrooxidans* that encode enzymes involved in the fixation of atmospheric nitrogen. These two nitrogen-fixing (nif) genes allow this iron-oxidizing bacterium to assimilate nitrogen directly from the atmosphere, sparing it the requirement for combined nitrogen (i.e., ammonia or nitrate) typical of most bacteria and of all higher animals and plants. Thus, the nif genes are potentially useful in strain improvement and vector construction for this metal-oxidizing bacterium. (A vector is a genetic element that can replicate and transfer genes from one bacterium to another.) Genes encoding enzymes of the biosynthetic pathways of the amino acids leucine and proline have been isolated and shown to be functional in an *E. coli* host, thereby demonstrating that a broad latitude of functions encoded by *T. ferrooxidans* genetic material are efficiently expressed in *E. coli* (a desirable host for genetic manipulations because of its well-developed molecular genetics).

We have also identified the gene encoding adenosine triphosphate (ATP) sulfurylase, an enzyme in the sulfur assimilatory pathway of *Thiobacillus*. We cloned the gene on a 4.7-kilobase insert in the plasmid pBR322. (The plasmid pBR322 is an autonomously replicating, circular DNA molecule present in *E. coli* that can be transferred from one bacterium to another and that can be used to insert and amplify any gene of choice.) Our work represents the first time this gene has been studied and characterized in *Thiobacillus*. Because it is a key gene in the sulfur assimilatory pathway of a bacterium that can also use sulfur in a dissimilatory, energy-producing way, its study is critical to the understanding of the overall sulfur metabolism of *Thiobacillus*. In fact, *T. ferrooxidans* can use reduced sulfur compounds (i.e., sulfide, sulfur, and thiosulfate) as the sole energy source. The gene encoding the *Thiobacillus* sulfurylase is functional when tested in an *E. coli* mutant that completely lacks such activity. Using an assay we recently developed, we measured the enzymatic activity of the *Thiobacillus* sulfurylase expressed in this mutant and found it to be present at levels similar to those found in the *T. ferrooxidans* cells. In contrast with the ATP sulfurylase from sulfate-grown *E. coli*, synthesis of the *T. ferrooxidans* enzyme expressed in *E. coli* is neither repressed by exogenous cysteine nor derepressed by exogenous, reduced glutathione. Thus, it appears that the *T. ferrooxidans* enzyme is under different genetic control than that of *E. coli*.

We isolated a new plasmid from a *T. ferrooxidans* strain and found it to be 11 to 12 kilobases in size. Although the plasmid, as isolated, carries no known genes that can be used as selective markers, genes for antibiotic and metal resistance found in some related strains (see the Figure) can be cloned into the plasmid to provide the necessary selection. The possibility of engineering the newly isolated plasmid with appropriate selective markers, together with its convenient small size, make it potentially useful in the construction of a genetic vector for the reintroduction of cloned genes into *T. ferrooxidans* cells.

During FY88, we will continue to characterize the genes we have already isolated. Future applications involving the use of the genes we are studying will require extensive knowledge of their structures and functions. We will use the gene from *C. pasteurianum* involved in the reduction of selenate to elemental selenium as a probe to detect the analogous gene in naturally occurring bacteria from the Kesterson Reservoir and other sites that are heavily contaminated with selenium. Such an approach could serve to identify a bacterial species even more suitable for direct use in decontamination or as a source of genetic material for genetic

engineering of an even more efficient bacterial strain. An important component in the genetic engineering of microorganisms is the development of new methods for the transfer, uptake, and maintenance of plasmid DNA into organisms. Construction of shuttle vectors for *Clostridium* and *Thiobacillus* will be a high priority for next year. Our approach will be to use the newly isolated plasmid as a vector for *Thiobacillus* and, in the case of *Clostridium*, to adapt a plasmid from a related bacterium for the same purpose.

References

Hanna, M. L., G. L. Bush, E. Garcia, and R. T. Taylor (December 1986), "Reduction of Selenium Oxyanions by *Escherichia coli* versus *Clostridium pasteurianum*," Genetic and Environmental Toxicology Association Meeting, Palo Alto, Calif.

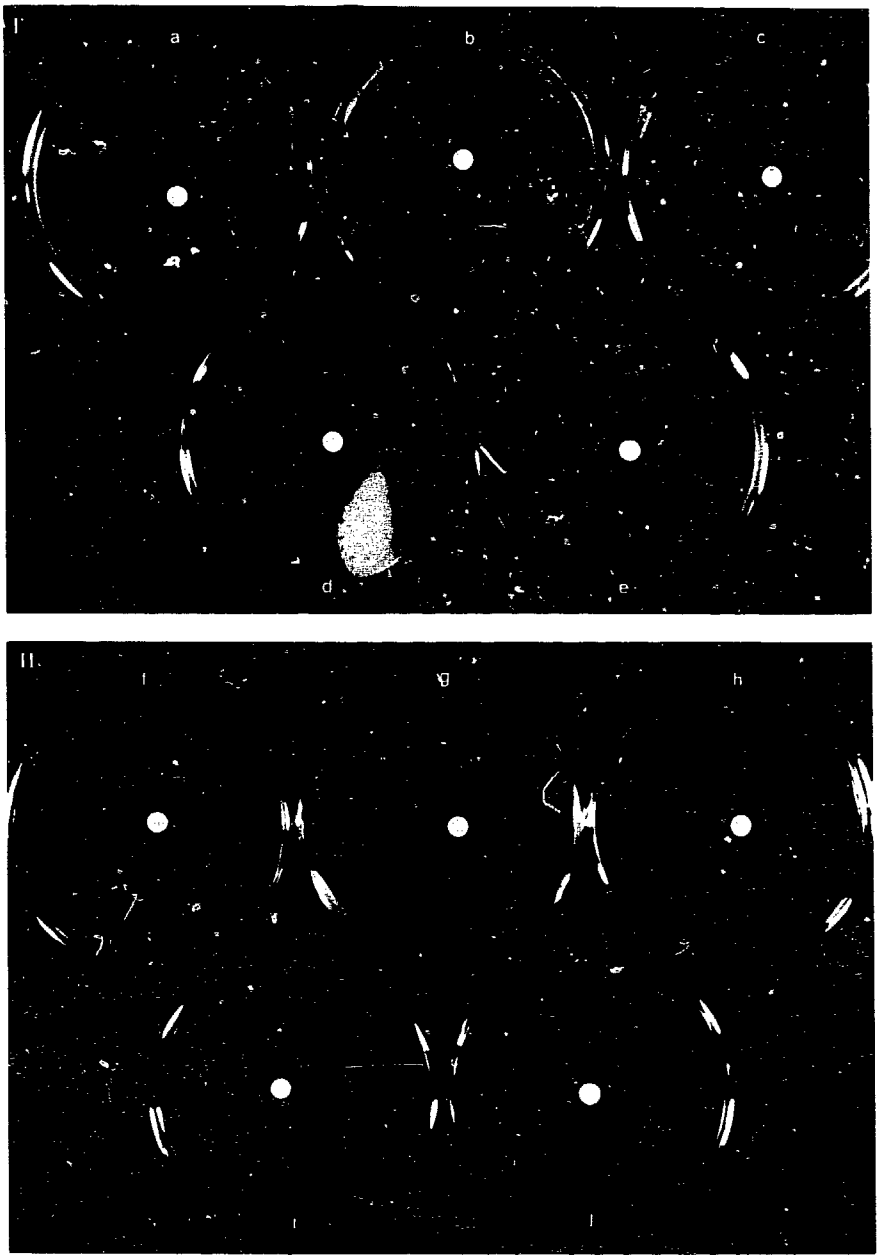

Screening of several *T. ferrooxidans* strains for heavy-metal resistance. We tested five *T. ferrooxidans* strains for sensitivity against mercury and nickel. After pouring a large number of cells into each plate, we placed a disk containing appropriate amounts of the metal in solution in the center of the plate. The killing of cells creates a clear zone around the disk. Panel I shows plates in which we added nickel: (a) strain ATCC 13598, (b) ATCC 21834, (c) ATCC 14119, (d) ATCC 23270, and (e) ATCC 33020. Panel II shows plates in which we added mercury: (f) ATCC 21834, (g) ATCC 13598, (h) ATCC 23270, (i) ATCC 33020, and (j) ATCC 14119. Increased resistance response to the metal by a given strain is indicated by a smaller zone of growth inhibition. Strain ATCC 14119 shown in (c) is the only strain to display complete resistance to nickel, making it an excellent candidate as a source from which to derive a nickel-resistance gene that can be used as a selective marker for a cloning vector. Panel II shows the extreme sensitivity displayed by all *Thiobacillus* strains tested against mercury.

Glycophorin Somatic Mutation in Patients Undergoing Radiation Therapy

Principal Investigators:
Ronald H. Jensen and
William L. Bigbee

After applying the glycophorin assay to blood samples from cancer patients undergoing various amounts of partial-body radiation therapy, we observed no significant induction of glycophorin A variant erythrocytes or correlation between the frequency of these variant cells and radiation dose or percentage of bone marrow irradiated.

Our glycophorin A (GPA) somatic cell mutation assay uses monoclonal antibodies, which are reagents tagged with fluorescent dyes, and the technique of high-speed flow sorting to count the frequency of rare, variant erythrocytes (red blood cells). The assay identifies those erythrocytes that fail to express a normal form of the protein GPA on the cell surface. These variant cells appear to result from *in vivo* mutations at the GPA locus in erythrocyte progenitor cells.

Previous studies demonstrated elevations of the variant frequency in blood samples from individuals exposed to chemical mutagens (Langlois et al., 1986; Bigbee et al., 1987) and from survivors of the atomic bomb at Hiroshima who were exposed to whole-body irradiation (Langlois et al., 1987). Our results on the effects of exposure to chemical mutagens indicate that the induced, elevated variant frequencies are transient in those individuals studied to date. However, we observed a highly significant linear relation between variant frequency and estimated whole-body radiation exposure in atomic bomb survivors sampled 40 years after exposure. To better understand the response of the assay to radiation exposure, we extended our work to cancer patients receiving radiotherapy.

We applied the assay to 92 blood samples from cancer patients undergoing high-energy radiotherapy and to 54 volunteer donors from LLNL who served as controls. In contrast to previous results obtained with blood samples from individuals exposed to moderate doses of whole-body radiation, we observed no significant induction of GPA variant erythrocytes (see the Table). In addition, we found no correlation between either the percentage of bone marrow irradiated or radiation dose and the GPA variant frequency. Our results suggest that partial-body irradiation in therapeutic doses effectively sterilizes the exposed bone marrow, leaving essentially no surviving stem cells to record mutations.

References

Bigbee, W. L., R. G. Langlois, R. H. Jensen, A. W. Wyrobek, and R. B. Everson (1987), "Chemotherapy with Mutagenic Agents Elevates the *In Vivo* Frequency of Glycophorin A 'Null' Variant Erythrocytes," *Environ. Mutagen.* **9**(8), 14.

Langlois, R. G., W. L. Bigbee, and R. H. Jensen (1986), "Measurement of the Frequency of Human Erythrocytes with Gene Expression Loss Phenotypes at the Glycophorin A Locus," *Hum. Genet.* **74**, 353.

Langlois, R. G., W. L. Bigbee, S. Kyoizumi, N. Nakamura, M. A. Bean, M. Akiyama, and R. H. Jensen (1987), "Evidence for Increased Somatic Cell Mutations at the Glycophorin A Locus in Atomic Bomb Survivors," *Science* **236**, 445.

Table Frequency of variant erythrocytes following radiation treatment.

Group	Number of individuals	Mean variant frequency ($\times 10^{-6}$)	Standard deviation ($\times 10^{-6}$)
Untreated controls	54	10.9	± 6.9
Pretreatment patients	4	9.5	± 2.9
30 to 120 days[a]	15	15.3	± 12.1
121 to 365 days[a]	26	11.9	± 8.6
1 to 5 years[a]	30	14.3	± 8.9
More than 5 years[a]	17	14.5	± 2.3

[a]Time following the start of radiation therapy in cancer patients.

Nuclear Magnetic Resonance Imaging: Structure and Function of Living Roots

We are using nuclear magnetic resonance imaging in new applications that allow us to make noninterfering, in situ observations of processes fundamental to the growth of plant roots.

Principal Investigators:
John J. Koranda and
Joseph H. Shinn
Co-Investigators:
Hugo H. Rogers[a] and
Paul A. Bottomley[b]

[a]U.S. Department of Agriculture, Auburn, Ala.
[b]General Electric Corp., Schenectady, N.Y.

The fundamental processes in living plant roots have been historically difficult to observe. Thus, phenomena such as vascular flow, growth under stressful stimuli, and mycorhizzal influences (the symbiotic association of a root with a fungus) on water and nutrient absorption remain subjects of considerable speculation in current research.

Our objective was to perform preliminary experiments on living roots with nuclear magnetic resonance (NMR) imaging. This unique and noninvasive tool yields two- and three-dimensional material density maps and is well suited for detecting protons. Such proton-spin resonance imaging in large-bore, high-resolution NMR imaging devices is available in industrial and medical facilities. The major goal of our research was to elicit interest and research support for a consortium of university and government facilities.

As a result of our initial funding, we conducted experiments showing for the first time how root systems can be observed within soil, without interference by free water, but with some effects from common media constituents, such as ferromagnetic particles in soil minerals. We also constructed a noninterfering dual-pressure chamber to enclose live plants and to control vascular flow during NMR experiments. Preliminary results indicate that noninvasive NMR imaging of plant root systems is a practical tool for investigating root and soil distribution in many agricultural soils at any stage of soil-water stress.

References

Cure, W. W. and H. H. Rogers (1987), "Magnetic Resonance Imaging for the Study of Plant Roots In Situ," *Tech. Papers Am. Soc. Photogram. Remote Sensing* **1**, 285.

Daley, P. F., J. H. Shinn, and J. J. Koranda (1987), "Nuclear Magnetic Resonance Imaging: An Innovative Method for the Study of Structure and Function of Plant Roots," Workshop on Innovation in Ecology: Technology and Theory, Gaithersburg, Md., April 21-22.

Rogers, H. H. and P. A. Bottomley (1987), "In Situ Nuclear Magnetic Resonance Imaging of Roots: Influence of Soil Type, Ferromagnetic Particle Content, and Soil Water," *Agronomy J.* **79**(6), 957.

Biological and Ecological Impacts of Nuclear War

Principal Investigators:
Lynn R. Anspaugh and
James R. Kercher

Our experimental results from growing conditions simulating nuclear winter suggest that soybeans and loblolly pine show no significant yield loss under reduced light and chilling for one to two weeks; however, plant development was delayed. The results of our simulations using models of soybeans were in good agreement with experiment.

The objective of our research is to determine the biological and ecological effects that would arise from changes in global climate after a hypothetical nuclear war. We first assembled a group of experts to prepare a research agenda for assessing ecological effects (Kercher et al., 1985). To implement the recommendations of this group, we are carrying out coordinated experimental and modeling studies on individual plants from selected species. In addition, we have undertaken modeling studies at the community and regional scales. The coordinated studies lay the foundation for an assessment of the effects of nuclear winter on agricultural systems. The community and regional studies assess the recovery potential of unorganized ecosystems.

We have completed our analysis of data from experiments conducted at the University of Wisconsin Biotron. In this work, soybeans and loblolly pine were subjected to two conditions simulating nuclear winter for several weeks (Rose et al., 1987). We reduced the temperature to 15°C and light by 99%. Tables 1 and 2 summarize our findings for soybeans and pine, respectively. We found no significant effect on growth or yield for the two species; however, growth was arrested during the time spent under conditions of nuclear winter. The time to achieve a set growth stage was therefore delayed by the length of exposure to nuclear winter conditions. Our results are in sharp contrast to the marked reduction in yield for wheat and potatoes (Rose et al., 1986).

Table 1. **Seed weight of soybeans in final harvest after a nuclear winter scenario.**

Treatment	Seed weight/ plant (g)
Control	63.6 ± 6.9
1 week nuclear winter	52.1 ± 17.1
2 weeks nuclear winter	55.3 ± 9.6

In our program on agricultural modeling, we are comparing the results of existing crop models to the Wisconsin experiments. Such model calibration will lay the foundation for assessing the agricultural effects of nuclear winter. We acquired two crop models, SOYGRO and GLYCIM, that calculate soybean seed weight over time. These models were developed by two independent sets of researchers. The Figure shows that both models compare well with the experimental results on yield. SOYGRO reflects the observed time delays as well.

In our program on natural ecosystems, we have developed a simulator of the vegetation dynamics over a forested region. We constructed the regional simulator, VISTA, by using an existing LLNL code, SILVA, on the gridpoints of a

Table 2. **Days to harvest from onset of nuclear winter scenario and total shoot weight for loblolly pine.**

Treatment	Number of days to 3 full-growth flushes	Dry weight (g)
Control	103 ± 15	28.7 ± 7.8
1 week nuclear winter	105 ± 18	33.7 ± 15.9
2 weeks nuclear winter	118 ± 17	39.2 ± 16.7
4 weeks nuclear winter	118 ± 17	29.0 ± 11.2
6 weeks nuclear winter	139 ± 5	32.2 ± 11.5

region. (SILVA is a model of the local dynamics of forest communities.) VISTA allows us to examine forest recovery and regrowth for extreme scenarios involving tree kill in a given area. However, the area must be revegetated by mechanisms of natural spread from remaining forests. We are currently testing the behavior of this model.

Preliminary computations using VISTA indicate that reforestation in a region, which depends on tree maturation and seed dispersal, is quite regular and deterministic for the dominant species. The movement of subdominant species is, on the other hand, irregular and stochastic.

During FY88, we will extend our work at the University of Wisconsin to test other plant species, such as those associated with grassland, and find the threshold of the observed responses of wheat and potatoes to reduced light and temperature. We will also compare model results with those from wheat and potato experiments for purposes of calibration and modification. By selecting the calibrated models that perform best, we can begin to develop a computational framework for the global assessment of crop loss for selected species. Finally, we will incorporate experimental data on seed dispersal into the forest spread simulator and assess rates of recovery of natural ecosystems under various scenarios.

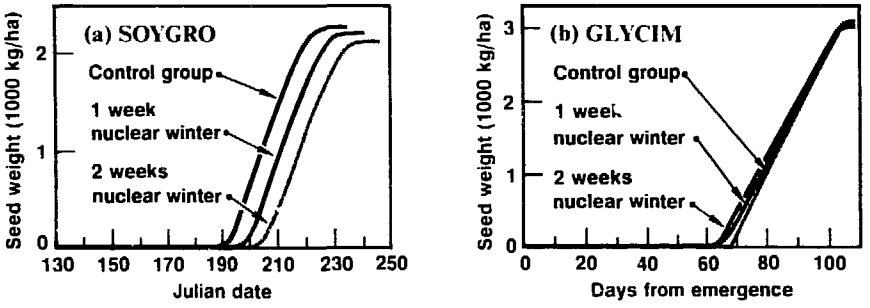

(a) The SOYGRO computer simulation of seed growth versus days of the year. This simulation of one and two weeks of nuclear winter conditions in soybeans shows delayed development of plants. (b) The GLYCIM computer simulation of seed growth versus number of days since seedlings emerge from the soil. This simulation of one and two weeks of nuclear winter conditions shows no significant reduction in soybean yield. These results agree with our experimental data from the University of Wisconsin.

References

Kercher, J. R., H. A. Mooney, and G. R. Grow (1985). *Research Agenda for Ecological Effects of Nuclear Winter*. Lawrence Livermore National Laboratory, Livermore, Calif., UCRL-53588.

Rose, E., J. Palta, B. McCown, T. Tibbetts, and M. Vinotti (1987). "Productivity of Loblolly Pines and Soybeans under a Nuclear Winter Scenario" (abstract). *Plant Physiol. Supplement* **83**, 71.

Rose, E., J. Palta, B. McCown, T. Tibbetts, and M. Vinotti (1986). "Productivity of Winter Wheat and Potatoes during a Nuclear Winter Scenario" (abstract). *Agron. Abstracts 1986 Ann. Meeting Am. Soc. Agron.*, p. 19.

The Compact Torus

Overview

Charles W. Hartman

The main objective of this project is a "proof-of-principle" experimental demonstration of the acceleration and focusing of plasma rings magnetically confined by the fields of a compact torus. Achieving this objective will enable us to construct higher-energy accelerators and to test applications. At higher energy, the compact torus accelerator can provide the basis for an efficient, low-cost inertial fusion driver. At the present energy scale, we can test applications to magnetic energy storage, a fast-opening switch, an ultra-high-power microwave source using rf compression, magnetic fusion, and weapons research.

We began construction of the plasma ring accelerator experiment (RACE) facility in April 1985 and completed it in April 1986. Since then, we have been operating the facility and have achieved our experimental goals roughly on schedule. Using RACE's magnetized coaxial gun, we demonstrated plasma-ring formation by July 1986 and acceleration of plasma rings by September 1986. Since then, we have controlled electrode-material contamination of the plasma enough to reduce the ring's mass to about 20 μg, raising its velocity to about 1500 km/s and its kinetic energy to 20 kJ with an initial accelerator-bank energy of about 65 kJ (a conversion efficiency of 30%).

We are currently testing the focusing of accelerated rings, adding improved diagnostics, and enhancing system performance. Improved diagnostics will lead to a greater and more detailed understanding of acceleration and focusing in this device.

To improve system performance, we will install a magnetic barrier coil at the muzzle of the ring-formation gun and a crowbar switch on the accelerator capacitor bank. We expect the barrier coil to inhibit the emergence of trailing plasma from the gun after the ring forms. The crowbar switch will reduce insulator contamination by preventing the accelerator's capacitor bank from ringing, thereby enabling us to increase the accelerator's energy. Both improvements will allow us to extend the range of the accelerator's operating parameters in the present experiment and determine scaling laws for future, higher-energy accelerators.

In FY87, the Compact Torus project received $1,017,000 in IR&D operating funds and $86,000 in equipment funds.

FY87: $1,017,000
FY88: $800,000

The Compact Torus

Principal Investigators:
Charles W. Hartman and
James H. Hammer

We have demonstrated the formation and acceleration of compact torus plasma rings. Initial tests produced high-mass rings; however, successive improvements in controlling mass evolution from the gun electrodes have resulted in near-optimum ring mass for acceleration. We have achieved acceleration of 20-μg rings to a velocity of ~150 cm/μs and kinetic energy of ~20 KJ for an efficiency of >30%. The observed ring formation and acceleration are roughly in agreement with numerical calculations of the ring trajectory, simulations with a two-dimensional magnetohydrodynamic (MHD) code, and analytic predictions. We have initiated tests of ring focusing and are now nearing the completion of improvements in diagnostics and system performance.

A compact torus is a magnetically confined plasma ring, where the conducting plasma and entrained toroidal ($\mathbf{B}_\theta$) field are linked by a dipole-like, poloidal ($\mathbf{B}_r$, $\mathbf{B}_z$) field. The magnetic fields are produced largely by plasma currents and are convected along when the plasma undergoes translation. Such properties and the observed ruggedness of compact toroids make them an ideal "macroparticle" for acceleration. Our work is providing the basis for a higher-energy accelerator that can serve as an efficient, low-cost inertial fusion driver.

Figure 1 shows a compact torus plasma ring located between the accelerator electrodes. To form the plasma ring, the solenoid capacitor bank is first discharged to establish a magnetic flux inside the gun center electrode and a radial fringe field near the muzzle of the gun. Pulse gas valves are then opened, and after the gas has spread across the electrode space, the gun capacitor bank is discharged. Plasma and the $\mathbf{B}_\theta$ magnetic field formed by the gun discharge are expelled from the gun entraining the pre-established $\mathbf{B}_r$, $\mathbf{B}_z$ field of the solenoids. The combined fields and plasma expand past the gun muzzle; after reconnection, they form a compact torus plasma ring in the accelerator interelectrode space. After the ring drifts past the accelerator feed slot, the accelerator capacitor bank is fired, accelerating the ring as in a coaxial rail gun.

Focusing of an accelerated plasma ring takes place as the ring enters the conical electrode section at the far-right end of the accelerator shown in Figure 1. The ring momentum carries the ring toward the apex of the cone, while the compact torus field, which is constrained by the electrodes, decreases in major and minor radius to focus the magnetically confined plasma. Because the plasma pressure is low ($\beta \ll 1$), the nearly force-free ring field undergoes self-similar focusing, decreasing the ring length as well. Neglecting drag forces and plasma pressure, a maximum compression ratio $R_0/R_{min} = U_K/U_m$ is reached where the ring's entering kinetic energy is converted to magnetic energy. (Here, R_0 is the initial ring radius, R_{min} is the minimum ring radius, U_K is the kinetic energy at the end of the acceleration region, and U_m is magnetic energy at the end of the acceleration region.) For a high-speed ring, focusing times are typically tens of nanoseconds, allowing the possibility of achieving the high focal energy densities required for an inertial fusion driver, as shown in Figure 2.

Apparatus. Figure 1 shows the Plasma Ring Accelerator Experiment (RACE) apparatus as presently configured. The gun and accelerator electrodes are mounted in a 1.54-m-diam, 6.75-m-long aluminum vacuum tank. The tank is pumped by a turbomolecular pump and two cryopumps to a base pressure of typically 2×10^{-7} Torr. The magnetized, coaxial plasma gun has a 35-cm-diam, 50-cm-long, stainless-steel outer electrode from the breech step to the muzzle step and a 20-cm-diam, stainless-steel inner electrode. Eight fast-acting pulse gas valves are located near the center of the outer electrode. An outer solenoid is

positioned as shown, and an inner solenoid is located inside the inner electrode.

The outer gun electrode is extended 4 m at 50-cm diam, forming the outer accelerator electrode. The 20-cm-diam inner accelerator electrode is brought in through the center of the inner gun electrode and is coaxial within the outer electrode. A 2-m-long focusing cone forms the muzzle end of the accelerator electrode assembly.

FY87 Progress. Our initial tests on the RACE facility were designed to demonstrate formation of compact torus plasma rings in the accelerator configuration. Our tests quickly confirmed the predicted formation process and verified the basic structure of the ring field using insertable B-loop probes. We found that the rings have approximately the predicted length, drift at about the Alfvén velocity (typically 10 to 20 cm/μs) in the accelerator region, spread axially at about the Alfvén velocity, and decay during 2-m drift down the accelerator with a lifetime of ~30 μs. The ring magnetic energy was 2 to 10 kJ at the 50-kJ gun bank energy, consistent with predicted efficiencies.

We have developed several codes to evaluate ring acceleration and applications. The RAC zero-dimensional ring acceleration code (Hartman et al., 1986) and the hydrodynamic and magnetic (HAM)

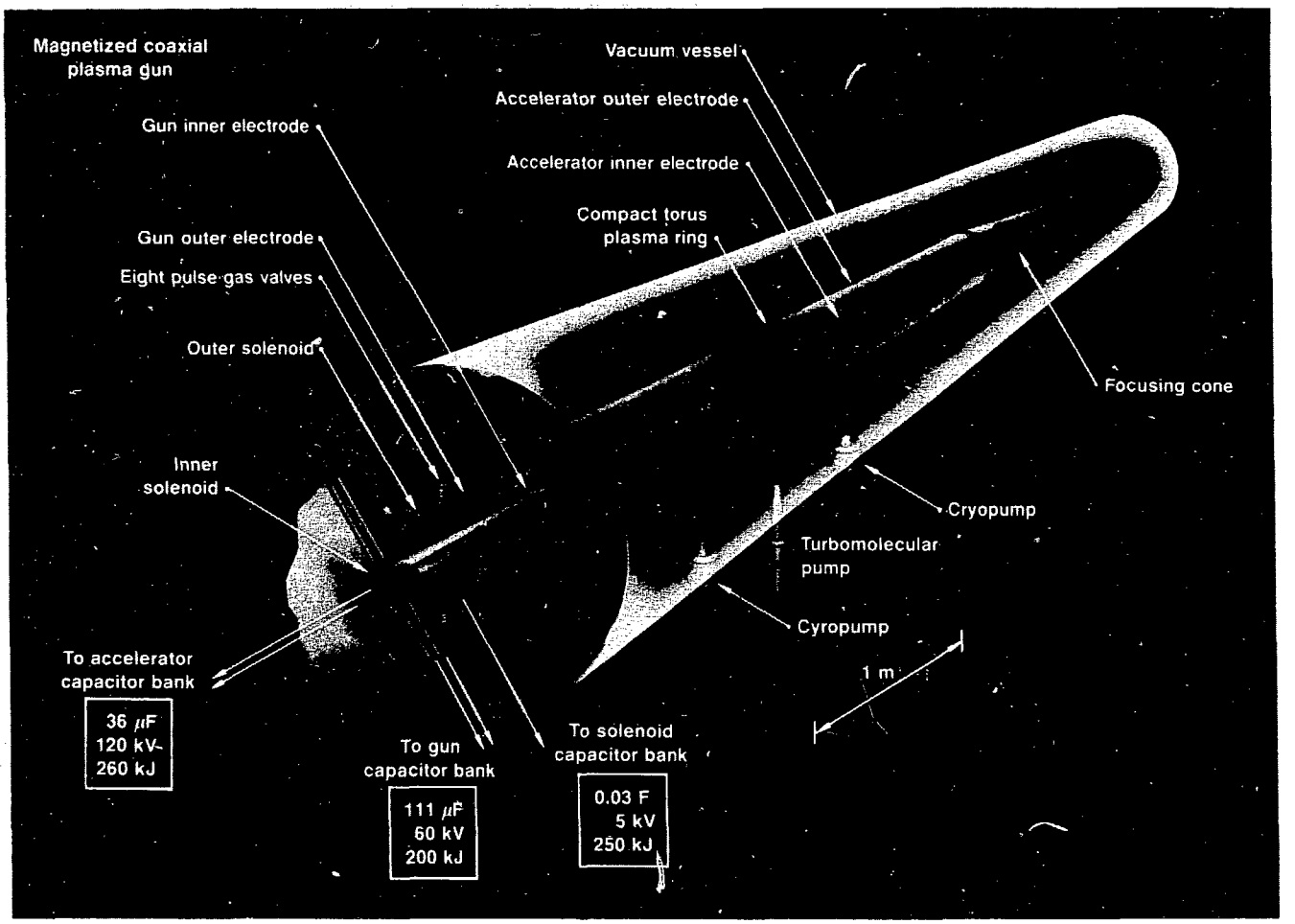

Fig. 1. The RACE apparatus as configured October 1987. The initial magnetic field of the gun is established by discharging the electrolytic solenoid capacitor bank through solenoids located outside the gun outer electrode and inside the gun inner electrode. Eight magnetically driven gas valves admit roughly 1 atm·cm³ of gas. The gun capacitor bank feeds the gun through a low-inductance array of coaxial cables and collector plates. Discharge currents typically have a 2-μs risetime and a 500-kA peak current. The accelerator capacitor bank is isolated from ground and has a parallel-plate transmission line that connects to the gun inner electrode and the coaxial inner electrode of the accelerator. A compact torus undergoing acceleration by the B_θ field is shown in the middle of this drawing.

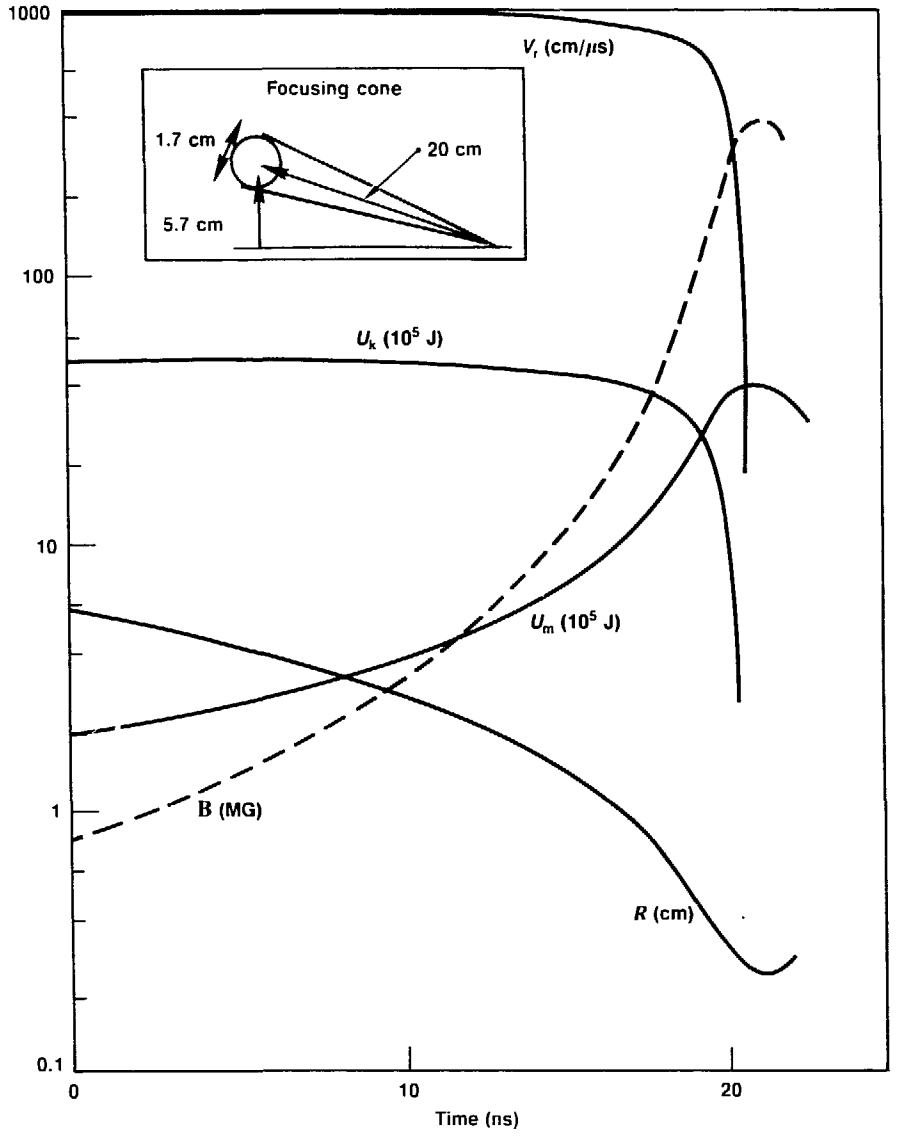

Fig. 2. Illustration of the potential for high-energy density states of a focused compact torus plasma ring. This calculation uses the RAC code and a precompression cone. A ring with radius R = 50 cm is first compressed to 5.7 cm in 10 μs by discharging a 9.3-MJ, 120-kV capacitor bank. Following 0.5-μs acceleration, the 10^{-4}-g ring enters the focusing cone, shown at the top, with a velocity of 10^9 cm/s and 5 MJ of kinetic energy. The ring then reaches its minimum radius R = 0.23 cm and maximum field. Inertia of the cone and the slow speed of ablative wall material allow the high-speed ring to outrun wall effects. A target would intercept the ring at R = 0.5 cm, $U_{kinetic}$ = 4.8 MJ, and the ring ions would deposit 1.6 × 10^{16} W total power (3.4 × 10^{16} W/cm²) in 0.3 ns.

two-dimensional MHD code (Maxom and Eddleman, 1978) have begun to show quantitative agreement with experiment.

The RAC code calculates the trajectory of a fixed-mass ring in conical or straight coaxial electrodes. The code accounts for magnetic forces derived from the discharge of the accelerator bank, the ring's magnetic field, and drag due to eddy currents in nearby walls. Ring plasma properties are obtained from volume-average heat flows, including ohmic, compression, and acceleration heating, and radiation and thermal conduction losses. During FY87, we extended the RAC code to include unequal electron and ion temperatures and improved models of nonadiabatic acceleration heating. We discuss comparisons of the RAC code with experiments later in this article. We also ran the HAM code with successively improved input and wall conditions and obtained reasonable agreement with experiment, as shown in Figure 3.

Tests of ring acceleration following our initial demonstration of ring formation verified the predicted acceleration process of a nearly constant mass ring accelerated with low drag forces by the accelerator $\mathbf{B}_\theta$ field. These tests were conducted with the final 2 m of the accelerator linear rather than conical. Predicted acceleration limits, based on destabilization of Rayleigh-Taylor modes, were exceeded without serious disruption of the ring. We achieved values of

$$F_{ring}/F_{ring\ predicted} = B^2_{\theta ring}/B^2_{\theta ring} \approx 1$$

compared with predicted

$$B^2_{\theta ring}/B^2_{\theta ring} \leq 0.4.$$

Here, F_{ring} is the force applied to the ring for acceleration, and $F_{ring\ predicted}$ is

the internal force holding the ring together. For

$$B^2_{\theta acc}/B^2_{ring} > 1,$$

we observed the predicted "blow-by" phenomenon, where the $B^2_{\theta acc}$ field pushes by the ring at the accelerator center conductor.

Comparison of the accelerated ring trajectory measured by magnetic field probes near the outer electrode with a fixed mass yielded good agreement with the RAC code for a ring mass $M = 500$ μg. The initial ring velocity of 17 cm/μs increased to 40 cm/μs after 2 m of acceleration, corresponding to a kinetic energy of 40 kJ, or 40% of the initial accelerator bank energy.

The typical ring mass of ~500 μg is greater by a factor of about 10 than the optimum ring mass required to match the electrical time constant $(L_{acc}C)^{1/2}$ (where L_{acc} = accelerator inductance) of the accelerator bank to the inertial time constant l_{acc}/V_{ring} of the ring (where l_{acc} = accelerator length and V_{ring} = ring velocity). To reduce the ring mass, we installed 0.010-in.-thick tantalum sheet liners in the gun. The liners present a more refractory surface to the plasma than the original electropolished stainless-steel surfaces. Through a series of experimental tests with progressively increased liner coverage, discharge cleaning, and careful adjustment of the gun parameters, we reduced the ring mass to ~10 to 20 μg by mid-FY87. The determining factors in adjusting the gun parameters are avoidance of post-ring plasma and field ejected from the gun, which block the acceleration field from reaching the ring.

We have accelerated low-mass plasma rings from initial velocities ranging from 50 to 100 cm/μs up to 300 cm/μs (Hammer et al., 1987). Figure 4 shows a comparison of ring position measured by magnetic probes over time with the trajectories calculated using the RAC code. The best-fit $M = 17.5$ μg trajectory has an initial velocity of 50 cm/μs and a final velocity of 150 cm/μs, which corresponds to about 20 kJ of kinetic energy. The ring magnetic energy is estimated to be about 2 kJ, giving

$$U_K/U_m \approx 10.$$

We obtained similar agreement in a comparison of the ring position measured by magnetic probes and the location of the accelerator current sheath, as determined by the voltage and current at the accelerator breech. The location of the current sheath at the ring position indicates that acceleration fields are applied directly to the ring rather than to trailing plasma mass. The accelerator voltage and current can be used to calculate the energy input to the accelerator.

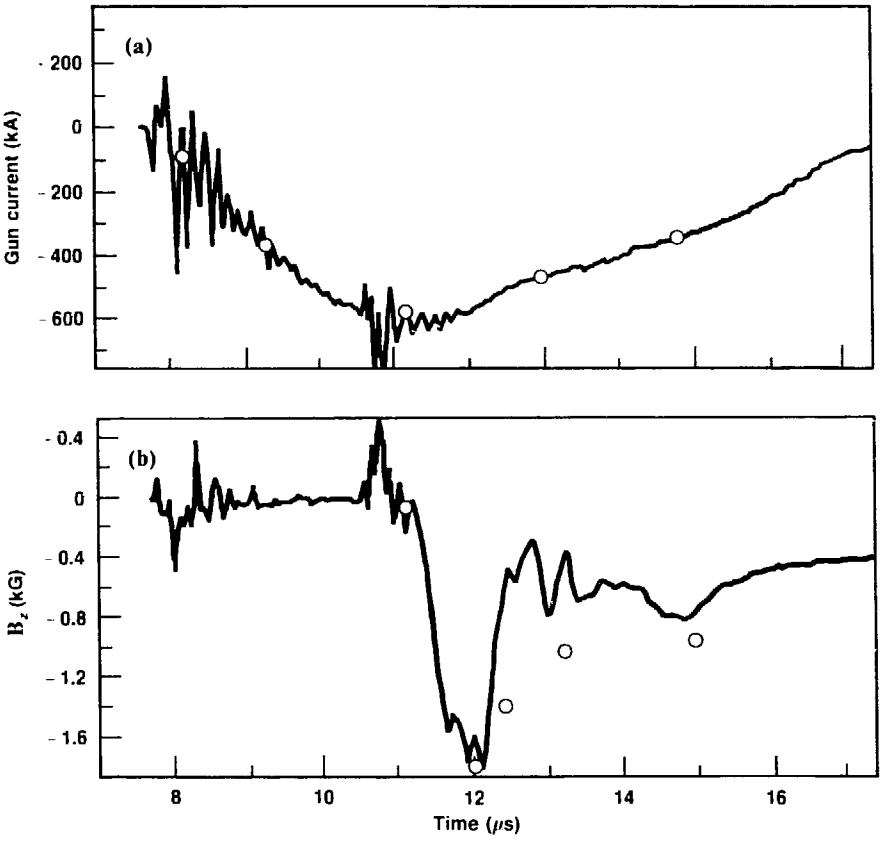

Fig. 3. Comparison of ring formation with the two-dimensional MHD code (calculations are shown as data points) with (a) measured gun current and (b) B_z field at the wall 20 cm past the outer electrode step. Departures of B_z following the peak suggest that reconnection occurs more rapidly in the experiment than in the code for this example. The magnitude of the late B_z depends critically on gun parameters and varies from shot to shot.

$U_{in} = \int VI\, dt$,

and the inductively stored energy,

$U_L = L(t)I^2/2$.

Neglecting sheath drops and other losses, we can calculate a "kinetic energy" at any point along the acceleration,

$U_K = U_{in} - U_L$,

which is in good agreement with the RAC code fit shown in Figure 5, giving independent confirmation of the ring kinetic energy.

Since mid-FY87, we have concentrated on improving electrode surfaces, developing more diagnostics, and fabricating and installing a 2-m-long focusing cone. All electrode surfaces are now covered with tantalum liners, and we have initiated tests of ring acceleration and focusing.

FY88 Objectives. Our main objectives for FY88 are to improve system performance, to document in greater detail the ring acceleration process with more extensive diagnostics, and to test the focusing of rings. We will also study scaling of ring acceleration to higher energy (the full capability of the RACE capacitor bank is 260 kJ).

Limitations of RACE parameters arise from two sources: the necessity of avoiding post-ring-formation plasma and field ejected from the gun, and the ringing current of the accelerator bank, which erodes electrode material and deposits it on the accelerator insulator vacuum interface. Avoidance of post-ring plasma requires that we carefully adjust the gun parameters, particularly the solenoid field strength and gas input timing, so that the reconnected solenoid field can inhibit further plasma expulsion by the gun. To overcome this limitation, we are constructing a "snipper coil" assembly, which will enable us to introduce a magnetic barrier to post-ring plasma. The barrier field will be provided by a single-turn coil located at the gun muzzle. We will avoid the deposition of electrode material on the accelerator insulator by using a rail-gap crowbar that is now under construction.

In terms of increased diagnostics, we will install a CO_2 single-beam interferometer in the first quarter of FY88. We have initiated visible-light spectroscopy in collaboration with the Air Force Weapons Laboratory, and we intend to extend spectroscopic studies to the vacuum ultraviolet. Development of calorimeter probes, Faraday cup probes, a dynamic pressure probe, and an ion energy analyzer are in progress.

Given our continued success in proving the principles of ring acceleration and focusing, we will begin planning for experimental tests of applications, such as the fast-opening switch, a high-power microwave source, and fueling and current drive for magnetic fusion devices. If scaling studies show positive results, we may initiate plans for a 2-MJ RACE II experiment to reach higher energy densities as a step toward a full-scale inertial confinement driver. Although the physical size of the accelerator would not increase rapidly, a full-scale inertial confinement driver would require roughly 20 MJ of bank energy. Figure 6 shows a pathway in parameter space leading to an inertial fusion driver.

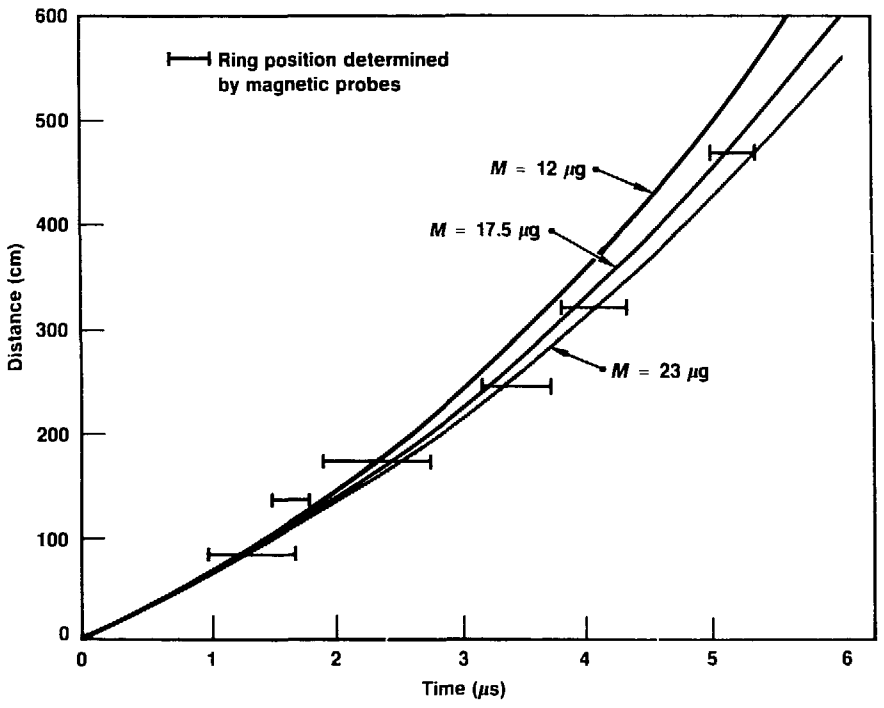

Fig. 4. Ring position measured by magnetic probes at the outer accelerator electrode compared with parameterized calculations for three ring masses using the RAC code. For the best-fit RAC calculation with M = 17.5 μg and an initial speed of 50 cm/μs, the calculated final ring speed is 150 cm/μs and the kinetic energy is 20 kJ. Time is measured from initiation of the accelerator bank discharge, and distance is measured from the gun muzzle.

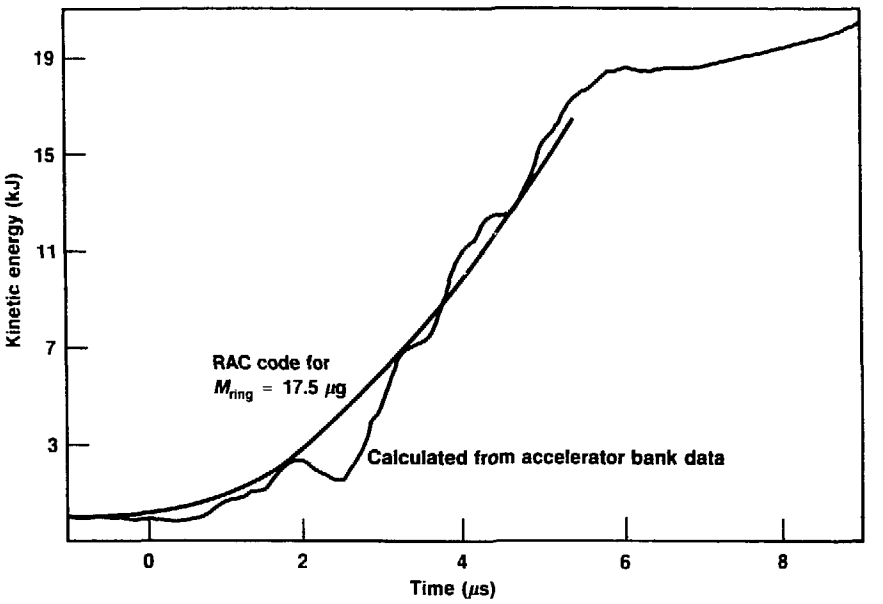

Fig. 5. Comparison of ring kinetic energy calculated by the RAC code for the best-fit conditions of Figure 4 and the "kinetic energy" calculated from the voltage and current measured at the accelerator breech.

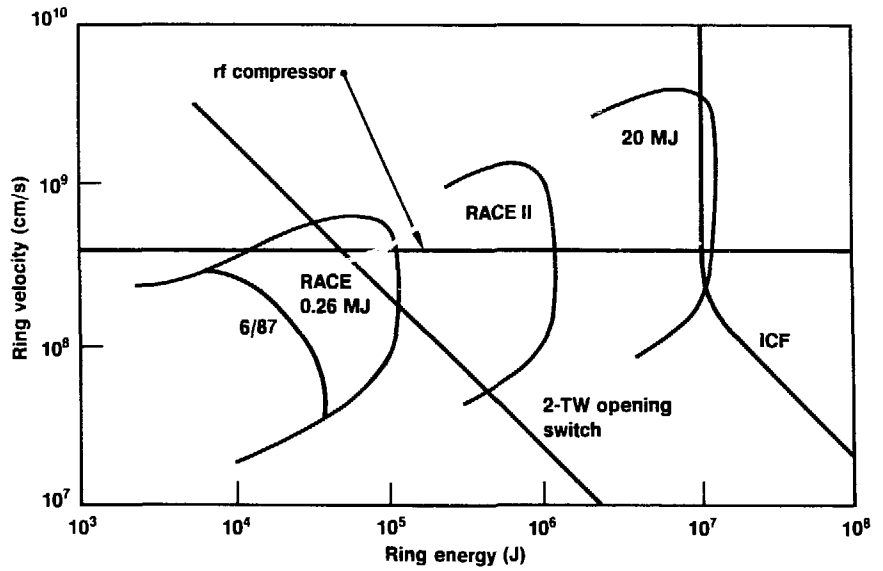

Fig. 6. Overview of parameter space related to the development of plasma ring acceleration for driving inertial confinement fusion. The inertial confinement fusion parameters are based on efficient coupling of the ring ion kinetic energy to hohlraum radiation. This diagram also shows applications of the RACE accelerator to an radio-frequency (rf) compressor source and to a 2-TW, fast-opening switch. The curve labeled 6/87 shows the envelope of available parameter space that had been explored as of June 1987 in the RACE experiment.

References

Eddleman, J. L., J. H. Hammer, and C. W. Hartman (1986), "Modeling of High Power Source by Plasma Ring RF Compression," *Bull. APS* **31**(9), 1485.

Hammer, J. H. and C. W. Hartman (1982), "Application of Accelerated Compact Toroids," *Proc. Fifth Symp. Physics Technol. Compact Toroids*, Seattle, Wash.

Hammer, J. H., C. W. Hartman, and J. L. Eddleman (1987), *Results from the RACE Compact Torus Acceleration Experiment*, Lawrence Livermore National Laboratory, Livermore, Calif., UCRL-96828.

Hartman, C. W., J. L. Eddleman, and J. H. Hammer (1986), "Plasma-Ring, Fast-Opening Switch," *IEEE Conf. Record Abstracts*, Saskatoon, Canada.

Hartman, C. W., J. L. Eddleman, J. H. Hammer, and D. L. Meeker (1986), "The Compact Torus Plasma Ring Accelerator—A New Type Driver for Inertial Confinement Fusion," *Proc. Fourth Internat. Conf. Emerging Nuclear Energy Systems*, Madrid, Spain; Lawrence Livermore National Laboratory, Livermore, Calif., UCRL-93786.

Hartman, C. W. and J. H. Hammer (1984), *Acceleration of a Compact Torus Plasma Ring, A Proposed Experimental Study*, Lawrence Livermore National Laboratory, Livermore, Calif., LLL-PROP-191.

Hartman, C. W. and J. H. Hammer (1986), *Proposed Experimental Study of the Plasma Ring Opening Switch*, Lawrence Livermore National Laboratory, Livermore, Calif., LLL-PROP-00198.

Maxom, S. and J. Eddleman (1978), "2-Dimensional Magnetohydrodynamic Calculations of the Plasma Focus," *Phys. Fluids* **21**, 1856.

Supercomputer Research and Development

Overview

A. Carl Haussmann

The overall goals of the supercomputer R&D effort are to develop the tools and techniques needed to design, manufacture, package, test, and maintain the supercomputers of the 1990s; to build advanced demonstration supercomputers for scientific applications; and to create the supporting software needed to make these computers into useful systems. Some of the codes and technology packages we have developed have already proved useful to industry. We will continue this technology transfer to demonstrate the merits of both the computer system and the design and manufacturing technologies used to produce it.

In addition to IR&D support, our supercomputer R&D program is funded by the U.S. Navy's S-1 project, the Very-High-Speed Integrated Circuits (VHSIC) laser pantography program of the Department of Defense, and some related Strategic Defense Initiative Office (SDIO) projects.

The current-generation research computer—the Advanced Architecture Processor (AAP)—is under construction. The supercomputer configurations we are considering, such as the AAP, require extensive software development, both for applications programs and for major extensions of the Structured Computer-Aided Logic Design (SCALD) tool set we developed. These software extensions must also be linked to hardware implementation (such as supporting design tools) and to appropriate computer-aided manufacturing tools (such as laser pantography).

Laser pantography and its supporting technologies, which enable a computer-controlled laser to "write" transistors, conductors, and insulators directly onto a silicon substrate, hold the prospect of wafer-scale integration of electronic assemblies containing millions of transistors. They should permit putting a computer equivalent to the AAP on one 10- to 15-cm-diam silicon wafer, and should make it economically feasible to produce one-of-a-kind circuits ranging from semicustom gate-array chips to custom supercomputers. Fabrication turnaround times of minutes (for a chip) to days (for a supercomputer) appear possible.

A major product of our supercomputer R&D program has been the SCALD concept and its early implementations. The acceptance of this technology by industry (SCALD concepts are now world standards) was one of the Department of Energy's technology transfer successes. It led to an array of private sector companies with several million dollars in annual sales.

This year we focused much of our IR&D funds on computer-aided design (CAD) tools for both laser pantography and the S-1 project. As they are developed, the tools are being distributed through the CAD software outlet at University of California (UC), Berkeley.

Less provable, but probably true, is that the existence of our computer center and the S-1 project has stimulated the industry to produce far larger memories. This last year has also seen the initial transfer of laser pantography technology into the commercial sector.

It is in this country's interest to stimulate additional advanced thinking in supercomputer research and development. Our project is a positive force in this arena, providing spin-offs in the form of the tools, techniques, and concepts that are at least as important as the computer itself. Progress on the S-1 project's AAP implementation has been steady; laser pantography advances have been excellent.

The total direct funding from all sources was $19.1 million in FY87; the project received $1,525,000 in FY87 from IR&D.

Computer-Aided Design Tools for Very Large Scale Integration (VLSI CAD)

Principal Investigator:
Walter S. Scott

This project is developing a vertically integrated set of tools for computer-aided design, manufacture, and testing of hybrid wafer-scale digital systems. In FY87, we developed tools for three CAD tasks: placing components, routing the wires that connect them, and testing the finished design. The tools we develop are widely distributed to industry and academia.

We are developing vertically integrated tools with which to design and manufacture hybrid wafer-scale digital systems. A hybrid system consists of several silicon chips mounted onto a single substrate (in this case, a silicon printed circuit board, or PCB) that routes signals, distributes power, and removes heat. We exploit novel manufacturing techniques developed by LLNL's laser pantography project, techniques that allow rapid fabrication of digital systems with multiple levels of metal transmission lines for high density and performance. The laser pantography process allows rapid repair, during fabrication, of the inevitable manufacturing defects. Previous attempts at wafer-scale integration (WSI) have been unsuccessful, largely because of formidable problems with manufacturing that limit the yield of usable circuits.

In FY87, we developed tools for three CAD tasks: optimally placing components in a VLSI system, routing the wires that connect components, and testing the finished design. In particular, we developed these tools:

- A placement program, Panzer, that uses simulated annealing to determine near-optimal component placement in gate-array, wafer-scale silicon PCBs and in conventional board-level layouts.
- A semiautomatic routing tool, a hint router, that finds optimal point-to-point wiring paths. The designer supplies hints that guide the router; the amount of guidance is at the discretion of the designer.
- Fully automatic routing tools for both gate-array and wafer-scale layouts.
- A novel approach to testing printed circuit boards for hybrid wafer-scale systems.

Panzer: Integrated-Circuit (IC) Placement. Panzer places structures such as gate arrays, hybrid wafer-scale silicon PCBs, or conventional PCBs in fixed locations. The system uses simulated annealing (Kirkpatrick et al., 1983) to minimize established wire length. Its basic strategies are derived from those used in the TimberWolf placement and routing package (Sechen and Vincentelli, 1986), which is oriented toward standard-cell arrays that are organized in rows of cells of a common height but with arbitrarily varying widths. For our purposes, components must lie in fixed locations—a constraint that required development of entirely new algorithms for Panzer.

Simulated annealing, the underlying approach used by Panzer to minimize wire length, is a Monte Carlo-like technique for solving large classes of combinatorial optimization problems. The annealing process starts with an initial solution that is perturbed to generate a new solution. If this new solution is better, it becomes the new starting point. However, if the solution is worse, it can still be accepted, with a probability that depends on the length of time the annealing process has been running. During early stages, the probability of accepting a worse configuration is high, while in later stages, the probability drops to zero. This ability to move to intermediate solutions that are slightly worse than the previous solution allows simulated annealing to avoid local minima.

We have used Panzer to place a number of gate-array and silicon PCB designs; we are now extending it to support more types of gate arrays and also conventional PCBs such as those used in the S-1 AAP processor design. Any components in a design can be preplaced; Panzer automatically places remaining components in such a way as to minimize the total length of wire required to connect them. Panzer can completely place a 3500-gate-equivalent bipolar array in under one hour of Sun-3/260 CPU time.

Semiautomatic Routing with Hints. Often in custom, high-performance designs, it is necessary to route certain critical signals along carefully chosen paths before automatically routing the remaining signals. We have developed a semiautomatic tool for routing such individual signals in

a completely placed circuit layout. The router uses hints to allow designers (or other CAD tools) to suggest all or part of a signal's path to the router, causing the router to generate a path that follows the hints as closely as possible while adhering strictly to the design rules. This tool is particularly useful for pre-routing critical nets, and we believe it will also be important in the repair of silicon PCBs (discussed below). It is implemented as part of the Magic IC layout system (Ousterhout et al., 1985) and is capable of using any number of routing layers to make its connections.

In addition to allowing designer hints, the implementation of the router is novel in two other aspects. First, it uses corner-stitching, a new, gridless data structure that gives the router performance superior to traditional Lee-style (wavefront) maze-routing algorithms and that also makes the router's runtime independent of scale.

Second, the router uses a number of search heuristics to speed its performance dramatically without reducing its generality. The gross structure of the layout is preprocessed to facilitate accurate estimates of cost to completion during routing and hence effective pruning of misdirected partial routes. A windowed search-strategy slowly shifts the focus from the start-point toward the goal. This permits the consideration of alternatives at all stages of routing without blowing up into an exhaustive search. Another mechanism, blooming, allows limited heuristic expansion of paths, subordinate to the general cost-based search. With blooming, line-expansion style heuristics can be used without sacrificing the flexibility of general maze-routing.

The combination of corner-stitching and the above heuristics enables the router to perform interactively on large designs; each successive route takes only a few seconds to perform on a Sun-3/260 workstation. In fact, as the Table indicates, the router's performance is close to the theoretical optimum on typical large designs.

Automatic Integrated Circuit Routing. While the hint-following router described above is useful for making individual, critical connections, other tools are needed to route most wiring in a design. Along these lines we have developed a suite of routers, all based on the Magic IC layout system, for routing gate-array-scale and wafer-scale designs.

The first router can route a 3500-gate-equivalent array in under one hour of Sun-3/260 CPU time. It accepts as input a Magic net list and a partially prerouted Magic layout (typically containing prewired power/ground and critical nets). The output is a Magic layout of the completed routing. Novel in this router are its ability to exploit automatically all available routing space over the tops of gate-array macros and the algorithm it uses for congestion control during the global routing phase to ensure 100% routability.

The second router is intended for silicon PCBs and is based on the YACR channel router developed at UC Berkeley and the global router described above. It generates higher-quality routing (shorter wires and fewer vias, the name given to holes through the insulating structure to allow signal transfer between levels of metallization) than the gate-array router, but at the cost of reduced flexibility. This router allows only limited prewiring, instead of avoiding obstacles as does the gate-array router.

Our experience with the shortcomings of both routers has led us to develop a third router intended to cover the complete spectrum of routing scenarios. This router, unlike its two predecessors, will work on an arbitrarily large number of layers, making it useful for multilayer silicon PCBs and modern gate-array designs. Designs with three or more levels of metal use a "sea-of-gates" organization in which routing regions are defined implicitly by the absence of pre-existing metal, rather than explicitly as rectangular channels between rows of subcomponents. Figure 1 shows the compact and simple wiring possible because this third router uses corner stitching as its underlying data structure, is able to rip up portions of nets to explore alternative routings, and includes a robust suite of routing strategies ranging from simple two-segment to arbitrary maze-routers. In

Table. The hint router's fast-search feature approaches the theoretical optimum on typical large designs and outperforms conventional maze routing algorithms (Lee and Tiles). The single-row example involves routing across one row of a standard-cell design; the subchip example involves routing across a large standard-cell subchip that contains 1200 transistors.

Algorithm	Paths considered	
	Route across single row of subchip	Route across entire subchip
Lee	1.0×10^7	4.5×10^7
Tiles	1.01×10^4	6.3×10^4
Fast search	142	235
Optimal	60	100

developing this router, we are focusing on improving the set of strategies available to it and on extensively measuring the effectiveness of these strategies.

All of these routers make use of the global via-minimizer we developed, which eliminates vias from routing. The via-minimizer uses a collection of simple pattern-recognition rules but by operating on the entire design is able to eliminate far more vias than possible with channel routers alone. We have observed via reductions of 20 to 40% over the gate-array router and of 10 to 30% over the silicon PCB router.

Silicon PCB Testing. We developed a new strategy, smart substrate, to test silicon PCBs for defective wires before their repair by laser pantography. A smart substrate is a set of fault-tolerant complementary metal-oxide semiconductor (CMOS) testing circuits fabricated in a silicon wafer by conventional processing before it becomes a PCB. These testing circuits (see Figure 2) are used to automatically test the silicon PCB for shorts and opens once its wires have been deposited and to measure the resistances of its wires.

Technology Transfer. We believe that the tools we develop benefit from being used as widely as possible, and we have made an effort to transfer our tools to industry as soon as they are ready. We have already transferred several of the tools described above to industrial and university beta-test sites, including Stanford University, New York University, UC Berkeley,

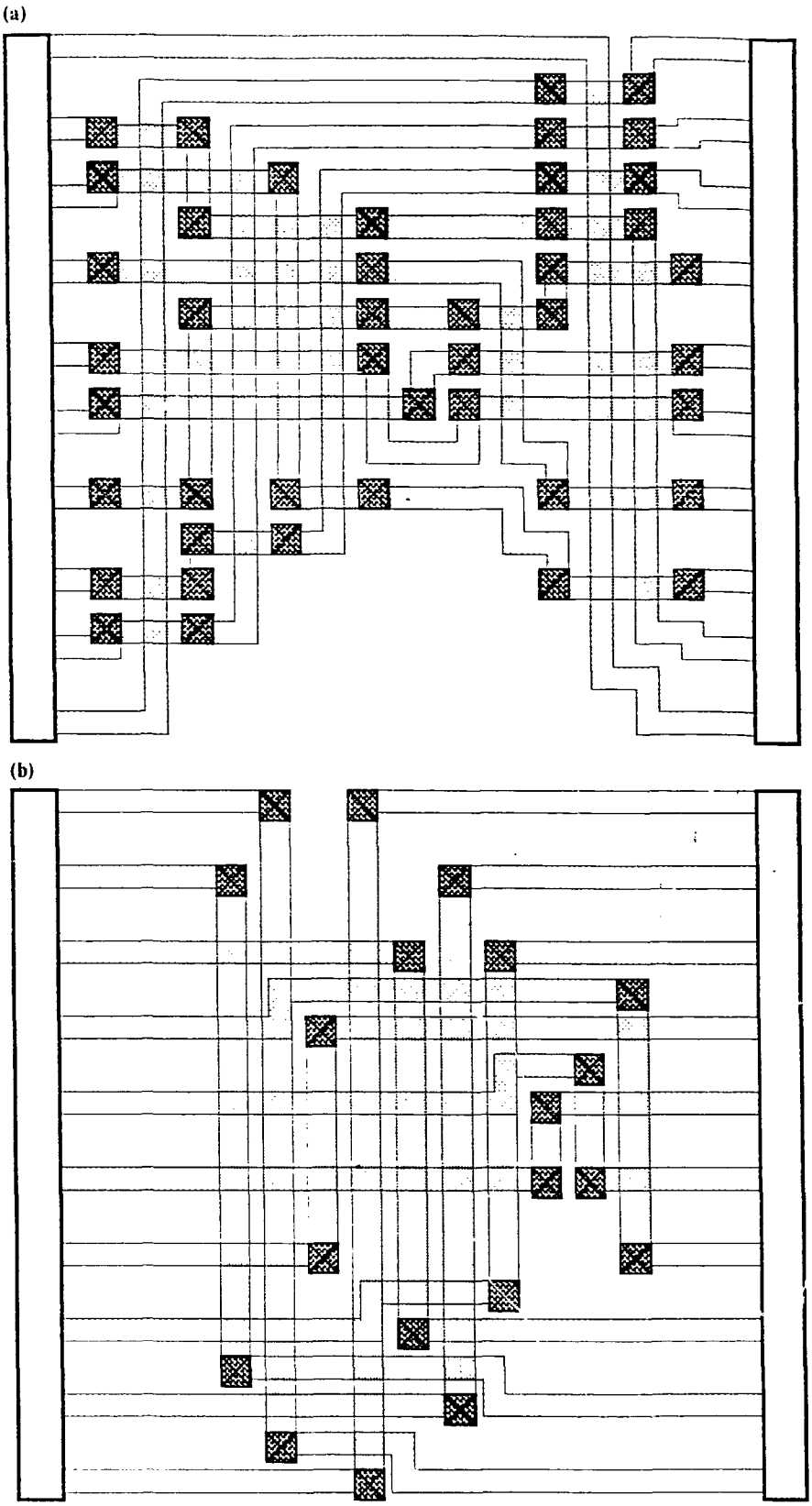

Fig. 1. Comparison of the output from (a) an early Magic router and (b) the compact and simple routing possible with the multilayer router.

Digital Equipment Corporation's Western Research Library, and LSI Logic Corporation. In addition, most of our tools are being included in UC Berkeley's VLSI tools distribution; this distribution typically reaches over 200 domestic industry, university, and government sites.

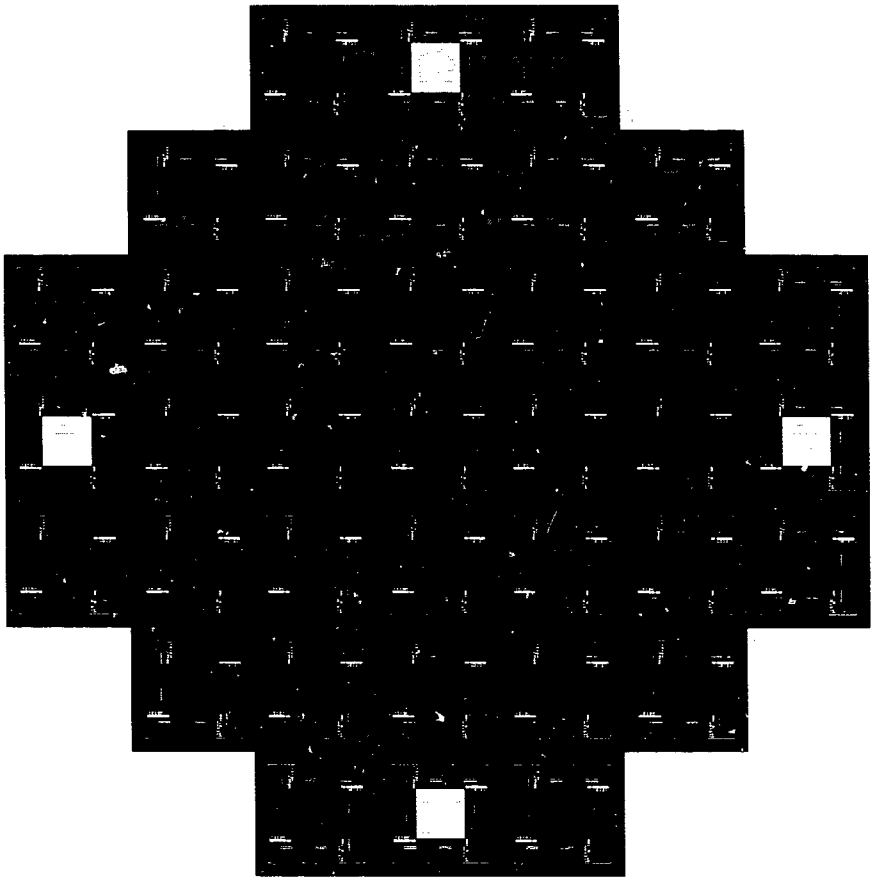

Fig. 2. Checkplot of the layout for all chip sites in an entire 4-in. wafer.

References

Kirkpatrick, S., C. D. Gelatt, and M. P. Vecchi (1983), "Optimization by Simulated Annealing," *Science* **220**, 671.

Ousterhout, J. K., G. T. Hamachi, R. N. Mayo, W. S. Scott, and G. S. Taylor (1985), "The Magic VLSI Layout System," *IEEE Design and Test of Computers* **2**(1), 19.

Sechen, C. and A. S. Vincentelli (1986), "TimberWolf 3.2: A New Standard Cell Placement and Routing Package," *Proc. 23rd Design Automation Conf.*, 432.

FY87: $780,000

S-1 High-Performance Computer Development Project

Principal Investigator:
Jeffrey M. Broughton

Our goal is to develop the high-performance computer environment that will be needed in the 1990s for the mathematical simulation of complex physical phenomena. We are addressing issues in computer architecture, design, fabrication, operating systems, and applications languages. The project, which began in 1977, has completed two generations of prototype systems; in FY87, we completed the design of and began testing a third-generation system.

The charter of the S-1 project is to develop high-performance computer systems for advanced applications in numerical and symbolic data processing, command and control, and simulation—vital areas for the national security and the health of the economy. We plan to exploit the full potential of silicon-based digital circuitry and, ultimately, develop the technology for producing custom computers rapidly and economically. Computers customized for specific applications could significantly outperform general-purpose computers. Toward this end, the S-1 project has undertaken a research program to develop appropriate multiprocessor architecture, computer-aided design, and advanced software.

Computer Architecture. The Advanced Architecture Processor (AAP) is being developed to demonstrate a multiprocessor interconnection technique (Moldenhauer et al., 1987) that is suitable for linking any number of supercomputer processing elements, including those with customized architectures.

We began by developing a uniprocessor. Its design was verified by executing large codes, including the Amber operating system, through the SCALD logic simulator (see "Computer-Aided Design Techniques"). We have shown that the AAP uniprocessor system can support scientific, symbolic, and general-purpose computation at a sustainable rate of 33 million instructions per second. Construction of the uniprocessor prototype has begun.

We are now validating the design of the multiprocessor version of AAP. Functional processors in a multiprocessor are connected with a global bidirectional ring network. The network can be easily extended by adding new nodes; each node provides a bandwidth of 1.6 gigabytes per second.

We developed protocols to support synchronization and memory consistency between cooperating processors. We are investigating optimistic synchronization (Jensen et al., 1987), a novel mechanism for implementing exclusive data access with higher-level, nonatomic operations. Caches are placed between the main memory and the CPU to hold frequently used data. A cache-coherency procedure assures that a cache accurately reflects the data in the memory, even though multiple copies are held within the multiprocessor. Our unique contribution has been a distributed dictionary approach suitable for nonbroadcast, packet-switched networks (Bruner et al., 1987).

High component densities are necessary for high performance. Initially, the AAP will use a combination of semi-custom gate-arrays and special packaging to achieve this goal. Logic chips are mounted on small ceramic printed circuits in which passive components are embedded, saving between 100 and 200% in circuit area. The system is cooled by direct immersion; the walls of the cooling vessel are the PC boards themselves, permitting debugging and maintenance to be carried out on the dry sides of the boards. In FY87, we completed prototypes of all mechanical parts of the packaging system and subjected them to extensive testing. In the longer term, it is our intention to reimplement the AAP in a wafer-scale circuit technology currently being developed by LLNL's laser pantography project.

Computer-Aided Design Techniques. Design time must be significantly reduced if customized computer architectures are to be produced in a timely and cost-effective fashion. One goal of the S-1 project has been to fully automate the design process. Our Structured Computer-Aided Logic Design (SCALD) has made it possible for a small staff to create complex systems very quickly. The SCALD concept has been transferred to industry; these design and simulation tools have spawned an array of private-sector companies.

In FY87, we continued to develop a test-pattern generation program to permit automated testing of SCALD-designed hardware. The program,

which is based on a significant new algorithm, can generate tests for nearly 100% of the gates in a combinatorial circuit.

System Software. We are developing software that will make the S-1 computers applicable for computing problems in academia, industry, and business, as well as defense. With the Amber operating system, we have adapted modern software techniques (such as single-level stores and high-level languages) for supercomputing and for the simulation problems of concern to defense researchers.

Over the past year, we modified the Amber operating system to operate on the AAP hardware base. This version of the computer was used to verify that our overall design is operating correctly.

References

Bruner, J. D., G. W. Hagensen, E. H. Jensen, J. C. Pattin, and J. M. Broughton (1987). *Cache Coherency on the S-1 AAP*, Lawrence Livermore National Laboratory, Livermore, Calif., UCRL-97646.

Jensen, E. H., G. W. Hagensen, and J. M. Broughton (1987), *A New Approach to the Exclusive Data Access in Shared Memory Multiprocessors*, Lawrence Livermore National Laboratory, Livermore, Calif., UCRL-97663.

Moldenhauer, V. Y., P. M. Farmwald, O. T. Anderson, J. C. Pattin, J. M. Broughton (1987), *Ring Interconnection Network for the S-1 AAP Multiprocessor*, Lawrence Livermore National Laboratory, Livermore, Calif., UCRL-97650.

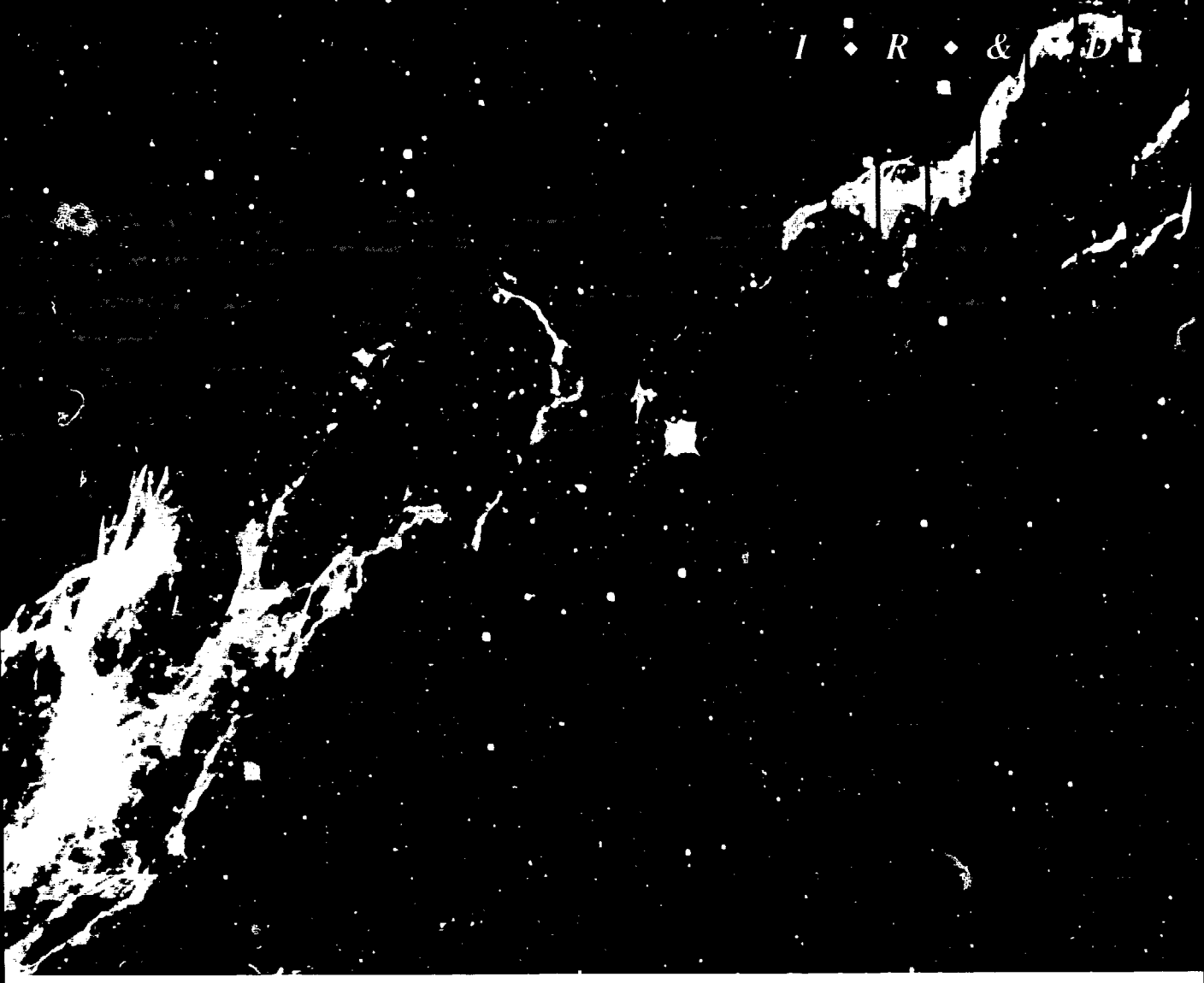

University of California Institutes

Lawrence Livermore National Laboratory

University of California Institutes

Overview

Claire E. Max

Several University of California (UC) advisory committees have reiterated the importance of increased scientific collaboration among staff members at the national laboratories and scientists located on UC campuses. The new contract between the Department of Energy and UC re-emphasizes the importance of such collaboration. This type of interaction has advantages for Laboratory staff members, who gain professional enrichment, closer contacts with the academic community, and new expertise in fields that are under-represented at the national laboratories. Likewise it carries advantages for campus researchers, who obtain access to unique Laboratory facilities and expertise, particularly in applied fields. In recent years, several joint UC-LLNL Institutes and Programs have been established, with the goal of enhancing campus-Laboratory collaboration in areas of overlapping interests and expertise.

In FY87, new LLNL guidelines were established. To be considered for status as a joint UC-LLNL Institute, a proposed project must be in a field where there is a genuine overlap of interest and expertise between the Laboratory and at least one UC campus. The Institute must be proposed and supported by an LLNL program or department to assure it an advocate within the Laboratory. Once established, a joint Institute must obtain funding from all of the following:

- Either a campus, a research unit, or the system-wide administration within the University of California.
- At least one LLNL program or department.
- The LLNL Institutional Research and Development Program.

Oversight of these joint Institutes at LLNL is provided by an Institutes Program Coordinator, who on behalf of the LLNL Director is responsible for monitoring the performance and quality of the existing Institutes, for approving the formation of new joint Institutes, and for maintaining the interface with the University on policy issues.

The four current UC-LLNL joint Institutes are at various stages of maturity:

- The Program for Analytical Cytology, approved by the Regents in 1982 as a joint program of LLNL and the UC San Francisco campus.
- The LLNL branch of the Institute of Geophysics and Planetary Physics, approved by the Regents in 1982 as the fifth branch of a University-wide Multicampus Research Unit.
- The Plasma Physics Research Institute, a new project with UC Davis, which was begun last year and is currently under review in the Office of the President of UC for official status.
- The Institute for Scientific Computing Research, a new project undertaken jointly by the LLNL Computation Department and by participants from the UC Berkeley campus.

All of these joint programs are currently functioning at LLNL, sponsoring collaborative research, post-doctoral and student researchers, workshops, and seminars. At present, the first two collaborative projects listed above receive funds from the system-wide administration of UC, as well as from other campuses, LLNL, and national funding sources. The system-wide funding is used to sponsor small awards to UC campus researchers for collaborative projects with LLNL. The second two projects are awaiting the designation of official status within the University.

Institute of Geophysics and Planetary Physics

Overview

Claire E. Max

The LLNL branch of the Institute of Geophysics and Planetary Physics (IGPP) was established by the Regents of the University of California in 1982. Its purpose is to make LLNL's unique facilities and expertise available to outside researchers, primarily those associated with UC. The program also broadens the scientific horizon of LLNL researchers by encouraging collaborative and interdisciplinary work with University scientists. At present, the IGPP at LLNL has three research centers:

- The Center for Geosciences, headed by George Zandt.
- The High-Pressure Physics Research Center, headed by William Nellis.
- The Astrophysics Research Center, headed by Charles Alcock.

This year the IGPP also took on administrative responsibility for the new UC Accelerator Mass Spectrometry program at LLNL.

The IR&D program provides funding for IGPP's administrative and secretarial costs at LLNL and provides half the salaries of the three Center heads. The Physics and Earth Sciences Departments contribute scientific and technical personnel to IGPP.

At the core of LLNL's IGPP program is a group of research grants open to scientists from all UC campuses. These peer-reviewed grants, which are jointly funded by the UC Regents and by LLNL's IR&D program, have been awarded annually since FY83. Typical grants range from $5000 to $20,000 and are used for research projects in seismology, geochemistry, cosmochemistry, high-pressure physics, and astrophysics. In recent years, we have received about twice as many qualified proposals as we could support. Figure 1 shows the breakdown of UC participants by IGPP research center since the program's start. Figure 2 shows the breakdown by campus, also since 1983; about 60% of the participants have come from Northern California campuses.

The grants help support visiting graduate and postgraduate researchers, experimental facilities for visiting researchers, and supercomputer time. The

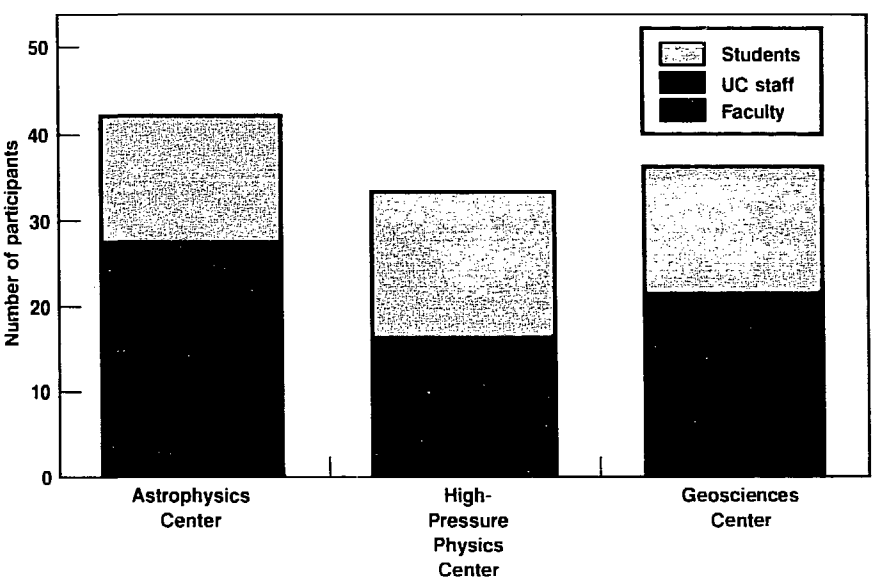

Fig. 1. Division of UC campus participants among the three IGPP research centers at LLNL.

opportunity for University faculty and students to use LLNL's supercomputers has been a prominent component of the program.

Several advanced facilities are available to researchers visiting the IGPP at LLNL. The High-Pressure Physics Research Center has the two-stage, light-gas gun, the diamond-anvil-cell laboratories, a piston-cylinder apparatus, and facilities for synthesizing and characterizing specimens at high temperatures and pressures. The Center for Geosciences has a variety of digital, broadband seismographic equipment available. The Astrophysics Research Center maintains a state-of-the-art image-processing facility for analyzing and displaying astronomical data.

For data analysis, the powerful analysis software LLNL has developed for seismic research can be run on Prime and Sun minicomputers. Grant recipients also have access to a network of Sun workstations and to the Cray supercomputers of the National Magnetic Fusion Energy Computer Center. The latter can be accessed through a local node in one of the IGPP/LLNL buildings and are at present used most extensively by the Astrophysics Research Center.

In addition to providing grants for campus researchers, the IGPP strives to provide an intellectual focal point for University-LLNL interactions. To further this goal, the IGPP runs a weekly seminar series, helps host University visitors for periods ranging from a few days to a full sabbatical year, and sponsors conferences and workshops. The most recent workshops concerned the new brilliant Supernova 1987a in the Large Magellanic cloud (this workshop was held at LLNL), new techniques for ground-based astronomical observations (held at UC Santa Cruz), and studies of the interactions between the Earth's crust and upper mantle (held at LLNL).

Overall, the Laboratory's IGPP program received $1,408,000 in IR&D operating funds in FY87 plus $98,000 for capital equipment.

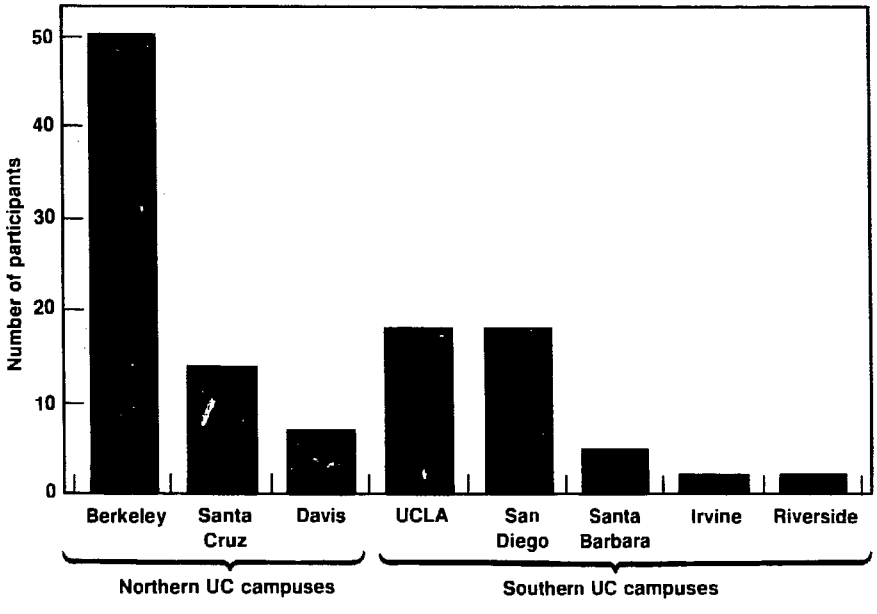

Fig. 2. Division of IGPP-LLNL participants among the eight Northern and Southern California campuses of UC.

Emission Spectra from Simple Shocked Liquids

Principal Investigator:
Malcolm F. Nicol[a]
Co-Investigators:
Neil C. Holmes and
Susanna Johnson[a]

[a]University of California, Los Angeles.

Chemical spectroscopists at UCLA and shock-wave physicists at LLNL are collaborating to investigate the nature of chemical reactions during shock compression of simple organic molecules. We are studying liquids of the type thought to exist in the outer planets and in high explosives, for example, CH_4, C_nH_n, CO, N_2, C_5H_5N, and a mixture called "synthetic Uranus." In experiments at the LLNL two-stage, light-gas gun, we subjected these liquids to pressures and temperatures representative of the interiors of the outer planets. Our goal is to understand not only the broad thermal background, but also the origin and kinetics of optical emission of C_2 and other chemical species that contribute sharp spectral features. Spectra are measured with a very sensitive 1000-channel detector in a 50-ns time interval. This year, we conducted experiments to determine whether any spectral features were generated by background effects in the target chamber of the gas gun. We coupled the specimen holder and spectrometer with optical fibers and found that the observed strong C_2 emission actually came from background sources, that the optical fibers eliminate background contributions, and that use of optical fibers makes alignment of the experiment more flexible and efficient.

Conductivity of Mantle Rocks between 20 and 700° C

Principal Investigator:
Steven Constable[a]
Co-Investigator:
Alfred G. Duba

[a]University of California, San Diego.

In order to interpret sea-floor electromagnetic sounding data collected at the Scripps Institution of Oceanography, UC San Diego, we have undertaken laboratory studies at LLNL of the electrical conductivity of representative upper mantle rocks in the temperature range from 20 to 700°C. Conductivity data from existing studies of single-crystal olivine at upper mantle temperatures have proved important in the interpretation of electromagnetic sounding data. Because the upper mantle includes polycrystalline rocks, we measured the electrical conductivity (in an atmosphere of controlled oxygen fugacity) of dunite with a grain size <1 mm and a magnesium/iron ratio between 5 and 8. We obtained reproducible results by using a very slow heating and cooling rate (20°C/hour) and by annealing the sample at 700°C for several hours. The resulting conductivity of 7×10^{-3} S/m at 700°C is consistent with the single-crystal data. This result contradicts previously held notions that grain boundary impurities and defects enhance the conductivity of olivine in upper-mantle rocks. The measured activation energy of 0.50 eV for the dunite conductivity is lower than that of single-crystal olivine at higher temperatures and may reflect a different conduction mechanism at the relatively low temperatures of these experiments.

Statistical Mechanics and Phase Equilibria of Ionic and Geophysical Systems

Principal Investigator:
Mark S. T. Bukowinski[a]
Co-Investigators:
Marvin Ross, Lars Stixrude,[a] and
Amotz Agnon[a]

[a]University of California, Berkeley.

We are investigating the thermodynamic properties of ionic and covalent materials under the pressure and temperature conditions prevailing in planetary interiors. We have two specific goals: First, we want to generate accurate theoretical simulations of silicate liquid structures and their response to pressure. We believe this will shed some light on the suggestion that, below some threshold depth in the Earth, magmas sink rather than rise to the surface. The impact of this suggested behavior on planetary evolution would be tremendously significant, but supporting data are thus far inconclusive. We are developing a theoretical model of the potential surface for liquid and solid silica that is based on spectroscopic data for silicate molecules. The model includes covalent effects and is independent of any liquid- or solid-state data. The model accurately reproduces the structure and compressibility of quartz and coesite. We believe that it will simulate silica liquids and glasses more accurately than do any previous models.

Our second goal is to produce a potential-energy model that accurately represents the general elastic properties of oxides. Such information is necessary to interpret seismic velocity profiles in the Earth's interior. However, at present, only the compressibility of some relevant minerals is reasonably well constrained and theoretically understood. Shear velocities are unknown for the relevant minerals beyond 3 GPa (30 kbar), and no accurate theoretical means of extrapolation in pressure and temperature exist. We have developed a parametric many-body-potential model that accurately reproduces elastic constants, including the large violations of the Cauchy relations in the cubic alkaline earth oxides. This potential model will be further refined and used in Monte Carlo, lattice dynamics, and integral-equation simulations of cubic oxides and silica liquid and solid phases.

Dynamic Response of Fully and Partially Fluid-Filled Saturated Rock: Experimental and Theoretical Investigations

Principal Investigators:
William Goldsmith[a] and
Michael M. Carroll[a]
Co-Investigators:
Brian P. Bonner,
Raymond C. Y. Chin, Ali Imam,[a]
and Baruch Revisn[a]

[a]University of California, Berkeley.

Knowledge of the dynamic response of partially fluid-saturated rocks is important for understanding the propagation of seismic waves. Applications include interpreting regional teleseismic data and differentiating between seismic signals from explosions and those from natural sources. Most work in this field involves dry rocks, although partially saturated rocks are more representative for field applications. The purpose of our theoretical and experimental study is to determine the effects of fluid in rocks on constitutive properties, microscopic deformation behavior, and wave propagation. Nugget sandstone specimens prepared at LLNL are loaded dynamically using the air guns and Hopkinson-bar apparatus at UC Berkeley, and stresses up to 2 kbar are achieved. Macro- and microstructures are investigated at LLNL, where quasi-static tests are performed as well. The theoretical treatment generalizes the pore collapse model for dry porous materials to include fluid-filled inclusions.

Computing the Resonance Frequency Spectra of a Rectangular Parallelopiped Single Crystal of Monoclinic Symmetry

Principal Investigators:
Orson L. Anderson[a] and
Shigero Yamamoto[a]
Co-Investigator:
Alfred G. Duba

[a]University of California, Los Angeles.

We used the LLNL Cray computers to compute the elastic constants of trigonal and monoclinic crystals by the rectangular parallelopiped resonance method. We found the elastic constants of Al_2O_3 (trigonal class) by inverting data of the first 29 measured modes and improved convergence for a 300 × 300 matrix. For a matrix of this size, we found excellent agreement between the experimental spectrum and the calculated spectrum. We extended the program to include clinopyroxene (monoclinic) symmetry, but we need an experimental measurement of a monoclinic crystal to further test the program.

Dynamic High-Pressure Processing and Synthesis of Novel Materials

Principal Investigator:
M. Brian Maple[a]
Co-Investigators:
William J. Nellis,
John Neumeier,[a] and
Milton Torikachvili[a]

[a]University of California, San Diego.

We are synthesizing metastable materials with novel crystalline structures and microstructures by combining UC San Diego's expertise in fabricating specimens and characterizing structure and physical properties with LLNL's capability in shock-wave physics. These new materials are created at high pressures, densities, and temperatures, and may be superior to other materials for superconducting or magnetic applications. Specimens are subjected to shock pressures up to the megabar range and temperatures of several thousand degrees kelvin; the shock process creates pressure quench rates that are sufficiently fast to produce metastable structures—structures frozen in the extreme formation conditions, such as cannot be created by conventional processing techniques. We are specifically attempting to synthesize metastable solid phases of potentially high-T_c superconductors and superconductors with ultrahigh critical magnetic fields. We have shown that powder can be compacted in a copper matrix by shock pressures in the 100-kbar range and completely melted and rapidly solidified by pressures in the 500-kbar range. We are currently attempting to shock-compact the new high-T_c (90 K) oxides in a copper matrix to synthesize superconducting wire.

Design and Construction of a Furnace for Elasticity Measurements of Geophysical Materials at Temperatures between 1000 and 1700 K

Principal Investigators:
Orson L. Anderson[a] and
Shigero Yamamoto[a]
Co-Investigators:
Alfred G. Duba and
Takayasu Goto[a]

[a]University of California, Los Angeles.

Until last year, the experimental furnace available to us could measure elastic constants of minerals at temperatures no higher than 1200 K. Temperatures in excess of 1700 K are needed for geophysical applications. We designed a furnace that can keep the temperature of the acoustic transducers below 800 K, while the specimen is at 1800 K. We have measured the elastic constants of corundum at 1800 K and are currently extending the measurements of forsterite to this new temperature range.

Teleseismic Studies in the Long Valley Caldera

Principal Investigator:
William A. Prothero, Jr.[a]
Co-Investigators:
George Zandt and Lee Steck[a]

[a]University of California, Santa Barbara.

We are studying teleseismic *P* waves recorded on an array of portable, three-component seismic stations in California's Long Valley Caldera. Previous efforts to locate possible magma bodies were hampered by a lack of resolution, exclusive reliance on *P*-wave energy, or reverberations in shallow low-velocity layers (in the case of reflection profiling). Bodies of liquid or partial melt, if they exist, should cause large conversions of compressions to shear energy at the liquid-solid interface. Teleseismic *P* waves are ideal signal sources in searching for such effects because they pass through the structure of interest from below and at moderate angles of incidence.

We deployed 3 three-component, digital, broadband, teleseismically triggered seismic stations on the resurgent dome of the Long Valley Caldera for two months. Twenty events were recorded; of these, we selected the ones with clear, impulsive *P* waves. The Figure shows depth contours in kilometers for the inferred origin of the earliest shear arrival, based on a one-dimensional ray-tracing approximation and the velocity model of Hill et al. (1985). Each number represents a data point. Our results agree well with those of other researchers.

For the northwestern anomaly, our depth lies between that of Sanders (1984) and Hill et al. (1985) and represents a smaller body than that of Sanders

Teleseismic Studies (continued)

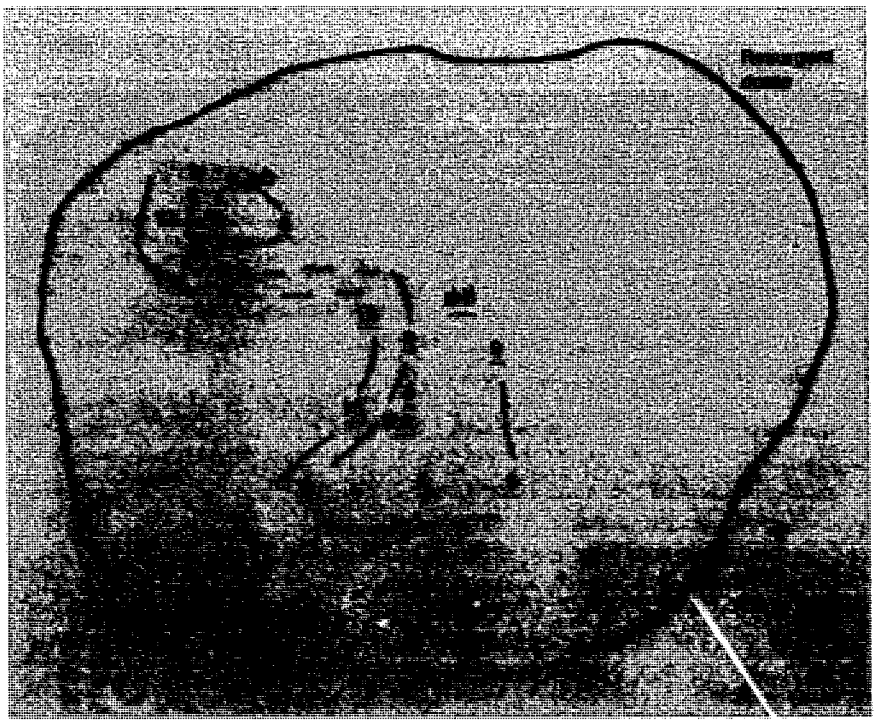

Depth contours for first converted shear arrivals at the three portable recorders, A, B, and C. A fourth recorder was briefly installed but was extremely noisy and thus abandoned. Numbers indicate data-point depths in kilometers.

(1984). The depth of the southern anomaly seen in our data is not well constrained. A single data point suggests that it is shallow (4 km), while other points indicate a depth of from 8 to 9 km. A shallow depth for this interface would correlate well with the results of Sanders (1984) and of Elbring and Rundle (1986). Our results indicate an overall smaller body than Sanders (1984) suggests for this area.

References

Elbring, G. J. and J. B. Rundle (1986), "Analysis of Borehole Seismograms from Long Valley, California: Implications for Caldera Structure," *J. Geophys. Res.* **91**, 12,651.

Hill, D. P., E. Kissling, J. H. Leutgert, and U. Kradolfer (1985), "Constraints on the Upper Crustal Structure of the Long Valley-Mono Craters Volcanic Complex, Eastern Calif., from Seismic Refraction Measurements," *J. Geophys. Res.* **90**, 11,135.

Sanders, C. O. (1984), "Location and Configuration of Magma Bodies Beneath Long Valley, California, Determined from Anomalous Earthquake Signals," *Proc. of Workshop XIX on Active Tectonics and Magmatic Processes Beneath Long Valley, Eastern California* **1**, 221.

Trace Elements and Isotope Geochemistry of Cretaceous/ Tertiary Boundary Sediments: Identification of Extraterrestrial and Volcanic Components

Principal Investigator:
Stanley V. Margolis[a]
Co-Investigators:
G. Price Russ III and
Eric Doehne[a]

[a]University of California, Davis.

We are studying a series of critical Cretaceous/Tertiary boundary samples taken near Zumaya and Sopelano, Spain, with the aim of distinguishing whether platinum and related metals in these transitional sediments are of extraterrestrial or volcanic origin. We devised new techniques for preparing samples and increased the sensitivity of inductively coupled plasma mass spectrometry (ICP-MS). We are ready to proceed with trace element and strontium isotopic analyses.

Extinctions of several groups of marine invertebrates are associated with negative oxygen and carbon isotope excursions that took place during the last million years of the Cretaceous period at Zumaya. These isotope excursions indicate major changes in ocean thermal regimes, circulation, and ecosystems that may be related to multiple extraterrestrial or volcanic events during latest Cretaceous time.

Preliminary analyses indicate the presence of iridium, platinum, arsenic, and nickel at the boundary, along with microparticles of possible extraterrestrial origin. Our research will provide important data on the possible cosmic, volcanic, or diagenetic origins of these trace element concentrations, their relation to biotic extinctions, and their distribution during the last million years of the Cretaceous period.

Seismological Studies of Core Transition Zones

Principal Investigator:
Lane R. Johnson[a]
Co-Investigators:
Fred E. Followill and
Phil Cummins[a]

[a]University of California, Berkeley.

The seismological data, expertise, and experience available at LLNL, UC Berkeley, and the Center for Computational Seismology at Lawrence Berkeley Laboratory were combined to study the transition zone between the outer and inner cores of the Earth. The high-quality digital data of the Regional Seismic Test Network provide a unique opportunity to use teleseismic body waves for studying fine details of Earth structure. A new hybrid method makes it possible to calculate body waves that have interacted with the Earth's inner core in an accurate, complete, and efficient manner. This approach allows exploration of completely general models of the transition zone between the Earth's inner and outer cores. We developed computer codes and then used the resulting calculations to interpret observations of core phases in different distance ranges. The results argue strongly for a transition zone less than 5 km thick and an increase in P velocity of between 0.6 and 0.7 km/s. The calculations also indicate how observational data might be used to make inferences about the S velocity and attenuation below the transition zone in the inner core.

Gravity Flow of Granular Solids: A Comparison of Experimental Measurements and Discrete-Particle Calculations

Principal Investigator:
Ronald L. Shreve[a]
Co-Investigators:
Otis R. Walton and
Thomas G. Drake[a]

[a]University of California, Los Angeles.

Measurements from essentially two-dimensional granular-flow laboratory experiments conducted at UCLA were used to determine the values of numerical constants for two-dimensional (2DSHEAR) and three-dimensional (3DSHEAR) discrete-particle computer models developed by the Granular-Flow Project at LLNL. From over 300 collisions of 6-mm-diam cellulose acetate spheres, we experimentally determined the normal coefficient of restitution to be 0.84 and the effective coefficient of sliding friction to be 0.4. Using these experimental values, we varied the ratio of the shear to normal stiffnesses in the 2DSHEAR model to best fit the experimental collision trajectories and determined that the ratio is 0.9—in agreement with our estimate from measurements of the material properties of the spheres. Detailed measurements of the mean velocity, mean rotation, granular temperature, rotational temperature, and density have been made from UCLA films of three steady, nearly uniform, gas-like flows at a single channel inclination and two values of mass flux. We are presently undertaking a comparison of the experimental flows with the computer simulations to completely validate the model.

Generation of Surface Waves from the Collapse of Explosion Cavities

Principal Investigator:
Leon Knopoff[a]
Co-Investigators:
Keith Nakanishi and
Frank Leader[a]

[a]University of California, Los Angeles.

We are using broadband three-component data from the Regional Seismic Test Network to investigate the excitation of surface waves that result from the collapse of cavities formed by underground nuclear explosions. Horizontal dispersive surface waves, called Love waves, are observed to be excited by both the explosions and collapses, which are assumed to be dilatational sources. By modeling the source mechanism that generates these surface waves, we hope to better understand the role of tectonic strains in the excitation of surface waves by underground nuclear explosions.

The first stage of this project was to prove that the horizontally polarized surface waves observed for the collapse events were indeed Love waves. This we have shown by matching the observed dispersion, for the collapse events, with the Love wave dispersion experimentally determined from the explosion events. The second stage of the project is to use the observed phase spectra of the surface waves to determine the mechanism for exciting the surface waves for the collapse events. We developed an optimized filter to extract the phase of the Love waves since the low signal-to-noise level made standard techniques ineffective. We are now analyzing the source mechanism.

Porosity and Hydrothermal Alteration Determined from Wireline Logs: Salton Sea Geothermal Field, California

Principal Investigator:
Wilfred A. Elders[a]
Co-Investigators:
Paul W. Kasameyer and
Hsiang-Yuan Lei[a]

[a]University of California, Riverside.

The Salton Sea Geothermal Field (SSGF), located near the southeastern end of the Salton Sea in Southern California, on the delta of the Colorado River, is one of the largest geothermal fields in the world. Boreholes penetrating this hypersaline system, with brines containing 25 wt% of total dissolved solids, have encountered temperatures as high as 350°C at only 2 km depth. Because the SSGF is located in sedimentary strata, well-logging interpretation techniques developed for use in oil fields can be applied effectively.

The major objective of this investigation is to study different wireline logs used in determining porosity and to establish the relation between wireline log properties and hydrothermal alteration in response to the reaction between the sediments and the hot brines. We began with a detailed study of the porosity and resistivity of one well, State 2-14. Subsequently, two more wells, Magmamax #3 and #2, were investigated for comparison. We added data from three more wells—Magmamax #1, I.I.D. #2, and Sinclair #4—to study the logging responses regionally. The mode of the neutron porosity distribution at each depth was plotted. The inflection points of this plot occurred in the 20 to 30°C temperature range. The same is true for modes plotted for density porosity, sonic porosity, and resistivity. These depth-versus-porosity frequency plots show a regional porous zone at a temperature range of 220 to 235°C, which is identified with a regional reservoir. After we compared the neutron, density, and sonic porosity logs, we identified the minerals enriched in intra-layer water, the radioactive minerals, the zones lacking consolidation, the fractures, and the rugose borehole. This study demonstrates the feasibility of identifying zones of varying porosity and hydrothermal alteration from borehole wireline logs. These techniques will be useful in future explorations of potential geothermal fields.

Spatio-Temporal Variations in Coda *Q* before the Mt. Lewis Earthquake in Fremont, California

Principal Investigator:
Karen C. McNally[a]
Co-Investigators:
George Zandt, Teresa Hauk, and
Glenn Nelson[a]

[a]University of California, Santa Cruz.

The temporal decay in seismic energy arriving after the main ray-arrival (coda) is a measure of the attenuation property of the medium through which seismic waves propagate. This measure is quantified by the coda quality factor $Q_c(\omega)$, which is a function of frequency and is related to inverse attenuation. A difference in Q_c between early and late lapse times has been suggested to be a precursor to a large earthquake. The objective of the present study is to determine whether temporal variations in Q_c can likewise be observed as a precursor to a moderate earthquake ($M_L = 5.7$). Temporal Q_c variations could result from increasing local stress change and consequent microcracking before a main shock. Such an effect might be observed months to years before a moderate earthquake. So far the search for Q_c variations has yielded mixed results. The density of stations and the high quality of digital seismograms from the Lawrence Livermore Seismic Network may enable us to observe a Q_c variation related to the Mt. Lewis main shock.

The Mt. Lewis earthquake, $M_L = 5.7$, occurred on March 31, 1986, 10 km south of California's Livermore Valley. We can determine $Q_c(\omega)$, using Sato's single-scattering model, for earthquakes located within 10 km of the main shock and recorded at three nearby stations by the Lawrence Livermore Seismic Network from January 1, 1980 through December 31, 1986. Sato's single-scattering model predicts that the coda decays as $-\omega(t - t_s)/Q_c$, after spreading corrections. Deviations from a linear fit may result from differing forward- and back-scattering coefficients, the onset of multiple scattering, clipping, low signal-to-noise ratios, unmodeled arrivals after the *S* wave, or aftershocks. Our

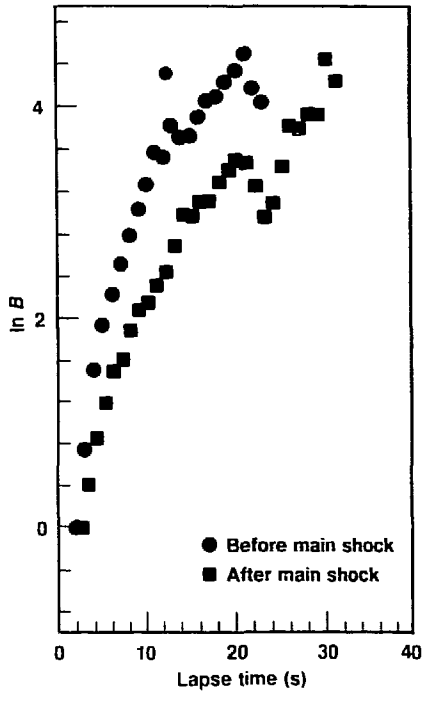

Average ln *B* vs $(t - t_s)$ at 6 Hz for all unclipped events at station CDV. The slopes defined by the data points are related to attenuation ($1/Q_c$). Note that the attenuation at short lapse time (<12 s) decreases after the main shock, but after 12 to 14 s, the slopes are the same.

data are taken at short distances (<15 km) and mostly at lapse times less than 25 s—conditions suitable for the single-scattering model. We find that for events located in the main shock source region, early and late lapse-time Q_c differ significantly before, but not after, the main shock. The Figure illustrates this difference for all unclipped events recorded at station CDV at 6 Hz. We computed the average Q_c for all three stations: Before the main shock, $Q_c = 141.9 \pm 28.5$ before 14 s and 294.5 ± 29.2 after 14 s; after the main shock, $Q_c = 195.4 \pm 48.2$ before 14 s and 241.9 ± 57.8 after 14 s. For events not in the source region, differences in early and late lapse-time Q_c exist but do not significantly decrease after the main shock. These preliminary results suggest that the Q_c change before a main shock may be a promising candidate for detecting behavior precursory to earthquakes. Further studies will determine whether spatial variations in Q_c may be biasing these observed temporal variations.

Simultaneous Hypocenter and Velocity Structure Inversion of the Santa Barbara Channel Region

Principal Investigator:
William A. Prothero, Jr.[a]
Co-Investigators:
John J. Zucca and
William J. Taylor[a]

[a]University of California, Santa Barbara.

We are using a new three-dimensional hypocenter-velocity structure inversion program to determine both the seismic velocity structure and earthquake hypocenter distribution in the Santa Barbara Channel and also the velocity structure of the volcanic region of Medicine Lake, California. Travel times from chemical explosions with known locations and origin times can also be included in the inversion procedure. Input data for this computer program includes explosion locations, trial hypocenter locations, *P*-wave travel times, and an initial velocity model. We invert for a more accurate velocity structure and hypocenter locations, by minimizing the residuals with least-squares statistical adjustments. Our main objective was to improve the algorithm so that a solution for the Santa Barbara Channel could be found. Improvements include: adding a new three-dimensional ray tracer, use of the difference in *S*- and *P*-wave arrival times to constrain hypocenter locations, and developing a velocity-model smoothing filter that allows convergence to a solution in sparse datasets.

Many problems arose while analyzing the Santa Barbara Channel data. The complexity of the velocity structure, the sparseness of the dataset, and poor convergence to a solution caused difficulties, even with the help of the new ray tracer. The complex velocity model demanded more velocity nodes (unknowns) than the data could actually resolve. This problem was overcome by applying a moving, weighted velocity average to the "information holes" after each iteration, so that the model stayed consistent. Convergence to a solution was then achieved with greatly reduced travel-time residuals from the known shot locations. The new hypocenter locations also look very promising. We have shown that this technique can yield useful information from sparse datasets.

Work with the Medicine Lake dataset is proceeding, and results will be covered in a later report.

Laboratory Astrophysics with Laser Plasmas

Principal Investigator:
Steven M. Kahn[a]
Co-Investigators:
Roger W. Falcone,[a]
Richard A. London,
Richard W. Lee,
William W. Craig,[a]
Jonathan Schachter,[a] and
Bradford Wargelin[a]

[a]University of California, Berkeley.

Development of high-sensitivity spectrometers for future x-ray space observatories such as the NASA Advanced X-Ray Astrophysics Facility and the ESA X-Ray Multi-Mirror Mission will soon provide high-quality soft x-ray spectra for most classes of cosmic sources. Among the most interesting objects for study are the accretion-powered sources (e.g., cataclysmic variables, x-ray binaries, active galactic nuclei) in which soft x-ray spectral features are formed in a photoionized nebula produced by the transfer of x-radiation from a powerful central source outward through a cooler, surrounding medium. Unfortunately, limitations in our knowledge of some important atomic physics and radiation-transfer processes may severely hamper our interpretation of the data for these cases. Laser-produced plasmas offer a useful experimental medium for studying some of these issues because they share important properties with the astrophysical photoionized nebulae:

- They are usually significantly overionized relative to their electron temperature (after the initial burst of energy deposition).
- They are often optically thick to the prominent resonance line radiation.

Both properties are thought to be quite important in shaping the emergent short-wavelength spectra.

We have developed and partially completed two independent laser plasma experiments designed to elucidate important x-ray transfer processes that are believed to occur in cosmic accretion-powered sources like cataclysmic variables, x-ray binaries, and active galactic nuclei. The first involves the measurement of K- and L-shell photoabsorption cross sections for intermediate ions of carbon. This is performed with two laser plasmas, one to provide the partially ionized absorbing medium, and the other to provide the backlit continuum radiation. The Figure is a schematic of the experiment under way at the Janus Research Laser Facility at LLNL.

The second experiment involves a laboratory demonstration of the Bowen fluorescence mechanism, an optical pumping process associated with wavelength coincidences between resonance transitions of He II, O III, and N III. A premixed volume of helium, oxygen, and nitrogen is photoionized into the appropriate states by a high-temperature laser plasma in close proximity. The irradiated gas cools and enters a recombination-dominated state, in which

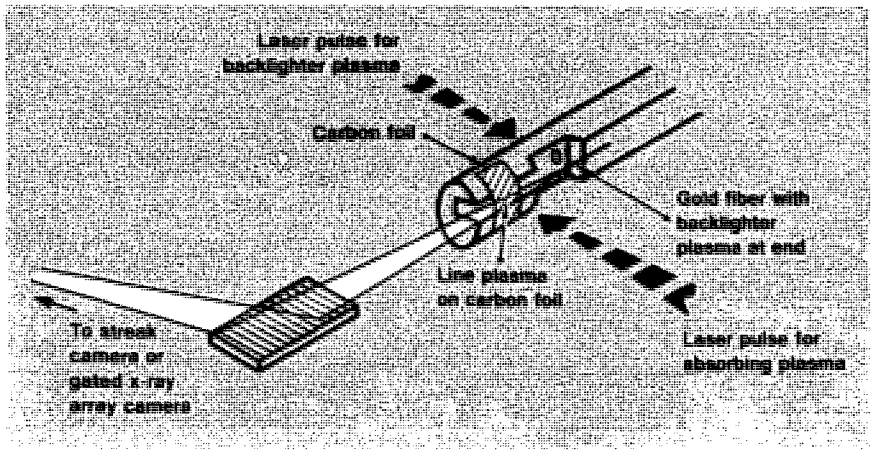

A schematic of the target configuration used for experimental measurements of carbon-ion photoabsorption.

the Bowen process should provide the dominant excitation mechanism for a series of characteristic optical and ultraviolet emission lines. Preliminary aspects of this experiment have been studied with a desk-top laser plasma facility on the Berkeley campus. In association with this project, we have also carried out some new Bowen line observations of astrophysical sources including high-ionization Seyfert 2 galaxies and several prominent x-ray binaries. We measured oxygen and He II P β Bowen fluorescence lines in ScoX-1 that represent the first such observations for this object.

Precision Fabrication of Grazing Incidence Glass Optics

Principal Investigator:
Stuart Bowyer[a]
Co-Investigator:
James Bryant

[a]Space Sciences Laboratory, University of California, Berkeley.

The original goal of this project was to develop a joint UC Berkeley/ LLNL capability in advanced polishing techniques for grazing incidence optics. Details of a broad plan to implement such a capability are currently under development.

In the meantime, IR&D funds were used to support work on another joint LLNL-Space Sciences Laboratory project: the LLNL Multiobject Spectrometer, led by Dr. Jean Brodie. In this device, 100 small prisms that can be moved by computer control to observe different objects in an astronomical field are connected by optical fibers to a single spectrograph. Since the telescope would otherwise observe only one object at a time, a hundredfold improvement in efficiency will be possible. The project itself has developed sufficiently so that it has now attracted major LLNL and UC Regents' funding.

Laboratory Development of a Phasing Camera for the Keck Telescope Segmented Mirror

Principal Investigator:
Gary Chanan[a]
Co-Investigators:
Jordin Kare, Terry Mast,[b] and
Jerry Nelson[b]

[a]University of California, Irvine.
[b]Lawrence Berkeley Laboratory, Berkeley, Calif.

The Keck Telescope, currently under construction by the University of California and California Institute of Technology, is scheduled for completion in 1990. Its primary mirror consists of 36 hexagonal segments 0.9 m on a side and arranged in three concentric rings, for an effective diameter of 10 m. An active electromechanical control system holds the relative position of adjacent edges to a high degree of accuracy (10 nm) and stability (stable for days), but this system does not determine where the segments are to be initially positioned. To achieve diffraction-limited images in the infrared, this positioning must accurate within 100 nm. We have been developing an optical device, or phasing camera, for this purpose. We have set up a simple benchtop prototype of the phasing camera, using a laser, a beam-spreader, and a commercial charge-coupled device. We built a 19-element lenslet array by close-packing commercial lenses (10 mm in diameter) and reducing their apertures to the required submillimeter diameters. Our calculations and simulations show that the aberrations introduced by the camera optics must correspond to an image asymmetry of no more than 1.5% (which in turn corresponds to a peak-to-peak comatic distortion of a tenth-wave) if the telescope phasing tolerances are to be met. In fact, we found that we could attain residual asymmetries of $1.0 \pm 0.5\%$ with this setup. This demonstrates that the camera concept is sound and that the associated optical tolerances are attainable.

The Use of the MACSYMA INTENSR Package in Quantum Gravity and Cosmology

Principal Investigator:
James B. Hartle[a]
Co-Investigators:
Beverly K. Berger and
Kristin Schleich[a]

[a]University of California, Santa Barbara.

Einstein's General Theory of Relativity is a very successful theory of gravity in the domain of classical mechanics. However, until recently, all attempts to reconcile the General Theory with quantum mechanics have been unsuccessful. We have been studying the quantum behavior of general relativity in certain special circumstances and have been using computer manipulations at LLNL to handle the formidable algebraic expressions that arise.

One approach to quantizing Einstein gravity is to use a Euclidean functional integral to construct the states; this formulation allows the invariances of the theory to be displayed manifestly in the expressions for these physical quantities. However, an immediate problem occurs; the Euclidean Einstein action is unbounded below. Therefore, the functional integrals weighted by this action diverge. However, for asymptotically flat space times, Euclidean functional integrals in terms of the physical degrees of freedom are convergent by virtue of the positive energy theorem. We have shown through a series of formal manipulations that these kinematically convergent Euclidean functional integrals in the physical degrees of freedom are equal to Euclidean functional integrals over the full set of metric components weighted by a positive action. This action is the Euclidean Einstein action with the conformal component of the metric perturbation rotated to imaginary values.

In order to check this formal result, the Euclidean functional integral for the ground state for asymptotically flatspace times can be computed perturbatively with the prescription of conformal rotation and compared to the result of the same calculation done in terms of the physical degrees of freedom. To carry out this calculation to second order, one needs the third- and fourth-order terms of the perturbation expansion of the Einstein action including the surface terms. Our proposal was to use the MACSYMA ITENSR package,

which consists of symbolic computation software available at LLNL but not at UC Santa Barbara, to derive these terms to use in the verification of the equivalence of the conformally rotated functional integral to that in the physical degrees of freedom. We used MACSYMA to factor out the conformal part of the metric perturbation in these terms and derived the form of the action with the rotated conformal factor needed for the functional integral. Using the third-order term, we calculated the Euclidean functional integral for the ground state to first order in perturbation theory and found that it indeed was equal to that computed in terms of the physical degrees of freedom.

Plasma Astrophysics

Principal Investigator:
Jonathan Arons[a]
Co-Investigators:
Richard Klein, A. Bruce Langdon, Claire E. Max, David Alsop,[a] and David Burnard[a]

[a]University of California, Berkeley.

We studied radiation gas dynamics of gravitational accretion flows onto the magnetic polar caps of strongly magnetized neutron stars, with the goal of modeling the emission properties of accretion-powered x-ray pulsars. These calculations make major use of computer facilities at LLNL. The resulting models are being used to create synthetic spectra, whose comparison to the spectra of x-ray pulsars should tell us much about the physical conditions within the emission regions of these objects. Previous radiation-transfer models constructed with single values of the plasma density and temperature by other workers have failed to give a good representation of the detailed spectra, mainly because the radiation pressure observed requires drastic inhomogeneities in space and time. The dynamical models under construction provide the needed spatial and temporal structures as functions of the (observable) luminosity of the systems. In addition, substantial effort has been put into constructing a radiation transfer computer program, which uses the results from the dynamical models as input physical conditions, so as to create detailed synthetic polarimetric spectra. We have obtained the first computational evidence for overstable convection in plasma over the polar caps of the neutron star. These results suggest the presence of 10- to 100-ms fluctuations in the emergent spectra of these objects.

In a separate project, we have also studied the structure of relativistic shock waves in a collisionless, magnetized, positron-electron plasma. The goal here is to understand the acceleration of the relativistic particles that are the source of synchrotron emission in supernova remnants powered by pulsars. These studies make use of ZOHAR, a fully relativistic, electromagnetic, explicit particle-in-cell plasma-simulation code written by Langdon and Lasinski at LLNL. We used ZOHAR to model several examples of relativistic shocks during the last year. In all cases, a cold electron-positron plasma with magnetic field polarized directly across the flow was injected into the computational grid at relativistic speed. The plasma was allowed to bounce off the far end of the box. The interaction between the reflected and injected plasmas led to a well-developed shock propagating back up through the box, with shock speed in good accord with the expectations from the Rankine-Hugoniot conditions. The Crab nebula is the best known example of this type of system.

Astrophysical Studies of Carbon, Nitrogen, and Oxygen Isotopes

Principal Investigator:
Michael Jura[a]
Co-Investigators:
David S. Dearborn and
Isabel Hawkins

[a]University of California, Los Angeles.

It is well established that most material in the universe heavier than helium was synthesized in stars rather than in the big bang. However, the quantitative details of the process of nucleosynthesis and the resultant chemical evolution of the galaxy are still uncertain. Our goal is to help explain the history of element production in our galaxy. In particular, we concentrate on carbon, nitrogen, and oxygen (CNO), since these species are the most abundant elements after hydrogen and helium, and because the CNO tricycle is so important as an energy source within stars.

The Figure characterizes the evolution of 12 different stars whose masses range from 1 to 25 times the mass of the sun. We calculated surface isotopic CNO abundance ratios in stars with a wide range in masses and compared these ratios with existing observations; the goal is to set more stringent limits on uncertain reaction rates and to probe the depth of the stellar convective layer. We are analyzing optical observations obtained at Cerro-Tololo Inter-American Observatory and Lick Observatory to investigate the possibility of a $^{12}C/^{13}C$ abundance gradient in the plane of the galaxy. In addition, we plan to use spectral lines of the SiO molecule to obtain observations of the circumstellar shells around evolved red giants and to measure $^{16}O/^{17}O$ ratios to test further our theoretical predictions.

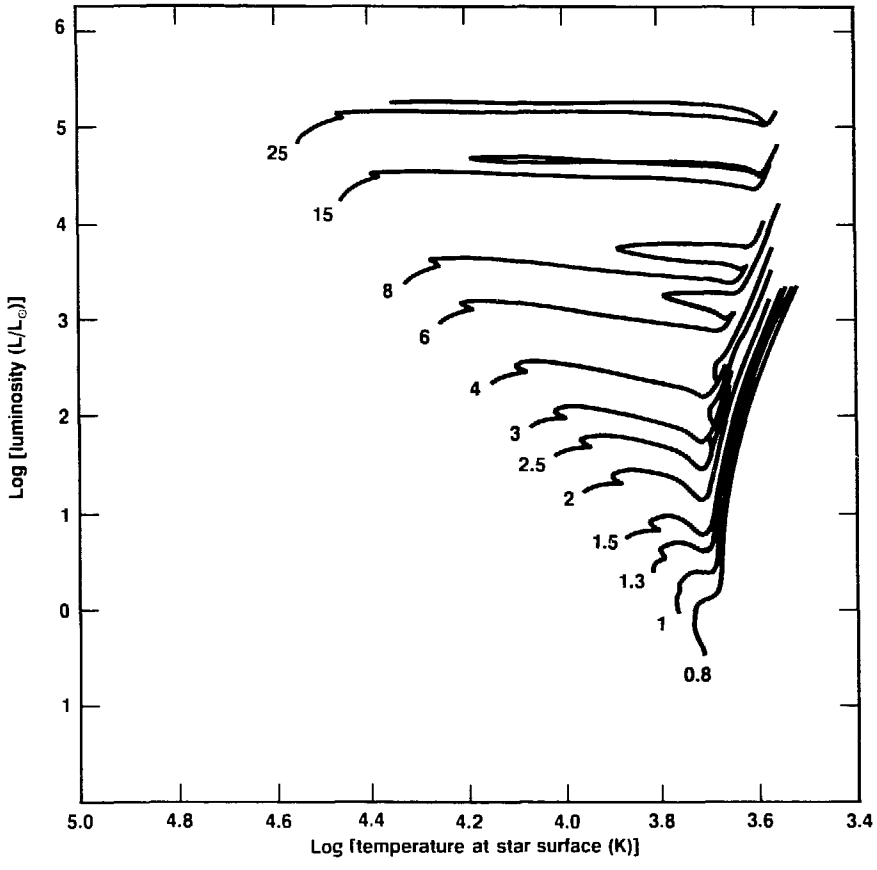

Evolution tracks for stars of different mass. The logarithm of the luminosity (in solar units) is plotted versus the surface temperature (K). Each track is labeled with the mass of the star (in solar units).

A Numerical Model of the Interface between Emission Line Clouds and Hot Intercloud Medium in Quasi-Stellar Objects and Seyfert Galaxies

Principal Investigator:
Richard C. Puetter[a]
Co-Investigators:
George Fisher, Steven Langer, and
Irwin Krinsky[a]

[a]University of California, San Diego.

One of the most interesting problems in the study of quasars and active galactic nuclei is the origin of the bright atomic emission lines from ions of abundant elements. These lines appear to originate in cool clouds that are embedded in a hot confining medium. The clouds are illuminated by intense radiation from the center of activity, and this radiation pumps the emission lines. Our primary goal was to explore the radiative hydrodynamics of the emission line clouds. During the past year, we modified an existing solar-flare computer code for application to this new quasar problem. We changed the code from a semi-infinite slab to a finite slab code, removing the one-stream radiative transfer calculation and replacing it with a two-stream approach. This allowed the specification of radiative boundary conditions on each side of the emission line cloud (ELC). We have also changed the boundary conditions to those appropriate to a finite ELC, including the imposition of an external source of ultraviolet or x-ray photons with a power-law energy spectrum. We have obtained a zeroth-order solution and are now exploring dynamical evolution. The zeroth-order solution is quite simple—a pure hydrogen atmosphere with hydrogen modeled as a two-level plus continuum atom. Energy balance has been imposed on the ELC, but we impose a temperature of 10^7 K at both boundaries; the temperature drops to 3×10^4 K at the cloud center.

In conclusion, we made significant progress in FY87 on modeling the emission line cloud/hot intercloud medium interface. We have made the necessary modifications to calculate the zeroth-order model, and we are now ready to study the dynamical evolution. Furthermore, preliminary investigations into how the UV and x-ray flux from a quasar may bloat the atmospheres of nearby stars look very promising and may provide an independent, productive avenue of research on the origins of quasar emission lines.

Implementation of AIPS on the Cray Computer at LLNL

Principal Investigator:
Robert H. Becker[a]
Co-Investigator:
Claire E. Max

[a]University of California, Davis.

Image processing and analysis is basic to all areas of observational astronomy. As the data rate from modern instrumentation increases, so does the demand for increased computing power for analysis. In order to make IGPP an effective environment for observational astronomers, it became clear that IGPP required an image-processing facility. Our original objective was very ambitious: to implement the Astronomical Image-Processing System (AIPS) on the Cray computers at LLNL. Developed by the National Radio Astronomy Observatory (NRAO), AIPS allows the user to create images from interferometric data. The success of this project depended on the release of AIPS by NRAO for use on the Cray Operating System (COS). When it became clear that the release would not be available, the goals were altered to support AIPS on the IGPP SUN 3-260 minicomputer, an IVAS image display, a laser printer, and a slide copier. This has been accomplished. AIPS is now operating on both computers. The IVAS is fully functional, and AIPS images can be displayed routinely as well as printed and reproduced on slides. An example of the IVAS capability is shown in the Figure.

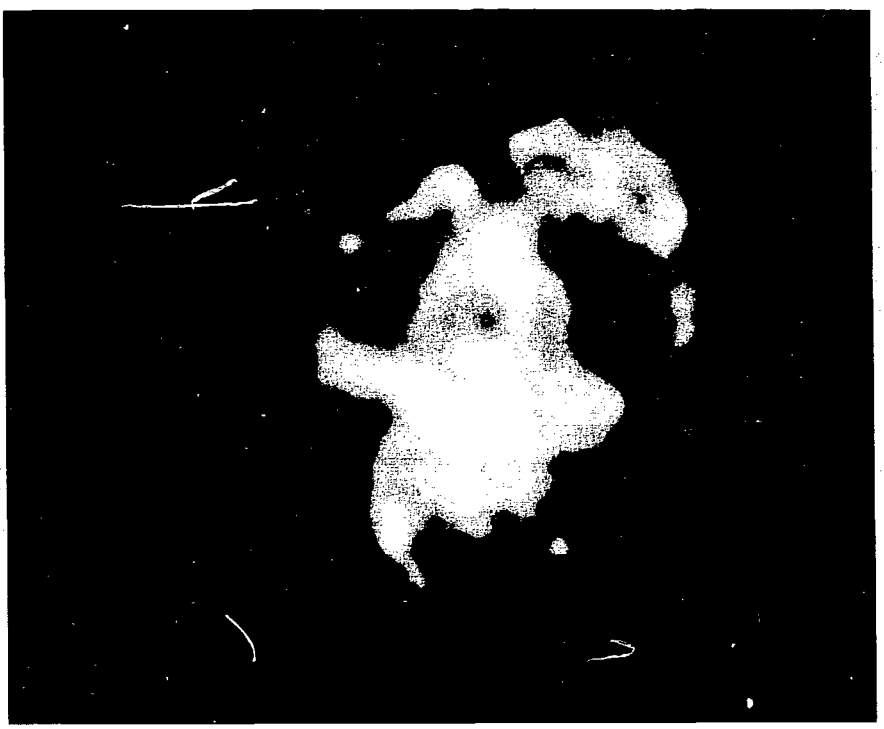

Image of the Crab supernova remnant, observed by the Very-Large-Array Telescope and processed at IGPP. The explosion that produced this object occurred in A.D. 1054.

Evolution of Low-Mass Stars, Substellar Objects, and Giant Planets

Principal Investigator:
Peter Bodenheimer[a]
Co-Investigators:
Hugh E. DeWitt,
Forrest J. Rogers,
Marvin Ross, and
Guy Stringfellow[a]

[a]University of California, Santa Cruz.

Our goals are to identify stages in the evolution of stars, substellar objects, and giant planets at which accurate equation-of-state (EOS) data are required for an adequate theoretical description of the evolution. We plan to obtain detailed EOS tables for a multi-component mixture with approximately the solar ratio of hydrogen to helium and with various degrees of enrichment (over solar abundances) of the heavy-element component. These tables are to be used to calculate the evolution of objects with substellar or planetary mass and thereby determine their observable properties.

Our calculations were aimed toward acquiring an accurate EOS for a gas with solar composition over the wide range of density-temperature parameter space appropriate for stars near and below the lower end of the main sequence and also for giant planets. The parameter space can be broken up into three separate regions: the strongly coupled plasma, where Coulomb corrections and screening become dominant factors in the EOS; the ideal gas regime, where density effects (0.001 to 1 $g \cdot cm^{-3}$) become important in the ionization process ("pressure ionization"); and the low-temperature regime, where molecule formation becomes important.

Most advanced EOS data now available are limited to the case of a one-component plasma. To extend these calculations over a wide parameter range in density and temperature and over a variety of possible compositions is a substantial project involving many subtleties in the physics. Our work has made it clear that a major commitment of time is required to obtain good and complete results for the EOS. However, this larger effort would be a timely one. What is needed is to improve upon the current standard tables for the solar mixture of elements and to provide a new state-of-the-art EOS for stellar calculations. Such an undertaking is feasible, but the time and resources available were not sufficient to complete the job.

Institute for Scientific Computing Research

Overview

Nora G. Smiriga

The Institute for Scientific Computing Research (ISCR) is devoted to research in scientific computing as a collaborative effort between UC and LLNL. At present, the ISCR is in a formative stage. In general, the ISCR plans to make LLNL's expertise in scientific computing and its computational facilities available to UC researchers.

The ISCR will first focus on strengthening research ties between LLNL and UC Berkeley. Our efforts will then expand to include all other UC campuses. Our main goals are to advance state-of-the art research in computer science and to foster research that will strengthen ties between the fields of computer science and scientific computing.

The IR&D program at LLNL provides ISCR funding for two postdoctoral fellows and one secretary. The ISCR also receives substantial contributions from the LLNL Computation Department. In the future, the ISCR plans to seek funds from the UC system-wide administration. During FY87, the ISCR supported two postdoctoral fellows, both of whom were jointly funded by IR&D and Physics Department funds.

Our FY87 activities centered on three basic areas of work: joint research efforts with UC Berkeley, site renovation at LLNL, and work toward formalizing the relationship between UC and LLNL. In April 1987, the ISCR held a joint workshop for LLNL and the UC Berkeley College of Engineering. The workshop's theme was problems in the computational sciences, and its primary goal was to determine the extent of common research interests between the two institutions. Twelve technical presentations by representatives of both LLNL and UC Berkeley dealt with several topics, including the application of large-scale numerical simulation techniques to a variety of problems.

Overall, the ISCR received $151,000 in funding for FY87.

Path Space Methods for Statistical Mechanics

Principal Investigator:
Thomas Buttke
Co-Investigators: Berni J. Alder
and Roy Pollock

The macroscopic properties of classical or quantum mechanical systems in thermodynamic equilibrium can be represented mathematically as averages of observables over high-dimensional configuration space. There are two approaches to making the numerical evaluation of such averages tractable: reducing the dimensionality of the space over which the integral is to be performed and using specialized quadrature formulas that exploit the structure of the specific integrals to be calculated. We investigated the possibility of a procedure proposed by Stratanovich for evaluating the high-dimensional integrals defining the partition function and its moments in classical and quantum statistical mechanics. In this approach, the integrals are expressed as the expected value of a functional Gaussian random walk in d-dimensional physical space. The functional can be expressed as a product of independent Gaussian random variables using Fourier transforms, thus reducing the calculation of the original problem to that of calculating a product of d-dimensional integrals. In the classical case, we formulated the algorithm to make the integrals amenable to highly accurate integration techniques. In particular, we removed the restriction that the Fourier transform be positive. We also developed variance reduction techniques based on the Wiener-Hermite expansions for use in the quantum case. We are now implementing these techniques for quantum mechanical calculations of the density functions for fermions in one, two, and three dimensions.

Vortex Methods in Three Dimensions

Principal Investigator:
Thomas Buttke
Co-Investigators: Phil Colella and
Scott Baden[a]

[a]University of California, Berkeley.

We are investigating fast algorithms for use in the study of turbulent, incompressible flow in three dimensions for the particle methods known as vortex methods. The underlying principle is that the influence of disjoint regions in a fluid is mediated through harmonic functions. Because these functions are infinitely smooth, and their derivatives decay rapidly, the influence of widely separated particles should be computable accurately using a reduced representation. The costs of such algorithms are essentially linear in the number of particles rather than quadratic. Two such methods have been proposed and tried in two dimensions. We are extending both algorithms to three dimensions to determine which one is optimal. We are also implementing techniques for generating arbitrary (nonradially symmetric) cutoff functions to improve the accuracy and efficiency of vortex methods. Our ultimate goal is to use the methods we are developing to study turbulence in both ordinary fluids and superfluids.

Maximally Discretized Molecular Dynamics

Principal investigator:
Michael Colvin
Co-Investigators:
Berni J. Alder and Tony Ladd

For the past three decades, molecular dynamics (MD) has been an essential tool in the field of statistical mechanics. However, the study of many interesting problems, such as fully formed hydrodynamical phenomena, will require at least a millionfold performance increase over the fastest available MD methods. To bridge this performance gap, we have developed a fast MD algorithm by simplifying the simulation model as much as possible without significantly affecting the physical properties of interest. In our two-dimensional MD model, the particles are hard hexagons moving on a coarse hexagonal grid, where each grid spacing equals one particle diameter. The particles are restricted to move in only six directions at a speed of either 0 or 1 grid space per timestep. Because the model involves the coarsest reasonable discretization of the particles' positions and velocities, we refer to it as maximally discretized molecular dynamics (MDMD). The Figure shows an MDMD system, where the dark hexagons are particles whose velocities are indicated by arrows. We have measured the collision rate, diffusion constant, and viscosity of the MDMD model. Our results agree well with our theoretical expressions for the MDMD transport coefficients and with the values for comparable simulations using conventional hard-disk MD. The computational advantage of MDMD over standard MD algorithms is significant. Our initial implementation of MDMD ran three orders of magnitude faster than comparable MD programs. Since the MDMD algorithm is inherently parallel, we feel that on massively parallel computers, such as the 65,000-processor connection machine, we should be able to gain an additional increase in performance by three orders of magnitude over that of standard MD methods.

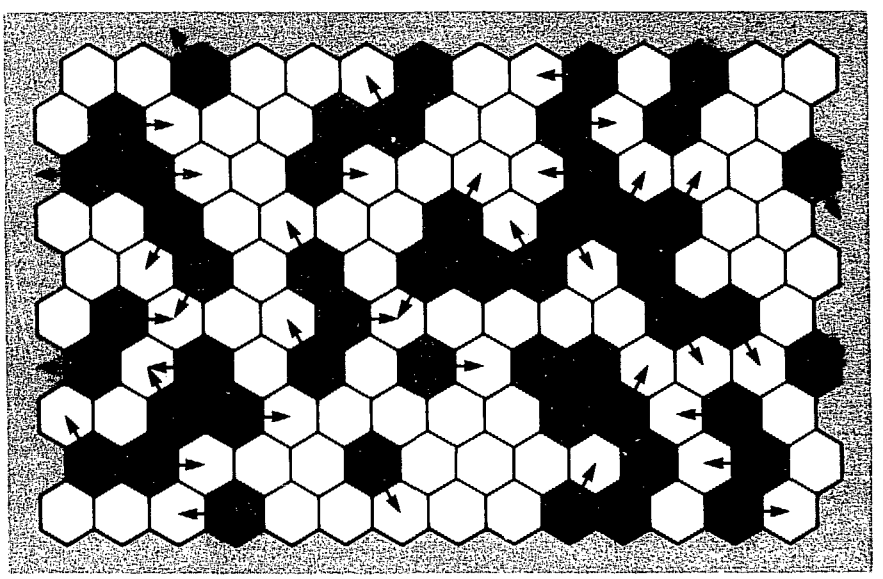

An MDMD system with dark hexagons representing particles whose velocities are indicated by the arrows.

Computer Models of Biological Visual Systems

Principal Investigator:
Michael Colvin
Co-Investigators:
Timothy S. Axelrod,
Donald Glaser,[a] Brent Beutter,[a]
and Tribhawan Kumar[a]

[a]University of California, Berkeley.

We take for granted our ability to instantly recognize a friend in a crowd of strangers; yet this simple task is far beyond the capabilities of today's electronic image-processing systems. Moreover, the perceptual feat is completed by our brain in less than ten neural "clock cycles," indicating that the visual system is extensively parallel and processes information along millions of channels simultaneously. The purpose of our project is to try to use neural engineering principles in the design of the primary image-processing system for the LLNL Wide-Field-of-View Telescope. Since the purpose of the telescope is to track moving objects against a stationary background, it is reasonable to look for biological systems that carry out the same task. Many studies have indicated that the visual systems of simple vertebrates, such as frogs, carry out just this task and have specialized "hardware" specifically for the detection of moving targets (i.e., food) against a stable background. Using physiological data, we are developing a computer model of retinas of the type found in simple visual systems. When complete, our computer model should be useful both in the development of the telescope tracking system and in research on biological visual systems.

Plasma Physics Research Institute

Overview

John Killeen

The Plasma Physics Research Institute (PPRI) is a new institute operated jointly by UC and LLNL. It is administered by LLNL and the College of Engineering at UC Davis, and receives support from the IR&D program, the UC Davis Department of Applied Science, and several LLNL programs. A proposal to establish the PPRI as an organized research unit of the University of California has been approved by UC Davis and LLNL, and is now under study at the Office of the President of UC.

Plasma physics is a scientific discipline fundamental to many of our major LLNL projects, especially the Magnetic Fusion Energy and Laser Fusion Programs. Over the years, the UC campuses and LLNL have developed several informal collaborative contacts to aid major plasma physics projects either at LLNL or on the campuses, but these contacts have usually been temporary and project-specific.

The PPRI's purpose is to strengthen basic and applied research in plasma science throughout the university. Faculty at virtually all of the campuses will benefit from the opportunities it will make available. It will also broaden and strengthen the plasma-physics graduate programs at the campuses and enhance the strong collaborative ties in plasma-physics research that already exist among LLNL and the campuses.

The PPRI will foster interaction among all of the university's organized research units and informally organized interdisciplinary groups with ongoing interests in plasma science. We anticipate strong collaboration with UCLA's Center for Plasma Physics and Fusion Engineering and with plasma scientists at UC Berkeley and at the various branches of the Institute of Geophysics and Planetary Physics (including the branch at LLNL).

During FY87, the PPRI has undertaken three major initiatives:

- Established a base of operations at LLNL.
- Sponsored a symposium on plasma physics research at the UC campuses and laboratories (held September 10-11, 1987).
- Established the Davis Diverted Tokamak at LLNL to study the basic physical processes governing the confinement and stability properties of a diverted plasma.

The equipment for the tokamak facility, which was fabricated at UCD, will also be used for current-drive experiments. In addition, we will have the benefit of equipment donated by Princeton Plasma Physics Laboratory, N.J., and GA Technologies, La Jolla, Calif.

In FY88, we plan three major experiments on the Davis Diverted Tokamak Facility: tokamak and divertor operation, rf-stabilization of the axisymmetric instability by lower hybrid current drive, and beat-wave current drive. We are engaged, with our UC Berkeley colleagues, in a joint numerical simulation project using a particle model. During the summer, we plan a visiting faculty program and another workshop on a special topic in plasma physics.

In FY87, the PPRI received $45,000 in IR&D funds.

Program for Analytical Cytology

Overview

Brian H. Mayall

The charter of the Program for Analytical Cytology (PAC) is to transfer technology by finding clinical applications for LLNL advances and by exposing clinical scientists to the conceptual approaches of analytical cytology. With analytical cytology, it is possible to quantify the properties of individual cells, rather than merely to measure the average characteristics of many cells in a test tube.

As a result of the PAC collaborative research and educational projects, we are now seeing broad benefits in the biomedical research community, mainly at UC San Francisco, but increasingly at the UC Berkeley, Davis, and Los Angeles campuses. The PAC activities are contributing significantly to the diagnosis, understanding, and treatment of many diseases and have made UC San Francisco a world leader in clinical applications of analytical cytology.

The PAC is funded by the UC Regents and uses those funds for mini-grants that serve as seed money supporting innovative and collaborative research projects. LLNL and UC San Francisco provide matching funds, primarily to support administration and teaching. Additional gifts from industry support postdoctoral fellows, and grants from the National Institutes of Health support collaborative research projects of demonstrated potential. More than 30 joint LLNL and UC San Francisco research projects have been funded through the PAC. More than half of these awards have led to collaborative research projects that now are being funded from sources outside the University.

In FY87, the PAC award program was curtailed because of funding uncertainties associated with renewal of the contract between UC and the Department of Energy. Nevertheless, the PAC has remained vital by consolidating past achievements. In addition, two postdoctoral fellows, on assignment to LLNL from UC San Francisco, have been supported through the PAC with funds contributed by an industrial donor.

The PAC has been active in advancing image cytometry at LLNL. Our prototype quantitative image processing system (QUIPS) is now in routine operation and has been duplicated to meet LLNL requirements for image cytometry.

In this section, we focus on four important efforts during FY87. First, we describe the expansion of the Laboratory for Cell Analysis, which is a unique PAC resource for cytometric applications at UC San Francisco. At the end of that discussion is a list of references to PAC-supported publications—an indication of the scope of PAC activities. In the abstracts that follow, we highlight our efforts in three areas: the detection of specific sequences of nucleic acids using in situ hybridization with antigen-labeled probes, the detection of chromosomal abnormalities using flow cytometry, and our new methods for detecting chromosome-linked genetic disorders in fetal cells isolated from maternal blood. Overall, the PAC received $180,000 for FY87.

Laboratory for Cell Analysis

Principal Investigator:
Mack J. Fulwyler[a]
Co-Investigators:
Brian H. Mayall, Joe Gray, Ronald H. Jensen, Barton L. Gledhill, Frederic Waldman,[a] Eileen King,[a] John Greenspan,[a] Daniel Stites,[a] and Karen Chew[a]

[a]University of California, San Francisco.

The Laboratory for Cell Analysis (LCA) is a most tangible manifestation of the PAC. Our 3,000-ft² research facility, located at UC San Francisco, now houses eight different cytometric systems (four flow sorters, a flow analyzer, and three image cytometers) that match and supplement the cytometric resources available through the PAC at LLNL. These systems make the PAC a unique resource for the applications of cytometry, a resource that probably is unsurpassed anywhere in the world. UC San Francisco has allocated funds for FY88 to renovate space for the LCA that will double its size. This renovation will allow us to continue expanding our collaborative research projects between LLNL and UC San Francisco.

References

Apicella, M. A., M. Shero, G. A. Jarvis, J. M. Griffis, R. E. Mandrell, and H. Schneider (1987), "Phenotypic Variation in Epitope Expression of the Neisseria Gonorrhoeae," *Infect. Immunity* **55**, 1755.

Balazs, M., J. Matko, J. Szollosi, L. Matyus, M. Fulwyler, and S. Damjanovich (1986), "Accessibility of Cell Surface Thiols in Human Lymphocytes is Altered by Ionophores or OKT-3 Antibody," *Biochem. Biophys. Res. Commun.* **140**, 999.

Dairkee, S. H., B. H. Mayall, H. S. Smith, and A. J. Hackett (1987), "A Marker that Predicts Early Recurrence of Breast Cancer" (letter), *Lancet* **8531**, 514.

Ficarra, G., K. B. Kaban, and L. S. Hansen (1987), "Central Giant Cell Lesions of the Mandible and Maxilla: A Clinicopathologic and Cytometric Study," *Oral Surg.* **64**(1), 44.

Haase, A., M. Brahic, L. Stowring, and H. Blum (1984), "Detection of Viral Nucleic Acids by In Situ Hybridization," *Methods in Virology*, H. Blum, K. Maramorosch, and H. Koprowski, Eds. (Academic Press, New York), vol. 7, p. 189.

Haase, A. T., H. Blum, L. Stowring, A. Geballe, M. Brahic, and R. Jensen (1985), "Hybridization Analysis of Viral Infection at the Single-Cell Level," *Clinical Laboratory Molecular Analysis* (Grune and Stratton, Inc., New York, N.Y.), p. 247.

LeBoit, P. E. and H. V. Fletcher (1987), "A Comparative Study of Spitz Nevus and Nodular Malignant Melanoma Using Image Analysis Cytometry," *J. Invest. Dermatol.* **88**, 753.

Mayall, B. H., C. Gadenne, E. B. King, K. L. Chew, L. A. Duarte, and N. L. Petrakis (1987), "Image Cytometry of Duct Cells from Benign and Malignant Breast Disease," *Clinical Cytometry and Histometry*, G. Burger and J. S. Ploem, Eds. (Academic Press, London), p. 414.

McHugh, T. M., D. P. Stites, C. H. Casavant, and M. J. Fulwyler (1986), "Flow Cytometric Detection and Quantification of Immune Complexes Using Human-C1q Coated Microspheres," *J. Immuno. Methods* **95**, 57.

Szollosi, J., L. Matyus, L. Tron, M. Balazs, I. Ember, M. Fulwyler, and S. Damjanovich (1987), "Flow Cytometric Measurements of Fluorescence Energy Transfer Using Single Laser Excitation," *Cytometry* **8**, 120.

Tron, L., S. Damjanovich, A. Aszalos, J. Szollosi, S. A. Mulhern, and M. J. Fulwyler (1986), "On the Role of Cell Surface Dynamics and Transmembrane Information Transfer: Cyclosporin A Changes Physical Properties of Cell Membranes," *Dynamics of Biochemical Systems* (Akademiai Kiado, Budapest, Hungary).

Waldman, F. M., M. J. Fulwyler, K. Hadley, and J. Schacter (1987), "Flow Cytometric Analysis of Chlamydia Trachomatis Interaction with L Cells," *Cytometry* **8**, 55.

Wyrobek, A. J., J. F. Moruzzi, B. H. Mayall, and B. L. Gledhill (1986), "Image Analysis of Human Sperm Morphology," *Environ. Mutagen.* **8**, 93.

Young, I. T., P. W. Verbeek, and B. H. Mayall (1986), "The Characterization of Chromatin Distribution in Cell Nuclei," *Cytometry* **7**, 467.

Nonradioactive In Situ Hybridization Using 2-Acetyl-Aminofluorene-Modified Probes

Principal Investigator:
Frederic Waldman[a]
Co-Investigators:
Joe Gray, Dan Pinkel, and
James E. Landegent

[a]University of California, San Francisco.

In situ hybridization with antigen-labeled probes allows for the nonradioactive detection of specific sequences of nucleic acids in microscopic preparations. The procedure involves chemical modification of probes with the low-molecular-weight compound 2-acetyl-aminofluorene (AAF). The covalently attached AAF groups are, in turn, detected after hybridization by specific antibodies to introduce nonradioactive labels, such as fluorescent dyes, deposits of enzyme products, or colloidal gold. We reduced the lower detection limit of nonradioactive in situ hybridization to allow chromosomal mapping of unique DNA sequences. We varied five aspects of the procedure to increase its sensitivity:

- Preparation of chromosomes prior to hybridization.
- Hybridization efficiency.
- Number of haptens (AAF groups) at target sites.
- Immunocytochemical detection through enhancement of the amount of marker deposited at the site of hybridized sequences.
- Microscopic visualization through use of reflection-contrast microscopy to detect localized deposits of enzyme products.

These efforts have allowed us to detect unique sequences as small as 15 kilobases.

Detection of Chromosomal Abnormalities with Flow Cytometry: Flow Karyotyping and Fluorescence Hybridization

Principal Investigator:
Mitchell Golbus[a]
Co-Investigators: Barb Trask,
Ger van den Engh, Dan Pinkel,
Jim Mullikin, and Joe Gray

[a]University of California, San Francisco.

Two methods to detect chromosomal abnormalities are flow karyotyping and fluorescence hybridization in suspension. For flow karyotyping, chromosomes are isolated from mitotic (dividing) cells, stained with two DNA-specific dyes, and then analyzed on a dual-beam flow cytometer. High chromosome resolution now allows us to discriminate among all human chromosomes, except for chromosomes 10 to 12, and many homologs. In a blind study of amniotic cultures, we detected 8 of 8 numerical abnormalities and 7 of 7 translocations by flow cytometry. In most cases, we were able to identify the chromosomes involved and to confirm the breakpoint. For fluorescence hybridization, nuclei obtained during interphase (when cells are not dividing) are hybridized in suspension to antigen-AAF-labeled probes for the DNA sequence. The bound probe is immunochemically labeled with a fluorescent dye, and nuclei are then analyzed in a dual-beam flow cytometer. Probe fluorescence following hybridization to human-chromosome-specific DNA is proportional to the number of chromosomes. Nuclei from normal males (46,XY), normal females (46,XX), and abnormal males (47,XYY) are clearly discriminated on the basis of such probe fluorescence after hybridization with a repetitive sequence probe that is specific for chromosome Y. We can now quantify target sequences as small as 1 megabase with this procedure.

Cytogenetic Analysis of Fetal Cells from Maternal Blood

Principal Investigator:
Susan Fisher[a]
Co-Investigators:
Joe Gray, Lo-Chung Yu,
Maria Pallavicini, Dan Pinkel,
Caroline Damsky,
and Mitchell Golbus[a]

[a]University of California, San Francisco.

Our goal is to develop procedures that allow the detection of selected chromosome-linked genetic disorders (e.g., Down's syndrome) in fetal cells isolated from maternal blood (see the Figure). We are now working on two fronts: to develop techniques enabling us to identify and determine the frequency of fetal cells in maternal blood, and to detect chromosome aberrations involving chromosome 21 in interphase cells. We are measuring fetal-cell frequencies in maternal blood by using fluorescence hybridization with probes that are specific for the Y chromosome to selectively stain fetal cells in the blood of women carrying male fetuses. The fetal cells will be selectively stained using fetal-cell-specific monoclonal antibodies and then purified using either cell sorting or immuno-affinity column separation. We will detect numerical aberrations in interphase fetal-cell nuclei using fluorescence in situ hybridization with chromosome-specific probes. Individual chromosomes tend to be tightly localized during interphase; the number of chromosomes of one type can be determined by counting the number of fluorescence domains after fluorescence hybridization. We are currently nearing completion of developing probes for chromosome 21.

Nuclei of cytotrophoblasts (cells from the placenta, which are shed into the mother's blood) from a male fetus. We identify the Y male sex chromosome by fluorescence in situ hybridization so that it becomes visible as a small spot in the nucleus of each cell. In this photograph, the Y chromosome is clearly visible in the two nuclei from a male fetus. (The third nucleus from a maternal cell has no Y chromosome.) We are now developing procedures to analyze these cells in the mother's blood. If successful, the approach should greatly reduce the need for amniocentesis to detect genetic problems.

I ◆ R ◆ & ◆ D

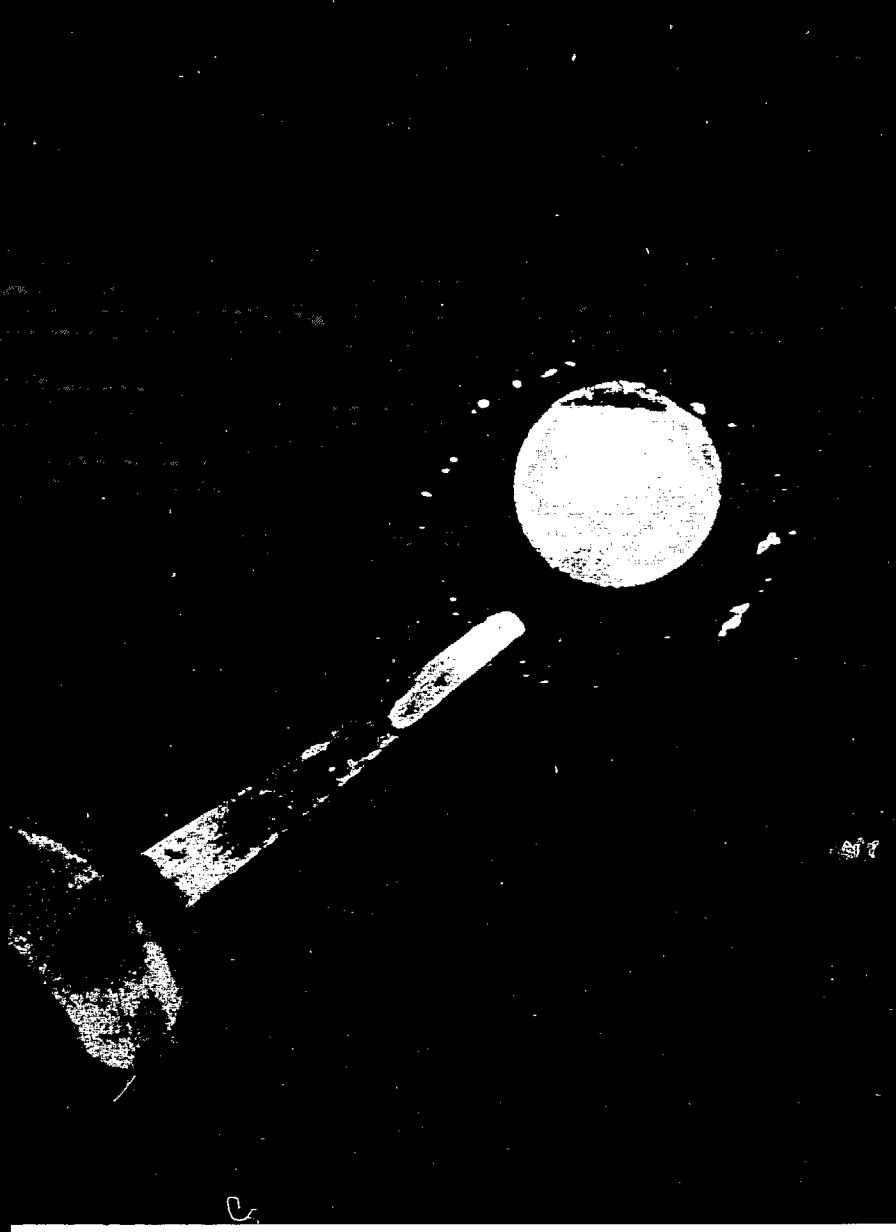

Individual Awards

Lawrence Livermore National Laboratory

Individual Awards

Overview

Richard A. Ward

The IR&D Awards are grants given to individual LLNL investigators in open competition with all staff members. These awards provide a way to give "seed funding" outside of the usual programmatic channels. Because of the intense competition for the limited funds available, the Research Committee focuses on projects that stand a good chance of blossoming into self-sustaining LLNL programs able to generate their own funding.

The selection criteria for FY87 proposals (consistent with Department of Energy guidelines) were:

- Scientific or technical quality.
- Impact on LLNL or the general scientific community.
- Leverage for future funding. (The seed-funding concept was extremely important in the committee's consideration of promising new directions for science and technology in fields of general interest to LLNL programs.)

The Research Committee consisted of 18 members appointed by and reporting to the Director. Chosen to represent the wide diversity of scientific disciplines pursued at LLNL, members serve for a maximum of three years. After all written proposals were submitted, two members interviewed each principal investigator and reported back to the full committee. The committee ranked each proposal in order of overall scientific excellence and pertinence to LLNL's scientific mission, so as to make the best use of the available funds.

The projects range from theoretical studies and computational simulations to building and conducting full-scale laboratory experiments, and span an impressively large range of disciplines. The following descriptions cover a few of the proposals chosen for funding.

One team proposed to continue its work using the time-projection chamber (TPC) at Stanford Linear Accelerator Center to study the interactions of 15-GeV electrons with nuclei in the Positron Electron Project (PEP) storage ring (see page 166). Such electrons are direct probes of the quark and gluon structure in nuclei, turning what was "background noise" in elementary-particle experiments into a primary source of information about electron-nucleon interactions. Continued funding will make possible further analysis of events already collected at the TPC and provide design support for constructing a dedicated nuclear physics facility in one of the six PEP interaction regions.

In the biomedical sciences, a proposal led to the development of techniques to follow cell division and lifetimes of individual lymphocytes in mice (see page 175). The ultimate aim is to measure changes in these parameters after exposure to mutagenic agents. Flow cytometric analysis of newly made DNA, coupled with analysis of cell surface markers and the DNA, will be monitored with monoclonal antibodies.

As a continuing spin-off of our positron source, another team proposed to produce high Rydberg states of positronium with a two-step laser-excitation process (see page 197). Such long-lived positronium states have significantly reduced positron-electron overlap, increasing the lifetime to annihilation. If successful, this project could benefit work on dense positronium for gamma-ray lasers and experiments to test the equivalence principle of general relativity on purely leptonic matter.

In chemistry and materials science, a researcher proposed to use a slightly cross-linked polystyrene template in synthesizing dense explosives (see page 184). Higher-density cyclic homologs of explosives such as HMX have long

Overview (continued)

been sought because they would be significantly more powerful than the less-dense material. Success with this method would be a boon not only to explosives synthesis but also to organic synthesis in general.

Several projects developed computer codes to model diverse physical processes. One such project (page 160) would continue dynamical calculations on the nonlinear growth of instabilities in radiation-driven stellar winds to determine whether acoustical noise at the base of the wind near the star's surface can be amplified or always dies away to a steady state.

Another project would include (in an existing stellar-evolution model) the effects that would follow if hypothetical massive particles such as axions and Majorana neutrinos were generated in a star's core (see page 163). Contrasting the evolution of these model stars with the observed Hertsprung-Russell distribution will make it possible to set limits on the myriad "ons" and "inos" called for in recent theories.

In FY87, the Research Committee considered 125 proposals requesting $15,800,000 in funding that included 1744 hours of supercomputer time. Of these, 38 individual awards were granted for a total of $3,697,000, including $41,000 for capital equipment. The funding for individual proposals ranged from a high of $180,000 to a low of $20,000. The disciplines of the funded proposals closely match the Laboratory-wide distribution of scientific disciplines.

Analysis of Fluid Inclusions Using Micro-Infrared Spectroscopy

Principal Investigators:
Roger D. Aines and
William L. Bourcier

By using micro-infrared spectroscopy, we determined the presence and composition of liquid and gaseous species in fluid inclusions within natural minerals and synthetic materials. We have begun to quantify the analysis using synthetic fluid inclusions of known compositions. Our technique can analyze fluid inclusions in natural minerals and reveal information about the temperature and pressure of mineral formation and the composition, source, and evolution of the fluid phase.

Fluid inclusions trap representative samples of those fluids present during the time the host mineral was formed. Knowledge of the composition of the fluids trapped in an inclusion provides key information on the process of mineral formation.

Because most inclusions are small (5 to 50 μm), analyses of fluid inclusions by conventional techniques have been difficult. However, recent advances in micro-infrared spectroscopy have made it possible to analyze sample volumes of typical fluid inclusions. Our investigation was aimed at determining the capabilities and limitations of this technique and developing procedures that quantify the analysis.

We demonstrated that useful spectra can be obtained for fluid inclusions that have the size and compositional range of common natural materials. The Figure shows a spectrum of a 45-μm fluid inclusion containing a mixture of water, carbon dioxide, light hydrocarbons, and a CH_4-CO_2 hydrate solid phase. The side peaks near the broad peak for water are due to light hydrocarbons. The carbon dioxide peak is shifted to higher wave numbers than are characteristic of free carbon dioxide because that component is present primarily in the hydrate solid phase.

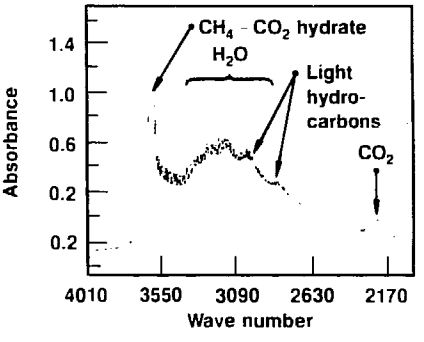

Infrared spectrum of a 45-μm fluid inclusion in the mineral quartz containing a mixture of water, carbon dioxide, light hydrocarbons, and a solid CH_4-CO_2 hydrate.

We used a suite of synthetic fluid inclusions containing mixtures of water and carbon dioxide of known composition to attempt to quantify our technique. Such quantification is difficult because of the irregular geometries of fluid inclusions and the corresponding effect on light paths through a sample. We are continuing to develop a satisfactory procedure for the quantitative analysis of fluid inclusions.

Reference

Bourcier, W. L. (1986), "A Computer Program for Calculation of Fluid Inclusion Phase Equilibria in the System H_2O-NaCl-CO_2-CH_4-H_2S with Applications to Mississippi Valley-Type Ore Deposits" (abstract), *Trans. Am. Geophys. Union* **U-67**(44), 1258.

FY87: $99,000

Three-Dimensional Hydrodynamic Studies of Relativistic Heavy-Ion Collisions

Principal Investigator:
Carol T. Alonso
Co-Investigators:
James R. Wilson,
Jonathan A. Zingman, and
Thomas L. McAbee

We are modeling relativistic heavy-ion collisions with a fully covariant, three-dimensional hydrodynamic model for nucleons combined with a dynamic Monte Carlo pion model. The modeling allows us to examine how assumptions about the nuclear equation of state both at zero and finite temperatures can affect experimental observables.

With the advent of accelerator facilities for studying relativistic heavy-ion collisions, physicists can investigate nuclear matter under extreme conditions of density and temperature. The flow of matter is reflected in the distribution of both nuclear fragments and pions generated during a collision. We have developed the first fully relativistic, three-dimensional hydrodynamic collision model that incorporates pions dynamically. We treat pion generation, transport, scattering, and absorption with cross sections derived from experimental data.

Our relativistic hydrodynamic model can handle collisions at arbitrary impact parameters. We have tested the model against analytic shock solutions to show that we can accurately handle flow at relativistic factors, such as $\gamma = 1$ to 10, which are comparable to those obtainable at current and proposed accelerators. We have studied various aspects of the nuclear equation of state (EOS), including compressional (zero-temperature) behavior, the behavior of effective masses for the nucleon and higher resonances, and the effects of various thermal EOSs. We have begun to study how these factors affect the flow of nuclear matter and pion production and are attempting to match the somewhat limited experimental data to identify the most important effects.

Although our model correctly treats pion dynamics, it appears to produce about the same number of

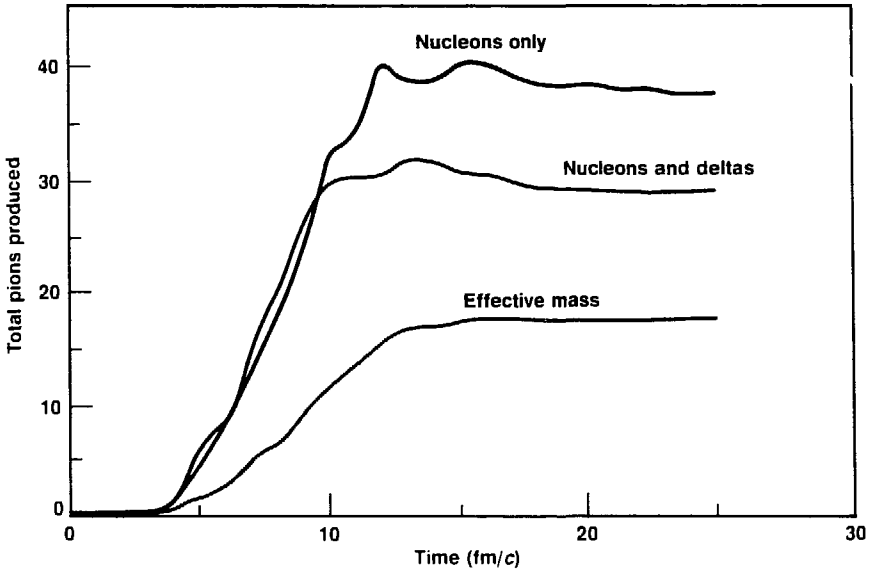

Pion production histories versus time, in units of femtometer/speed of light, with nucleons only in the thermal EOS, with nucleons and deltas in the thermal EOS, and with an effective mass in both the thermal and ground-state EOS.

pions as predicted by previous static chemical models, implying achievement of equilibrium for at least a short time. This result suggests that our model needs an additional channel for pion production from resonance decay. Calculations with three different EOSs using nucleons only, nucleons and deltas, and nucleons with an effective mass (see the Figure) still produce only 80% of the pions observed experimentally for lanthanum on another layer of lanthanum at 1350 MeV.

Our results point out the necessity for further refinements to the model. In particular, we need to include pion production from delta resonance decay to match observed pion multiplicities, and we need nuclear fluid viscosity to reproduce results on experimental flow.

References

Molitoris, J. J., D. Hahn, C. T. Alonso, I. Collazo, P. D'Alessandris, T. L. McAbee, J. R. Wilson, and J. A. Zingman (1987), *Relativistic Nuclear Fluid Dynamics and VUU Kinetic Theory*, Lawrence Livermore National Laboratory, Livermore, Calif., UCRL-97270.

Zingman, J. A. (1987), *Nuclear Stopping and Energy Deposition in the Flux Tube Model*, Lawrence Livermore National Laboratory, Livermore, Calif., UCRL-97269.

Zingman, J. A., T. L. McAbee, J. R. Wilson, and C. T. Alonso (1987), *Introduction and Guide to LLNL's Relativistic 3-D Nuclear Hydrodynamics Code*, Lawrence Livermore National Laboratory, Livermore, Calif., UCID-21126.

Zingman, J. A., T. L. McAbee, J. R. Wilson, and C. T. Alonso (1987), *Relativistic 3-D Nuclear Hydrodynamics with Monte Carlo Pions*, Lawrence Livermore National Laboratory, Livermore, Calif., UCRL-97153.

FY87: $153,000
FY88: $148,000

Scanning Tunneling Microscopy

Principal Investigator:
Walter Bell
Co-Investigators:
Wigbert J. Siekhaus,
Bruno Marchon,[a] David Ogletree,[a]
and Miquel Salmeron[a]

[a]Lawrence Berkeley Laboratory,
Berkeley, Calif.

We have developed a scanning tunneling microscope that operates in air at atmospheric pressure. It can determine the physical structure of surfaces with a resolution of 1 Å in plane and better than 0.1 Å normal to the surface plane. We demonstrated its ability to differentiate between different atomic species by identifying the structure of sulfur atoms adsorbed onto molybdenum(001). Its capabilities open the way for in situ studies of surface structure and reactivity at high pressure.

The study of geometry and the electronic structure of surfaces at elevated pressures is of great importance in understanding the behavior and the properties of real materials in corrosion, passivation, electrochemistry, catalysis, and other areas of science and technology. Until recently, most surface-sensitive techniques have been restricted to ultra-high-vacuum (UHV) environments. The pressure gap of some 10 orders of magnitude makes it difficult to infer explanations of surface phenomena at high pressures from information obtained in UHV. The advent of scanning tunneling microscopy (STM) (Binnig et al., 1982) has provided the opportunity to study surface phenomena such as corrosion, wetting, and catalysis at operating pressures.

Figure 1 shows the main features of the microscope we built. A tripod of piezoelectric ceramic serves to manipulate the tunneling tip probe made of 1-mm wire (60% platinum/40% rhodium) cut with a wire cutter at an angle of 45°. Electric fields applied in the ceramic legs through evaporated metallic contacts induce strain, which moves the tip around. In our instrument, the tripod provides a maximum tip range of 15,000 Å in all directions, with displacement control of better than 0.1 Å. Square pictures 100 Å on a side can be acquired in less than a minute.

Here is a description of how our instrument operates. Imagine an atom at the end of an atomically sharp metallic needle close to the surface of a conducting material. If the gap between the needle and the surface is 5 Å, an applied bias of several tens of millivolts will induce nanoampere current flows. Electrons can flow across the gap because of

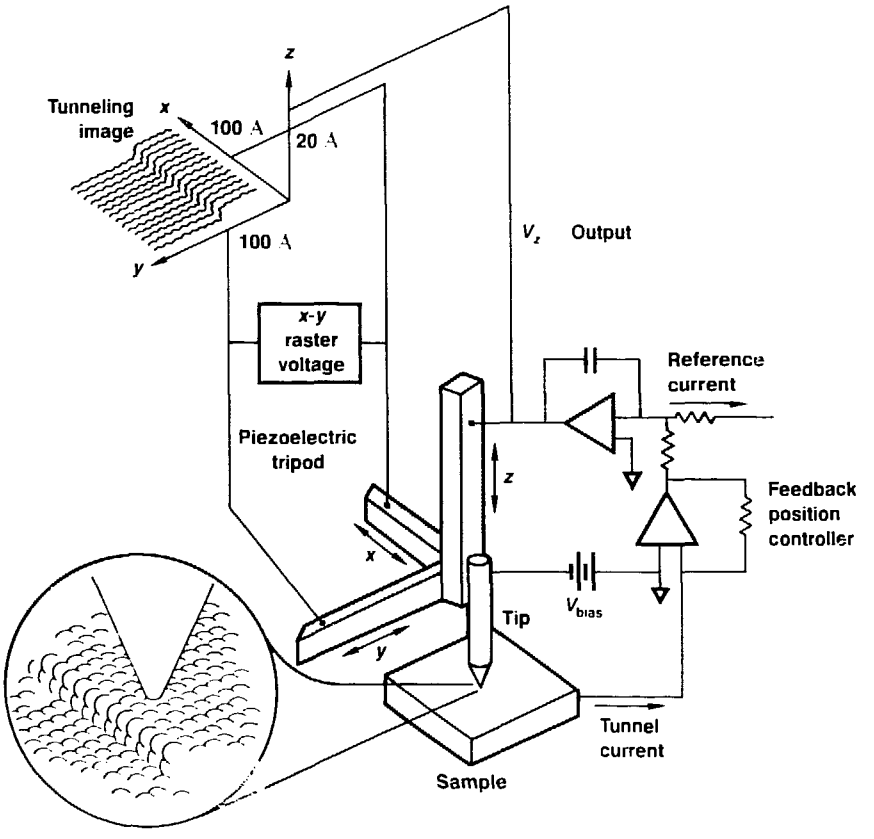

Fig. 1. The scanning tunneling microscope.

the quantum-mechanical tunneling effect. The current I is given by

$$I \approx \exp - \beta\sqrt{\mu}s$$

where β is a scaling constant, s is the gap distance, and μ is the local electronic barrier height. The current typically decreases by an order of magnitude for every Å in gap spacing. We have used three operating modes: the constant-current mode, the constant-height mode, and the local barrier-height mode.

In the constant-current mode, the needle scans across the surface laterally while its distance from the surface is adjusted to keep a constant tunneling current, and a topograph of the surface is obtained in the recorded trajectory of the tip.

In the constant-height mode, the needle scans across without height adjustment. A topograph is obtained in the recorded tunneling current. Figure 2 shows such a topograph of the basal plane surface of pyrolytic graphite. As mentioned in the literature (Park and Quate, 1986), the STM "sees" only every second atom on the graphite surface because only every second atom has electronic states easily accessible to tunneling.

In the local barrier-height mode, the tip-to-surface gap distance is modulated at a frequency above the feedback loop cutoff, such that the mean distance and, therefore, the mean value of the tunneling current is maintained at a constant level. The amplitude of the ac part of the instantaneous tunnel current, as measured by a lock-in amplifier, is directly related to the square root of the local barrier height, according to the equation given above.

Figure 3 shows a 60- × 30-Å region of ordered sulfur atoms adsorbed (under UHV conditions) onto an atomically clean molybdenum(001) surface. The image was taken in barrier-height mode after several days' exposure to air. Large parts of the crystal surface (for example, around the ordered structure in Figure 3) could not be atomically resolved in this experiment, possibly because of partially conductive contaminants or highly oxidized spots on the surface.

The important result of our work is that it proves that atomic-resolution imaging for adsorbate atoms on metals can be achieved by using STM in an ordinary air environment. To our knowledge, it is the first time that an atomically resolved structure has been imaged in barrier-height mode.

In FY88, we plan to use our scanning tunneling microscope to investigate the paths and sites of superconductivity in high-temperature superconductors. We seek to determine whether superconductivity is uniform or localized.

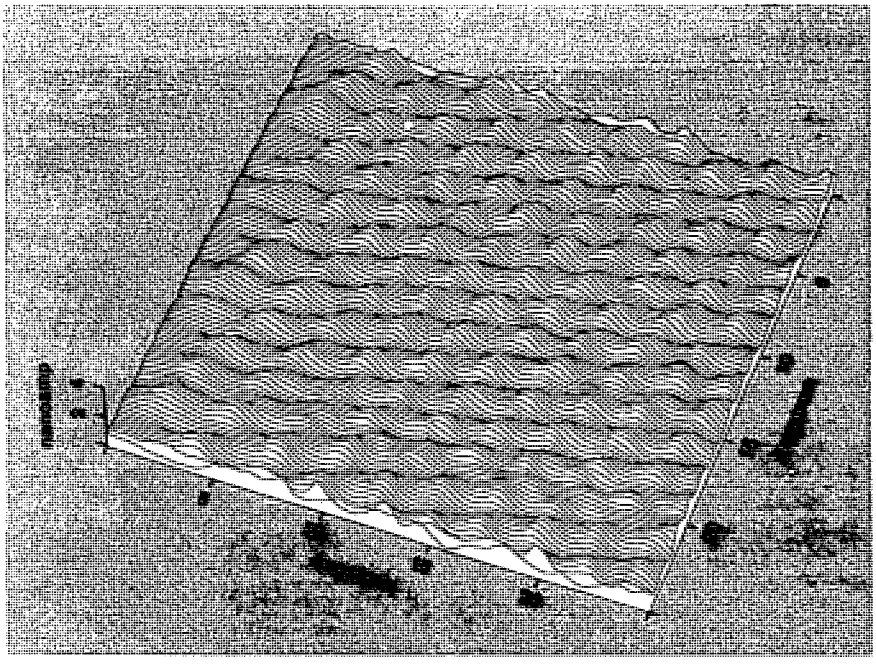

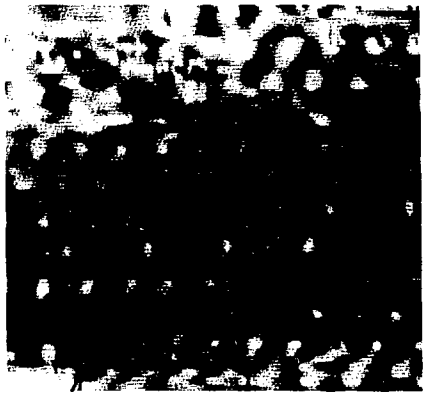

Fig. 2 (*Top*). Topograph of the basal plane surface of pyrolytic graphite.

Fig. 3. STM image, recorded in the barrier-height mode, of a 60- × 30-Å region of ordered sulfur atoms adsorbed onto molybdenum(001).

References

Binnig, G., H. Rohrer, C. Gerber, and E. Weibel (1982), "Surface Studies by Scanning Tunneling Microscopy," *Phys. Rev. Lett.* **49**, 57.

Park, S. and C. F. Quate (1986), "Tunneling Microscopy of Graphite in Air," *Appl. Phys. Lett.* **48**, 112.

FY87: $116,000

New Hamiltonian Lattice-Gauge Theory Computational Scheme

Principal Investigator:
Stewart D. Bloom
Co-Investigators:
Grant J. Mathews and
Neal J. Snyderman

We have carried out mass-gap and string-tension calculations within the Hamiltonian formulation of the SU(2) lattice-gauge theory. Our calculational scheme, carried to higher order than ever before, reproduces the results of Monte Carlo calculations. We have begun to include dynamical quarks in these calculations.

There is a clear need for a fast new computational method for the theory of strong interactions. Monte Carlo calculations in the action formulation of lattice-gauge theories take hundreds of hours of Cray computer time to approach the continuum limit for the pure SU(2) and SU(3) gauge theories. In the full theory with dynamical quarks, these Monte Carlo calculations become hundreds of times more complex.

Special dedicated supercomputers are being built to deal with this well-defined but overwhelming computational problem. As an alternative, the Hamiltonian formulation is in three rather than four dimensions, and we have been able to remove all of the problem's translational redundancy and much of its combinatorial redundancy. Also, in our calculational formulation, adding dynamical quarks to the pure gauge theory increases the calculation's complexity only moderately.

In our formulation, to compute the physical observables we determine only the connected matrix elements of powers of the Hamiltonian with respect to a variational state. With this algorithm, we computed, in the SU(2) lattice-gauge theory, powers of the Hamiltonian up to $\langle H^{12} \rangle$ for the vacuum and $\langle H^{11} \rangle$ for the string tension, two and four powers higher, respectively, than in previous calculations.

Using the more efficient algorithms developed by R. Rainsberger of LLNL, we hope to extend our calculations four higher powers of the Hamiltonian. We are also generalizing the matrix-element code to SU(3).

With dynamical quarks on the lattice, a real test of how well we are actually approaching the continuum limit is to compute the mass of the η' meson. We are now calculating the analogue of this problem in the much simpler massive Schwinger model in one spatial dimension. If this calculation is as successful as the SU(2) gauge field computations were, then we shall have made a significant step toward demonstrating the capability to analyze quantum chromodynamics quantitatively.

References

Hasenfratz, P. (1986), "Nonperturbative Methods in Quantum Field Theory," *Proc. 13th International Conference on High Energy Physics*, Berkeley, Calif., July 1986, p. 169.

Horn, D., M. Karliner, and M. Weinstein (1985), "The t Expansion and SU(2) Lattice Gauge Theory," *Phys. Rev. D* **31**, 2589.

Mathews, G., N. Snyderman, and S. Bloom (1987), "SU(2) Lattice Gauge Theory and the Convergence of the t Expansion," *Phys. Rev. D* **36**, 2553.

Laboratory Simulation of Seismic Wave Propagation at Depth

Principal Investigator:
Brian P. Bonner
Co-Investigator:
David L. Kohlstedt[a]

[a]Cornell University, Ithaca, N.Y.

We are conducting laboratory experiments to study mechanical disturbances equivalent to those caused by a passing seismic wave on refractory silicates at high temperature and pressure. We are simulating conditions in the earth's upper mantle to determine the origin of the low-velocity, high-attenuation zone, one of the earth's dominant seismic features.

Although seismic evidence demonstrating the presence of a region of low velocity and high attenuation in the upper mantle has been available for at least forty years, the origin of the phenomenon remains controversial. The most direct approach to this problem is through laboratory simulations, which have not been done because low-frequency, high-temperature, high-pressure experiments are inherently difficult.

Our project emphasizes upgrading our experimental facility and synthesizing upper-mantle analogue materials. We need to improve the existing facility to produce torsional vibrations (equivalent to seismic shear waves) and to reach the high temperatures (1300°C) required for the relevant simulation. Well-characterized synthetic mantle analogues must be fabricated for the experiments because natural materials include grain-boundary contaminants formed in the near-surface environment that can dramatically alter the velocity and attenuation of seismic waves.

The experimental apparatus is a forced torsional oscillator designed to test samples under simultaneous high-pressure and high-temperature conditions. We extract the seismic properties of the sample by dividing transducer outputs proportional to the torque and twist of the sample, and then compute the time-dependent shear modulus. This year we installed the pressure vessel, developed powder-pressing dies for sample synthesis, constructed a new furnace with molybdenum windings, and fabricated new proximity detectors for high-pressure operation. We obtained test data at atmospheric pressure for polymethylmethacrylate (PMMA), a commercial-grade lucite (see the Figure). We used this polymer in preliminary experiments because its anelastic properties are similar to those inferred from seismic data for upper-mantle rocks.

Our colleagues at Cornell University used the gel precipitation technique to prepare ultrafine grain samples of polycrystalline olivine having negligible porosity, with and without partial melts. We characterized the materials, ideal for our simulation experiments, with electron microscopy and found no grain-boundary contaminants.

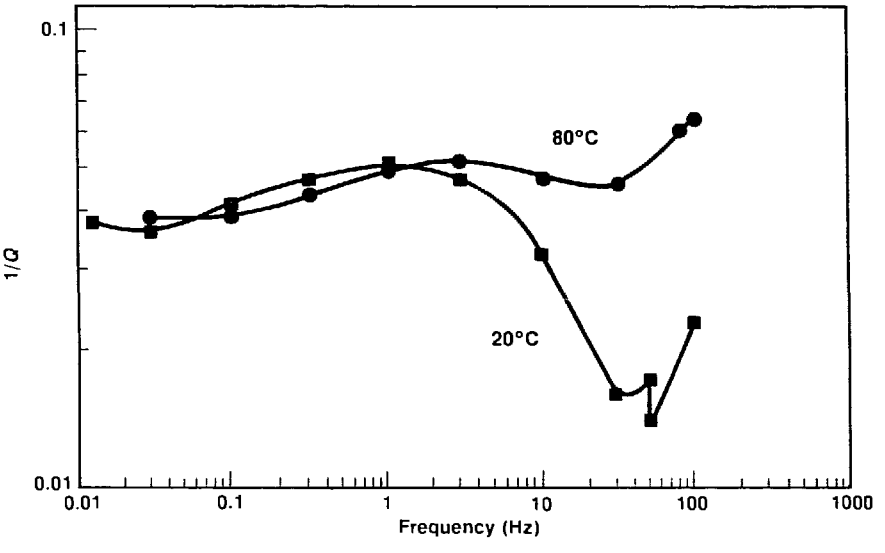

The tangent of the phase angle between applied torque and the resulting twist, $1/Q$ (a measure of mechanical damping) for PMMA as a function of frequency. Increases in damping with temperature are associated with motions of side groups attached to the main polymer backbone.

FY87: $161,000
FY88: $151,000

High-Order Multiphoton Absorption

Principal Investigator:
E. Michael Campbell
Co-Investigators:
Michael D. Perry,
Abraham Szöke, and
Otto Landen

We studied multiphoton ionization of argon, krypton, and xenon at intensities in excess of 10^{14} W/cm^2 using a well-characterized, tunable picosecond dye laser. The laser tunability permitted us to systematically study the influence of intermediate multiphoton resonances on the ionization probability. Experiments on nonresonant multiphoton ionization demonstrated that the production of multiply charged ions occurs via a mechanism of sequential ionization. Results were in excellent agreement with a general theoretical model that includes the effect of the ionic Coulomb field and the intense laser field on the outgoing photoelectron.

Advances in laser technology have resulted in the ability to produce intense electromagnetic fields that approach or even exceed the internal field experienced by outer electrons in rare-gas atoms. A series of experiments performed since 1982 at such intensities has resulted in the observation of unexpected phenomena. The initial observation of the production of multiply charged ions as high as U^{10+} under collisionless conditions demonstrated that large amounts of energy could be efficiently absorbed from an intense laser field by an isolated atom (Luk et al., 1983). Experiments by Kruit et al. (1983) and Bucksbaum et al. (1987) on the nonresonant multiphoton ionization (MPI) of xenon at 1.06 μm dramatically demonstrated the absorption of additional photons beyond the minimum required to ionize the atom. This phenomenon has been named "above-threshold ionization." A series of experiments by Perry et al. (1987) measuring the absolute yield of multiply charged ions in nonresonant MPI as a function of laser intensity demonstrated a weak dependence of the ionization probability on the details of the internal atomic structure. These experiments and several others have shown that lowest-order perturbation theory does not provide an adequate description of MPI at high field strengths.

Such a breakdown of perturbation theory is not surprising. By definition, the application of perturbation theory is not valid when the strength of the perturbation approaches that of the primary interaction. In the experiments cited, the strength of the applied field was a significant fraction of the internal field experienced by the outer atomic electrons. Furthermore, the outgoing photoelectron wave function is substantially modified from the conventional "free" electron wave function by the presence of the intense field. Thus a new approach is required that goes beyond perturbation theory to describe MPI in intense laser fields.

One such theory (Keldysh, 1965) suggests that the "dressing" of the electron with photons from the field plays an important, if not dominant, role in determining the ionization probability. Other researchers have suggested that the excitation of collective oscillation of entire shells of electrons may be responsible for the production of multiply charged ions (Luk et al., 1983).

We have measured the absolute yield of multiply charged ions of argon, krypton, and xenon produced within a well-characterized focal volume as a function of laser intensity. From this work, we were able to provide quantitative data that could be compared directly with emerging theories. We found the Keldysh theory to be in good agreement with the experimental results for the production of only the first charge state of each species. We attribute the breakdown of the Keldysh theory to a neglect of the Coulomb field of the residual ion.

We developed a generalized theory that accounts for the effect of the Coulomb field of the residual ion on the outgoing electron (Perry et al., 1987). Our theory is in excellent agreement with experimental results for the production of even the highest charge states observed (for example, Xe^{8+}) with no adjustable parameters.

The Figure shows the dependence of threshold intensity, defined as the intensity at which ionization probability is 10^{-4}, on the ionization potential of the parent atom or ion. The smooth, monotonic behavior suggests a weak influence of internal atomic structure on the ionization probability.

In another experiment (Landen et al., 1987), we made the first observation of resonant enhancement in MPI at intensities exceeding 10^{13} W/cm^2. Once again, determination of the absolute ion yield within a well-characterized intensity distribution permitted quantitative modeling of the experiment. The results were the extraction of several important atomic parameters for krypton. The parameters include the determination of the optical Stark shift and photoionization cross sections of several of the 4d and 5d excited states.

We have also constructed an experimental station to measure photoelectron energy and angular distributions resulting from MPI. This station will substantially add to our ability to investigate MPI and has already yielded some surprising results.

Our project will continue during FY88 and will include an investigation of a scheme to produce vacuum-ultraviolet stimulated emission using resonantly enhanced MPI and a continued search for evidence of multiply excited states. We also hope to activate a new extreme ultraviolet spectrometer to be used in examining fluorescence resulting from the decay of high-lying atomic states excited by multiphoton absorption.

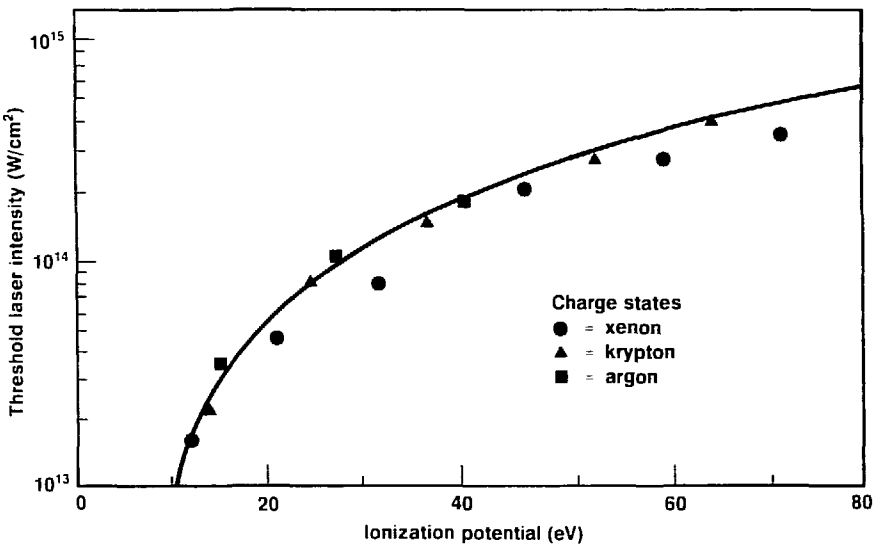

Threshold laser intensity, defined as the intensity at which the ionization probability is 10^{-4}, as a function of ionization potential of a given charge state. The curve is obtained as described by Perry et al. (1987).

References

Bucksbaum, P. H., R. K. Freeman, M. Bashkansky, and T. J. McIlrath (1987). "Role of the Ponderomotive Potential in Above-Threshold Ionization." *J. Opt. Soc. Am. B* **4**, 760.

Keldysh, L. V. (1965). "Ionization in the Field of a Strong Electromagnetic Wave." *Sov. Phys. JETP* **20**, 1307.

Kruit, P., J. Kimman, H. G. Muller, and M. J. van der Viel (1983). "Electron Spectra from Multiphoton Ionization of Xe at 1064 and 532 nm." *Phys. Rev. A* **28**, 248.

Landen, O. L., M. D. Perry, and E. M. Campbell (1987). "Resonant Multiphoton Ionization of Krypton by Intense UV Laser Radiation." *Phys. Rev. Lett.* **59**, 2558.

Luk, T. S., H. Plummer, K. Boyer, M. Sahidi, H. Egger, and C. K. Rhodes (1983). "Anomalous Collision-Free Multiple Ionization of Atoms with Intense Picosecond UV Radiation." *Phys. Rev. Lett.* **51**, 110.

Perry, M. D., O. L. Landen, A. Szöke, and E. M. Campbell (1987). "Multiphoton Ionization of the Noble Gases by an Intense (10^{14} W/cm^2) Dye Laser." *Phys. Rev. A* **37** (in press).

Perry, M. D., A. Szöke, O. Landen, and E. M. Campbell (1987). *Nonresident Multiphoton Ionization: Theory and Experiment*. Lawrence Livermore National Laboratory, Livermore, Calif., UCRL-96943.

Nonlinear Instabilities in Line-Driven Stellar Winds

Principal Investigator:
John I. Castor
Co-Investigators:
Stanley P. Owocki[a] and
George B. Rybicki[b]

[a]University of California, San Diego.
[b]Harvard-Smithsonian Center for Astrophysics, Cambridge, Mass.

We studied the nonlinear growth of instabilities in a radiatively driven stellar wind using numerical hydrodynamics and analytic theory. Our goal was to learn about the nonlinear structures that result from the known, violent instability of stellar winds and to explain the observations of x-ray emission in terms of shocks.

Our major focus was to construct a code to calculate the hydrodynamics of a stellar wind, taking into account the important body force on wind material due to absorption and scattering of radiation by an ensemble of resonance lines. This body force dominates the force due to gas pressure and is sensitive to the flow velocity owing to Doppler-effect corrections to spectral line transfer. The response of the force to variations in velocity causes the wind instability.

We have made hydrodynamic calculations with different approximations for the radiation force. The simplest is the Sobolev approximation, which is a dependence on only the local velocity gradient. Another is the absorption approximation, in which only the momentum transferred to matter at the first photon scattering is counted in the force, as if photons were then absorbed. The wind is known to be unstable in this approximation, as supported by numerical results.

Our computational results indicate that the situation in the nonlinear regime may be more complex. If stellar wind structure is modeled to approximate the steady-state structure, then further evolution indicates stability. However, natural evolution from an arbitrary initial state appears never to attain the steady state, but shows a quasiperiodic behavior in which a train of waves continually passes through the wind. The waves are generated as small-amplitude oscillations near the sonic point of the flow, the origin of which is unclear.

In a real star, many mechanisms can produce small-amplitude motions near the stellar photosphere; thus, the waves shown by our simulations are certain to exist. In other simulations, we applied small-amplitude waves explicitly as a boundary condition. Our results were similar to those without such wave input, supporting our conclusion concerning robustness of the wave phenomena.

Nonlinear development of the waves leads to the formation of shock waves and a general kinematic picture that is in accord with most inferences made from observations of the winds of hot stars. Our remaining quantitative questions stem from two uncertainties: the actual wave amplitude that depends on the source of excitation and the effect of temperature scaling required for a feasible simulation. We require more computational resources before addressing the major question concerning the effect of the absorption approximation.

References

Castor, J. I., S. P. Owocki, and G. B. Rybicki (1987), "Mass Loss from Pulsation Hot Stars With and Without Radiative Driving," *Proc. 1987 Trieste Workshop on Pulsation and Mass Loss in Stars*, L. A. Willson and R. J. Stalio, Eds. (Reidel Publishing Co., Dordrecht, Netherlands).

Owocki, S. P., J. I. Castor, and G. B. Rybicki (1987), "Nonlinear Dynamics of Instabilities in Line-Driven Stellar Winds," *Instabilities in Luminous Early-Type Stars*, H. J. Lamers and C. W. deLoore, Eds. (Reidel Publishing Co., Dordrecht, Netherlands), p. 269.

Owocki, S. P., J. I. Castor, and G. B. Rybicki (1987), "Shock Formation from the Nonlinear Evolution of Instabilities in Line-Driven Stellar Winds," *Bull. Am. Astron. Soc.*, **19**, 703.

Owocki, S. P., J. I. Castor, and G. B. Rybicki (1986), "A Time-Dependent Line-Driven Wind Model Not Based on the Sobolev Approximation," *Bull. Am. Astron. Soc.*, **18**, 953.

FY87 $102,000

Implicit Particle Simulation of Velocity-Space Transport and Electric Potentials in Magnetized Plasmas

Principal Investigator:
Bruce I. Cohen
Co-Investigators: Alex Friedman, Charles K. Birdsall,[a] Edward Morse,[a] Richard Procassini,[a] and Julian C. Cummings[a]

[a]University of California, Berkeley.

We developed a one-dimensional, implicit, particle-simulation code incorporating binary Coulomb collisions, wave heating, ionization, and charge exchange to simulate velocity-space transport and electric potentials in magnetized plasmas. This new simulation tool addresses long transport times and is an efficient alternative to Fokker-Planck codes that have intrinsic limits on flexibility in applications to complex configurations.

Our goal was to perform self-consistent computer simulations of both velocity-space transport and the evolution of the plasma electric potential. To do so in an efficient manner, we combined relativistic, implicit, particle simulation with optimized Monte Carlo methods. The new simulation tool, TESS, is a flexible and efficient alternative to Fokker-Planck codes widely used in plasma physics. Our simulation model is particularly suited to many magnetic fusion configurations and will be applied first to the study of electrostatic end plugging and the formation of electrostatic thermal barriers in tandem mirrors.

TESS is characterized by:

- Relativistic, implicit particle simulation.
- Multispecies, self-consistent, shielded Coulomb collisions.
- An arbitrary, complex, multiregion domain in configuration space.
- Simulation of all important axial physics in a tandem mirror device. The model includes end loss, magnetic mirrors, wave heating, ionization, charge exchange, and electrostatic plugging.

We embedded TESS in the Basis computing system (Dubois and Moteller, 1987), tested the code implementation of special relativity, coded and tested the quasilinear model of electron and ion cyclotron heating, and coded and tested the charge exchange and ionization subroutines. We also added necessary memory management and bookkeeping to account for particle sources and losses. We have now completed testing and begun substantial physics applications.

We compared the results of wave heating studies in TESS to those obtained in the existing MCPAT Monte Carlo code (Rognlien, 1983) and have begun simulations of a simple mirror and a wave-heated tandem mirror. We also identified and scoped out for near-term action a benchmark test comparing TESS with the SMOKE Fokker-Planck code (Matsuda and Stewart, 1986). Our work will continue under the auspices of M Division and the Plasma Physics Research Institute at LLNL and with the theory and particle simulation group of the Electrical Engineering and Computer Science Department at the University of California, Berkeley.

References

Dubois, P. F. and Z. C. Moteller (1987), *Basis User's Manual*, Lawrence Livermore National Laboratory, Livermore, Calif., M-189.

Friedman, A., A. B. Langdon, and B. I. Cohen (1981), "A Direct Method for Implicit Particle-in-Cell Simulation," *Comments Plasma Phys. Contr. Fusion* **6**, 225.

Matsuda, Y. and J. J. Stewart (1986), "A Relativistic Bounce-Averaged Fokker-Planck Code for Mirror Plasmas," *J. Comp. Phys.* **66**, 197.

Rognlien, T. D. (1983), "Frequency Splitting and Collisional De-Correlation for Removing Superadiabatic Barriers in ECRH Experiments," *Nucl. Fusion* **23**, 163.

FY87: $105,000

Ion-Molecule Reactions for Enhanced Selectivity in Chemical Analysis

Principal Investigators:
Richard W. Crawford,
Thomas T. Coburn, and
Philip E. Miller

We increased the specificity of triple quadrupole mass spectrometry by using three types of ion-molecule reactions. The reactions were applied to the determination of ammonia using proton exchange and of carbon monoxide using charge exchange in real time in a complex mixture. We identified reactions using addition formation, thought to be specific to classes of oxygen-containing compounds.

Triple quadrupole mass spectrometry (TQMS) is one of the most specific instruments for analysis of complex mixtures. TQMS is a form of tandem mass spectrometry in which ions are mass-selected in the first analyzer. Selected ions enter a collision cell, and the product ions from collision are scanned by a second analyzer. However, the TQMS technique becomes less specific when applied to small molecules (with molecular weights less than 50). Several small molecules, such as ammonia (NH_3) and carbon monoxide (CO), are critical to understanding the chemistry of fossil-fuel pyrolysis.

Our objective was to explore several classes of ion-molecule reactions as a method for increasing the selectivity of TQMS. In particular, we studied specific ion-molecule reactions employing proton exchange, charge exchange, and adduct formation as alternatives to the method of collisionally activated dissociation classically used in TQMS.

We have completed the development of methods for detecting and determining low levels of NH_3 in the presence of steam and hydrocarbons (Crawford et al., 1987; Oh et al., 1987). We used isobutane as a proton-transfer agent to preferentially ionize ammonia by forming NH_4^+. The isobaric interference from water is minimal because water ionizes primarily to form H_3O^+. We applied this technique to the determination of NH_3 during the pyrolysis of a variety of oil shales, tar sands, and buddingtonite, which is a nitrogen-containing mineral.

We developed a charge-exchange method for the determination of CO in the presence of nitrogen and hydrocarbon isobaric interferences. By selecting the proper collision gas, CO^+ preferentially charge-exchanges with that gas, and the collision gas ion is detected. This technique is now routinely used for the determination of CO evolution kinetics during pyrolysis of oil shales, tar sands, and coals.

We also explored the formation of reactive gases that are selective for specific functional groups by using reactants with the potential for adduct formation. Oxygen-containing species are of particular interest in the pyrolysis of polymers and fossil fuels. We found that addition products are generally favored over adducts because the collision between ion and reactive gas imparts excess energy to an intermediate that can be lost only by fragmentation. For example, when the acetone ion collides with iodobenzene, neutral water and HI fragments are formed, leaving the allylbenzene ion. Using iodobenzene as the reactive collision gas, we formed addition products with ketones, a cyclic ether, alcohols, and thiophene (sulfur heterocycle). Water and HI were stable neutral fragments. Products were not formed with acetates, straight-chain ethers, trimethylamine, or methyl acetamide. We obtained similar results using iodine in place of iodobenzene as the collision gas. Such information will allow us to detect certain homologous series with specific functional groups in a complex mixture.

References

Crawford, R. W., T. T. Coburn, P. E. Miller, and M. S. Oh (1987), "Isobutane CI for On-Line Determination of Ammonia from Oil Shale," *Proc. Thirty-Fifth ASMS Conf. Mass Spectrosc. Allied Topics* (ASMS, East Lansing, Mich.), p. 977; to be published in *Fossil Fuel Analysis by Mass Spectroscopy*.

Oh, M. S., R. W. Taylor, T. T. Coburn, and R. W. Crawford (1987), *Ammonia Evolution during Oil Shale Pyrolysis*, Lawrence Livermore National Laboratory, Livermore, Calif., UCRL-95618; to be published in *Energy and Fuels*.

FY87: $30,000

Neutrinos, Elementary Particles, and Their Consequences

Models in high-energy particle physics predict a variety of unobserved elementary particles. We explored the conditions for which the existence of such particles lead to a conflict with observed astronomical phenomena.

Principal Investigator:
David S. Dearborn

The current constraints on elementary particles are based on the success of stellar evolution theory to explain the broad range of behavior observed in stars. In particular, the observed violation of charge-parity conservation can be explained by postulating the existence of a particle called an axion. While some such particle is indeed likely to exist, theory contributes little to our knowledge of its properties, couplings, and strengths. Unlike axions, neutrinos are weakly interacting elementary particles that are known to exist. The well-known problem concerning the solar neutrino flux requires only a 4% drop in the central temperature of a star for a solution. Such findings are indicative of the accuracy with which stars are now modeled.

We developed a code that is capable of reproducing the standard solar model formulated by Bachall and Ulrich. We used this code to study the uncertainties due to the equation of state and opacity. We then explored the implication of these uncertainties on the parameter space necessary for resonant neutrino oscillations to resolve the neutrino problem.

We also examined the effect of strengths of various couplings, such as the axion-photon coupling, on the evolution of stellar models. Although previous attempts have been made to set astrophysical limits, those efforts were based on finding conditions where axions would affect stars, but not necessarily conflict with observed behavior. We set our astrophysical limits by comparing the calculations, with axions included, to the observed luminosity function of clusters. We also calibrated the results of earlier papers to determine the true limit.

Our future work will be directed toward improving our ability to numerically model stars. Within this framework, we will search for more restrictive astrophysical tests of the properties of elementary particles.

References

Dearborn, D., G. Marx, and I. Ruff (1987), "A Classical Solution to the Solar Neutrino Problem," *Prog. Theor. Phys.* 77, 2.

Raffelt, G. and D. Dearborn (1987), "Bounds on Hadronic Axions from Stellar Evolution," *Phys. Rev. D* (in press).

Raffelt, G. and D. Dearborn (1987), "Bounds on Weakly Interacting Particles from Observational Lifetimes of Helium-Burning Stars," *Phys. Rev. D* (in press).

FY87 $140,000
FY88 $70,000

Doppler-Free Spectroscopy of Multiply Charged Ions Using Recoil Ion Sources

Our aim was to demonstrate experimentally a new and promising technique of Doppler-free spectroscopy for multiply charged ions. We designed, constructed, and tested the gas target cell and high-resolution crystal spectrometer to be used in experiments at the Lawrence Berkeley Laboratory Super HILAC accelerator.

Principal Investigator:
Daniel D. Dietrich
Co-Investigators:
Chris T. Chantler,[a]
William A. Hallet,[a]
J. Martin Laming,[a] and
Joshua D. Silver[a]

[a]University of Oxford, England.

Our major objective is to demonstrate the ability to obtain spectra of multiply charged ions, which are limited only by the inherent properties of the diffraction crystals that are used. We selected as reference lines the resonant lines in one- and two-electron argon. These transitions have been previously measured, with Doppler broadening as the limitation, in a recoil ion source with a resolution $\lambda/\Delta\lambda$ of approximately 2800, where it was necessary to carefully model satellite line intensities to extract an absolute wavelength accuracy of 5 parts per million. This result gives a 1.5% test of the ground-state ($1s_{1/2}$) Lamb shift and is currently the most accurate measurement of any high-Z Lamb shift. Improving the instrumental resolution by one order of magnitude will decrease the uncertainties in the Lamb shift by more than one order of magnitude. The latter improvement arises because resolving more satellites will simultaneously simplify the line shape and provide more constraints on the model used to predict any remaining unresolved satellite line intensities.

We will perform our measurements at the Lawrence Berkeley Laboratory (LBL) Super HILAC accelerator using the intense uranium beam. The experiment will measure the x-ray spectra of recoil ions produced in a cell filled with argon gas by observing the hydrogenic Lyman α radiation along the beam axis. Because the atoms in the gas cell are lighter than uranium, the ions recoil primarily at 90° to the direction of the incident beam. The low velocity of the recoil ions, coupled with observations that are orthogonal to their motion, results in spectra that are essentially free of Doppler broadening.

During the first year of our two-year award, we developed and tested a gas cell and a spectrometer. We tested both components during separate experiments performed at the University of Oxford tandem accelerator. The Figure shows our experimental arrangement for the recoil ion experiment. We used an 81-MeV Br^{5+} beam from the Oxford tandem accelerator to bombard neon gas. We observed the $1s^2\,{}^1S_0 \rightarrow 1s2p\,{}^1P$ transition in helium-like neon with a KAP crystal. The resolution was limited by this crystal spectrometer. A spectrometer with much better resolution has been built and tested for use with the much shorter wavelengths from an argon recoil source; however, we need the 1-GeV U^{40+} beams available at the LBL Super HILAC accelerator to produce usable amounts of hydrogen and helium-like argon. We were granted six days of beam time at the LBL Super HILAC accelerator by the Physics Advisory Committee and scheduled our experiment for late 1987.

Tandem accelerators produce heavy ions, such as bromine ions, at energies far below the Coulomb

barrier for nuclear interactions. However, the Super HILAC can produce uranium ions at energies above the Coulomb barrier. The resulting nuclear interactions will produce a significant quantity of neutrons and minimum ionizing radiation, which will be sources of noise in our detectors. Therefore, most of our efforts in initial experiments will be aimed at optimizing beam energy, gas-cell pressures, and window conditions. We will schedule subsequent experiments in early 1988 to perform actual measurements on the Lyman α radiation (2p → 1s) in argon to provide the first test of our technique.

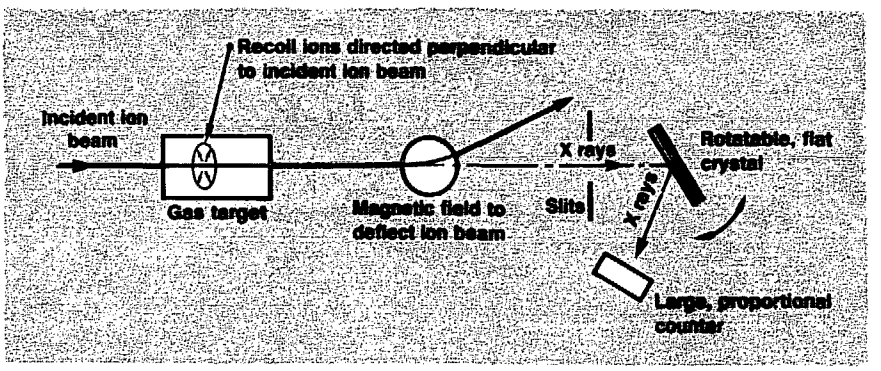

Experimental setup for longitudinal observation of x rays from recoil ions produced by bombardment with a highly charged, heavy-ion beam.

The Search for Quark Phenomena in Atomic Nuclei

Principal Investigator:
Frank S. Dietrich
Co-Investigator:
Karl A. Van Bibber

Using the time-projection chamber (TPC) in the Positron Electron Project (PEP) storage ring at the Stanford Linear Accelerator Center (SLAC), we completed a pilot experiment on the interaction of 14.5-GeV electrons with nuclei. On this experience, we based a preliminary design for a dedicated nuclear physics facility at PEP and outlined the physics program to be performed with it.

We have begun a program to observe the many particles that emerge when high-energy electrons scatter from nuclear targets. Under certain conditions, deep inelastic scattering transfers all the energy and momentum from an incident electron to a single quark in the target nucleus. We expect such experiments to yield fundamental information on how quarks propagate through nuclear matter and on the mechanism by which an energetic quark turns into a jet of observable particles. PEP's electron beam can have any energy from 6 to 15 GeV, an ideal capability for such studies. The other requirement is an ultrathin (gas-jet) target.

To glimpse the types of events obtainable, we performed a short test run at SLAC's existing TPC detector facility, using a simple gas-injection target. With colleagues from other institutions, we organized the Workshop on Electronuclear Physics with Internal Targets in January 1987. Here we reported the results of this experiment. We also formed a collaboration among about 30 scientists from 12 institutions to plan and carry out a nuclear physics program at PEP.

We have assumed responsibility for designing the gas-jet target and are now measuring density profiles in an existing supersonic jet target. We acquired a computer code that models particle production in deep inelastic scattering and used its predictions to optimize the spectrometer design (shown in the Figure with a typical computer-modeled nuclear event).

In this experiment, a large-angle magnetic spectrometer downstream of the target measures momenta of the scattered electrons and of the energetic secondary particles associated with the struck quark. In addition, neutron detectors and solid-state-detector telescopes for nuclear fragments will help us analyze how the target nucleus responds to a deep-inelastic-scattering reaction on one of its constituent nucleons. A proposal to construct this facility will be submitted to the Department of Energy in early 1988.

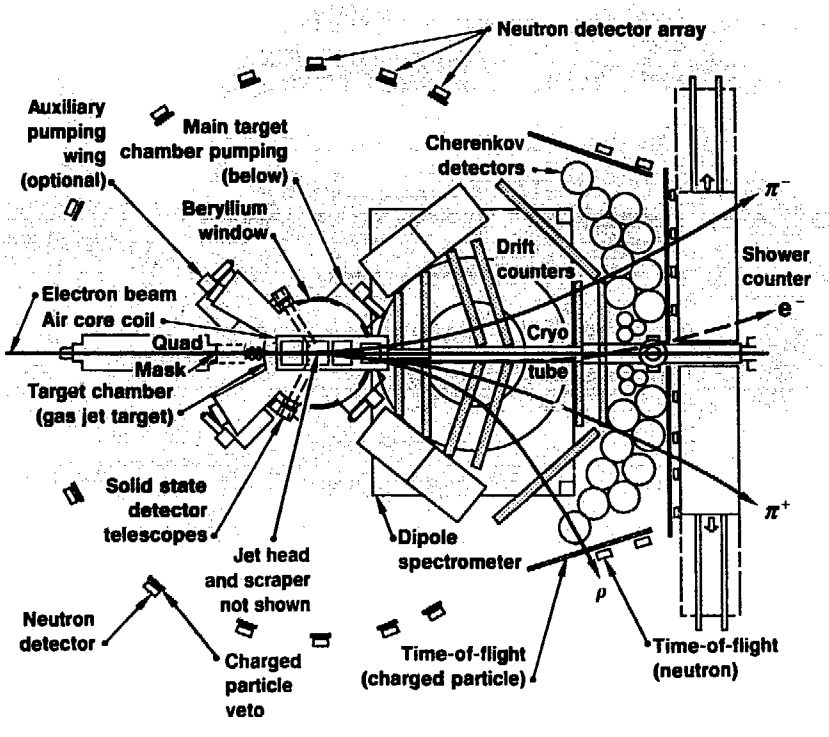

Sketch of the proposed nuclear physics facility for the PEP electron-storage ring showing particle trajectories in a typical event (ρ-meson production from a proton target).

Reference

Melnikoff, S. O. (1987). "Nuclear Physics at PEP: Recent Results Using the Time Projection Chamber." *Proc. Workshop on Electronuclear Physics with Internal Targets*, SLAC Rept. 316, p. 111.

Atomic Physics Studies at the LBL ECRIS

We have built a low-energy beamline at the Lawrence Berkeley Laboratory (LBL) electron cyclotron resonance ion source (ECRIS) so that we can measure cross sections for electron impact excitation in multiply charged ions.

Principal Investigator:
Patrick O. Egan
Co-Investigators:
Sophie Chantrenne and
Michael H. Prior[a]

[a]Lawrence Berkeley Laboratory, Berkeley, Calif.

Electron-impact excitation in highly charged ions is a key process in many of the high-temperature plasmas we study, but there are almost no experimental data on excitation cross sections for such ions. To fill this need, we have built a low-energy atomic-physics beamline onto the high-current ECRIS at LBL's 88-in. cyclotron. We will measure the cross sections with a new type of instrument, a merged-beam, electron-energy-loss spectrometer (EELS) that we have developed, built, and commissioned.

Our EELS spectrometer (see the Figure) uses trochoidal analyzers (crossed electric and magnetic fields) to merge an electron beam of known energy (30 to 500 eV) with the beam of highly charged ions from the ECRIS and then analyzes the emerging electrons to determine what proportion have transferred energy to (i.e., excited) the charged ions and how much energy they lost in the process. This mode of operation makes our spectrometer (EELS) sensitive to all transitions, whether optically allowed or forbidden. The long merged-beam interaction region and the use of a position-sensitive detector give this spectrometer more sensitivity than more conventional techniques used for singly ionized systems.

We have finished building the EELS spectrometer and are now testing it. In FY88, after installing it at Berkeley, we plan to complete a first sequence of experimental measurements on eight-times ionized argon (Ar^{+8}).

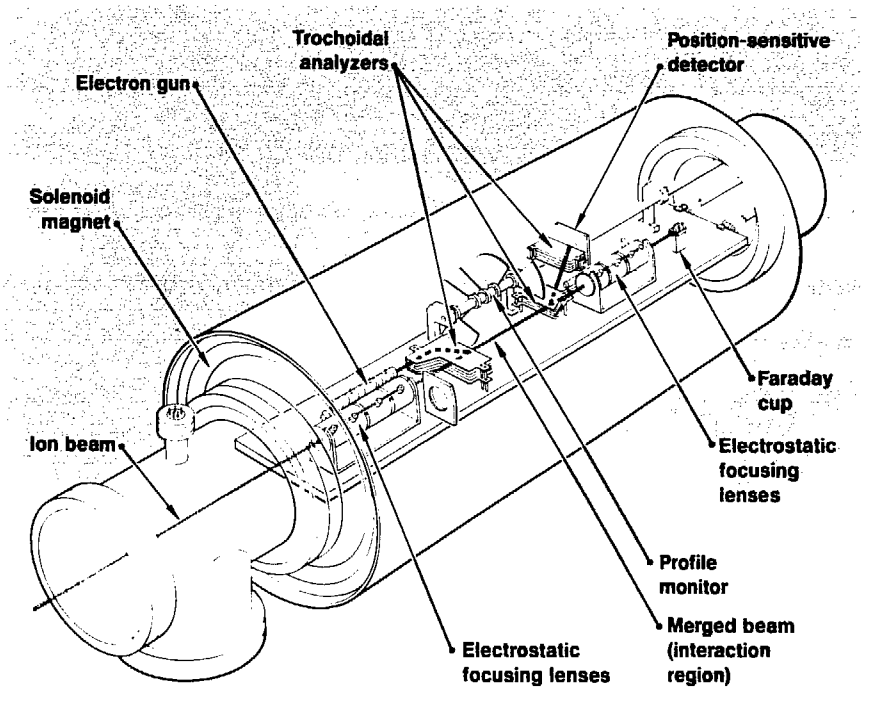

The electron-energy-loss spectrometer (EELS). A trochoidal analyzer merges the beam from an electron gun with the ion beam from the ECRIS. Another analyzer extracts the electrons, and a position-sensitive detector records those that lost energy by exciting ions in the beam.

The Search for Quantum Chaos

Principal Investigators:
Michael D. Feit and
Stewart D. Bloom

We are looking for possible chaotic (unpredictable) behavior at a subatomic level where processes are governed by quantum mechanics.

Long-range weather forecasts turn out to be unattainable, not because we lack computer power or proper initial measurements, but because the underlying phenomena are chaotic (i.e., unpredictable in practice). In chaotic phenomena (e.g., weather, earthquakes, the stock market), insignificant events can trigger processes that build up with time, ruining the forecast. The question is, can such unexpected behavior also occur in the subatomic realm? To find out, we are studying chaotic behavior in processes governed by quantum mechanics.

To look for chaotic behavior in a macroscopic process, one follows the fate of two particles that started out side by side to see how far apart they get as time goes on. If they diverge exponentially, the rate (known as the Liapunov index) helps to define regions of stability and chaos within a process's parameter space. We are seeking to define a quantum equivalent to the Liapunov index.

To do this, we converted a system of codes (VLADI), originally used for shell-model calculations in atomic and nuclear physics, to the study of nonlinear, coupled systems in many dimensions and tested it against previous two-dimensional calculations (Feit and Fleck, 1984). We have also generalized the VLADI code to three dimensions and made a preliminary study of a three-dimensional system of coupled oscillators using a cyclic coupling via the nonlinear Henon-Heiles potential (Benettin et al., 1976), which has been studied in two dimensions, both classically and quantum mechanically. Both cases yield visual qualitative evidence of chaotic behavior in the way bound orbits evolve with time.

We are presently setting up to calculate the quantum Liapunov indices using three-dimensional quantum orbits in the energy range of the previously calculated classical orbits. These results should help us understand the correspondence between quantum and classical deterministic chaos.

References

Benettin, G., L. Galgani, and J. Strelcyn (1976), "Kolmogrov Entropy and Numerical Experiments," *Phys. Rev. A* **14**, 2338; also see references therein.

Feit, M. D. and J. A. Fleck, Jr. (1984), "Wave-Packet Dynamics and Chaos in the Henon-Heiles System," *J. Chem. Phys.* **80**, 2578.

Calculation of Alloy Phase Diagrams from First Principles

Principal Investigator:
Michael J. Fluss
Co-Investigators:
Patrice E. A. Turchi and
Didier de Fontaine[a]

[a]University of California, Berkeley.

Last year, for the first time, we developed methods for calculating alloy phase diagrams from first principles. These ab initio calculations provide the experimentalist with information that, earlier, could only be obtained in the laboratory. Our methods now extend to noncoherent phase diagrams, in particular those involving fcc and bcc crystalline structures. We also investigated the possibility that various ordered states occur in complex structures.

The task of calculating alloy phase diagrams from first principles is both practical and challenging: practical because the study of alloy properties depends critically on the relevant phase diagrams and challenging because such calculations must accurately combine quantum-mechanical and statistical thermodynamic contributions. The methods we developed to perform these calculations can be compared advantageously with experiments such as photoemission, Compton scattering, and positron annihilation.

Our approach was to adapt the Generalized Perturbation Method (GPM) to a first-principles model of electronic band structure, namely the Korringa-Kohn-Rostoker-Coherent Potential Approximation (KKR-CPA). In the case of complex crystalline structures, the GPM was adapted to the Tight Binding Approximation (TBA-CPA). Both models lead to the calculation of the concentration-dependent effective cluster interactions that make up the configurational part of an alloy's total energy. We then used the band-structure results in a statistical model—the Cluster Variation Method (CVM)—to obtain the phase diagram of a given alloy system and its related thermodynamic properties. Therefore, starting with the simple knowledge of the number of electrons for each alloy constituent, we can deduce the stability properties at temperature $T = 0$ K and the thermodynamic quantities at $T \neq 0$ K.

It is commonly assumed that complex structures can have only one ordered phase. But preliminary studies of the ground states of the Ising model for the A15 crystalline structure indicate that several ordered phases can exist. We have begun to investigate their stability properties and have developed CVM models to compute phase diagrams involving them.

We also investigated noncoherent phase diagrams. Using the simplest TBA-CPA-CVM scheme, we studied the thermodynamic properties of a transition-metal binary alloy exhibiting fcc and bcc solid-solution phases and ordered intermetallic-compound phases. The prototype system chosen for this study was Ti-Rh (or Ti-Ir). We obtained good agreement with experiment. The resulting phase diagram shows that stable and metastable phase equilibria in this class of binary systems can be understood on the basis of competition between fcc and bcc solid-solution tendencies, each lattice contributing its own set of ordered superstructures (see the Figure).

We used the KKR-CPA-GPM approach to make detailed band structure calculations on Pd-V, Pd-Rh, and Ni-Al systems. These led to stability properties at $T = 0$ K that are in good agreement with experimental results. The GPM was also used to determine the specific competition between ordered $L1_2$ and DO_{22} states and to estimate antiphase boundary energy, which is, in the case of Ni_3Al, in good agreement with the experimental value.

Our plans for FY88 call for

- Studies of multicomponent and magnetic alloy systems.
- Experiments with the model systems used in our calculations to measure the momentum densities of annihilating electron-positron pairs. We will compare the results of these experiments with those obtained from our calculations.

References

Howell, R. H., P. Meyer, I. J. Rosenberg, and M. J. Fluss (1985), "Two-Dimensional Electron-Positron Momentum Measurements at a Copper Single-Crystal Surface," *Phys. Rev. Lett.* **54**, 1698.

Sluiter, M., P. E. A. Turchi, F. Zezhong, and D. de Fontaine (1987), "Tight Binding Calculation of Ti-Rh Type Phase Diagram," *Phys. Rev. Lett.* (in press).

Stocks, G. M., D. M. Nicholson, F. J. Pinski, W. M. Butler, P. Sterne, W. M. Temmerman, B. L. Gyorffy, D. D. Johnson, A. Gonis, X. G. Zhang, and P. E. A. Turchi (1987), "Ab Initio Theory of the Ground State Properties of Ordered and Disordered Alloys and the Theory of Ordering Processes in Alloys," *Proceedings of the Material Research Society Symposium* **81**, 15.

Turchi, P. E. A., A. Gonis, X. G. Zhang, and G. M. Stocks (1987), *Configurational Energies in Terms of Effective Cluster Interactions in Binary Substitutional Alloys: Connection Between the Embedded Cluster Method and the Generalized Perturbation Method*, Lawrence Livermore National Laboratory, Livermore, Calif., UCRL-96787.

Turchi, P. E. A., G. M. Stocks, W. H. Butler, D. M. Nicholson, and A. Gonis (1987), *First Principles Study of Ordering Properties of Substitutional Alloys Using the Generalized Perturbation Method*, Lawrence Livermore National Laboratory, Livermore, Calif., UCRL-96786.

Turchi, P. E. A., M. Sluiter, and D. de Fontaine (1987), "Prototype fcc-Based Binary Alloy Phase Diagrams from Tight Binding Electronic Structure Calculations," *Phys. Rev. B* **36**, 3161.

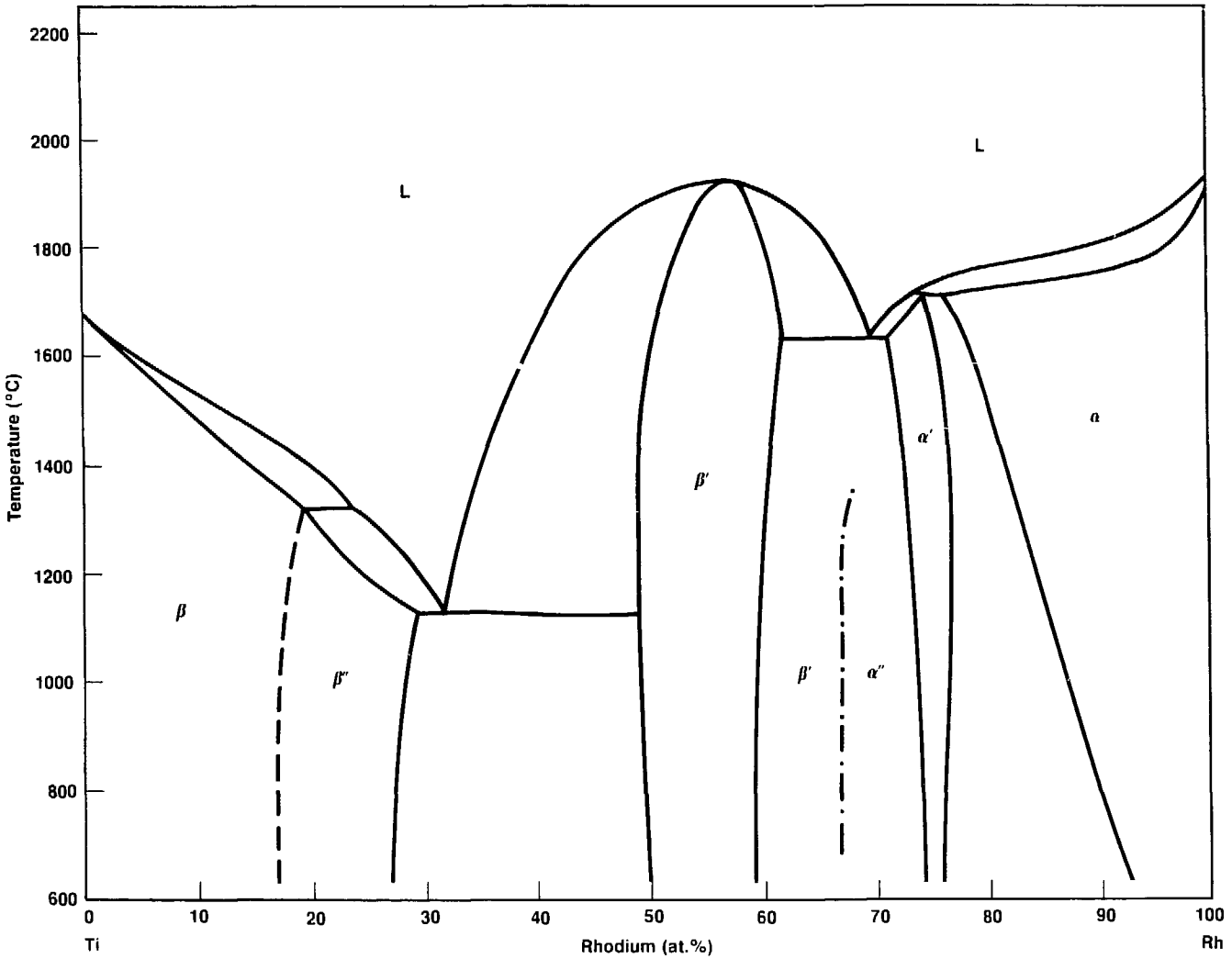

Calculated phase diagram for a Ti-Rh-like binary system. The phases are: L = liquid, α = fcc (solid solution), α′ = LI_2 (ordered phase), α″ = LI_0 (metastable ordered phase), β = bcc (solid solution), β′, β″ = B2 (ordered phase).

Petrologic, Isotopic, and Chemical Modification of Deep Continental Crust

Principal Investigators:
William Glassley,
Sidney Niemeyer,
Frederick J. Ryerson, and
Henry F. Shaw

We investigated how fluids control the chemical, isotopic, and petrologic characteristics of rocks 20 to 30 km deep in the earth. In order to establish mechanisms that influence crustal evolution, we must identify the source of these fluids and their effect on the continental crust. In rock samples from Sri Lanka, we identified the source and composition of these fluids, the effect the fluids had on the crust, and the mechanisms responsible for the observed effects.

The role fluids play in the evolution of deep (>15 km) continental crust has been difficult to establish because good exposures of such terrains at the earth's surface are rare. The earth's mantle could be the source of such fluids, but significant transfer of mass from the mantle to the crust would be required. Debate persists about the chemical and isotopic effects such fluids would have crustal material. It is difficult to rigorously evaluate the source, volume, and composition of fluids that may be derived from the mantle and may have interacted with continental crust.

To resolve these issues, we studied well-exposed deep crustal material in Sri Lanka. We were specifically interested in identifying the source, composition, and chemical and isotopic effects of the fluid in deep crustal material.

In addition to field relationships, chemical and isotopic data demonstrate that fluid which interacted with the deep crustal rocks was rich in carbon (primarily as CO_2 but also with significant CH_4). In some cases, fluids passing through the rocks deposited graphite, leading to dehydration reactions that produce pyroxenes from biotite and hornblende. Chemical changes include enrichment of U, Th, and La in the pyroxene-bearing rocks. Isotopic redistribution in Rb-Sr, Sm-Nd, and K-Ar systems was limited to small regions associated with formation of the pyroxene-bearing assemblages. The source of the carbon-rich fluid was marble, which released the fluid during decarbonation reactions at high temperature. Little evidence supports the view that mantle degassing contributed the fluid to the crust in this area. A model for fluid genesis within the crust is consistent with the observations.

References

Glassley, W. E., F. J. Ryerson, H. Shaw, and S. Niemeyer (1987). "Mineral Stability and Element Mobility in Fluid-Bearing Systems under Deep Crustal Conditions." *NATO Advanced Study*, D. Bridgwater, Ed. (Reidel Publishing Co., Dordrecht, Netherlands).

Glassley, W. E., H. Shaw, F. J. Ryerson, S. Niemeyer, and P. B. Abeysinghe (1986). "Marble-Derived Carbon-Rich Fluids and Amphibolite to Granulite Transformation: Field and Laboratory Evidence from Sri Lanka." *Trans. Am. Geophys. Union* **67**, 1256.

Shaw, H., S. Niemeyer, W. Glassley, F. J. Ryerson, and P. B. Abeysinghe (1987). "Isotopic and Trace Element Systematics of the Amphibolite to Granulite Facies Transition in the Highland Series of Sri Lanka." *Trans. Am. Geophys. Union* **46**, 464.

Laser Interactions with Positrons and Positronium Bound to Solids

Principal Investigator:
Richard H. Howell
Co-Investigators:
Klaus-Peter Ziock
and Frank Magnotta

We conducted experiments on metallic and insulating samples to investigate the positron surface interaction and to determine the nature of the mechanism that binds positrons to material surfaces. We obtained complete data on the emission of positrons and positronium from alkali-halide crystals. We also observed a new photon-surface effect while searching for photodesorbed positrons.

Describing the positron-surface interaction and particularly the mechanism for binding positrons to a surface is a significant theoretical problem requiring a full account of the many-body electron-positron correlation. To provide new data on that interaction, we are studying the photon desorption of positrons from a metallic surface by synchronizing the light pulses from an excimer laser with the intense, pulsed positron beam at the LLNL 100-MeV electron linac. We developed a new vacuum chamber with new positron diagnostics to detect the results of the photon-interaction experiments and to obtain better basic positron data.

With this system we were able to record changes in the amount and energy of positrons or positronium for each positron beam pulse. With metallic samples, there was no evidence of single-photon desorption contributing to increased emission of either positrons or positronium. Since the upper limit set by these data is well below estimates based on simple potential-well descriptions of the positron surface binding, a better theoretical description of positron surface binding is needed.

The new effect we found, which could only be observed easily with positrons, involved a large change (about -0.4 eV) in the negative positron work function when the surface was irradiated with laser light. There was no corresponding change in the positronium energy.

The positron interaction in insulating materials is more complicated and incompletely understood. We have surveyed the emission properties of several alkali-halide insulators with wide band gaps. We observed the formation and diffusion of positronium and determined the deformation potential for these materials. Similar measurements planned for solid rare gases were delayed due to difficulties in delivery of a displex helium refrigerator.

References

Howell, R. H., I. Herman, F. Magnotta, I. J. Rosenberg, and K. Ziock (1987), "Photon Desorption of Positrons Bound at a Metal Surface," *Bull. Am. Phys. Soc.* **32**, 899.

Howell, R. H., I. J. Rosenberg, and T. McMullen (1987), "Dynamics of Positronium Formation in an Insulator," Lawrence Livermore National Laboratory, Livermore, Calif., UCRL-96716.

A New Low-Z Radiative Opacity Code

Principal Investigator:
Carlos A. Iglesias
Co-Investigators:
Forrest J. Rogers,
Brian G. Wilson, and
Roger K. Ulrich

We have developed a new radiative-opacity code for elements lighter than copper to address current problems in astrophysics. Using a better treatment of the atomic physics involved, the code significantly raises the Rosseland mean opacity appropriate for models of Cepheid Variable stars.

A vital factor in models describing how a star shines is its opacity, which governs the rate at which light formed inside can get out. Since there is no way to measure this opacity directly, we depend on theoretical models. Because of the complexity of the problem, past calculations used approximations that may affect their accuracy.

Our new code is based on a many-body quantum statistical treatment that provides both equation-of-state and occupation numbers (Rogers, 1986). It is a detailed configuration-accounting approach that defines the bound states in the theory in terms of one-electron parametric potentials that systematically include density effects. Solving the Dirac equation with these analytic potentials yields energies and wave functions from which the code computes photon absorption cross sections that, for isolated atoms, are comparable to those of atomic-structure codes.

Briefly, our code considers photoionization processes individually for every subshell in all configurations of the various ion stages. The calculation is done in the central field and in the dipole approximation. The code also calculates the allowed bound-bound dipole transitions explicitly for every configuration and computes oscillator strengths either in LS or intermediate coupling. It computes inverse bremsstrahlung by solving the Schrödinger equation for the scattering states in the parametric potentials and then by computing the dipole matrix elements. It treats free-electron photon scattering by assuming weakly coupled electrons but with quantum corrections to the electron-structure factor (Boercker, 1987).

Calculations with the new code (Iglesias et al., 1987) show that the Rosseland mean opacity may be significantly above that of the standard Astrophysical Opacity Library (Huebner et al., 1977) for densities and temperatures important to Cepheid models. Much of the increase is due to an improved treatment of the atomic physics. The systematic treatment of density effects will also allow us to study the dense interiors of stars.

References

Boercker, D. B. (1987), "Collective Effects on Thomson Scattering in the Solar Interior," *Astrophys. J. Lett.* **316**, L95.

Huebner, W. F., A. L. Merts, N. H. Magee, and M. Argo (1977), *Astrophysical Opacity Library*, Los Alamos National Laboratory, Los Alamos, N. Mex., LA-6760-M.

Iglesias, C. A., F. J. Rogers, and B. G. Wilson (1987), "Reexamination of the Metal Contribution to Astrophysical Opacity," *Astrophys. J. Lett.* **322**, L45.

Rogers, F. J. (1986), "Occupation Numbers for Reacting Plasmas: The Role of the Planck-Larkin Partition Function," *Astrophys. J.* **310**, 723; also see references therein.

Expert-System Mesh Generator[a]

Principal Investigators:
Rowland R. Johnson and
Richard Ziolkowski

Our objective was to investigate the application of expert-system techniques to the problem of automatic mesh generation for both modeling and simulation codes. We determined that such a capability is both needed and feasible, and identified pertinent research issues not addressed in existing expert systems.

The objective of our research was to investigate the application of expert-system techniques to the problem of automatic mesh generation for modeling and simulation codes. Much of our meshing problem is similar to the problem treated by existing expert systems that handle the task of designing a given object.

In general, a design problem is stated as a set of constraints and allowable design decisions. The meshing problem has the physical object's shape and modeling considerations as its constraints. Partitioning and cell formulation represent the allowable design decisions, and the design process centers on how such decisions interact. Interactions must be determined by making a design decision and observing the implications. An implication from a design decision may collide with an implication from other decisions or constraints. Such a collision produces an anomaly, the severity of which is represented on the interval $(0, \infty)$. In essence, the design process is a search for a set of design decisions for which resulting collisions have minimal total severity.

We developed a prototype system to gain better understanding of the issues we must address. Our prototype handles a restricted set of circumstances and uses the inferencing techniques developed for the seismic event analyzer. The seismic system is easily modifiable and provides a mechanism to explore different solutions for mesh applications.

Design expert systems require forward-chain inferencing and usually achieve search with dependency-directed backtracking. The disadvantage of search with backtracking is that it can become slow. The inferencing technique used in the seismic event analyzer is a forward-chaining, assumption-based, truth-maintenance system developed because it models closely the technique used by seismologists. Its desirable characteristics for our meshing application include search without backtracking, making it faster than current design expert systems. Its basic mechanism can also be extended to allow reasoning about trade-offs of design decisions in a direct way. Because such direct reasoning is not currently included in design expert systems, research was required for our extensions.

We gained an understanding of the problems involved in expressing geometric descriptions. Our application required that geometric objects, such as quadrilaterals, be located, tested, and manipulated. The description of a quadrilateral as four, straight, connected lines can be used as a matching operand when attempting to locate a diagonal. The problem is that four such matches can be found for the same quadrilateral due to the symmetry of the quadrilateral with respect to the description. All the obvious solutions have disadvantages.

We have now gained considerable insight into extending the techniques of assumption-based reasoning for use in the meshing application. These techniques appear to be highly attractive because they allow for the direct expression of reasoning strategies about design trade-offs.

[a]This project was accomplished in four months of the original twelve months planned for its duration.

A New Approach to the Study of Lymphocyte Dynamics

Principal Investigator:
Irene M. Jones

The ability to quantify dividing cells in animal tissues is a key to predicting the genetic consequences of exposure to mutagenic agents. We developed a method to quantify dividing lymphocytes in mice and to monitor the lifespan of the newly formed cells by labeling their genetic material (DNA) with bromodeoxycytidine (BrdCyt). Our method employs a monoclonal antibody and flow cytometry to detect cells that have incorporated the labeling material.

Studies of mice exposed to radiation and toxic chemicals indicate that the frequency of lymphocytes with induced mutations depends on the proportion of dividing cells in a target tissue. The persistence of lymphocytes (their lifespan and that of their progeny) and their migration also affect mutant frequency. To predict the genetic consequences of exposure to mutagens, we needed a method that would allow us to quantify dividing lymphocytes and to monitor their persistence.

Our approach was to label the DNA of dividing cells by incorporation of BrdCyt. This label is diluted and eventually disappears as a cell and its progeny divide. We detected the BrdCyt in individual cells by staining them with a BrdCyt-specific monoclonal antibody (Vanderlaan et al., 1986) and then analyzed the cells on a flow cytometer. By exposing mice to BrdCyt for various periods and analyzing their cells at different intervals after labeling, we were able to determine the proportion of cells dividing at any specific time and the length of time that the labeled cells survived. We tried to distinguish lymphocytes from other labeled cells by identifying cell-surface antigens with specific monoclonal antibodies.

In most cases, exposure to BrdCyt for short periods did not disrupt normal population dynamics. We studied cells of the bone marrow, thymus, and spleen. After a two-day exposure to BrdCyt, labeled cells were found to persist for as long as three weeks in the spleen. In contrast, labeled cells rapidly disappeared from the bone marrow and thymus because cells in these organs are immature and continue to divide, or they mature and then migrate to other tissues.

At the level of BrdCyt used (50 μg/h), a 3-day exposure proved to be toxic, producing labeled cells that were no longer able to divide. In one experiment, BrdCyt was toxic after only a 12-h exposure—a result we do not understand. The detection sensitivity for BrdCyt could not be increased enough to allow the use of lower, presumably less toxic, levels.

We found it difficult to label lymphocytes simultaneously with BrdCyt and with monoclonal antibodies specific to the cell type. The harsh chemical treatment used to detect BrdCyt incorporation prevented good discrimination among cell types.

References

Crippen, T. L. and J. M. Jones (1987), *A New Method to Study the Dynamics of Lymphocyte Populations*, Lawrence Livermore National Laboratory, Livermore, Calif., UCRL-95957.

Vanderlaan, M., B. Watkins, C. Thomas, F. Dolbeare, and L. Stanker (1986), "An Improved High-Affinity Monoclonal Antibody to Iododeoxyuridine," *Cytometry* 7, 499.

Calculational and Experimental Studies of Metallic Ceramics

We have studied the properties of metallic ceramics to find new containment materials. The monosulfides and monophosphides of lanthanoids and actinides give the best combination of properties for molten metal containment.

Principal Investigators:
Oscar H. Krikorian and
Paul G. Curtis

Metallic ceramics are metal-rich compounds, such as W_2B, Ta_4C, and CeS, that combine some of the desirable characteristics of metals (high electrical and heat conductivities) with those of ceramics (high melting point, high hardness, and good corrosion resistance). A combination of metallic, ionic, and covalent bonding is present in these materials. Our objective was to evaluate which metallic ceramics have the best characteristics as containment materials for molten metals.

By comparing borides, carbides, nitrides, phosphides, sulfides, and selenides, we found that monosulfides (MS) and monophosphides (MP) of lanthanoids (includes scandium, yttrium, lanthanum, and the lanthanides) and actinides have the best combination of characteristics for molten metal containment. We found that the class of compound and type of bonding in metallic ceramics affect such properties as thermodynamic stability, heat capacity, thermal expansivity, and microhardness (Krikorian, 1986a, 1986b, and 1987b). We fabricated specimens of CeS and determined their solubility and wettability in contact with molten aluminum (Al), uranium (U), and iron (Fe) (Krikorian, 1987a).

The MS and MP compounds are advantageous because the sharp peak in thermodynamic stability in the lanthanoid-actinide regions reduces the potential for most molten metals to compete for S and P constituents. Thermodynamic stability peaks in the periodic table are much broader for borides, carbides, nitrides, and oxides; selenides are similar to sulfides, but with lower melting points. The metallic constituent in MS and MP is usually also resistant to molten metal interaction. High melting points (2500 to 3300 K) and nearly invariant compositions with temperature minimize melt contamination by MS and MP compounds, and high thermal conductivities give good thermal stress resistance. Thus, MS and MP materials should be useful as monolithic containers, such as crucibles, and coatings on many metal alloys. Durable, fracture-free coatings should result from selecting a good match in thermal expansion between coating and substrate.

We developed methods for calculating heat capacities that predict the terms for dilatation and harmonic lattice vibration. We also developed a generalized expression to predict thermal expansivities based on atomization energy and microhardness.

After experimental exposures of CeS to molten metals, we found that Al begins to react with CeS at ~1200 K without wetting, dissolves Ce but not S, and forms a thin layer of Ce_2S_3 at the interface. At 1360 K, Al wets and spreads over the CeS surface and dissolves ~0.1 at.% Ce. We found that U does not wet or react with CeS at 1673 K. At 1873 K, U wets and spreads on the surface and dissolves ~0.01 at.% S, which precipitates on cooldown. Finally, Fe wets CeS at 1873 and 1973 K but does not spread on the surface or react. Our studies, which are backed by thermodynamics, confirm that some metals, such as Al, interact preferentially with the metallic constituent in CeS, whereas U interacts with the S constituent. Nevertheless, the degree of reaction remains low.

References

Krikorian, O. H. (1987a), *Synthesis of CeS and Interactions with Molten Metals*, Lawrence Livermore National Laboratory, Livermore, Calif., UCRL-96023; to be published in *High Temp–High Press*.

Krikorian, O. H. (1987b), *Thermal Expansivity Correlations for Refractory Materials with the NaCl-Type Structure*, Lawrence Livermore National Laboratory, Livermore, Calif., UCRL-96022; submitted to *High Temp–High Press*.

Krikorian, O. H. (1986a), "Development of Accurate Estimation Methods for Calculating Heat Capacities of Refractory Materials," *Thermophysical Properties*, B. Wang et al., Eds. (China Academic Publishers, Beijing, China), p. 151.

Krikorian, O. H. (1986b), "Development of Accurate Estimation Methods for Calculating Thermal Expansivities of Hard Materials," *Science of Hard Materials*, E. A. Almond et al., Eds. (Adam Hilger Ltd., Bristol, U.K.), p. 137.

Production of a VUV Laser

Principal Investigator:
Richard W. Lee
Co-Investigator:
Roger W. Falcone[a]

[a]University of California, Berkeley.

We have demonstrated a new class of short-wavelength laser near 100 nm in xenon and krypton. We measured lifetimes and quenching of the lasing states, measured Auger branching ratios, developed a simple model predicting gain and time evolution of laser output, observed multipass gain, and developed a sensitive soft-x-ray detection system for experiments.

We have demonstrated gain in a new type of short-wavelength (or VUV) laser system. In our experiments, soft x rays emitted from a laser-produced plasma ionize a 4d inner-shell electron in neutral xenon gas. The resulting highly excited Xe^* atoms rapidly undergo Auger decay to various excited states of Xe^{++}. The relative Auger decay rates and level degeneracies are such that a population inversion is created between Xe^{++} $5s^25p^6\,{}^1S_0$ and $5s^25p^5\,{}^1P_1$, and gain is observed at the transition wavelength, which is 108.9 nm. The analogous transition in krypton, Kr^{++} $4s^24p^6\,{}^1S_0$ to $4s^24p^5\,{}^1P_1$, has been similarly inverted and shows gain at 90.7 nm.

Our experimental apparatus used to demonstrate gain consists of a neodymium-doped-glass laser pulse from the 20-J, 1-ns Janus laser, which was focused on a tantalum target to form a thin, 9-cm-long soft x-ray source. Radiation from the resulting plasma ionizes xenon or krypton gas in a channel opposite the plasma. We varied the length of the gain region and detected a nonlinear increase of emission from gas in the channel with pumped length using a vacuum spectrometer and soft x-ray streak camera. We observed gain at the Xe^{++} 108.9-nm transition and in krypton at 90.7 nm.

Our measurement of lifetimes of the upper and lower laser levels used a novel technique that combines time-correlated photon counting with a high-repetition-rate, laser-produced plasma x-ray source. Because collisional quenching of the excited ions occurs at gas pressures on the order of 1 Torr, we obtained data at various pressures to extrapolate the natural lifetime to zero pressure. The Table shows measured lifetimes and collisional quenching coefficients.

We measured the relative decay intensities on the transitions for the xenon laser system (the upper level decays primarily on the 108.9-nm transition, while the lower level decays at 84.0, 90.1, 91.5, and 98.1 nm). A rough measure of the inversion ratio due to Auger pumping is 1:0.3, including degeneracies, into the upper and lower laser states.

We also developed a time-dependent computer simulation to model the systems. The model takes into account amplified spontaneous emission, predicts the temporal behavior of the output, and relates predicted local gain coefficients to the experimentally measured gain. The model predicts a fitted gain parameter of 0.95 cm^{-1}, which is in reasonable agreement with the measured gain of 0.8 cm^{-1}. The behavior of the amplitude and pulse length of the output appears to be reasonably accurately simulated using this model with only one empirical parameter. We therefore conclude that amplified spontaneous emission is the dominant process determining the behavior of the system.

Further studies of photo-pumped lasers at shorter wavelengths will probably require development of

ultrashort-pulse-length (100-fs), laser-produced plasma x-ray sources because lifetimes scale as the inverse square of wavelength. Many such schemes exist in the literature, but only recent technological advances in short-pulse laser technology make these schemes possible.

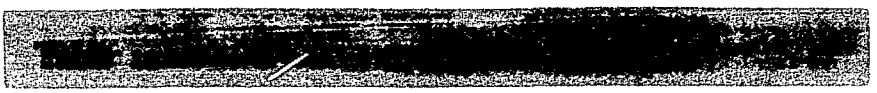

Transition	Wavelength (nm)	Decay time (ns)	Collisional quenching $(Torr \cdot s)^{-1}$
Xe upper $5s^15p^5{}^1P_1$ to $5s^05p^6{}^1S_0$	108.9	4.75 ± 0.15	$2.8 \pm 0.2 \times 10^7$
Xe lower $5s^25p^4{}^3P_0$ to $5s^15p^1{}^1P_1$	90.2	20.5 ± 2.0	$2.3 \pm 0.5 \times 10^7$
Kr upper $4s^1 4p^5{}^1P_1$ to $4s^04p^6{}^1S_0$	90.7	2.0 ± 0.1	$3.4 \pm 0.6 \times 10^7$
Kr lower $4s^24p^4{}^1D_2$ to $4s^14p^5{}^1P_1$	78.6	4.5 ± 0.3	$1.8 \pm 1.1 \times 10^7$

References

Kapteyn, H. C., R. W. Lee, and R. W. Falcone (1986), "Observation of a Short-Wavelength Laser Pumped by Auger Decay," *Phys. Rev. Lett.* **57**, 2939.

Kapteyn, H. C., M. M. Murnane, and R. W. Falcone (1987), "Time-Resolved Measurements of Short-Wavelength Fluorescence from X-Ray Excited Ions," *Opt. Lett.* **12**, 663.

Kapteyn, H. C., M. M. Murnane, R. W. Falcone, G. Kolbe, and R. W. Lee (1986), "Measurements on a Proposed Short-Wavelength Laser System in Xenon III," *Multilayer Structures and Laboratory X-Ray Laser Research*, N. M. Ceglio and P. Dhez, Eds. (SPIE, Bellingham, Wash.), vol. 688.

FY87 $58,000

Doppler-Free Annihilation Radiation from Ultra-Cold Positronium

We are studying a way to cool positronium (Ps) to within 0.1 K of absolute zero with lasers. This work may benefit ultra-high-resolution spectroscopy and even lead to a gamma-ray laser.

Principal Investigators:
Edison P. Liang and
Jon C. Weisheit
Co-Investigators:
Charles D. Dermer and
Brian M. Palmer

We are investigating the prospect of using a newly developed laser technique to cool ortho-Ps to extremely low temperatures before it decays away (in about 140 ns). We are examining what kind of laser we would need and how low it could drive the temperature. We are also using a collisional-radiative model of the Ps-level populations produced by recombination of thermal positrons and electrons to study the atomic physics of the ortho-para conversion in Ps collisions. This process is of interest because it inhibits efficient cooling at high densities (para-Ps decays in about 0.1 ns).

Ultra-cold Ps is a unique system—a pure quantum gas with negligible interatomic forces. Radiation from ultra-cold Ps would have almost no Doppler broadening, greatly benefitting high-resolution spectroscopy. Studies of the time-dependent development of a Bose-Einstein condensate from cold Ps would also benefit. Demonstration of laser cooling of Ps could also have spin-offs in antimatter technologies.

Perhaps most intriguing is the possibility of making a 0.511-MeV annihilation gamma-ray laser. This would require using 203-GHz microwaves to spin-flip the cold ortho-Ps into the para-Ps state. Under suitable conditions the 0.511-MeV gamma rays released might stimulate more annihilations.

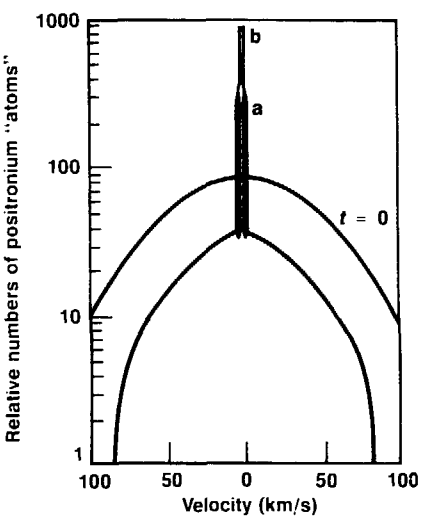

Positronium velocity distributions from a one-dimensional numerical simulation of laser cooling, with $t = 0$ representing the initial room-temperature distribution: (a) the distribution after 140 ns (one ortho-Ps lifetime) with laser illumination at saturation intensity and at wavelengths longer than the 1s → 2p transition frequency; (b) the distribution with the laser light cut off at a slightly lower frequency to reduce stimulated emission from low-velocity Ps.

The Figure shows Ps velocity profiles after one ortho-Ps lifetime for two different ideal laser profiles, which illuminate the red Doppler wing of the 1s → 2p transition of ortho-Ps. About 16% of the original Ps is cooled to low temperature. Analytic studies suggest that we can obtain similar results with three-dimensional laser cooling. To demonstrate cooling of Ps, we could illuminate the system with a second laser tuned to the 2p → 3d transition of cold Ps only and look for a change in the annihilation rate.

Reference

Liang, E. P. and C. D. Dermer (1987), "Laser Cooling of Positronium," submitted to *Opt. Commun.*

Laser Damage Mechanisms in Optical Polymers

Principal Investigators:
Richard Lyon,
Richard Cristensen,
Jack Campbell, and
Howard Powell
Co-Investigator:
Marvin Kong

Organic polymer glasses have the potential for use as laser optical components in aerospace applications. But these materials have low optical strength compared with inorganic glasses. They are prone to damage by pyrolysis and fracture associated with particles trapped in the polymer. We used computer models to predict the scaling of damage threshold with laser pulse length for micron-size particles. These predictions show a good correlation with experimental results.

The apparently low optical strength of organic polymeric glass compared with inorganic glass has been attributed to damage mechanisms, such as pyrolysis and fracture, associated with trapped particles that absorb laser light (Dyumaev et al., 1983; O'Connell and Saito, 1983). The low decomposition temperature of typical polymers precludes the high processing temperatures that volatilize or solubilize contaminants in inorganic glass. However, researchers have observed that increased molecular mobility near a second-order transition in polymeric materials can arrest damage propagation and increase the damage threshold to that of high-optical-strength inorganic glass (Dyumaev et al., 1982).

Recognizing the potential of polymeric glasses as lightweight laser optical components in aerospace applications, we set out to study the mechanisms of laser damage due to particulate contaminants. Ultimately, we hope to identify chemical and mechanical properties that contribute to high optical strength.

One of our objectives in FY87 was to distinguish between the chemical and the mechanical events leading to damage. We planned to accomplish this by developing computer models of pyrolysis and fracture mechanics. We would use the models to evaluate the time scales of these processes relative to the laser pulse. Another objective was to determine the influence of molecular mobility on microfracture occurring in the nanosecond time scale of the laser pulse. This would be accomplished by correlating modeling results with experimental studies of laser damage occurring at wavelengths of 1.06 μm in characterized polymer glasses. A third objective was to characterize chemical processes by decomposition kinetics and intrinsic absorption.

We developed a thermal pyrolysis model that couples heat-transport and polymer-decomposition kinetics at particle sites. Using a fast-pyrolysis technique, we determined the required kinetic parameters for 10 candidate polymers spanning a range of chemical composition and mechanical properties.

We also derived relations that allow us to obtain polymer relaxation spectra from measured dynamic mechanical properties. We then used the spectra in a coupled heat-transport/fracture model. Modeling results suggest that visible, single-shot damage is a rapid, fracture-dominated process occurring in nanoseconds during the laser pulse. These results indicate that the single-shot damage threshold should decrease with the reciprocal square root of the particle size and also has a strong logarithmic dependence on pulse length. Laser damage resulting from pyrolysis is a relatively slow, cumulative process occurring in milliseconds. It exhibits a weak logarithmic pulse-length dependence but has a complex relation to particle size. Preliminary experimental data support these conclusions.

References

Dyumaev, K. M., A. A. Manenkov, A. P. Maslyukov, G. A. Matyushin, V. S. Nechitailo, and A. M. Prokhorov (1983), "Transparent Polymers: A New Class of Optical Materials for Lasers," *Sov. J. Quantum Electron.* **13**, 503.

Dyumaev, K. M., A. A. Manenkov, A. P. Maslyukov, G. A. Matyushin, V. S. Nechitailo, and A. S. Tsaprilov (1982), "Influence of Viscoelastic Properties of the Matrix and of the Type of Plasticizer on the Optical Strength of Transparent Polymers," *Sov. J. Quantum Electron.* **12**, 838.

O'Connell, R. M. and T. T. Saito (1983), "Plastics for High-Power Laser Applications: A Review," *Optical Engineering* **22**, 393.

Transparent Glass-Crystal Composites for Laser Hosts

Principal Investigators:
John E. Marion, Janet B. Davis, and Stanley Stokowski

We investigated the feasibility of combining glass and crystals to form highly transparent composites for use as active laser materials. To make these transparent composites, we introduced crystallites into a glass that had been tailored for a precise refractive-index match.

Traditionally, both glasses and single crystals have been used separately as laser host materials. We sought to produce a laser host made of a composite combining the ease of formation and low cost of a glass with the desirable laser and thermomechanical properties of a crystal. Our approach was to introduce crystallites into a glass that had had its properties tailored to match those of the crystal—principally its refractive index and thermal expansion properties. Other researchers have produced glass-ceramic laser hosts (Müller and Neuroth, 1973), but these exhibit unacceptable optical loss due to scattering from the crystallites. Efforts at minimizing crystallite size to reduce optical loss succeeded only in cutting loss to about 4% per centimeter. For efficient laser performance, optical loss must be less than 0.1% per centimeter.

In our experiments, we first selected promising crystals. Then we chose glass systems that had some overlap in refractive index with the chosen crystal. By developing compositional phase diagrams with sets of contours of constant refractive index and constant thermal expansion, we manipulated the composition of the glass system so that its properties matched the crystal properties.

Our most successful combination was a five-component lanthanum borate glass matched to spinel crystal ($MgAl_2O_4$). The refractive indices matched within 10^{-4}, and thermal expansion was within 1×10^{-7} per °C. Our calculations indicate that this match is close enough for us to achieve our optical-loss goal (<0.1% per cm) when the spinel particles are 1 mm in diameter.

We found that the two most successful methods for forming the composites were:

- Casting the spinel crystals into the glass as it was poured.
- Imbedding spinel crystals into a pressed, dried sol-gel of the glass and then heating the composite to full density.

We discovered that the concept of a glass-crystal composite formed by using these methods has severe limitations. In the first method, dissolution of the crystal by the glass was so rapid that the small particles, which are required to minimize scattering, dissolved before the glass became homogeneous. In low-temperature castings from sol-gel glasses, devitrification, even of very stable glasses, occurred at the glass-crystal interface. Also, the boundary layer surrounding the crystal in the glass always had a different refractive index even when that of the bulk glass and the crystal were the same. We conclude that the feasibility of this concept for producing highly transparent, inexpensive laser hosts is marginal.

Reference

Müller, G. and N. Neuroth (1973), "Glass Ceramic—a New Laser Host Material," *J. Appl. Phys.* **44**, 2315.

FY87: $36,000

Three-Dimensional, Relativistic Hydrodynamic Simulations of Compact, Interacting Binary Systems

Principal Investigators:
Grant J. Mathews and
James R. Wilson
Co-Investigators:
Charles R. Evans[a] and
Steven L. Detweiler[b]

[a]California Institute of Technology, Pasadena.
[b]University of Florida, Gainesville.

We have developed a three-dimensional relativistic hydrodynamics code for describing how two neutron stars can coalesce. We will use this code to study the dynamics of coalescing systems and their associated gravitational radiation.

The details of how two neutron stars spiral toward each other and collapse into one is still an unsolved problem in astrophysics. Such objects may be the most efficient gravity-wave generators in the universe and an important source of heavy elements in the interstellar medium. We have written a three-dimensional, relativistic hydrodynamics code to compute the dynamics of coalescence and the associated gravity waves from such systems.

Our code uses a time-explicit Eulerian scheme with an adaptive grid—an approach that is most amenable to solving the relativistic field equations and that works well on one- and two-dimensional relativistic problems. These calculations use the ADM (or 3 + 1) formulation of general relativity. We picked a Cartesian grid to avoid finite-differencing problems near coordinate singularities and to produce simpler and more symmetric solutions to the relativistic field equations.

Our main emphasis in FY87 was to find the fastest scheme for solving the relativistic field equations. Our final choice uses a conformally flat three metric, approximates the radiation reaction from a moment expansion, and determines the lapse function, shift vector, and extrinsic curvature by solving elliptic equations. This approximate field-equation solution gives the exact structure for a single neutron star on the grid and is therefore more accurate than a post-Newtonian approximation. We have successfully followed the orbits of two relativistic polytropic neutron stars on the grid and have introduced a more efficient advection scheme. We are now upgrading the code to use a realistic neutron-star equation of state and are finishing our method for solving the field equations.

References

Evans, C. R. (1987), "Gravitational Radiation from Collisions of Compact Stars," *Thirteenth Texas Symposium on Relativistic Astrophysics*, M. P. Ulmer, Ed. (World Scientific, Singapore), p. 152.

Evans, C. R. and G. J. Mathews (1987), "Shock-Driven Neutronized Wind from Binary Neutron Star Coalescence as a Site for the *r*-Process," *Origin and Distribution of the Elements*, G. J. Mathews, Ed. (World Scientific, Singapore), p. 617.

Mathews, G. J., C. R. Evans, and J. R. Wilson (1986), "Relativistic (3 + 1) Dimensional Hydrodynamic Simulations of Compact Interacting Binary Systems," *Advances in Nuclear Astrophysics*, E. Vangioni-Flam et al., Eds. (Editions Frondieres, Gif Sur Yvette, France), p. 211; also published as Lawrence Livermore National Laboratory, Livermore, Calif., UCRL-95416, and *Bull. Am. Astron. Soc.* **18**, 930.

Fokker-Planck Simulation of Space Plasma Phenomena

Principal Investigator:
Yoshiyuki Matsuda
Co-Investigator: Kang T. Tsang[a]

[a]Science Application International Corporation, McLean, Va.

Using a relativistic, two-dimensional Fokker-Planck code, we studied the auroral kilometric radiation by obtaining self-consistent solutions for wave emission and electron distribution. Comparisons of our numerical results with spacecraft observations and data analysis show that a quasilinear process combined with other relevant processes can explain the observed emission.

We developed a relativistic, two-dimensional Fokker-Planck code to study space plasma phenomena and to specifically investigate the auroral kilometric radiation (AKR). The AKR is believed to be the earth's most intense wave emission. The leading candidate for generation of this emission is a cyclotron maser instability that is due to energetic electrons of 1 to 10 keV with a loss-cone distribution. We used this numerical approach to study the time-evolution and steady-state behavior of the AKR and the self-consistent electron distribution. Our work will help to provide a quantitative understanding of the origin of the AKR and to elucidate several characteristic features observed by spacecraft.

Our study is based on a quasilinear theory of the cyclotron maser instability, including the effects of Doppler shift, radiation loss, and electron source and sink. Simulations of the AKR emission perpendicular to the magnetic field (see the Figure) show the saturation amplitude of radiation to be higher than estimates from spacecraft data. We also studied the effect of the perpendicular spatial variation of the magnetic field by applying a linear theory. We found growth rates similar to those obtained by a local theory and an indication of wave energy losses from the source region by propagating waves.

More refined simulations indicate that we can obtain an electron distribution similar to those actually observed, and a quasilinear process combined with other processes can be a viable mechanism for quantitatively explaining the observed AKR. However, for a model distribution of energetic electrons used in our study, emission is strongest in the direction almost perpendicular to the magnetic field. This result requires further study because analyses of spacecraft data indicate that emission deviates significantly from the perpendicular direction. Our results illustrate the advantages of our numerical approach and realistic models in quantitatively studying many space plasma phenomena.

Reference

Tsang, K. T. and Y. Matsuda (1987), "Quasilinear Simulation of Auroral Kilometric Radiation," *Trans. Am. Geophys. Union* **68**(16), 385.

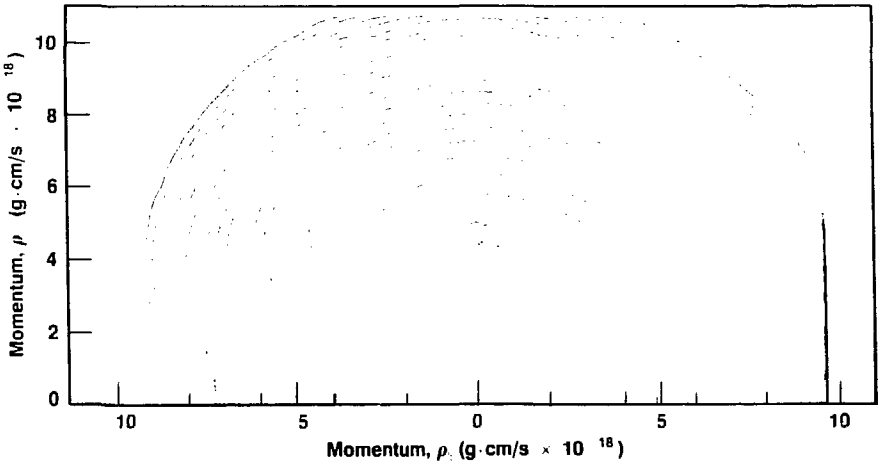

Electron distribution function in momentum space ($p_\parallel$, $p_\perp$) at a steady state reached by the quasilinear process alone. Flattening in the vertical direction is caused by wave-particle interactions. The magnitude ratio for successive contour lines is 0.56.

FY87: $162,000
FY88: $149,000

Synthesis of Dense, Energetic Materials Using Polymer Supports

We have conducted exploratory studies on the use of polymer supports for the preparation of dense, energetic materials. During FY88, we will undertake the synthesis of several new high-explosive materials that are potentially more energetic than HMX.

Principal Investigator:
Alexander R. Mitchell

Our overall objective is to develop innovative approaches for the synthesis of high explosives that are more energetic than HMX. Figure 1 shows the structure of this important military explosive, which has a density of 1.90 g/cm^3. Significantly higher densities, estimated at 2.09 g/cm^3, have been predicted (Nielsen, 1973) for the 12- to 14-member ring homologs (I, n = 6 to 7) of HMX. Attempts by other researchers to prepare such compounds have failed, thereby indicating the need for alternative strategies with respect to synthesis.

The 1984 Nobel Prize for Chemistry was awarded to Merrifield for pioneering the use of polymer supports in synthetic organic chemistry and inventing solid-phase peptide synthesis (Merrifield, 1986). While the application of polymer supports in the field of high-explosive synthesis is untried, it may well provide the innovative thrust that is needed to obtain energetic compounds currently beyond our reach with existing technologies. Figure 2 shows the final steps in the preparation of a larger-ring HMX compound (I, n = 6).

Earlier research on polymer-supported synthesis of cyclic peptides (Mitchell and Merrifield, 1985) suggested the approach we are currently exploring. We prepared the polycarbamate support (denoted as IIa in Figure 2) that is employed in our scheme in a three-step sequence from 1% crosslinked polystyrene (50-µm beads). We investigated several low-molecular-weight models for the conversion of structure IIa to I via structure III. Modeling studies substantiated our approach, and they unexpectedly revealed a mild nitrolysis reaction that may significantly enhance our capabilities to synthesize new explosives.

During FY88, we will pursue the approach shown in Figure 2 to its conclusion. At the present state of refinement, we expect that a mixture of cyclic methylenenitramines (I, n = 3, 4, 5, 6, 7 ...) will be produced. We will use chromatographic separation based on molecular sizing (gel-permeation chromatography) to isolate the product (I, n = 6).

We will also develop a polymer template (structure IIb) containing carbamate trimer units to limit the number of cyclic products (I, n = 3, 6, 9, 12 ...), thereby making the preparation of the HMX homolog (I, n = 6) more accessible. Finally, we will examine the scope and limitations of the recently discovered nitrolysis reaction, expecially with respect to synthesis of larger-ring homologs of HMX and other HMX-like compounds.

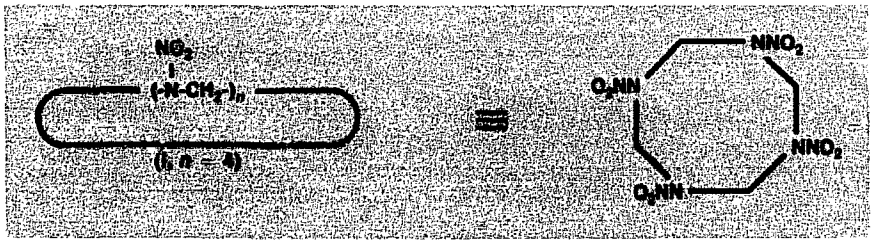

Fig. 1. Two structural representations of HMX (I, n = 4), which is an important military explosive. The number of methylenenitramino groups is represented by n. HMX is a cyclic methylenenitramine having an eight-member ring and a density of 1.90 g/cm^3.

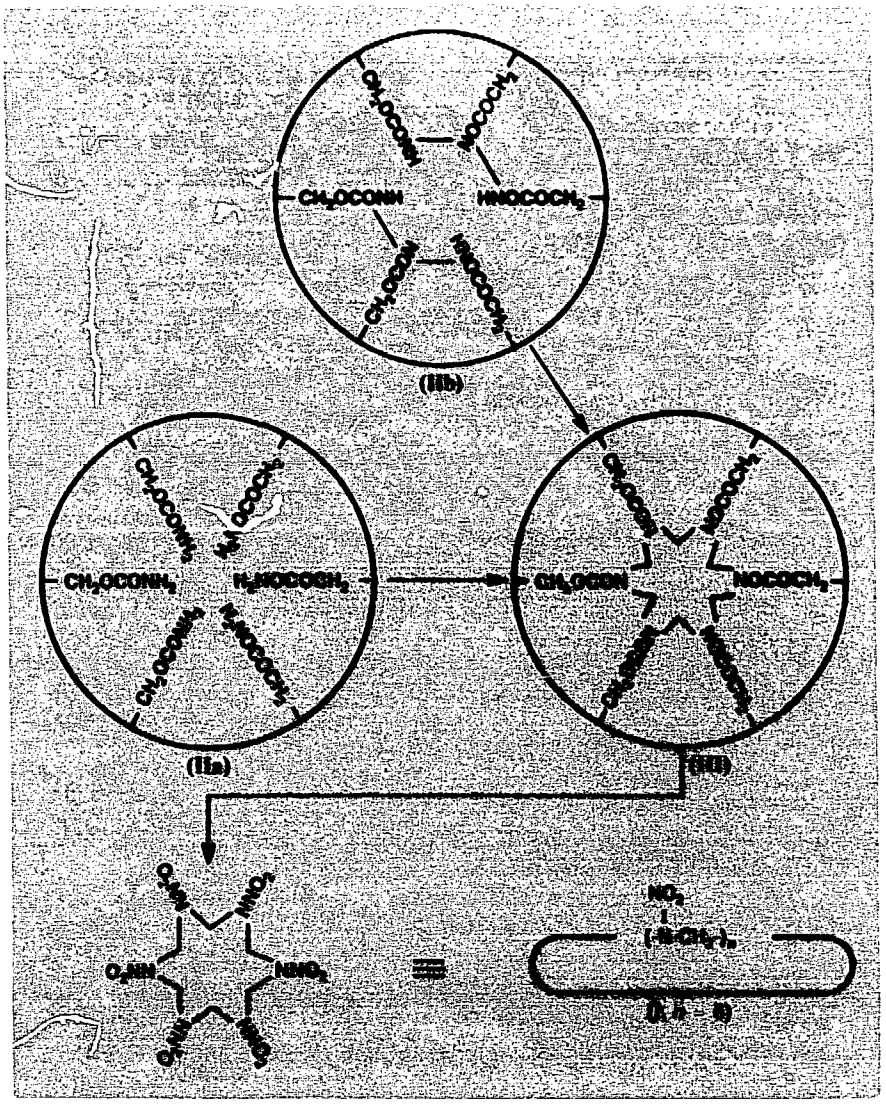

Fig. 2. Use of polycarbamate supports (IIa and IIb) to prepare an HMX homolog (I, $n = 6$). Polymers IIa and IIb serve as templates for the formation of the polymer-supported HMX precursor (III). A combination of acidolysis and nitrolysis steps releases the target molecule I from III.

References

Merrifield, R. B. (1986), "Solid Phase Synthesis," *Science* **232**, 341.

Mitchell, A. R. and R. B. Merrifield (1985), "Peptide Cyclizations on Polystyrene Supports: A Study of Intrasite and Intersite Reactions," *Peptides: Structures and Function*, C. M. Deber, V. J. Hruby, and K. D. Kopple, Eds. (Pierce, Rockford, Ill.), p. 289.

Nielsen, A. T. (1973), *Calculation of Densities of Fuels and Explosives from Molar Volume Additive Increments*, Naval Weapons Center, China Lake, Calif., technical publication No. 5452.

Modeling Gallium Arsenide Solid-State Devices

Principal Investigators:
William J. Orvis,
Gizzing H. Khanaka, and
Jick H. Yee

We developed two computer models to calculate gallium arsenide (GaAs) device operation and failure. The models are useful for both design problems and understanding device operation and failure during application of an electromagnetic pulse or other high-power electronic threat. Initial results indicate that GaAs is more sensitive than silicon to high-power failures.

GaAs is a material used in high-speed electronic devices because of its high mobility and direct band gap. High mobility causes high electron velocities; a direct band gap results in short minority carrier lifetimes. Both effects increase the speed of an electronic device by allowing charge carriers to be rapidly added to or removed from the active region of the device. Shorter lifetimes also result in a higher radiation tolerance.

The objective of our modeling efforts is to calculate transient device operation and failure at the high power levels expected during an electromagnetic pulse, lightning, or other electromagnetic transient. In the first of two models, we use only a single type of electron with average transport properties. The details of this model are identical to those for our silicon model (Orvis and Yee, 1985). In the second model, we use one electron continuity equation for lower-valley electrons and one for upper-valley electrons. A third continuity equation calculates hole densities in the valence band. Transitions between the upper and lower valleys are handled with a simple relaxation equation to the equilibrium densities after a specified lifetime. Transitions between the valence band and the two conduction bands are modeled with a Shockley-Reed-Hall and an optical emission/absorption recombination equation. These equations, together with Poisson's equation, the heat flow equation, and an external circuit equation, form a set of stiff, coupled, nonlinear partial differential equations solved with an implicit finite-difference scheme.

Our initial calculations involved a small-signal diode with the same configuration as the silicon bipolar 1N4148 diode. The Figure shows the short-pulse failure threshold energy versus pulse length for a silicon and a GaAs device calculated by applying a high-voltage pulse to the diode and integrating its operation until some point in the device reached 800 K.

In silicon, the forward-bias failure threshold is higher than the reverse-bias threshold because heating is not concentrated in the small junction volume as it is during reverse bias. In GaAs, the forward-bias failure threshold is significantly lower due to the formation of a Gunn domain, which causes the heating to be localized and thus requires much less energy to reach a failure temperature. The change in character at the 0.1-ns pulse width is due to the switch between substrate conduction with upper-valley electrons at short pulses and lower-valley electrons at long pulses.

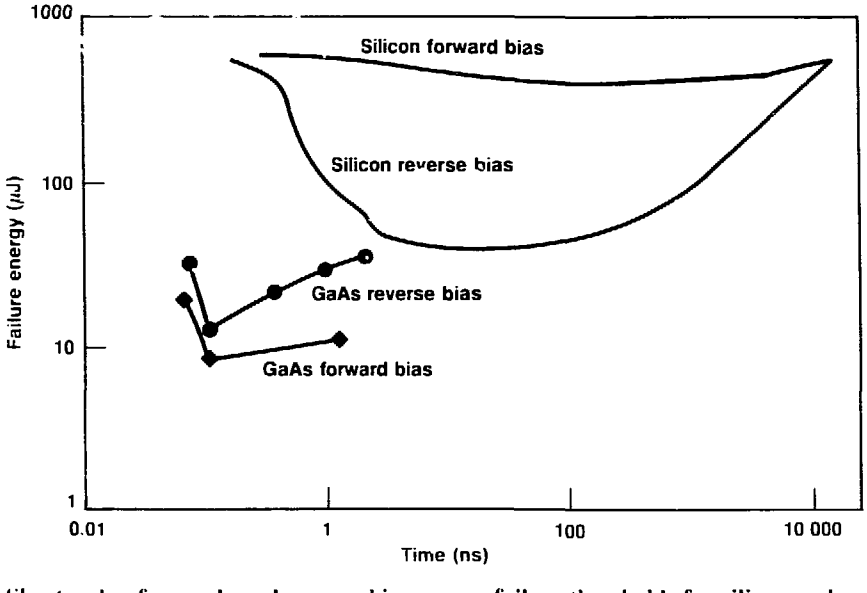

Short-pulse, forward- and reverse-bias energy failure thresholds for silicon and GaAs versions of the 1N4148 diode.

Reference

Orvis, W. J. and J. H. Yee (1985), *Semiconductor Device Modeling with BLRN42*, Lawrence Livermore National Laboratory, Livermore, Calif., UCID-20602.

FY87: $88,000
FY88: $111,000

Detection and Quantitation of Gene Expression Through Fluorescence Measurements

Principal Investigator:
Maria Pallavicini

All biological processes, including abnormal ones, are controlled by the selective expression of specific genes. Thus the capability to detect and quantify gene expression is an important step toward understanding abnormal processes such as uncontrolled cell proliferation and tumorigenesis. We have demonstrated this capability through two fluorescence-measurement techniques: in situ fluorescence hybridization and quantitative fluorescence microscopy.

Biological processes, such as cell proliferation and differentiation, are controlled by the selective expression of specific genes. When the expression of certain genes is altered, problems such as uncontrolled cell proliferation and tumorigenesis can develop.

A gene is expressed when the DNA sequence representing that gene is transcribed into messenger RNA (mRNA), and the mRNA is translated into proteins needed for cell function. Our goal is to develop cytologic techniques that employ fluorescence to quantify the levels of specific mRNAs and their protein products in single cells.

By exposing a mutant cell system to elevated temperatures, we caused it to express high levels of c-myc mRNA (1000 copies per cell) and its associated protein product. Our initial work was devoted to characterizing and subcloning this cell line to provide a homogeneous population.

We hybridized the cellular c-myc mRNA in situ with a biotinylated c-myc DNA probe. The hybridization protocol included cell fixation in paraformaldehyde, a 12-h hybridization period, and stringent wash conditions. We were able to detect the resulting RNA-DNA hybrids by using avidin conjugated with fluorescein. Using quantitative image analysis, we then measured the fluorescence intensity per unit area. Our measurements showed that the fluorescence increased steadily during the first 60 min of heat treatment and reached a plateau thereafter. These data demonstrated the feasibility of in situ fluorescence hybridization to quantify mRNA in cells on microscope slides. Currently, the sensitivity of this method is limited by background fluorescence associated with nonspecific sticking of the avidin. We have begun the development of several procedures to reduce the background fluorescence and increase sensitivity.

In another experiment, we used monoclonal antibodies linked to Texas Red dye to detect intranuclear c-myc protein in cells on slides and in suspension. We then quantified the fluorescence of the cells in suspension by flow cytometry. These studies demonstrate that the c-myc protein product can be detected in cells in suspension under conditions needed for detection of mRNA. Thus, in principle, it is possible to detect c-myc transcription and c-myc translation simultaneously in individual cells.

In FY88, we plan to develop the use of flow cytometry for the detection and quantitation of specific mRNAs. We will compare the sensitivity of this method with that of quantitative image analysis. As we improve the sensitivity of our flow cytometric techniques, we will apply fluorescence hybridization to analyses of c-myc gene expression in cells with fewer copies of the c-myc gene. Successful use of flow cytometry for quantifying gene expression will facilitate research in defining the relation between specific gene sequences and cellular function.

References

Pallavicini, M. G., J. W. Gray, D. Pinkel, and F. Wurm (1987), "Detection and Quantitation of Gene Expression by In Situ Fluorescence Hybridization," *Cytometry*, Supplement 1, 992.

Wurm, F. W., K. A. Gwinn, O. Papoulas, M. G. Pallavicini, and R. E. Kingston (1987), "Developments in Biological Standardization," *Proceedings of the European Society of Animal Cell Technology Meeting*, Israel (in press).

FY87 $100,000
FY88 $87,000

Generation of High Electrical Potentials in a Plasma

Principal Investigator:
Richard F. Post

We are assembling an experimental apparatus for a proof-of-principle test of a new way to generate very high transient electrical potentials in a magnetically contained, hot-electron plasma. Possible applications include particle accelerators for heavy-ion-driven inertial fusion or for high-energy particle physics.

Years of research at LLNL and elsewhere have provided a good theoretical understanding of the confinement of plasmas by magnetic mirrors. Theory predicts that if one were to suddenly (e.g., in 10 ns) subject a mirror-confined, hot-electron plasma (i.e., one consisting of low-energy ions and several-megavolt electrons) to a localized additional mirror midway between the main mirror fields, a transient electric potential about as large as the electron energy (i.e., millions of volts) will be generated in the plasma. If we link together a row of such regions and time the transient potentials to coincide with the arrival of a bunched beam of ions, we would have an accelerator resembling an rf linac. The foreseen advantages include high current, precise shaping of the space-charge fields (to optimize beam focusing), and potentially lower costs. In connection with the LLNL advanced test accelerator (ATA) induction linac, we have already developed the pulsed-power technology needed to generate the rapidly rising local mirror field.

We are now constructing a small-scale mirror facility in which to test the concept for comparison with theory. One of two critical factors in this investigation is the mean energy of the electrons, which we will measure by observing the x-ray (bremsstrahlung) spectrum emitted by the plasma. The other, the peak value of the potential, we will gauge by the acceleration of an axially injected low-current particle beam. The two measurements need not be concurrent: First we will generate the hot-electron plasma and measure its x-ray spectrum, and then we will install the pulsed mirror and ion source and measure the beam acceleration.

During FY87, we published an analysis of the concept and made additional theoretical calculations necessary for the design of the experiment. We procured (or fabricated) and assembled all the major equipment items for the experiment. We checked out the vacuum system and tested the two microwave transmitters. We finished testing the microwave coupling system and are now installing and testing auxiliary equipment.

Reference

Post, R. F. (1987), "Generation and Control of High Transient Electrical Potentials within a Mirror-Confined Plasma," *Phys. Rev. Lett.* **58**, 878.

Ab Initio Calculation of Pressure-Induced Ruby R-line Fluorescence Shifts

Principal Investigators:
Marvin Ross and Nicholas Winter

We have carried out Hartree-Fock calculations on the lowest quartet and doublet states of ruby (Al_2O_3:Cr^{+3}) using a cluster approximation for the crystal. The widely used pressure scale, based on the pressure-induced shift of ruby R-line fluorescence, is calibrated only to 1 Mbar and may have underestimated by 10% the highest pressures attained experimentally (about 5 Mbar).

Diamond-anvil cells permit the study of material properties at pressures up to 5 Mbar. There is no way to measure the pressure directly in such a cell, however. Instead, the shift of ruby's fluorescence wavelength with pressure is used as a secondary calibrant.

Because this standard has been accurately calibrated only to 1 Mbar, measurements at higher pressures must rely on extrapolation. We have been carrying out theoretical calculations of how the fluorescence wavelengths of Cr^{+3} and V^{+2} ions in alumina and magnesium oxide (MgO) hosts vary with pressure to put multimegabar pressure measurements on a sound theoretical basis.

The R-line fluorescence of ruby is usually assigned to the $^2E_g \rightarrow {}^4A_{2g}$ transition. Our Hartree-Fock calculations found two low-lying doublet states, ^2E and ^2A, at about the same energy above the ground state. The calculated shifts of the fluorescence with pressure are in good overall agreement (±10%) with the experimental ruby data (Mao et al., 1986).

The calculations also found a second ^2E state at a slightly higher energy that showed a strong fluorescence shift with pressure. We are investigating the possibility that the measured ruby fluorescence shifts are due to a combination of these low-lying doublet states.

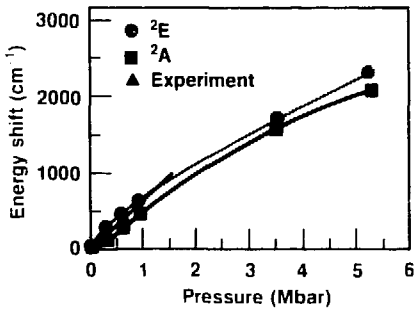

Comparison of the experimental data of Mao et al. (up to 1 Mbar) with our calculated shift in frequency of the ^2E and ^2A fluorescence lines in ruby (Al_2O_3:Cr^{+3}) as a function of pressure.

We conclude that the widely used pressure scale may have underestimated the highest pressures attained in diamond-anvil experiments (4 to 5 Mbar) by about 0.5 Mbar, and our calculations of the R-line fluorescence of Cr^{+3} in MgO support this conclusion. We are now improving our theoretical calculations to include the effects of configuration interaction and spin-orbit coupling.

Reference

Mao, H. K., J. Xu, and P. Bell (1986), "Calibration of the Ruby Pressure Gauge to 800 kbar Under Quasi-Hydrostatic Conditions," *J. Geophys. Res.* ***91***, 4673.

Liquid Metal Surface Chemistry

Principal Investigator:
Wigbert J. Siekhaus
Co-Investigators:
William McLean II,
Mehdi Balooch,[a] and
Donald R. Olander[a]

[a]University of California, Berkeley.

Modern science has developed sophisticated analytical techniques that enable us to probe the chemistry of material surfaces. Some of those we use are: Auger electron spectroscopy, microcinematography, and modulated molecular beam residence time spectroscopy. Although such techniques are commonly used to study electronic components or catalysts, we applied them, for the first time, to liquid metals. Among the metals we investigated are uranium, uranium alloys, and bismuth.

Over the last twenty years, powerful techniques such as low-energy electron diffraction (LEED), Auger electron spectroscopy (AES), x-ray-induced photoelectron spectroscopy (XPS), microcinematography, and modulated molecular beam residence time spectroscopy (MBRS) have been used to study the surface properties of materials. These techniques were commonly applied to materials used in the electronics industry, such as silicon, germanium, and gallium arsenide, and to catalysts, such as platinum, iron, and silver. But, at the start of our project, they had never before been used to study the surface chemistry of liquid metals.

Our work includes studies of

- The kinetics of the reaction between Cl_2 gas and clean liquid indium, lead, bismuth, tin, and gallium surfaces.
- The kinetics of the reaction between H_2O and a clean liquid uranium surface.
- The growth kinetics of uranium oxide on a clean liquid uranium surface.
- The solubility and surface segregation of oxygen in liquid uranium.
- The sticking coefficients and probabilities of reaction for H_2O, N_2, O_2, CH_4, C_2H_2, and CO_2 gases with the surfaces of clean liquid uranium and two liquid uranium alloys.

We studied all the reactions by MBRS, a technique in which a modulated beam of reactant gas strikes the liquid metal surface, which is held in an ultra-high-vacuum environment. Gaseous reaction products were detected by a mass spectrometer. For reactions that yield no gaseous product, we monitored the disappearance of the scattered reactant as a function of temperature to determine the reaction probability. The reaction of Cl_2 with the low-melting-point metals and the reaction of H_2O with uranium and uranium alloys are examples of processes that yield gaseous products, whereas the reactions of N_2 and O_2 with uranium and uranium alloys do not.

We also used AES to study the reaction of H_2O with the uranium surface and microcinematography to monitor the growth of uranium oxide (McLean and Siekhaus, 1986).

Our studies determined the surface-segregation coefficient of oxygen and the solubility of oxygen in pure uranium at temperatures close to the melting point. No other data of this kind were available for such low temperatures. Having obtained solubility data over a range of temperatures, we then established a reliable heat of solution for oxygen in liquid uranium.

The chlorine reaction results are being published in a series of articles. The most interesting concerns the reaction with bismuth (Balooch et al., 1986). The Figure shows the probability of an incoming chlorine molecule reacting with the surface and also shows the phase lag of the

Table Reaction probabilities and accommodation coefficients for reactions of gases with liquid uranium and uranium alloys.

Gas molecule/liquid material	Reaction probability	Accommodation coefficient
H_2O/U	0.4	0.6
O_2/U	0.7	0.6
CH_4/U	$<10^{-3}$	0.3
C_2H_2/U	0.6	0.3
N_2/U (See Balooch et al., 1987.)	—	—
CO_2/U	0.03	0.1
CO/U	$<10^{-3}$	0.1
H_2O/(U, Fe)	0.2	0.6
H_2O/(U, Cr)	0.2	0.6
O_2/(U, Fe)	0.6	0.6
O_2/(U, Cr)	0.6	0.6
CO_2/(U, Fe)	0.03	0.1
CO_2/(U, Cr)	0.03	0.1

reaction product with respect to the scattered reactant. This phase lag is roughly proportional to the time needed to complete a reaction, so that a phase lag of 45° at 20 Hz corresponds to a reaction time of 12.5 ms. Bismuth is a semimetal in the solid state but changes its electronic structure at the melting point to become a metal. Of all the metals investigated, bismuth alone exhibits a dramatic change in the reaction probability at the melting point: The product changes from $BiCl_3$ to BiCl, the reaction probability drops from 0.1 to 0.002, and the reaction time drops by a factor of 2 as bismuth changes from solid to liquid. This dramatic change will be used to corroborate controversial results purporting to show that the surface of lead melts tens of degrees centigrade before the bulk melts. We will make careful temperature measurements to determine whether the reaction probability for bismuth indicates that it too undergoes surface melting before bulk melting.

All other metals, including uranium and uranium alloys, show a smooth increase in reaction probability as the temperature increases through the melting point. The uranium results (Balooch et al., 1987) are summarized in the Table. The thermal accommodation coefficients in the Table represent the fraction of the surface temperature acquired by the cold molecule scattered by the surface and are, therefore, a measure of the gas-surface interaction in the adsorption well. The alloys investigated show only a small reduction in the reaction probability, approximately proportional to the nonuranium content of the alloy independent of the alloying element.

With IR&D support, we have originated the field of liquid-metal surface science, working with elements and alloys important to present and future Department of

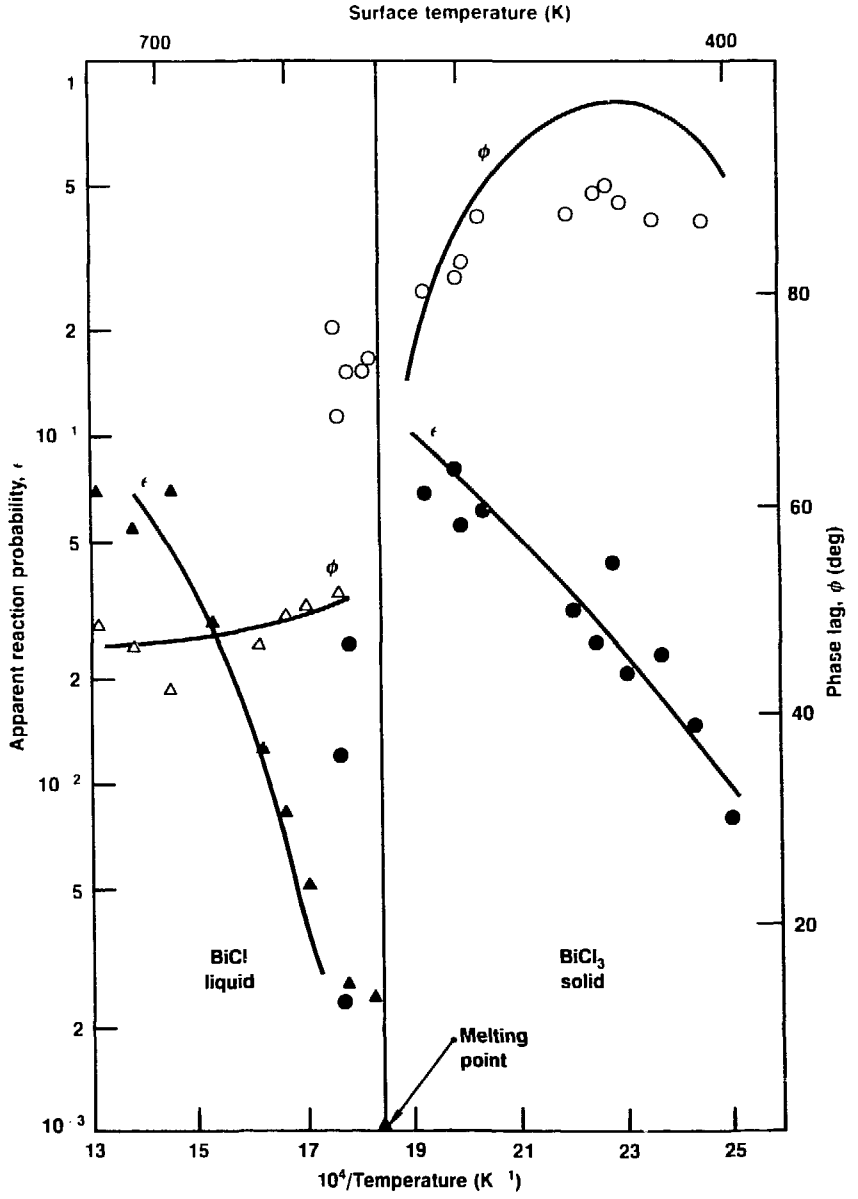

Apparent reaction probabilities and phase lags for $BiCl_3$ and BiCl as functions of surface temperature. The solid lines are based on a theoretical model.

Energy projects. We plan to continue this work on aluminum, lithium, uranium, and plutonium.

References

Balooch, M., W. J. Siekhaus, and D. R. Olander (1987), "The Reaction of Gases with Liquid Uranium and Its Alloys," *J. Oxidation* (in press).

Balooch, M., W. J. Siekhaus, and D. R. Olander (1987), "The Reaction of Water Vapour and Oxygen with Liquid Uranium," *J. Oxidation* (in press).

Balooch, M., W. J. Siekhaus, and D. R. Olander (1986), "Reactions of Chlorine with Liquid Metals, 3. Bismuth," *J. Phys. Chem.* **90**, 1671.

McLean, W. II and W. J. Siekhaus (1986), "The Reaction of Water Vapor with a Clean Uranium Surface," *J. Less Common Metals* **122**, 101.

Microcalorimeters for X-Ray Spectroscopy

Principal Investigator:
Eric H. Silver
Co-Investigators:
Simon Labov, Charles Hailey, Frederick Goulding,[a] Norman Madden,[a] Donald Landis,[a] Jeffrey Beeman,[a] Eugene Haller,[a] Gary Chanan,[b] James Rutledge,[b] Gary Bernstein,[c] Paul Richards,[c] and Steven M. Kahn[c]

[a] Lawrence Berkeley Laboratory, Berkeley, Calif.
[b] University of California, Irvine.
[c] University of California, Berkeley.

We are developing a microcalorimeter for pulse-counting x-ray spectroscopy. When the device is operated between 100 and 300 mK, it will offer a broad-bandwidth capability, nearly 100% efficiency above 1 keV, and the high resolution power of a Bragg crystal spectrometer.

The merits of microcalorimetry below 1 K for high-resolution x-ray spectroscopy are now widely recognized on theoretical grounds. By combining the high efficiency and broadband spectral sensitivity of traditional photoelectric detectors with the high-resolution capabilities characteristic of dispersive spectrometers, a microcalorimeter could potentially revolutionize spectroscopic measurements of astrophysical and laboratory plasmas.

In principle, a calorimeter can be any material that exhibits a perceptible temperature increase after it absorbs a single photon. For the temperature rise to be measurably large, the material must possess a small heat capacity. This heat capacity can be achieved below 1 K in crystals with small dimensions because the volume heat capacity of an ideal crystal theoretically drops with the third power of temperature. In an ideal microcalorimeter, the photon-induced temperature rise must be measured above background temperature noise caused by the intrinsic lattice vibrations in the detector. This phonon noise manifests itself as thermal fluctuations with a root-mean-square value $\delta T = (kT^2/C)^{1/2}$. Here, T and C are the temperature and heat capacity of the detector, respectively, and k is the Boltzmann constant. The spontaneous Gaussian energy fluctuation ΔE is $2.35(kT^2C)^{1/2}$. For single-crystal germanium with dimensions of 1 mm × 1 mm × 100 μm at T = 100 mK, $C = 3.7 \times 10^{-14}$ J/K, and ΔE is 1 eV.

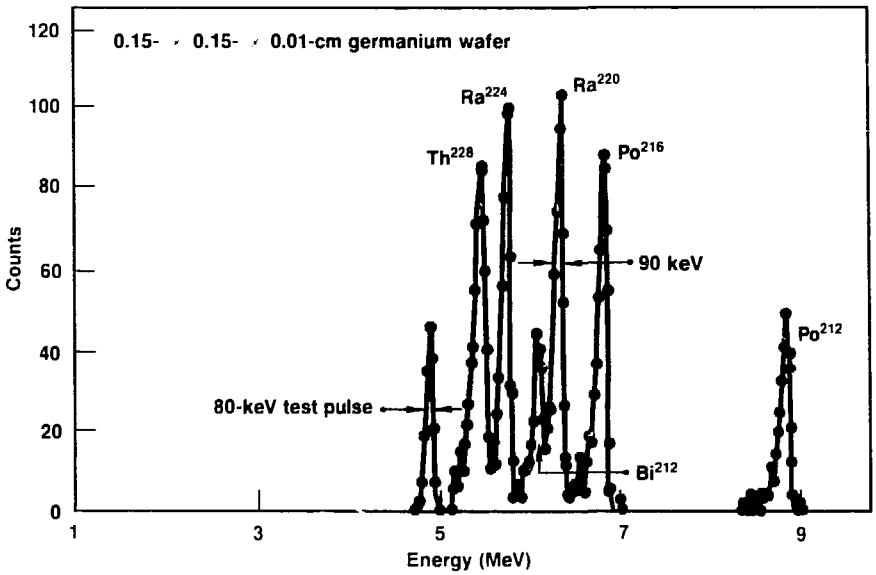

Alpha-particle spectrum obtained with a monolithic germanium calorimeter operating at 1.4 K. Peaks represent alpha-particle energies present in a multinuclide source.

In practice, additional contributions to the background signal arise from at least three sources:

- Johnson noise of the temperature-sensitive resistive element (thermistor) used to detect the temperature step.
- Electronic noise associated with the junction field-effect transistor (JFET) preamplifier circuitry.
- Mechanically induced microphonic noise.

Our primary objective is to make the latter two sources of noise small compared to the Johnson noise. We believe that careful calorimeter fabrication, coupled with today's most advanced JFETs, will allow us to accomplish this task. Furthermore, below the frequency set by the thermal decay time of the calorimeter, the Johnson noise at

0.1 K is less than the phonon noise. Above this corner frequency, Johnson noise dominates. Hence, phonon-noise-limited resolution should be theoretically achievable at low counting rates. Therefore, our second objective is to design a device whose thermal decay time is relatively short by present standards so that phonon-noise-limited energy resolution can be achieved at counting rates approaching 1 kHz.

We constructed prototype calorimeter/spectrometer/refrigeration systems to operate at 1.4 K and 0.3 K using well-developed infrared bolometric theory and laboratory techniques. Mastering the thermal and electronic techniques necessary to make calorimeters perform at these low temperatures has been the foundation of our experimental philosophy. Such mastery is clearly a prerequisite to commencing with experiments at 0.1 K, where the thermodynamic properties of materials are markedly different, and cooling by either adiabatic demagnetization (ADM) or He^3 dilution refrigeration is essential.

With both practicality and the capability of high counting rate in mind, we conceived of a new approach to low-noise pulse-counting electronics for microcalorimeters. The two circuit configurations under study are based on JFET preamplifiers with negative feedback that were developed for use with silicon and germanium charge-collecting detectors. Negative feedback significantly improves the temporal response of the preamplifier over previous techniques and has enabled us to measure the thermalization time of high-resistance germanium calorimeters.

We have introduced two new techniques for diagnosing calorimeter performance. First, we use a test capacitance input to exercise the entire electronic chain without irradiating the calorimeter. This technique provides for a combined measure of noise from all sources. Second, we use a controllable infrared LED to independently test operation of the calorimeter. This technique is a simple means for measuring thermalization time, thermal decay time, and, in conjunction with thermal conductance obtained from the calorimeter load curve, the heat capacity.

We are fabricating and studying the properties of composite and monolithic bolometers. Our monolithic bolometers are 1.5-mm × 1.5-mm × 100-μm wafers of single-crystal germanium doped via neutron-induced transmutation (NTD). The dopant level defines the degree to which sample resistance varies with temperature. We have learned to wedge bond aluminum wires to the germanium wafers to minimize total heat capacity. The Figure (Silver, 1987) shows an alpha particle spectrum obtained with such a monolithic calorimeter operating at 1.4 K. Peaks represent alpha particle energies present in a multinuclide source. The 90-keV width of the Ra^{220} peak is predominantly due to electronic noise (see the 80-keV-wide test pulse). We determined that the major contribution to this noise originates from approximately 100 pF of stray capacitance in the wiring harness, which effectively magnifies the intrinsically small JFET noise.

We performed concurrent experiments at 0.3 K and detected 30-keV x rays. These experiments suffered from identical problems with stray capacitance. Our plan is to reduce the stray capacitance to at least 10 pF and thereby make the effective JFET noise small compared to the other noise sources.

We are also exploiting techniques involving thin-film evaporation to fabricate composite bolometers. A film of germanium-gold alloy semiconductor serves as the thermal sensor and is evaporated on a sapphire x-ray absorber. We expect that the thin film will make good thermal contact with the sapphire substrate and thereby possess fast temporal properties.

Finally, we have constructed and begun testing an ADM refrigerator to cool the calorimeter to 100 mK. We have achieved a temperature of 50 mK and a holding time of more than 12 h at 100 mK. The success of its design will guide further development of flight-compatible devices.

After reducing stray capacitance, we expect our calorimeter resolution to be limited by Johnson and phonon noise. One of our goals for FY88 is a practical instrument with an energy resolution of approximately 60 eV for samples cooled to 0.3 K. We will also begin experiments in the ADM refrigerator at 0.1 K, fabricate new monolithic and composite calorimeters optimized for operation at 0.1 K, and investigate the behavior of these devices at varying phonon counting rates.

If the resolution of 1 eV is attainable at 0.1 K, then it would represent an improvement of two orders of magnitude over the best nondispersive spectrometers available today. It would then be possible to measure broadband spectra with the resolution power of a Bragg crystal, and measurements could be accomplished with almost unit efficiency rather than the usual 0.1% efficiency associated with crystal spectrometers.

Reference

Silver, E. H. (1987), "UV and X-Ray Spectroscopy of Astrophysical and Laboratory Plasmas," *Microcalorimeters for X-Ray Spectrosc., Proc. IAU Colloq.* **102**, 44.

Fabrication of Fully Stabilized, Multifilamentary NbN Superconductors

Principal Investigators:
Leonard T. Summers and
John R. Miller

Using a combination of physical vapor deposition and liquid-metal infiltration, we have demonstrated the technology for fabricating NbN superconductors in configurations suitable for large-scale magnet applications. We have produced prototype wires and are investigating conductor performance.

Unlike the present generation of technically important superconductors, NbN is insensitive to the effects of incident radiation and mechanical strain. Although laboratory samples have been produced, NbN has not been fabricated in a useful configuration. The objective of our research program is to demonstrate the feasibility of fabricating NbN in geometries that are suitable for large-scale fusion-energy applications.

We are studying the use of physical vapor deposition of NbN onto fine, multifilamentary substrates, i.e., graphite, followed by liquid-metal infiltration of a normal metal stabilizer, such as copper or aluminum. The resulting conductor is a fully stabilized, multifilamentary composite that may be suitable for use as magnet windings.

With the cooperation of Cordec, Inc., and Materials Concepts, Inc., we have successfully vapor-deposited NbN on substrates as long as 30 m using a continuous process. The NbN films we produced were uniform and have excellent adherence to the substrate. As expected, the critical currents in the films were low (<400 $A \cdot cm^{-2}$) but are readily improved by variation of the deposition parameters.

Infiltration of the normal metal stabilizer, a critical step in the fabrication of a useful conductor, was successful using aluminum. There appears to be no degradation of the NbN layer during the process, and electrical characterization is now in progress. Deposition of a copper stabilizer has proven to be difficult and requires further development. Additional development work is proceeding and is funded by Department of Energy Small Business Innovative Research (SBIR) grants awarded to the commercial vendors.

References

Summers, L. T. and J. R. Miller (October 1986), "The Development of Superconductors for Applications in High-Field, High-Current-Density Magnets for Fusion Research," Applied Superconductivity Conference, Baltimore, Md.

Summers, L. T., J. R. Miller, M. J. Strum, R. J. Weimer, and D. Kizer (June 1987), "The Influence of Liquid Metal Infiltration on the Superconducting Characteristics of NbN," International Cryogenic Materials Conference, Chicago, Ill.

Bacterial Reduction and Removal of Selenium

Principal Investigator:
Robert T. Taylor
Co-Investigator:
Emilio Garcia

Oxidized soluble forms of selenium in agricultural drainage and energy-associated wastes are polluting our natural waters. Reductive removal of selenate and selenite by bacteria is an attractive possibility for ridding wastes of these toxic compounds. We are working to determine the biological mechanisms by which bacteria reduce these compounds to insoluble, nontoxic elemental selenium (Se^0). With this knowledge, we can guide the genetic engineering of a soil bacterium to enhance its waste-cleansing properties.

Our goal is to determine the enzymatic-biochemical reactions by which *E. coli* and *C. pasteurianum* reduce selenium oxyanions to Se^0. Because *E. coli* live only in vertebrate intestines, they are not suitable for environmental applications. However, they are very useful in laboratory research. In contrast, C. *pasteurianum* grows only in the absence of oxygen (anaerobically) under low redox conditions, is ubiquitous in soils, can reduce a number of metallic ions to their elemental forms, and was reported recently to accumulate Se^0 in selenate-laden wastewater from a uranium mine (Kauffman et al., 1985). The ultimate purpose of our work is to guide the genetic engineering of either *C. pasteurianum* or a related soil isolate toward more effective removal of toxic forms of selenium.

We observed that cultures of *E. coli* reduce selenite, but not selenate, to Se^0, while those of *C. pasteurianum* reduce both (Hanna et al., 1986). It is important to clarify the comparative biochemistry of selenium reduction in these two microorganisms.

Of particular interest was the relation of selenium reduction to the metabolic assimilation of sulfur into the essential amino acid *L*-cysteine (Cys). It had been assumed that the pathway for this process would be the same for selenium because its chemical properties mimic those of sulfur. To test this assumption, we devised simple procedures to assay two enzymes that catalyze reactions in this pathway: ATP sulfurylase and sulfite reductase. We found that growing *E. coli* in a medium containing Cys repressed their ATP sulfurylase and sulfite reductase enzymes over thirtyfold. Yet, selenite was still converted to Se^0 as in nonrepressed sulfate-grown cultures. In addition, Cys-requiring E. *coli* mutants form as much intracellular Se^0 from selenite as the nonmutant parent cells. These and other experiments established that selenite reduction to Se^0 does not depend on the enzymes of inorganic sulfate assimilation.

Reduction of selenite, but not selenate, to Se^0 made *E. coli* an attractive cellular host for studying how *C. pasteurianum* converts selenate to selenite. To carry out this study, we cloned fragments of *C. pasteurianum* DNA into the *E. coli* plasmid pBR322. From a bank of 3000 clones, we identified one positive selenate reducer, pCP52-24. Cell suspensions of pCP52-24 consistently turn pink-brown when they are incubated with 10 to 25 ppm selenate, indicating reduction to Se^0. Unlike typical E. *coli*, this clone can also reduce molybdate and tellurate to elemental grey-black molybdenum and tellurium. Assays of extracts from clone pCP52-24 indicate that increased levels of ATP sulfurylase or a sulfurylase with a higher affinity for selenate (encoded by a *C. pasteurianum* gene) is not the biochemical basis for its selenate-reducing activity. We are now using an electrophoretic, ^{75}Se radiotracer method to obtain quantitative measurements of selenate conversion to Se^0 in cell extracts. Clone pCP52-24 may be expressing a special selenate reductase due to the inserted *C. pasteurianum* DNA fragment.

We plan to continue this potentially important line of research in cooperation with Binnie-California Corporation, Mendota, Calif., which operates a state-sponsored pilot plant for treating agricultural wastes. There, mixed cultures of anaerobic bacteria from mud sediments and sewage sludge have been used successfully to remove selenate from agricultural drainage water. We are interested in identifying the major bacterial species involved and the biochemical-genetic factors that control the rate of the process. Our new biochemical assays and the *C. pasteurianum*-DNA probe in clone pCP52-24 could be powerful tools in this endeavor.

References

Hanna, M. L., G. L. Bush, E. Garcia, and R. T. Taylor (December 1986), "Reduction of Selenium Oxyanions by *Escherichia coli* Versus *Clostridium pasteurianum*," *Proceedings of the Genetic and Environmental Toxicology Association*, Palo Alto, Calif.

Kauffman, J. W., W. C. Laughlin, and R. A. Baldwin (1985), "Microbial Treatment of Uranium Mine Waters," *Environ. Sci. Technol.* **20**, 243.

Formation of Giant Scattering Resonances in Heavy Atoms and Ions

Principal Investigator:
Stephen M. Younger

We have performed a systematic study of the formation and characteristics of giant scattering resonances in heavy atoms and ions using a specially modified distorted-wave computer code. Whereas it was initially thought that such structures were peculiar to a few ions in the periodic table, we have shown that they are a general feature of electron interactions with heavy elements.

In 1986, we discovered giant resonances in electron-impact-ionization cross sections for heavy elements. Our discovery prompted us to ask whether the phenomenon is specific to the few cases for which experimental data are available or whether it is a general feature of electron scattering from heavy atoms and ions. Such resonances have been shown to have a profound effect on the ionization balance and kinetics of plasmas containing heavy atoms.

We have performed a systematic study of the development of giant resonances in the electron-impact-ionization cross sections of elements preceding xenon in the periodic table and in other selected atoms and ions. Our study made use of our unique multiconfiguration, term-dependent, distorted-wave computer code. In addition to the interest arising from the pure physics aspects of this work, we have also considered the exploitation of giant resonances in designing low-cost, electron-beam-driven x-ray lasers.

To date we have completed a survey of the electron-impact-ionization cross sections for the singly charged ions Ag^+ to Ce^+ and for several other atoms and ions of particular interest. We found that the giant resonance behavior begins at iodine and continues to dominate the cross section through the rare-earth elements. Although giant resonance behavior is most pronounced for inner-subshell ionization, we also found significant effects for valence-subshell ionization. Efforts are now under way at several laboratories working in electron scattering to confirm our findings and predictions.

References

Younger, S. M. (1987), "Giant Resonance Effects in the Electron Impact Ionization of Heavy Atoms and Ions," *Phys. Rev. A* **35**, 2841.

Younger, S. M. (1987), "Systematics of Giant Resonances in the Electron Impact Ionization of Heavy Atoms and Ions," *Phys. Rev. A* **35**, 4567.

Production of Rydberg Positronium

Principal Investigator:
Klaus-Peter Ziock
Co-Investigators:
Richard H. Howell,
Kevin M. Jones,[a] and
Frank Magnotta

[a]Williams College, Williamstown, Mass.

Our goal is to excite positronium obtained from the LLNL linac to Rydberg levels and thereby create long-lived (~1-ms) positronium atoms. We plan to reach Rydberg levels using a two-step, resonant photon excitation, which allows simultaneous spectroscopy on the systems.

Positronium is the hydrogen-like bound state of an electron-positron pair, which is of interest from both fundamental and practical points of view. However, study and use of the system is complicated by its short lifetime. The lifetime of the longest lived of the two ground states is only 140 ns.

Our goal is to take thermal positronium produced at the LLNL electron linac and to promote it to the highly excited (Rydberg) quantum states. These states are of interest due to their long lifetimes, which can be up to 1000 times the lifetime of the ground state. Such atoms have potential applications as a tool for diagnosing and enhancing the technique of laser cooling applied to positronium. In addition, we might store cooled atoms for use in a stimulated-annihilation gamma-ray laser (Liang, 1986). Because few measurements have been performed in positronium beyond the first excited state, precision spectroscopy of some of the lower Rydberg levels is of fundamental interest.

We create Rydberg positronium via resonant, two-photon excitation. The atom is simultaneously subjected to co-propagating ultraviolet and red laser beams. Photons from the ultraviolet beam take the atom from the ground state to the first excited state; photons from the red beam shift the atom to the final level. The excited species drift toward a detector where field ionization occurs and the positron is trapped. Trapped positrons are transported to an off-axis microchannel plate for detection by an electric field crossed with the magnetic field used to focus the incoming positron beam. The ability to excite and ionize the atoms on the axis of the incoming beam significantly increases the solid angle of our detector over that of other configurations.

To date we have made the first trial runs with the entire experimental apparatus, including both the novel detector and laser system. The laser light is produced by simultaneously pumping two dye lasers with an excimer laser synchronized to the linac positron pulse. The light from one of the dye lasers is subsequently doubled to achieve resonance with the transition from the ground state to the first excited state.

During FY88, we will redesign several aspects of our experiment to improve the sensitivity. Our improvements include redesigning the vacuum-chamber windows to reduce the noise in the microchannel plate due to scattered light. We anticipate further improvements through an increase in the amount of ultraviolet light from the use of both a more efficient dye laser and newly developed, more efficient doubling crystals. We then plan to use the Rydberg states as a diagnostic tool in upcoming work that will be directed at achieving laser cooling of room-temperature positronium to millikelvin temperatures.

Reference

Liang, E. P. (1986). *Laser Cooling of Positronium and Stimulated Annihilation Radiation*. Lawrence Livermore National Laboratory, Livermore, Calif., UCRL-95117.

I ◆ R ◆ & ◆ D

Resource Requirements Author Index

Lawrence Livermore National Laboratory

Budget:

Institutional Research and Development Program — FY87

	Actual costs—FY87 (K$)	Projected costs—FY88 (K$)
Exploratory Research in the Disciplines	**7,653**	5,990
Biomedical and Environmental Research[a]	**100**	100
Chemistry and Materials Science	**1,076**	1,000
Computation	**1,084**	750
Earth Sciences	**1,196**	890
Engineering	**927**	500
Nuclear Chemistry	**970**	750
Physics	**2,300**	2,000
Director's Initiatives	**3,389**	6,070[b]
Biomedical and Environmental Research	**847**[c]	710
The Compact Torus	**1,017**[d]	800
Supercomputer Research and Development	**1,525**	1,500
University of California Institutes	**1,784**	1,980
Institute of Geophysics and Planetary Physics	**1,408**[e]	1,450
Institute for Scientific Computing Research	**151**	190
Plasma Physics Research Institute	**45**	150
Program for Analytical Cytology	**180**	190
Individual Awards	**3,656**[f]	3,361
38 projects funded in FY87; *26 projected for FY88*		
IR&D Administration	**318**[g]	599[h]
Totals		
Operating costs	**16,800**	18,000
Capital equipment	**260**	200

[a] Work in this category is described in the Director's Initiatives section of this report.
[b] Includes $3,060,000 projected costs for Director's Initiatives not funded in FY87.
[c] The Biomedical and Environmental Research Director's Initiative received an additional $35,000 for capital equipment, for a total of $882,000.
[d] The Compact Torus Director's Initiative received an additional $86,000 for capital equipment, for a total of $1,103,000.
[e] The Institute of Geophysics and Planetary Physics received an additional $98,000 for capital equipment, for a total of $1,506,000.
[f] Individuals were awarded an additional $41,000 for capital equipment, for a total of $3,697,000.
[g] Cost includes IR&D Annual Report FY86, salaries, and miscellaneous administrative expenses.
[h] Projected costs for FY88 include $250,000 in unallocated research funds.

Author Index

U.S. Government Printing Office: 1988 4 – 585-057 77482